



Eesti Maaülikool

Estonian University of Life Sciences

**INDUCTION OF VOLATILE ORGANIC COMPOUND
EMISSIONS FROM LEAVES UPON OZONE AND
METHYL JASMONATE (MeJA) TREATMENTS**

**TAIMELEHTEDE LENDUVÜHENDITE EMISSIOONI
INDUKTSIOON OSOONI JA METÜÜL JASMONAADI
MÕJUL**

SHUAI LI

A Thesis
for applying for the degree of Doctor of Philosophy
in Plant Physiology

Väitekirj
filosoofiadoktori kraadi taotlemiseks taimefüsioloogia erialal

Tartu 2018

Eesti Maaülikooli doktoritööd

**Doctoral Theses of the
Estonian University of Life Sciences**



Eesti Maaülikool
Estonian University of Life Sciences

**INDUCTION OF VOLATILE ORGANIC COMPOUND
EMISSIONS FROM LEAVES UPON OZONE AND
METHYL JASMONATE (MeJA) TREATMENT**

TAIMELEHTEDE LENDUVÜHENDITE EMISSIOONI
INDUKTSIOON OSOONI JA METÜÜL JASMONAADI
MÕJUL

SHUAI LI

A Thesis
for applying for the degree of Doctor of Philosophy
in Plant Physiology

Väitekirj
filosoofiadoktori kraadi taotlemiseks taimefüsioloogia erialal

Tartu 2018

Institute of Agricultural and Environmental Sciences
Estonian University of Life Sciences

According to the verdict No 6-14/17-2 of January 4, 2018 The Doctoral Committee of Environmental Sciences and Applied Biology of the Estonian University of Life Sciences has accepted the thesis for the defence of the degree of Doctor of Philosophy in Plant Physiology.

Opponent: **Dr. Silvano Fares**
Council for Agricultural Research and Economics (CREA)
Research Centre for Forestry and Wood
Arezzo, Italy

Supervisor: **Professor Ülo Niinemets**
Institute of Agricultural and Environmental Sciences
Estonian University of Life Sciences
Tartu, Estonia

Defence of the thesis:
Estonian University of Life Sciences, room 2A1, Kreutzwaldi 5, Tartu,
on February 26, 2018, at 12:15.

The English language was edited by Ülo Niinemets and Arooran Kana-gendran. The Estonian summary was translated and edited by Kaia Kask and Astrid Kännaste.

Publication of this thesis is supported by the Estonian University of Life Science and by the Doctoral School of Earth Science and Ecology created under the auspices of European Social Fund.

This study was supported by the Estonian Ministry of Science and Education (institutional grant IUT-8-3), the European Commission through the European Regional Development Fund (Centre of Excellence EcolChange, TK 131), and the European Research Council (advanced grant 322603, SIP-VOL+).



DoRa

ARCHIMEDES

© Shuai Li, 2018

ISSN 2382-7076

ISBN 978-9949-629-17-6

ISBN 978-9949-629-18-3 (pdf)

To my parents

为了祖国、科学和荣誉、以及我深爱着的人们

CONTENTS

LIST OF ORIGINAL PUBLICATIONS	9
DEFINITIONS OF ABBREVIATIONS AND SYMBOLS	10
1. INTRODUCTION	13
2. REVIEW OF THE LITERATURE	17
2.1. O ₃ uptake via stomata and leaf surface reactions	17
2.1.1. Stomatal O ₃ sinks	17
2.1.2. Non-glandular and glandular trichomes	17
2.2. Influence of O ₃ on leaf photosynthesis and VOC emissions. .	18
2.2.1. O ₃ effects on foliage photosynthetic characteristics	18
2.2.2. Volatile release from plants upon O ₃ stress	18
2.3. Influence of MeJA application on VOC emissions.	19
2.4. Kinetics of VOC emission upon different stresses	20
3. AIMS OF THE STUDY.....	21
4. MATERIALS AND METHODS	22
4.1. Plant material (Papers I-III)	22
4.2. Experimental set-up for the measurement of net assimilation rate, stomatal conductance to water vapour, and VOCs	23
4.3. Stress application (Papers I-III)	24
4.4. Gas-exchange measurement (Papers I-II)	25
4.5. Online monitoring of dynamics of plant volatiles (Papers I- III)	25
4.6. Volatile sampling and GC-MS analyses (Paper III)	26
4.7. Determination of trace gas emission rates (Papers I- III)	26
4.8. Quantitative characterization of elicitation of volatile emissions (Papers II-III)	27
4.9. Calculation of O ₃ uptake (Papers I-II)	29
4.10. Quantitative characterization of the protective role of glandular trichomes against O ₃ stress (Paper I)	30
4.11. Chlorophyll fluorescence measurements (Papers I-II)	30
4.12. Scanning electron microscopy analyses of density and morphology of leaf trichomes (Paper I)	30

5. RESULTS	32
5.1. Effect of acute O ₃ treatments on visible leaf damage and leaf physiological characteristics (Papers I-II)	32
5.2. Elicitation of VOCs caused by O ₃ and MeJA treatments (Papers I-III)	33
5.3. Trichome morphology, distribution and density (Paper I)	34
5.4. The relationships between non-stomatal O ₃ deposition and trichome types and density (Paper I)	35
5.5. Changes in physiological characteristics and LOX product emissions in response to O ₃ exposure in relation to glandular trichome density (Paper I)	36
5.6. Time courses of emissions of methanol, LOX products, MeSA, and mono and sesquiterpenes upon acute O ₃ and MeJA treatments (Papers II-III)	38
5.7. Maximum and total integrated O ₃ - and MeJA-elicited volatile emissions (Papers II-III)	40
5.8. Kinetics of foliage volatile emissions from <i>P. vulgaris</i> and <i>C. sativus</i> upon different O ₃ and MeJA treatments (Papers II-III)	43
6. DISCUSSION	47
6.1. Impact of non-stomatal O ₃ deposition rates, and type and density of trichomes on stomatal O ₃ uptake rates	47
6.2. Impact of elevated O ₃ on foliage photosynthetic characteristics	48
6.3. Emission of VOCs upon acute O ₃ and MeJA treatments in <i>P. vulgaris</i> and <i>C. sativus</i>	49
6.4. Time- and dose-dependent modifications of stress volatiles emitted upon acute O ₃ treatments in <i>P. vulgaris</i> leaves	51
6.5. Time- and dose-dependent modifications of stress volatiles emitted upon MeJA treatments in <i>C. sativus</i> leaves	52
CONCLUSIONS	54
REFERENCES	56
SUMMARY IN ESTONIAN	68
ACKNOWLEDGEMENTS	71
ORIGINAL PUBLICATIONS	73
CURRICULUM VITAE	157
LIST OF PUBLICATIONS	159

LIST OF ORIGINAL PUBLICATIONS

The current thesis is based on the following original publications:

- I. **Li, S.**, Tosens, T., Harley, P.C., Jiang, Y., Kanagendran, A., Grosberg, M., Jaamets, K., Niinemets, Ü. (2018) Glandular trichomes as a barrier against atmospheric oxidative stress: relationships with ozone uptake, leaf damage and emission of LOX products across a diverse set of species. *Plant Cell & Environment*, in press.
- II. **Li, S.**, Harley, P.C., Niinemets, Ü. (2017) Ozone-induced foliar damage and release of stress volatiles is highly dependent on stomatal openness and priming by low-level ozone exposure in *Phaseolus vulgaris*. *Plant Cell & Environment* 40, 1984-2003.
- III. Jiang, Y., Ye, J., **Li, S.**, Niinemets, Ü. (2017) Methyl jasmonate-induced emission of biogenic volatiles is biphasic in cucumber: a high-resolution analysis of dose dependence. *Journal of Experimental Botany* 68 (16), 4679-4694.

DEFINITIONS OF ABBREVIATIONS AND SYMBOLS

ABBREVIATION	DEFINITION
CCN	Cloud condensation nuclei
ESEM	Environmental Scanning Electron Microscope
GC-MS	Gas chromatography mass spectrometry
GGDP	Geranylgeranyl diphosphate pathway derived volatiles
LOX	Lipoxygenase pathway
MeJA	Methyl jasmonate
MeSA	Methyl salicylate
PTR-TOF-MS	Proton transfer reaction-time of flight-mass spectrometry
ROS	Reactive oxygen species
SOA	Secondary organic aerosols
VOC	Volatile organic compound

SYMBOL	DEFINITION	UNITS
ϕ_x	Emission rates of given VOC	$\text{nmol m}^{-2} \text{s}^{-1}$
F	Air flow rate through the chamber	mol s^{-1}
S	Leaf area enclosed in the chamber	m^2
$C_o(X)$	Concentration of the target VOC compound (compound X) measured at the chamber outlet	nmol mol^{-1}
$C_i(X)$	Concentration of the target VOC compound (Compound X) measured at the chamber inlet	nmol mol^{-1}
$C_c(X)$	The correction to account for the possible release of the given compound X released from the gas-exchange system components	nmol mol^{-1}
$\phi_{M1, X}$	Maximum emission rate at the first emission peak	$\text{nmol m}^{-2} \text{s}^{-1}$
$\phi_{M2, X}$	Maximum emission rate at the second emission peak	$\text{nmol m}^{-2} \text{s}^{-1}$

SYMBOL	DEFINITION	UNITS
Φ_x	Total amount of given VOC emitted over a certain time	$\mu\text{mol m}^{-2}$
t_{P1S}	Start of the first emission burst since the start of the O_3 exposure	h
t_{P1E}	End of the first emission burst since the start of the O_3 exposure	h
t_{P2S}	Start of the second emission burst since the start of the O_3 exposure	h
t_{P2E}	End of the second emission burst since the start of the O_3 exposure	h
D_{P1}	Duration of the first induced emission peak	h
D_{P2}	Duration of the second induced emission peak	h
t_{E1}	Time from the onset of O_3 exposure to the first emission elicitation	h
t_{E2}	Time from the onset of O_3 exposure to the second emission elicitation	h
t_{M1}	Time from the elicitation to the first emission maximum	h
t_{M2}	Time from the elicitation to the second emission maximum	h
τ_{I1}	Doubling-time for the increase of the emission during the first emission burst	h
τ_{D1}	Half-time for the decrease of the emission during the second emission burst	h
τ_{I2}	Doubling-time for the increase of emissions during the second emission burst	h
τ_{D2}	Half-time for the decrease of emissions during the second emission burst	h
k_{I1}	Rate constant for the initial increase of the emission during the first emission burst	h^{-1}
k_{D1}	Rate constant for the decrease of the emission during the first emission burst	h^{-1}
k_{I2}	Rate constant for the initial increase of emissions during the second emission burst	h^{-1}
k_{D2}	Rate constant for the decrease of emissions during the second emission burst	h^{-1}

SYMBOL	DEFINITION	UNITS
ϕ_{LO_3}	Rate of O_3 uptake by whole leaf	$\text{nmol m}^{-2} \text{s}^{-1}$
C_{in}	O_3 concentration in the air entering the chamber	nmol mol^{-1}
C_{out}	O_3 concentration in the air exiting the chamber	nmol mol^{-1}
$C_{O_3}^{\text{chamber}}$	O_3 destruction due to surface reactions by the empty chamber	nmol mol^{-1}
Φ_{LO_3}	Total amount of O_3 uptake by whole leaf	$\mu\text{mol m}^{-2}$
$C_{O_3}^i$	Intercellular O_3 concentration	nmol mol^{-1}
ϕ_{GO_3}	Rate of O_3 uptake by stomata	$\text{nmol m}^{-2} \text{s}^{-1}$
t_E	Start of O_3 exposure	h
t_P	End of O_3 exposure	h
Φ_{GO_3}	Total amount of O_3 uptake by stomata	$\mu\text{mol m}^{-2}$
Φ_{NGO_3}	Total amount of non-stomatal O_3 deposition	$\mu\text{mol m}^{-2}$
γ	O_3 uptake-weighted response	

1. INTRODUCTION

Plants produce a large amount of secondary metabolites including a variety of biogenic volatile organic compounds (VOCs), consisting of volatile isoprenoids, volatile products of lipoxygenase (LOX) pathway and saturated aldehydes (Guenther *et al.* 1995). It is known that these volatiles play major roles in the formation of atmospheric ozone (O_3), secondary organic aerosols (SOA) and cloud condensation nuclei (CCN) (Fehsenfeld *et al.* 1992; Carter 1994; Benjamin and Winer 1998; Claeys *et al.* 2004; VanReken *et al.* 2005; Sun and Ariya 2006; Carlton *et al.* 2009; Calfapietra *et al.* 2013). In addition, these volatiles play crucial roles in plant growth, development, communication, defense and protection (Sharkey and Singsaas 1995; Arimura *et al.* 2000; Kessler and Baldwin 2001; Loreto *et al.* 2001, 2004; Dudareva *et al.* 2006; Fares *et al.* 2008, 2010b, c; Dicke *et al.* 2009). For example, isoprene enhances plant thermotolerance (Sharkey *et al.* 2001) and increases the resistance of plant metabolism to atmospheric oxidants (Loreto *et al.* 2001) and protects cellular membranes from denaturation (Loreto *et al.* 2004).

Plant volatile emissions are either constitutive or induced upon a variety of stresses (Guenther *et al.* 1995, 2000; Heiden *et al.* 1999; Beauchamp *et al.* 2005; Copolovici and N  nemets 2010; Loreto and Schnitzler 2010; N  nemets 2010a; Brilli *et al.* 2011; Copolovici *et al.* 2012, 2014; Portillo-Estrada *et al.* 2015; Pazouki *et al.* 2016). Thus, volatiles can serve as reliable noninvasive markers for the detection of stress and for the detection of elicitation of stress-dependent processes such as programmed cell death, and stress response and recovery under given environmental conditions (Beauchamp *et al.* 2005). Therefore, these biomarkers can be useful in providing important insight into how specific stresses affect the plant and when critical thresholds for acute responses are reached. This makes it possible to explain how the magnitude and timing of these emissions scale with stress dose, and improve the overall mechanistic understanding of regulation of plant VOC emission upon stress.

Usually, constitutive emissions of VOCs consume 1-2% of the carbon fixed by photosynthesis, but when the plants are under stress, they enhance the emission rates of VOCs at the expense of photosynthesis; in stressed plants, VOC emissions can consume more than 10% of photosynthetically-fixed carbon (Fuentes and Wang 1999; Sharkey *et al.* 2008; Guenther *et al.*

1993; Niinemets 2010b; Copolovici *et al.* 2014). The majority of previous studies has focused only on the contribution of constitutive plant volatile emissions to global VOC budget. However, the overall impact of stresses such as acute O₃ exposure and simulated herbivory (including exposure to methyl jasmonate (MeJA) mimicking herbivory treatments) on volatile release from leaves is poorly understood. Particularly limited is the understanding of what is the effect of key environmental and biotic stresses on elicited volatile emission kinetics. Rapidly changing global environmental conditions result in increased stress level in plant ecosystems, and thus, the share of induced VOC emissions to global VOC budget is further expected to gain in importance (Loreto and Schnitzler 2010; Niinemets 2010a; Peñuelas and Staudt 2010). Therefore, it is necessary to investigate the influence of environmental factors on plant VOC emissions to predict how plants respond to climate change and to provide useful guidelines on environmental management policies for the future.

Average global O₃ concentration has approximately doubled since the pre-industrial time and it is expected to increase further (Vingarzan, 2004; Fowler *et al.* 2008; IPCC 2013; Monks *et al.* 2015; Ainsworth 2017). As a result, exposure to high O₃ concentrations dose significantly disturb plant growth and development as well as productivity (Long and Naidu 2002; Calatayud *et al.* 2003; Fiscus *et al.* 2005; Kollist *et al.* 2007; Wittig *et al.* 2009; Fares *et al.* 2010a, 2013b; Vahisalu *et al.* 2010; Avnery *et al.* 2011a, b; Ainsworth *et al.* 2012; Betzelberger *et al.* 2012; Wilkinson *et al.* 2012; McGrath *et al.* 2015), and these perturbations are expected to become more important in the future. Past studies have shown that enhanced emissions of VOCs such as methanol, LOX products and methyl salicylate (MeSA) are typically observed during and after O₃ fumigation (Heiden *et al.* 1999; Beauchamp *et al.* 2005). Therefore, atmospheric O₃ rise can be an important abiotic stress factor greatly influencing global volatile emissions.

Once O₃ enters the leaf, it can instantly react with the plasmalemma and trigger the release of reactive oxygen species (ROS), which eventually cause cellular damage or death, leading to hypersensitive reactions (Long and Naidu 2002; Wohlgemuth *et al.* 2002; Pasqualini *et al.* 2003; Beauchamp *et al.* 2005; Fiscus *et al.* 2005; Vahisalu *et al.* 2010). However, upon O₃ exposure, leaves typically close stomata (Kollist *et al.* 2007; Vahisalu *et al.* 2008; Vahisalu *et al.* 2010). Stomatal conductance has a dramatic impact on the degree of damage caused by elevated O₃ in plant cells regardless of the concentration of O₃ around the leaf surface. However, O₃-dependent

reduction in stomatal conductance limits CO₂ uptake and thus, declines the net assimilation rate.

In addition, apart from *de novo* synthesized VOCs emitted from leaves, glandular trichomes on leaf surface also exude semi-volatile or volatile organic compounds (Glas *et al.* 2012; Sallaud *et al.* 2012; Jud *et al.* 2016). These compounds react with O₃ on leaf surface providing an effective way of depleting O₃, they act as a sink for O₃ and thus, play a major role for surface uptake (non-stomatal O₃ deposition) before O₃ enters the leaf (Jud *et al.* 2016). Given these two different pathways for O₃ absorption, stomatal uptake and surface uptake, it is important to distinguish between O₃ exposure and stomatal O₃ uptake and non-stomatal O₃ deposition to accurately characterize the thresholds for acute responses.

Endogenous jasmonic acid (JA) and its methyl ester, methyl jasmonate (MeJA) are typically observed after plant wounding and herbivore damage (Farmer and Ryan, 1990; Baldwin *et al.* 1997). Once released into the air, MeJA has been shown to act as an important signaling molecule to trigger defense responses in neighboring plants or in non-impacted parts of the damaged plant (Farmer and Ryan 1990; Cheong and Choi 2003; Heil and Ton 2008). Thus, exogenous application of MeJA has often been used to simulate defense responses similar to responses elicited by physical wounding and biotic stress (Zhao and Chye 1999; Heijari *et al.* 2008; Tamogami *et al.* 2008; Kegge *et al.* 2013; Jiang *et al.* 2016).

The main purpose of this thesis was to study the overall impacts of elevated O₃ and MeJA stress on diverse set of plant species. We hypothesized that (1) Exposure of leaves to acute O₃ will lead to severe visible leaf injuries, reductions in leaf physiological activity, and elicitation of volatile emissions that will scale with the severity of O₃ treatment (**Papers I and II**); (2) Non-glandular trichomes will not protect plant leaves against elevated O₃, while glandular trichomes will serve as an important antioxidative barrier (**Paper I**); (3) The lower rate of stomatal O₃ uptake due to stomatal closure in darkness or pre-exposure to low-level O₃ during acute exposure (priming) will reduce O₃-induced leaf damage (**Papers II**); (4) MeJA treatment lead to an emission blend of methanol, LOX volatiles, and mono- and sesquiterpenes (**Paper III**), both the amount of volatile emitted and the response kinetics depend on stress dose (**Papers II and III**).

In this thesis, **Paper I** describes the O₃ sensitivity of 24 plant species pos-

sessing non-glandular and glandular trichomes on the leaf surface. **Paper II** presents the impact of acute O₃ stress on photosynthetic characteristics and volatile emission kinetics in *Phaseolus vulgaris* leaves. Finally, **Paper III** explores the emission kinetics of methanol, LOX volatiles, mono- and sesquiterpenes in response to MeJA stress in *Cucumis sativus* leaves.

2. REVIEW OF THE LITERATURE

2.1. O₃ uptake via stomata and leaf surface reactions

2.1.1. Stomatal O₃ sinks

Tropospheric ozone (O₃) is a major airborne pollutant and well-known to be harmful for human and plants. In the past decades, O₃ levels over the intermediate latitudes of the Northern hemisphere have been high enough to induce damage to crops (Emberson *et al.* 2009). As a strong polar oxidant, O₃ enters plants mainly through the stomata. Thus, stomatal conductance is a significant factor in controlling stomatal O₃ uptake by leaves (e.g. Kollist *et al.* 2007; Fares *et al.* 2013a, 2014).

2.1.2. Non-glandular and glandular trichomes

Many plant species possess glandular and/or non-glandular trichomes on leaf and stem surface (Wagner *et al.* 2004). Non-glandular trichomes are found in most angiosperms and in some gymnosperms and bryophytes with branched or unbranched structures. Density (number per surface area) of non-glandular trichomes varies greatly among species (Mathur and Chua 2000; Wagner *et al.* 2004). Non-glandular trichomes do not produce or secrete phytochemicals and serve primarily as a mechanical barrier against herbivores (Corsi and Bottega 1999; Werker 2000; Glas *et al.* 2012) or as a reflective screen against high solar radiation (Ehleringer 1981). As non-glandular trichomes are covered by a wax layer that consists of saturated hydrocarbons and that have a low reactivity with O₃ (Corsi and Bottega 1999), the effect of non-glandular trichomes in leaf O₃ resistance is expected to be minor, despite having a high surface area. Yet, the role of non-glandular trichomes in O₃ resistance has not been studied to our knowledge.

Glandular trichomes are specialized structures on the leaf surface in about 30% of all vascular plants (Fahn 2000). Two major types of glandular trichomes have been characterized, capitate and peltate trichomes. Both capitate and peltate glandular trichomes consist of one basal cell. Capitate glandular trichomes possess one or a few secretory cells at the tip of the stalk which consist of one or several stalk cells (Werker 2000; Maffei 2010), but peltate glandular trichomes consist of a (short) stalk cell that supports a head consisting of several secretory cells (Turner *et al.* 2000). Capitate glandular trichomes primarily produce and store smaller

quantities of diterpenes. They also primarily produce non-volatile or poorly volatile compounds such as defensive proteins acyl sugars and esters that are directly excluded onto the surface of trichome (Glas *et al.* 2012; Sallaud *et al.* 2012; Tissier 2012; Jud *et al.* 2016). Peltate trichomes mostly contribute to the production and storage of both volatile and semi-volatile organic compounds (Corsi and Bottega 1999; Turner *et al.* 2000; Gang *et al.* 2001; Wagner *et al.* 2004; Glas *et al.* 2012). Given that glandular trichomes have the capacity to produce, store and secrete large amounts of different classes of secondary metabolites, they could be potentially involved in the chemical reactions on leaf surface.

2.2. Influence of O₃ on leaf photosynthesis and VOC emissions

2.2.1. O₃ effects on foliage photosynthetic characteristics

Once O₃ enters the leaf interior and passes the cell wall aqueous phase, it can directly react with the plasmalemma and trigger the formation of reactive oxygen species (ROS), which can eventually lead to cellular damage or death (Long and Naidu 2002; Wohlgemuth *et al.* 2002; Pasqualini *et al.* 2003; Beauchamp *et al.* 2005; Fiscus *et al.* 2005; Fares *et al.* 2010a; Vahisalu *et al.* 2010). In general, acute O₃ exposure has been shown to reduce net assimilation rate, stomatal conductance and the quantum yield of primary photochemistry (Long and Naidu 2002; Calatayud *et al.* 2003; Fiscus *et al.* 2005; Flowers *et al.* 2007; Kollist *et al.* 2007; Guidi *et al.* 2009; Vahisalu *et al.* 2010; Fares *et al.* 2013b). Furthermore, exposure of leaves to O₃ leads to visible symptoms of injury including chlorotic or necrotic lesions on the leaf surface (Loreto *et al.* 2001; Pasqualini *et al.* 2003; Beauchamp *et al.* 2005; Fares *et al.* 2006; Vickers *et al.* 2009). As plant species have various O₃ quenching mechanisms such as stomatal closure to limit O₃ uptake and scavenging of O₃ by antioxidants in cells, the plant response to O₃ can be very complex (Loreto and Fares 2007; Fares *et al.* 2010a). In addition, mild stress itself can elicit priming responses leading to enhancing or reducing the sensitivity of subsequent stress episodes (Conrath *et al.* 2006; Heil & Kost 2006). Therefore, more experiments are needed to address the possible modification of acute O₃ resistance as primed by exposure to low concentration of O₃ and leaf surface structures.

2.2.2. Volatile release from plants upon O₃ stress

It has been shown that several constitutively emitted plant VOCs, particularly isoprene and monoterpenes protect leaves against O₃ stress (Loreto and Velikova 2001; Loreto *et al.* 2001, 2004; Vickers *et al.* 2009).

In general, constitutive *de novo* synthesized VOCs are emitted in a light and temperature dependent manner (Guenther *et al.* 2000; Niinemets *et al.* 2004). Apart from the environmental controls on the constitutive emissions in non-stressed conditions, many abiotic stresses such as temperature (Pazouki *et al.* 2016), wounding (Brilli *et al.* 2011), flooding (Copolovici and Niinemets 2010) and O₃ (Heiden *et al.* 1999; Beauchamp *et al.* 2005) alter the rate of constitutive emissions and can also trigger the release of other stress-dependent VOCs. In the case of O₃ stress, the emissions of several isoprenoids, methanol, volatile products of LOX pathway and methyl salicylate (MeSA) are typically induced during and after O₃ fumigation (Heiden *et al.* 1999; Beauchamp *et al.* 2005).

The extent of O₃-induced foliage damage depends on the severity of O₃ stress that is driven by the O₃ concentration at the time of exposure as well as by the cumulative leaf O₃ uptake during the exposure (Beauchamp *et al.* 2005; Wieser *et al.* 2013). As stomatal conductance controls the entry of O₃ into the leaf, the immediate photosynthetic responses to O₃ stress and ultimate leaf damage are significantly driven by the stomatal conductance before the exposure and by changes in stomatal conductance (Kollist *et al.* 2007; Vahisalu *et al.* 2008; Vahisalu *et al.* 2010). On the other hand, net assimilation rate directly depends on stomatal conductance and O₃-driven reductions in stomatal conductance can result in reductions in net assimilation rate even without physiological damage. Thus, tracking the stress volatile release in real time during and after stress periods can be much more informative for understanding the kinetics of stress development and propagation of O₃-induced lesions than monitoring changes in net assimilation rate (Beauchamp *et al.* 2005). Furthermore, due to the primary cellular damage caused by elevated O₃ itself and due to the secondary damage resulting from enhanced ROS production in cells, O₃ exposure can be used to gain an insight into the downstream signalling events that influence both plant defense responses and programmed cell death (Kangasjärvi *et al.* 1994; Rao and Davis 2001; Beauchamp *et al.* 2005).

2.3. Influence of MeJA application on VOC emissions

MeJA also mainly enters leaf intercellular spaces through stomata. MeJA application can trigger the emissions of several VOCs such as LOX products and various terpenoids (Rodriguez-Saona *et al.* 2001; Martin *et al.*

2003; Semiz *et al.* 2012; Kegge *et al.* 2013). Release of terpenoids reflects modification in the expression of terpene synthase genes and terminal enzymes in MeJA-treated leaves (Martin *et al.* 2003; Byun-McKay *et al.* 2006). The temporal emission patterns of VOCs are often associated with the severity of MeJA applications (Rodriguez-Saona *et al.* 2001; Martin *et al.* 2003; Semiz *et al.* 2012; Kegge *et al.* 2013). Interestingly, these volatile blends induced by MeJA treatment are very similar to those emitted upon herbivore attacks (Dicke *et al.* 1999; Rodriguez-Saona *et al.* 2001). These herbivore-induced volatiles serve as infochemicals for attracting herbivore enemies or eliciting defense pathways both in affected and neighboring plants (Dicke *et al.* 1999; Heil and Kost 2006; Heil and Ton 2008; Kappers *et al.* 2010), underscoring the biological significance of MeJA as an inducer for chemical signaling among plants.

2.4. Kinetics of VOC emission upon different stresses

Long-term continuous VOC kinetic studies are rare. Previously, Beauchamp *et al.* (2005) found that O₃-induced methanol release exhibited a biphasic emission pattern with two maxima, but emissions of LOX products and MeSA showed a monophasic pattern. However, biphasic emission of LOX products, ethylene and terpenoids have occasionally been found in response to pathogen infections (Mur *et al.* 2008; Toome *et al.* 2010; Wi *et al.* 2012). A complex temporal kinetics of volatile release during and after stress exposure might comprise both immediate stress responses and induction of systemic responses (Toome *et al.* 2010; Wi *et al.* 2012). Due to the complex temporal kinetic emission responses, quantitative relationships among stress treatments and the timing, and magnitude of induced volatile responses can be more informative to understand how plant key primary and secondary metabolic processes respond to stresses. However, most of the previous kinetic studies had been carried out with a low time resolution (from hours to days) except the ozone stress study of Beauchamp *et al.* (2005). Thus, there is a lack of quantitative information about the relationship between volatile emissions and the degree of stress. In particular, there is a scarcity of studies investigating the quantitative emission characteristics in response to given stress severity (stress dose), and therefore, inferences of the stress severity and degree of physiological damage cannot be currently made on the basis of past studies on volatile emissions.

3. AIMS OF THE STUDY

The overall objective of this thesis is to study how the presence of trichomes modifies the severity of O₃ treatment from a diverse set of plant species and what are the impacts of O₃ and methyl jasmonate (MeJA) treatments on time- and dose-dependent modifications in photosynthetic characteristics and VOC emission kinetics in *Phaseolus vulgaris* and *Cucumis sativus* leaves.

The specific aims of the thesis were:

1. To investigate the effects of acute O₃ and MeJA treatments on leaf photosynthetic characteristics and volatile emissions from a diverse set of plant species (**Papers I-III**).
2. To evaluate the possible protective role of glandular and non-glandular trichomes against O₃ stress (**Paper I**).
3. To examine the role of stomatal conductance in controlling ozone uptake, leaf injury and volatile release in *P. vulgaris* leaves (**Paper II**).
4. To estimate how acute O₃ and exogenous MeJA treatments alter the time kinetics of volatile release after initial stress applications and through recovery phase (**Papers II-III**).

4. MATERIALS AND METHODS

4.1. Plant material (Papers I-III)

For the **Paper I**, 24 species strongly differing in the extent of non-glandular and glandular trichome density and glandular trichome types were used. The species sampled included both cultivated and native species growing in the vicinity of Tartu, Estonia or grown from seed in the lab (Table 1). In brief, for plants grown from seed (seed sources: *C. sativus*: Seston Seemned OÜ, Estonia; *N. tabacum*: gift of I. Bichele, University of Tartu; *O. basilicum* and *S. lycopersicum*: SC Agrosel SRL, Romania; *P. vulgaris*: DALEMA UAB, Vilnius, Lithuania; the seed of *V. thapsus* were collected in the field in Estonia). After germination, the seedlings were replanted into 2 L plastic pots filled with commercial potting soil (Biolan Oy, Kekkila Group, Vantaa, Finland). The plants were grown in a plant growth room under the light intensity at leaf surface of 400 $\mu\text{mol m}^{-2} \text{s}^{-1}$ (HPI-T Plus 400 W metal halide lamps, Philips) for 12 h photoperiod, the temperatures of 24/20°C (day/night), and relative air humidity of 60% maintained throughout the experimental period.

Table 1. The source of 24 plant species investigated.

Site name	Coordinates	Part of collection	Species name
Species grown from seed			<i>C. sativus</i> , <i>Nicotiana tabacum</i> L. cv. W38, <i>Ocimum basilicum</i> L., <i>P. vulgaris</i> , <i>Solanum lycopersicum</i> L. cv. Pontica, <i>Verbascum thapsus</i> L.
Estonian University of Life Sciences (EULS)	58°23' N 27°05' E elevation 40 m	Seedlings and plants Leaves	<i>Betula pendula</i> Roth, <i>Geranium palustre</i> L., <i>Geranium pratense</i> L., <i>Urtica dioica</i> L., <i>Anchusa officinalis</i> L., <i>Arctium tomentosum</i> Mill, <i>Carduus crispus</i> L., <i>Tussilago farfara</i> L.
Ihaste, Tartu	58°21' N 26°46' E elevation 41 m	Plants	<i>Erigeron acer</i> L., <i>Erigeron canadensis</i> L., <i>Erodium cicutarium</i> L., <i>Silene latifolia</i> Poir
Pühajärve, Estonia	58°03' N 26°28' E elevation 131 m	Plants	<i>Geranium robertianum</i> L.
Gardens of Tartu city		Leaves	<i>Cucurbita pepo</i> L., <i>Lavandula angustifolia</i> Mill, <i>Mentha × piperita</i> L., <i>Rosmarinus officinalis</i> L., <i>Salvia officinalis</i> L.

For the seedlings and plants collected from the vicinity of the Estonian University of Life Sciences (EULS), Ihaste and Pühajärve, they were replanted in 2 L plastic pots containing the same commercial potting mix, and exposed to full sunlight under ambient environmental conditions throughout the experimental period. All plants were fertilized once in two weeks with a standard fertilizer with microelements (Biolan Oy, Kekkilä Group, Vantaa, Finland) and watered every day to maintain optimal growth conditions.

For the leaves collected from the vicinity of the EULS and the gardens of Tartu city, all plants sampled were grown in open areas exposed to full sunlight and ambient environmental conditions at the time of experiment. Terminal shoots with multiple leaves exposed to direct sunlight were collected in the morning, immediately recut under water and transported to the laboratory. After recut the cut ends of the shoots under water in the laboratory, a representative leaf was selected for measurements. Fully-expanded non-senescent leaves were used in all measurements.

Common bean (*Phaseolus vulgaris* L. cv. Saxa) and cucumber (*Cucumis sativus* cv. Libelle F1) were selected for the study of O₃ and methyl jasmonate (MeJA) treatment (**Papers II-III**). All plants were grown from seed (seed sources: *P. vulgaris*: DALEMA UAB, Vilnius, Lithuania; *C. sativus*: Seston Seemned OÜ, Estonia). After germination, the seedlings were replanted and kept in a plant growth room under the same conditions as explained above. Application of fertilizer and water was maintained to all plants at close to optimal levels till the completion of the experiment.

4.2. Experimental set-up for the measurement of net assimilation rate, stomatal conductance to water vapour, and VOCs

In **Papers I-III**, we used a custom-made temperature-controlled gas-exchange system with a temperature-controlled glass chamber for photosynthetic measurements, volatiles sampling and stress application (Copolovici and Niinemets 2010). Ambient air with a flow rate of $1.19 \times 10^{-3} \text{ mol s}^{-1}$ was passed through a charcoal filter and O₃ trap before entering the leaf chamber. The chamber air was mixed with a fan providing continuous high turbulence. The gas stream was divided between a reference flow (that was measured in the reference mode) corresponding to the air before entering the chamber, and a sample flow (that was measured in the measurement mode) corresponding to the gas leaving

the plant chamber. An infra-red dual-channel gas analyzer (CIRAS II, PP-Systems, Amesbury, MA, USA) and a proton transfer reaction-time of flight-mass spectrometer (PTR-TOF-MS, Ionicon Analytik GmbH, Innsbruck, Austria; See section 4.5 for further details of volatile measurement with PTR-TOF-MS) were connected to the chamber ports to measure CO₂ and H₂O concentrations and the intensity of VOC signals in the air entering and exiting the leaf chamber. In all measurements, leaf temperature was maintained at 25 °C, ambient CO₂ concentration was 380–400 µmol mol⁻¹ and light intensity at the leaf surface was set to 500 µmol m⁻² s⁻¹ when light was on.

4.3. Stress application (Papers I-III)

The plants were treated with different concentrations of acute O₃ (**Papers I and II**) and exogenous MeJA (**Paper III**). O₃ was generated by an O₃ generator with a quartz glass reaction chamber (Stable Ozone Generator, Ultra-Violet Products Ltd, Cambridge, UK) under UV light (λ=185 nm) (**Papers I and II**). O₃ concentrations in the chamber in- and outlets were measured with a UV-photometric O₃ sensor (Model 49i, Thermo Scientific, Massachusetts, USA). O₃ fumigation was started after stabilization of photosynthesis and VOC emissions, typically 20-30 min after leaf enclosure. In **Paper I**, the illuminated leaf was fumigated with a step-wise increase of O₃ concentration as follows: 100 ± 5 nmol mol⁻¹ of O₃ for 30 min, followed by 200 ± 10 nmol mol⁻¹ for 30 min, and so on, progressively increasing O₃ concentration by 100 nmol mol⁻¹ in every half-hour until the final maximum O₃ concentration was reached. The final maximum O₃ concentration was varied among plant species.

In **Paper II**, O₃ fumigation treatments of *P. vulgaris* leaves are described in detail in **Table 2**. Briefly, both the illuminated and darkened leaves of Treatments 1 and 2 were fumigated with 600 nmol mol⁻¹ O₃ for 30 min, and the illuminated leaf of Treatment 3 was exposed first to 200 nmol mol⁻¹ O₃ for 30 min, after which it was exposed to 600 nmol mol⁻¹ O₃ for an additional 30 min (**Table 2**).

Table 2. O₃ fumigation treatments on *P. vulgaris* leaves in **Paper II**.

	O ₃ concentration (nmol mol ⁻¹) and fumigation time (min)	Light intensity (μmol m ⁻² s ⁻¹)
Treatment 1	600 (30 min)	500
Treatment 2	600 (30 min)	0
Treatment 3	200 (30 min) + 600 (30 min)	500

In **Paper III**, the cucumber leaves were treated with following MeJA concentrations: 0 (control, 5% ethanol), 0.2, 2, 5, 10, 20, and 50 mM to obtain a gradient of MeJA dose response. Thereafter, the leaves were enclosed in the glass chamber for volatile emission measurements.

For all measurements, the treated leaves were harvested at the end of the measurements, and their area (J) and the quantitative degree of visible damage was estimated using ImageJ software (National Institutes of Health, Bethesda, MD, USA).

4.4. Gas-exchange measurement (Papers I-II)

After leaf enclosure, standard measurement conditions were established and continuous measurements of photosynthetic characteristics and trace gas exchange were started immediately with CIRAS II and PTR-TOF-MS. The leaf was kept under the standard conditions until the gas exchange characteristics reached a steady state, and these steady-state values were recorded and pertinent experiment treatments (O₃ exposure or MeJA treatment) were started. The net assimilation rate and stomatal conductance to water vapour per unit enclosed leaf area were calculated according to the equations of von Caemmerer and Farquhar (1981).

4.5. Online monitoring of dynamics of plant volatiles (Papers I- III)

A high-resolution PTR-TOF-MS was used to track the volatile release at trace levels in real time. The drift tube was kept at 600 V drift voltage at 2.3 mbar drift pressure and 60 °C temperature, corresponding to an E/N ≈ 130 Td in H₃O⁺ reagent ion mode (Graus *et al.* 2010; Brilli *et al.* 2011; Portillo-Estrada *et al.* 2015). The PTR-TOF-MS system was calibrated with a calibration standard mixture containing key volatiles of different classes (Ionimed Analytic GmbH, Austria). The data acquisition

software TofDaq (Tofwerk AG, Switzerland) was used to acquire the raw data and post-processed by PTR-MS Viewer software (PTR-MS Viewer v3.1, Tofwerk AG, Switzerland) (Jordan *et al.* 2009; Portillo-Estrada *et al.* 2015). Methanol and methyl salicylate (MeSA) were detected as the protonated parent ions at m/z of 33.034 and 153.088, respectively. The total amount of LOX product emission presented in this study is the sum of the dominant compounds with mass signals m/z 81.070 [hexenal (fragment)], m/z 83.085 [hexenol + hexenal(fragments)], m/z 85.101 [hexanol (fragment)], m/z 99.080 [(*Z*)-3-hexenal + (*E*)-3-hexenal (main)], m/z 101.096 [(*Z*)-3-hexenol + (*E*)-3-hexenol + (*E*)-2-hexenol + hexenal (main)] (Brilli *et al.* 2011; Portillo-Estrada *et al.* 2015). Total monoterpene emission was characterized by the parent ion with an m/z of 137.133 and by the mass fragment with an m/z 81.070, and total sesquiterpene emission by the parent ion with an m/z 205.195.

4.6. Volatile sampling and GC-MS analyses (Paper III)

The volatiles emitted by control and MeJA treated leaves of *C. sativus* were collected onto multi-bed stainless steel adsorbent cartridges using a portable air sampling pump (210-1003MTX; SKC Inc., Houston, TX, USA). The air from the glass chamber was passed through the adsorbent cartridges for 20 min at a suction flow rate of 200 mL min⁻¹ (4 L air) for quantification of volatile LOX products, mono- and sesquiterpenes, saturated aldehydes, GGDP pathway volatiles, and aromatic volatiles. Adsorbent cartridges were analyzed with the combined Shimadzu TD20 automated cartridge desorber and a Shimadzu 2010 Plus gas-chromatograph mass-spectrometer (GC-MS; Shimadzu Corporation, Kyoto, Japan) according to (Copolovici *et al.* 2009; Kännaste *et al.* 2014). The compounds were identified by comparing their mass spectra with those of authentic standards (Sigma-Aldrich, St. Louis, MO, USA), and using NIST 05 (National Institute of Standards and Technology) library of mass spectra (Adams 2001).

4.7. Determination of trace gas emission rates (Papers I- III)

Volatile emission rates (ϕ_x , nmol m⁻² s⁻¹) were calculated as

$$\phi_x = \frac{F}{S} [C_o(X) - C_i(X) - C_c(X)] \quad (\text{Eq.1})$$

where F is the flow rate through the chamber, S is the leaf area enclosed

in the chamber (m^2), $C_o(\text{X})$ is the concentration (nmol mol^{-1}) of the target VOC (compound X) measured at the chamber outlet and $C_i(\text{X})$ of that measured at the chamber inlet, and $C_c(\text{X})$ is the correction to account for the possible release of the given compound adsorbed on the gas-exchange system components (Beauchamp *et al.* 2005; N  nemets *et al.* 2011).

The total amount of target VOC emitted over the given time period (Φ_{X}) (nmol m^{-2}) was calculated as:

$$\Phi_{\text{X}} = \sum_{t_{\text{PS}}}^{t_{\text{PE}}} \Delta t \phi_{\text{X}}$$

where t_{PS} and t_{PE} are the start and end times of the target VOC emission release, Δt is the measurement time interval (10 s), and ϕ_{X} is the emission rate of the target VOC measured over this time interval (Beauchamp *et al.* 2005). The total emission values correspond to the whole experiment, from elicitation to the end of the experiment (Fig. 1).

4.8. Quantitative characterization of elicitation of volatile emissions (Papers II-III)

The kinetics of different volatile emissions showed a similar pattern that was characterized by an exponential increase shortly after initiation of the stress treatment until the emissions reached a maximum value, followed by a non-linear decay to the baseline emission (Fig. 1). We used first order exponential rise and decay kinetics models to estimate the time kinetics and the key quantitative characteristics of emission responses upon stress (Fig. 1 for acronyms and definitions of all quantitative characteristics). The exponentially increasing part of the response was quantitatively analyzed according to:

$$\phi(t) = \phi(t_{\text{PS}}) e^{k_1(t)} , \quad (\text{Eq. 3})$$

where $\phi(t)$ is the emission rate at time t and $\phi(t_{\text{PS}})$ is the VOC emission rate measured at the start of the emission burst following the start of O_3 exposure (baseline emission). The parameter k_1 is the rate constant for the initial increase of VOC emission rate, and the corresponding doubling-time (τ_1) for the emission burst is calculated as $\ln(2)/k_1$.

The decreasing part of the emission burst was analyzed quantitatively by:

$$\phi(t) = \phi_M e^{-k_D(t)}, \quad (\text{Eq. 4})$$

where ϕ_M is the maximum VOC emission rate. Analogously, the parameter k_D is the rate constant for the decrease of VOC emission rate, and the corresponding half-time (τ_D) for the emission burst is calculated as $\ln(2)/k_D$. Figure 1 shows VOC emission kinetics of this study, as well as the definition of key quantitative emission characteristics used above. When a second emission burst was present, the decay and rise characteristics for this second rise of emissions were also calculated (Fig. 1).

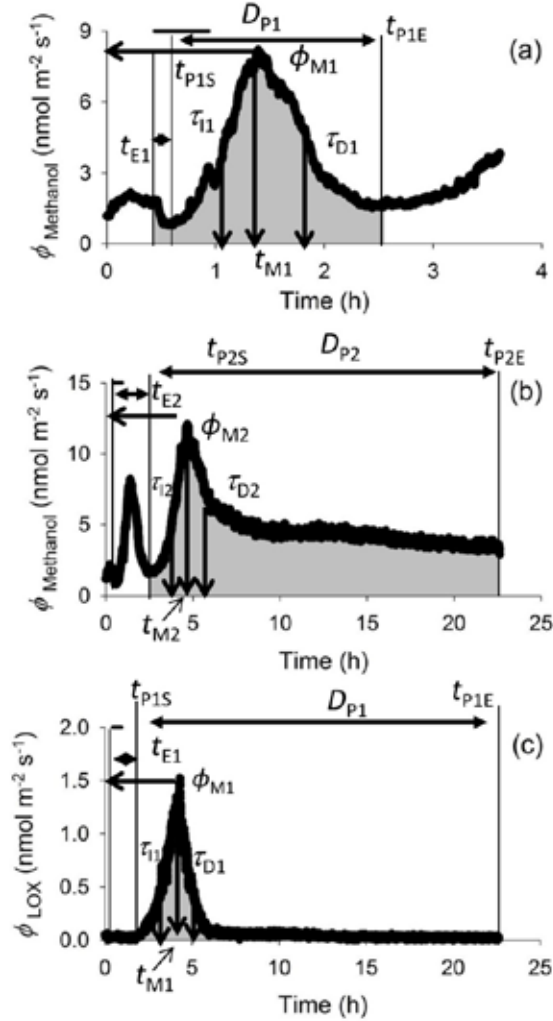


Figure 1. Representative time-courses of O_3 induced methanol and LOX volatile emissions from *Phaseolus vulgaris*, and definition of key variables characterizing the induction response (see Definitions of symbols) (**Papers II-III**).

4.9. Calculation of O₃ uptake (Papers I-II)

The rate of O₃ uptake by the leaf (ϕ_{LO_3} , nmol m⁻² s⁻¹) was calculated as:

$$\phi_{\text{LO}_3} = \frac{F}{S} (C_{\text{in}} - C_{\text{out}} - C_{\text{O}_3}^{\text{chamber}}) \quad (\text{Eq. 5})$$

where C_{in} and C_{out} are the O₃ concentrations in the air entering and exiting the leaf chamber (nmol mol⁻¹), $C_{\text{O}_3}^{\text{chamber}}$ is O₃ destruction due to surface reactions (“uptake”) by the empty chamber. We calculated C_{in} and C_{out} as the average value over a given time interval due to the fluctuations of concentration produced by the ozone generator and manual adjustment of C_{in} to account for changes in O₃ uptake during the exposure.

The rate of O₃ uptake by stomata (ϕ_{GO_3} , nmol m⁻² s⁻¹) was determined by:

$$\phi_{\text{GO}_3} = (C_{\text{out}} - C_{\text{O}_3}^i) \frac{g_s}{2.03} \quad (\text{Eq. 6})$$

where $C_{\text{O}_3}^i$ is intercellular O₃ concentration (nmol mol⁻¹), and 2.03 is the ratio of water vapor to O₃ diffusivities estimated from O₃ diffusion coefficient in air (Ivanov *et al.* 2007) and water vapour diffusion coefficient according to Chapman and Enskog theory (Niinemets and Reichstein 2003). $C_{\text{O}_3}^i$ was assumed to be zero (Laisk *et al.*, 1989; Moldau and Bichele, 2002). To be consistent with the C_{out} calculations, stomatal conductance (g_s) estimated across the O₃ exposure period.

The total amount of leaf and stomatal O₃ uptake (Φ_Y , where Y stands for either leaf, LO₃, or stomatal, GO₃, O₃ uptake) over the given exposure period (O₃ dose) was determined as:

$$\Phi_Y = \sum_{t_s}^{t_E} \Delta t \phi_Y \quad (\text{Eq. 7})$$

where t_s and t_E are the start and end times of O₃ exposure, Δt is the time interval of the O₃ exposure, and ϕ_Y is either the mean rate of ϕ_{LO_3} or the mean rate of ϕ_{GO_3} measured during this time interval (Beauchamp *et al.* 2005). Ultimately, the total amount of non-stomatal O₃ deposition (Φ_{NGO_3}), i.e. O₃ uptake by the leaf surface referred as non-stomatal O₃ deposition was calculated as:

$$\Phi_{\text{NGO}_3} = \Phi_{\text{LO}_3} - \Phi_{\text{GO}_3} \quad (\text{Eq. 8})$$

where Φ_{LO_3} is the total amount of O_3 uptake by the whole leaf and Φ_{GO_3} is the stomatal O_3 uptake.

4.10. Quantitative characterization of the protective role of glandular trichomes against O_3 stress (Paper I)

The plant response per unit O_3 taken up by the leaf or stomata (γ) was calculated as:

$$\Phi_Z/\Phi_Y = Z/\Phi_Y \quad (\text{Eq. 9})$$

where Z represents the percentage decrease (relative to the non-treated situation) of net assimilation rate, stomatal conductance and F_v/F_m or the total amount or maximum rate of LOX products emitted over a certain time.

4.11. Chlorophyll fluorescence measurements (Papers I-II)

To assess the activity of photosystem II (PS II) in the leaves before and after the O_3 treatment, a portable Imaging PAM chlorophyll fluorimeter and ImagingWin software (IMAG-MIN/B, Heinz Walz GmbH, Effeltrich, Germany) were used. After the leaf was fixed in the Imaging PAM, the leaf was dark-adapted for 30 min and then, minimum (F_o) fluorescence yield was measured. The leaf was further illuminated with a 500 ms pulse of saturating irradiance ($2700 \mu\text{mol quanta m}^{-2} \text{s}^{-1}$) to measure the maximum (F_m) dark-adapted fluorescence yield. The spatial-average maximum dark-adapted quantum yield of PSII, F_v/F_m was calculated as $(F_m - F_o)/F_m$.

4.12. Scanning electron microscopy analyses of density and morphology of leaf trichomes (Paper I)

We used a Zeiss EVO LS15 Environmental Scanning Electron Microscope (ESEM, Carl Zeiss AG, Jena, Germany) to study the trichome morphological characteristics. The fresh leaf adjacent to the leaf used for O_3 fumigation was sampled and viewed with a Zeiss ESEM at an acceleration voltage of 15 kV under the low vacuum mode. Images acquired from ESEM were analyzed with the Image J software. We estimated trichome

density from the middle zones of both leaf surfaces (adaxial and abaxial) avoiding major veins. The peltate or capitate glandular trichomes were identified as suggested by Ascensão and Pais (1998), Ko *et al.* (2007) and Baran *et al.* (2010).

5. RESULTS

5.1. Effect of acute O₃ treatments on visible leaf damage and leaf physiological characteristics (Papers I-II)

Stepwise increase of O₃ concentration during fumigation led to severe visible leaf injuries, and reductions in net assimilation rate, stomatal conductance to water vapour and the maximum dark-adapted quantum yield of photosystem II (PSII) (F_v/F_m) in species studied in **Paper I**. However, only the amount of stomatal and leaf O₃ uptake were strongly correlated with the amount of visible leaf damage (Fig. 8c and S3c in **Paper I**).

Leaves of *P. vulgaris* treated with O₃ showed severe visible leaf injury (Fig. 2a in **Paper II**) and remarkable reductions in leaf physiological activity including reductions in net assimilation rate, stomatal conductance to water vapour and the maximum dark-adapted photosystem II (PSII) quantum yield (F_v/F_m) (Fig. 2a and b). However, changes in leaf physiological activity depended on the exposure conditions, dark vs. light exposure, priming with low O₃ vs. immediated acute exposure (Fig. 2b). In addition, both stomatal O₃ uptake and the total amount of O₃ taken up by the leaves were strongly determined by stomatal conductance (Fig. 3 in **Paper II**) and a strong relationship was found between the accumulated stomatal O₃ uptake for the exposure period and the percentage of leaf area damaged (Fig. 2b in **Paper II**).

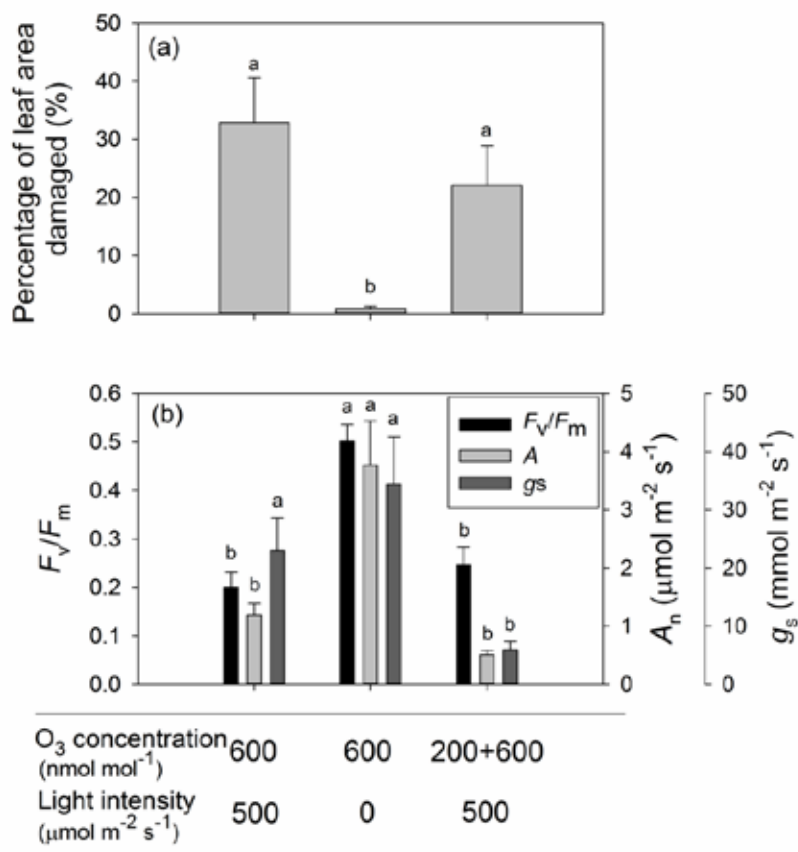


Figure 2. Percentage of leaf area damaged (a) and leaf physiological characteristics (the maximum dark-adapted photosystem II (PSII) quantum yield, F_v/F_m ; net assimilation rate, A_n ; stomatal conductance, g_s) in *P. vulgaris* leaves at 21 h after O_3 fumigation (b). The error bars indicate $\pm SE$ (reproduced from **Paper II**).

5.2. Elicitation of VOCs caused by O_3 and MeJA treatments (Papers I-III)

In **Paper I**, PTR-TOF-MS measurements were carried out in six species grown from seed and raised in an indoor growth facility (Table 1). All species included in this experiment were poor emitters of VOCs under non-stressed conditions. Leaf LOX product emission was significantly induced in response to the stepwise increase in O_3 treatments in all studied species (Fig. 8e and f in **Paper I**).

The release of plant stress volatiles such as methanol, LOX products and MeSA was highly enhanced in *P. vulgaris* by 600 $nmol\ mol^{-1}$ O_3 fumigation

under illumination and darkness (Fig. 4 in **Paper II**). However, MeSA emission was inhibited by pre-exposure of leaves to lower O₃ concentration of 200 nmol mol⁻¹ (Fig. 4c in **Paper II**).

Leaves of *C. sativus* treated with MeJA exhibited a rapid emission burst of methanol and classic LOX products, (*Z*)-3-hexen-1-ol, 3-hexenyl acetate, and *n*-hexanal (Fig.2 and Table 2 in **Paper III**). Mono- and sesquiterpene emissions were not significantly enhanced immediately after MeJA treatments, but limonene and Δ^3 -carene emissions were enhanced since 10 h after application of MeJA treatments (Table 2 in **Paper III**). In addition, emissions of the monoterpene linalool, and sesquiterpenes β -farnesene, α -cedrene, and β -caryophyllene were also identified at 10 h after the treatment with 10 mM and 20 mM MeJA (Table 2 in **Paper III**). In general, quantitative stress dose vs. emission relationships were observed during the recovery phase (Table 2 in **Paper III**).

5.3. Trichome morphology, distribution and density (**Paper I**)

Non-glandular trichomes with branched or unbranched structures were found on the leaf surfaces of the 24 studied species. Non-glandular trichome density greatly varied among species (Fig. 3; Table 1 in **Paper I**). Two types of glandular trichomes were identified in this study: peltate and capitate (Fig. 3). Capitate glandular trichomes were found in all species with density ranging from 1 mm⁻² in *C. pepo* to 90 mm⁻² in *R. officinalis*, but peltate glandular trichomes were present only in 12 species belonging to the family Lamiaceae (*O. basilicum*, *L. angustifolia*, *M. piperita*, *S. officinalis* and *R. officinalis*) and Geraniaceae (*E. cicutarium*, *G. pratense* and *G. robertianum*) and in *B. pendula*, *E. canadensis*, *S. latifolia* and *U. dioica* with density ranging from 5.9 mm⁻² in *G. robertianum* to 60 mm⁻² in *R. officinalis* (Table 1 in **Paper I**).

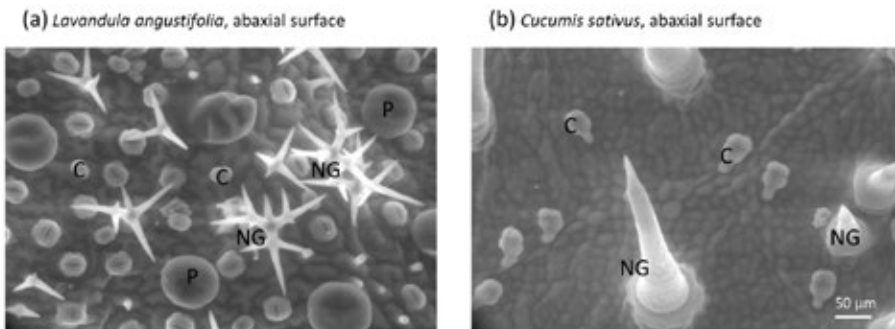


Figure 3. Environmental scanning electron microscope (ESEM) micrographs of (a) non-glandular (NG) and peltate (P) and capitate (C) glandular trichomes on the lower surface of *L. angustifolia* and (b) lower surface of *C. sativus* containing non-glandular (NG) and glandular capitate trichomes (C). Scale bars are shown in the bottom right (reproduced from **Paper I**).

5.4. The relationships between non-stomatal O_3 deposition and trichome types and density (**Paper I**)

The percentage of non-stomatal O_3 deposition was not correlated with the density of non-glandular trichomes (Fig. 3a in **Paper I**), however, it was positively correlated with the density of glandular trichomes (Fig. 4a). In fact, this positive correlation was also found across species possessing only capitate trichomes, and both capitate and peltate trichomes (Fig. 4b).

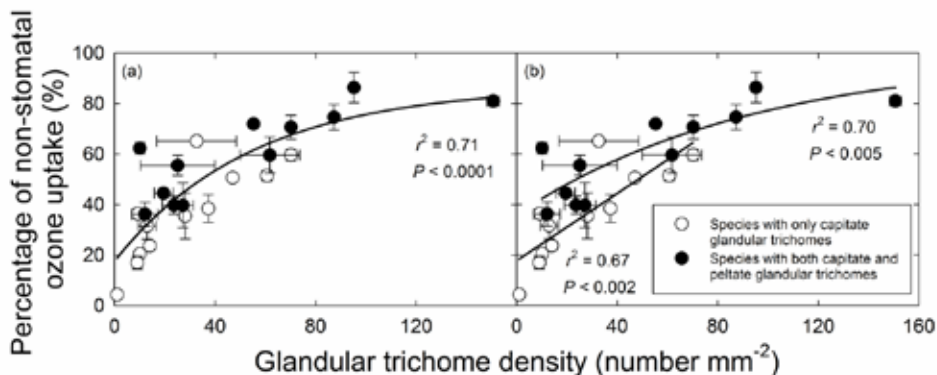


Figure 4. Relationships between the percentage of non-stomatal O_3 uptake and glandular trichome density (a), and percentage of non-stomatal O_3 uptake and glandular trichome density in species with capitate, and both capitate and peltate trichomes (b). In all cases, open symbols represent species with only capitate glandular trichomes and filled symbols represent species with both capitate and peltate glandular trichomes. The error bars indicate $\pm SE$. The glandular trichome density is shown in Table 1 in **Paper I** (reproduced from **Paper I**).

5.5. Changes in physiological characteristics and LOX product emissions in response to O₃ exposure in relation to glandular trichome density (Paper I)

The threshold minimum value of accumulated O₃ uptake causing acute response was determined to characterize O₃ dose effects on the photosynthetic characteristics and LOX product emissions. Glandular trichome density was significantly correlated with the threshold value of total leaf O₃ uptake, leading to decrease in net assimilation rate and stomatal conductance (Fig. 4a and c in **Paper I**). However, glandular trichome density was not correlated with the threshold value of total stomatal O₃ uptake (Fig. 4b and d in **Paper I**). In the case of LOX product emissions, only a weak correlation was observed with threshold of total leaf O₃ uptake, but there was no significant correlation with the threshold of total stomatal O₃ uptake (Fig. 4e and f in **Paper I**).

O₃-induced percentage reduction of net assimilation rate and stomatal conductance were negatively correlated with glandular trichome density (Fig. 5a and b). Less visible leaf damage was found in species with greater glandular trichome density under same amount of O₃ uptake by a leaf (Fig. 5c). The percentage reduction of F_v/F_m per ppb O₃ taken up by leaf was not correlated with glandular trichome density (Fig. 5d). In addition, no significant correlations were observed between glandular trichome density and absolute reduction of net assimilation rate, stomatal conductance and F_v/F_m , and percentage of visible leaf injury under same amount of stomatal O₃ uptake (Fig. S2a-d in **Paper I**).

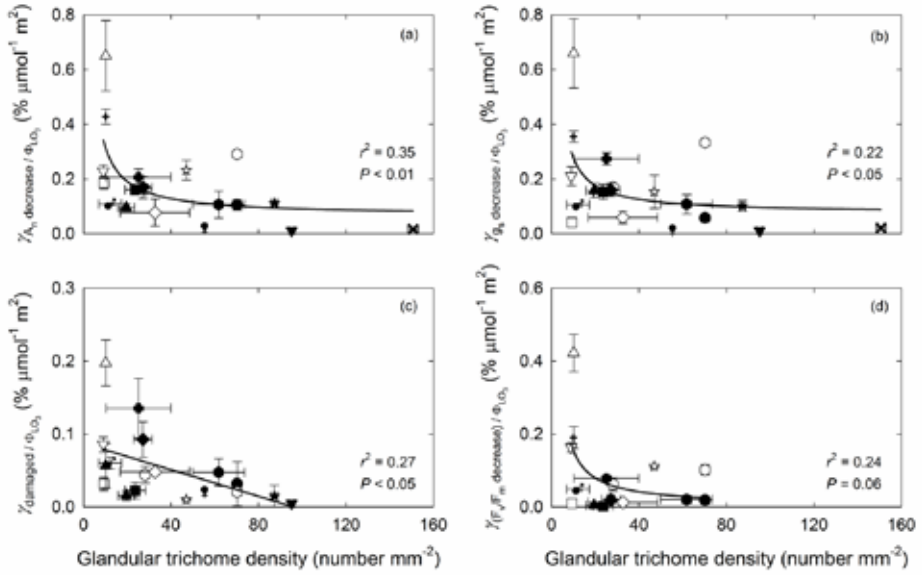


Figure 5. (a) The percentage decrease in net assimilation rate, (b) the percentage decrease in stomatal conductance, (c) the percentage of leaf area visibly damaged and (d) the percentage decrease in the dark-adapted maximum quantum efficiency of PSII (F_v/F_m) per unit leaf O_3 uptake in relation to glandular trichome density in *B. pendula* (filled circles, ●), *C. sativus* (open circles, ○), *E. acer* (open squares, □), *E. canadensis* (filled squares, ■), *E. cicutarium* (filled diamonds, ◆), *G. palustre* (open diamonds, ◇), *G. pratense* (filled hexagons, ●), *G. robertianum* (filled upward pointing triangles, ▲), *L. angustifolia* (filled downward pointing triangles, ▼), *M. × piperita* (filled stars, ★), *N. tabacum* (open hexagons, ○), *O. basilicum* (filled plus symbols, +), *P. vulgaris* (open upward pointing triangles, △), *R. officinalis* (filled crosses, ×), *S. officinalis* (filled Venus symbols, ♀), *S. latifolia* (filled Mars symbols, ♂), *S. lycopersicum* (open downward pointing triangles, ▽), *U. dioica* (filled Christian crosses, +), *V. thapsus* (open stars, ☆). In all cases, open symbols represent species with only capitate glandular trichomes and filled symbols species with both capitate and peltate glandular trichomes. The error bars indicate \pm SE (reproduced from **Paper I**).

In the case of total leaf O_3 uptake and stomatal O_3 uptake, glandular trichome density was negatively correlated with the total amount and maximum value of per ppb O_3 -induced LOX product emissions burst, and the correlations were non-linear (Fig. 6a, b; Fig. S2e and f in **Paper I**).

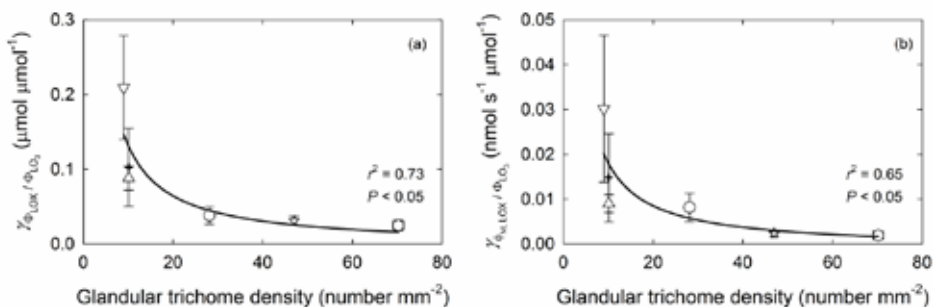


Figure 6. (a) The induction of total amount of LOX product emission and (b) the maximum rate of induced LOX product emission per unit leaf O_3 uptake in relation to glandular trichome density. Symbols are as defined in Fig. 5. The error bars indicate \pm SE (reproduced from **Paper I**).

Across species, both leaf O_3 uptake and stomatal O_3 uptake were not correlated with the percent decrease in net assimilation rate, stomatal conductance and F_v/F_m , but they were positively correlated with the percentage of leaf area visibly damaged (Fig. 8 and S3 in **Paper I**). Furthermore, both total leaf O_3 uptake and stomatal O_3 uptake were strongly correlated with the total LOX product emission and maximum LOX product emission rates (Fig. 8 and S3 in **Paper I**). However, non-stomatal O_3 uptake showed nonsignificant correlations with the percent decrease in net assimilation rate, stomatal conductance and F_v/F_m , amount of visible leaf damage and LOX product emissions (Fig. S4 in **Paper I**). In addition, percentage of non-stomatal O_3 uptake showed negative correlations with the percent decrease in F_v/F_m and nonsignificant correlations with the percent decrease in net assimilation rate and stomatal conductance, amount of visible leaf damage and LOX product emissions (Fig. S5 in **Paper I**).

5.6. Time courses of emissions of methanol, LOX products, MeSA, and mono and sesquiterpenes upon acute O_3 and MeJA treatments (**Papers II-III**)

In general, all O_3 -induced volatile emissions in *P. vulgaris* exhibited a sigmoidal rise to a peak value and then, decayed to near pre-fumigation values. Specifically, temporal emissions induced by O_3 fumigation were either biphasic with two maxima (methanol) or monophasic (LOX products and MeSA) (Fig. 4 in **Paper II**). A few minutes after the onset of acute O_3 fumigation ($600 \text{ nmol mol}^{-1}$, but not $200 \text{ nmol mol}^{-1}$) methanol emissions began to increase, peaking shortly after fumigation ended and

then rapidly declined. A second, much larger, burst of methanol emissions were observed 1-2 hours since O_3 fumigation and peaked several hours later. When the fumigation was carried out in the light (Fig. 4a, c, d and f in **Paper II**), methanol emissions began to fall rapidly (within 10 min) shortly after fumigation was ceased. When O_3 fumigation occurred in darkness (Fig. 4b and e in **Paper II**), similar to the situation in illuminated leaves, methanol emissions slightly increased upon the onset of fumigation. As with the illuminated leaves, when the fumigation period ended, methanol emissions levelled off. However, in contrast to illuminated leaves, the emissions remained constant in the dark for an additional 15 minutes. When the leaf was then illuminated, a second short burst of methanol emissions was observed, perhaps associated with rapid stomatal opening (Fig. 4e in **Paper II**). The induction of methanol emissions was less pronounced in the leaves exposed to a lower O_3 concentration of 200 nmol mol⁻¹, (Fig. 4f in **Paper II**). However, methanol emissions increased rapidly when the O_3 dosage was raised to 600 nmol mol⁻¹. In all cases, the second burst of methanol emission after O_3 treatments was larger and lasted longer.

In all cases, the exposure of *P. vulgaris* leaves to O_3 resulted in a single large burst of LOX product emissions starting 1-2 h since O_3 exposure and lasting for several hours. The burst of MeSA emissions showed similar pattern in leaves exposed to 600 nmol mol⁻¹ O_3 under illumination and in darkness, but it was not always found when the leaves were pre-exposed to 200 nmol mol⁻¹ O_3 (Fig. 4 in **Paper II**)

For MeJA-treated *C. sativus* leaves, the emission time courses were either biphasic with two maxima (LOX products; Fig. 2A and B in **Paper III**) or monophasic (monoterpenes, sesquiterpenes, and methanol; Fig. 2C and D in **Paper III**). An instant LOX volatile emission burst was elicited immediately after MeJA treatment and reached a maximum value in ~0.2–1 h. Then, it was followed by a slower burst elicited in 6–10 h after MeJA treatment, this second burst reached its maximum level in ~16–20 h (Fig. 2A and B in **Paper III**). In the case of mono- and sesquiterpenes, the emissions started in 2–6 h after MeJA treatments and reached a maximum value in ~15–25 h (Fig. 2C in **Paper III**). Methanol emissions started almost immediately after MeJA treatments, and reached a maximum value in ~0.5–1.5 h after the treatments (Fig. 2D in **Paper III**).

5.7. Maximum and total integrated O₃- and MeJA-elicited volatile emissions (Papers II-III)

The maximum emission rates of the first methanol emission burst were significantly greater in *P. vulgaris* leaves exposed to 600 nmol mol⁻¹ O₃ under illumination, followed by 200 + 600 nmol mol⁻¹ O₃ treatment under illumination, and 600 nmol mol⁻¹ O₃ treatment in darkness (Fig. 7a). A strong non-linear relationship was found between the total amount of O₃ uptake and the maximum emission rates of the first methanol burst (Fig. 5d in **Paper II**). In contrast, the maximum methanol emission rate of the second emission burst in leaves exposed to O₃ under illumination was significantly higher than that in leaves treated in darkness (Fig. 7a). In addition, the correlation between the total amount of O₃ taken up and the maximum emission rates of the second methanol emission burst was linear (Fig. 5d in **Paper II**). The leaves exposed to 600 nmol mol⁻¹ O₃ under illumination exhibited significantly higher maximum emission rates of LOX products than the leaves in the other two treatments (Fig. 7b). The maximum emission rate of LOX products was strongly and non-linearly correlated with total stomatal O₃ uptake (Fig. 5e in **Paper II**). However, there was no statistically significant difference in the maximum emission rate of MeSA among the leaves exposed to 600 nmol mol⁻¹ O₃ under illumination and in darkness (Fig. 7c). Furthermore, no MeSA emission was detected in leaves first exposed to 200 nmol mol⁻¹ O₃ prior to the exposure to 600 nmol mol⁻¹ O₃ (Fig. 7c).

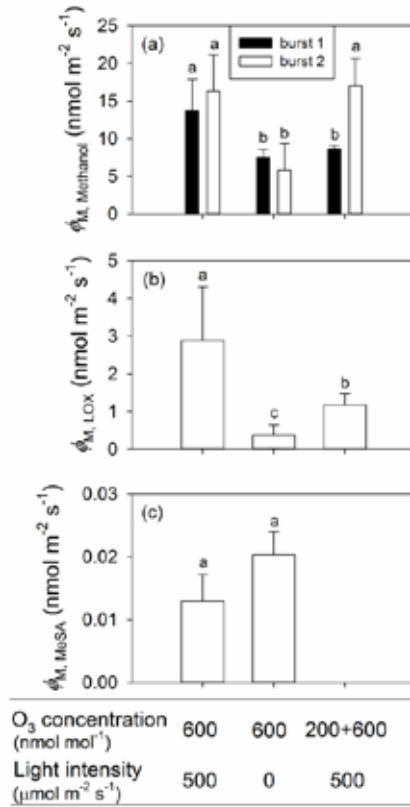


Figure 7. Maximum emission rates of methanol (a), LOX products (b) and MeSA (c) in O₃-exposed *P. vulgaris* leaves. The error bars indicate \pm SE (reproduced from **Paper II**).

The total amount of the first methanol emission burst was significantly higher in *P. vulgaris* leaves exposed to O₃ under illumination than in darkness, and its relationship with total O₃ uptake was linear (Fig. 6a and 9a in **Paper II**). Treatment differences in the total amount of the second methanol emission burst, LOX products and MeSA emissions were similar to differences in the maximum emission rates, and the correlations of these traits with total stomatal O₃ uptake were also similar with the correlations between total stomatal O₃ uptake and the maximum emission rates (Fig. 6c and d, Fig. 9a and b in **Paper II**).

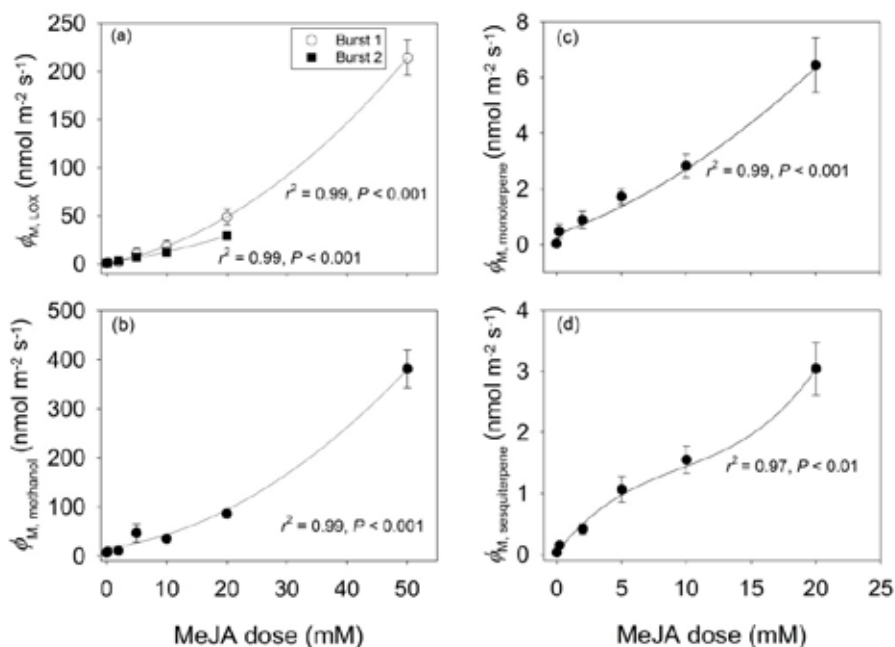


Figure 8. Maximum emission rates of LOX products (a), methanol (b) and mono- (c) and sesquiterpenes (d) in MeJA-treated *C. sativus* leaves. The error bars indicate \pm SE (reproduced from **Paper III**).

In MeJA-treated *C. sativus* leaves, both the maximum emission rate and the total integrated emissions of the volatile bursts scaled positively with the MeJA doses for both the faster and the slower MeJA responses (Fig. 8; Fig. 4 in **Paper III**). Non-linear correlations between the maximum emission rates of volatiles and MeJA concentration implied that the increases of the maximum emission rates were greater at higher MeJA concentrations of 10 to 50 mM (Fig. 8). For total integrated emission versus MeJA concentration relationships, the non-linearity of relationship was observed between the maximum emission rate and MeJA doses (Fig. 8; Fig. 4 in **Paper III**). In addition, both the emission maxima and total emissions scaled positively with the degree or leaf damage (insets in Fig. 3 and 4 in **Paper III**).

5.8. Kinetics of foliage volatile emissions from *P. vulgaris* and *C. sativus* upon different O₃ and MeJA treatments (Papers II-III)

The initial burst of methanol emissions began within about 10 minutes following the onset of O₃ exposure in all cases, but the second emission burst occurred earlier in leaves exposed to 600 nmol mol⁻¹ O₃ under illumination and in darkness than in leaves exposed to 200 nmol mol⁻¹ O₃ prior to the exposure to 600 nmol mol⁻¹ O₃ (Fig. 7a in **Paper II**). The burst of LOX products after the onset of O₃ fumigation occurred earlier in leaves exposed to 600 nmol mol⁻¹ O₃ under illumination than in leaves treated with 200 + 600 nmol mol⁻¹ O₃ under illumination, and 600 nmol mol⁻¹ O₃ in darkness (Fig. 7b in **Paper II**). In contrast, MeSA emission bursts occurred earlier in leaves exposed to 600 nmol mol⁻¹ O₃ in darkness than under illumination (Fig. 7c in **Paper II**).

The time from the onset of elicitation to the first methanol emission peak was significantly lower in leaves exposed to 600 nmol mol⁻¹ O₃ under illumination, but there was no statistically significant difference in the time from the onset of elicitation to the second methanol peak in all cases (Fig. 7d in **Paper II**). In contrast to the temporal kinetics of methanol emission in different O₃ treatments, the time from the onset of elicitation to the peak in emissions of LOX products was significantly greater in leaves exposed to O₃ under illumination than in darkness (Fig. 7e in **Paper II**). However, once elicited there was no statistically significant differences in the time from the onset of elicitation to the peak of MeSA emissions in different treatments (Fig. 7f in **Paper II**). Furthermore, the times from the onset of elicitation to the first methanol emission peak and to LOX emission peak were nonlinearly correlated with total amount of stomatal O₃ uptake (Fig. 9 c and d in **Paper II**).

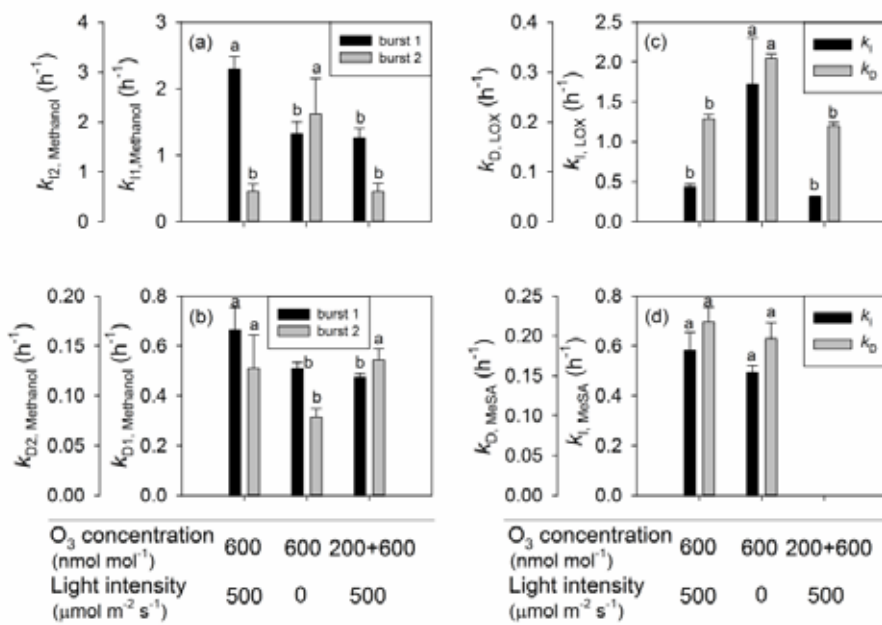


Figure 9. The rate constant for the initial increase for the first and the second emission burst of methanol (a), LOX products (c) and MeSA (d) and the rate constant for the decrease for the first and the second emission burst of methanol (b), LOX products (c) and MeSA (d) for three treatments in O_3 -exposed *P. vulgaris* leaves. The error bars indicate \pm SE (Paper II).

To further characterize the impact of O_3 on volatile emission kinetics, the induction (k_i , Eq. 3) and decay (k_d , Eq. 4) rate constants were determined. In fact, both the initial enhancement and decline in the first burst of methanol emission responses were faster in leaves exposed to 600 nmol mol⁻¹ O_3 under illumination than in leaves treated with 200 + 600 nmol mol⁻¹ O_3 under illumination, and 600 nmol mol⁻¹ O_3 in darkness (Fig. 9a and b). For the second burst of methanol, the initial enhancement of emissions was faster and the decline was slower in leaves exposed to O_3 in darkness than in those treated with O_3 under illumination (Fig. 9a and b). Similarly, both the rise and decay kinetics were much faster for the LOX product emissions in *P. vulgaris* leaves exposed to O_3 in darkness than that in leaves treated illumination (Fig. 9c). However, there were no statistically significant differences in either k_i or k_d of MeSA emissions in the leaves treated with O_3 (Fig. 9d).

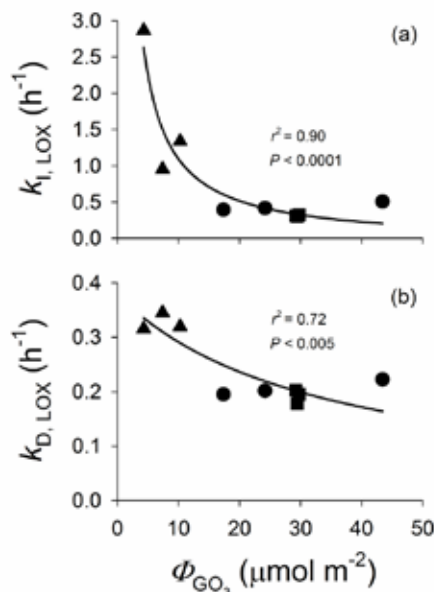


Figure 10. Correlation of the rate constant for the initial increase (a) and decrease (b) for the LOX products with the total amount of stomatal O₃ uptake (Φ) in O₃-exposed leaves of *P. vulgaris*. The filled circles (●) denote illuminated leaves fumigated with 600 nmol mol^{-1} O₃ for 30 min, the filled upward pointing triangles (▲) denote the leaves exposed to 600 nmol mol^{-1} O₃ for 30 min in darkness, and the filled squares (■) denote the illuminated leaves exposed first to 200 nmol mol^{-1} O₃ for 30 min and then to 600 nmol mol^{-1} O₃ for additional 30 min (reproduced from **Paper II**).

The rate constants for the initial increase (k_i , Fig. 10a) and decrease (k_d , Fig. 10b) for LOX product emission were negatively correlated with the amount of stomatal O₃ uptake. In addition, the rate constant for the initial increase for the second methanol emission burst was negatively correlated with the amount of stomatal O₃ uptake (Fig. 9e in **Paper II**), but the rate constant for the initial decrease for the second methanol emission burst was positively correlated with the amount of stomatal O₃ uptake (Fig. 9g in **Paper II**).

MeJA concentration significantly affected the timing of volatile emission responses from the leaves of *C. sativus*. The times to the maxima of the first and the second LOX emission bursts were negatively correlated with MeJA concentration, indicating that the maxima of LOX emission bursts occurred earlier at higher MeJA concentration (Fig. 5B in **Paper III**). In contrast, the maximum emission for the methanol emission burst occurred later at a higher MeJA concentration (Fig. 5C in **Paper III**). Similarly to LOX, the maxima of mono- and sesquiterpene emissions also occurred

earlier at higher MeJA concentrations, and this dose response was stronger for monoterpenes (Fig. 5D in **Paper III**).

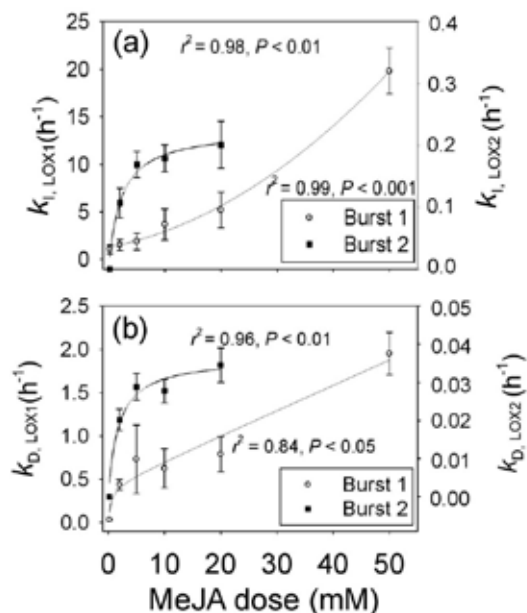


Figure 11. First-order rate constants for the initial rise (k_i ; a) and decline (k_d ; a) of the first ($k_{i, LOX1}$ and $k_{d, LOX1}$) and the second ($k_{i, LOX2}$ and $k_{d, LOX2}$) emission burst of LOX volatiles in relation to MeJA concentration in *C. sativus* leaves. The error bars indicate \pm SE (reproduced from **Paper III**).

Both the initial rise and decline of emissions were faster at higher MeJA concentrations for LOX compounds (Fig. 11a and b) and terpenoids (Fig. 7A and B in **Paper III**). However, both the rise and decline kinetics were much faster for the first LOX emission burst than for the second emission burst (Fig. 11a and b). The induction and decay rates were similar for mono- and sesquiterpenes, except for the response to the lowest MeJA treatment of 0.2 mM that barely induced sesquiterpene release (Fig. 7A and B in **Paper III**). For methanol, the rate constants k_i and k_d initially decreased over the MeJA concentration range of 0.2–5 mM, and they were weakly affected by MeJA concentrations >5 mM (Fig. 6C in **Paper III**). The duration of the emission burst increased with increasing MeJA concentration for all other compound classes (Fig 6D and 7C in **Paper III**), except for the first LOX volatiles (Fig. 6D in **Paper III**). In the case of the early LOX volatile release, the duration of the burst decreased between 2mM and 5 mM MeJA, and was thereafter invariable (Fig. 6D in **Paper III**).

6. DISCUSSION

6.1. Impact of non-stomatal O₃ deposition rates, and type and density of trichomes on stomatal O₃ uptake rates

Past studies have demonstrated that the interspecific variation in O₃ sensitivity among plant species can be significantly linked to leaf structure (e.g., leaf mass per unit area, LMA), leaf nitrogen concentration and life form (Franzaring *et al.* 1999; Hayes *et al.* 2007; Li *et al.* 2016). However, plant responses to acute O₃ exposure can quantitatively and qualitatively differ from the responses to chronic low to moderate level O₃ exposures (Heiden *et al.* 1999; Beauchamp *et al.* 2005; Calfapietra *et al.* 2013). Generally, as in our study (**Papers I and II**), stomatal O₃ uptake significantly drives the overall physiological changes (Beauchamp *et al.* 2005; Jud *et al.* 2016). Stomatal O₃ uptake can be affected by both stomatal conductance and the presence of glandular trichomes on leaf surface (Kollist *et al.* 2007; Fares *et al.* 2010b, 2013a, 2014; Jud *et al.* 2016). For example, Jud *et al.* (2016) reported that the glandular trichomes of *Nicotiana tabacum* play an important role in reducing stomatal O₃ uptake because a significant fraction of O₃ is scavenged on the leaf surface, thereby reducing the quantity of O₃ entering intercellular airspaces.

Both non-glandular and glandular trichomes are widely distributed on leaf surfaces and their density varied greatly among the 24 plant species studied (**Paper I**). As outlined in **2.1.2**, non-glandular trichomes mainly serve as a mechanical barrier against herbivore and pathogen attack (Corsi and Bottega 1999; Werker 2000; Glas *et al.* 2012), but little is known about their role as antioxidants against oxidative stress. In this study, we found that non-glandular trichome density was not correlated with the quantity of non-stomatal O₃ uptake (Fig. 3a in **Paper I**). This was consistent with the fact that non-glandular trichomes do not produce phytochemicals and are covered by a wax layer that has a low reactivity to O₃ (Corsi and Bottega 1999).

Although different types of trichomes produce different classes of secondary metabolites, high glandular trichome density is often associated with the enhanced emission of terpenoids and other defensive compounds (Gang *et al.* 2001; Amme *et al.* 2005). In our study, both capitate and peltate glandular trichome densities were strongly correlated with non-stomatal

O₃ uptake, reflecting the circumstance that the highly reactive chemical compounds may be synthesized in different types of glandular trichomes. Furthermore, our data indicated that the non-stomatal O₃ deposition contributed to more than 20% of total O₃ uptake by the leaves in most cases, consistent with the past observations in tobacco (Jud *et al.* 2016). This evidence indicates that higher O₃ depletion capacity of the leaf surfaces in certain plant species can reduce stomatal O₃ uptake. However, various reactive compounds are secreted and exuded from different types of glandular trichomes and the variation in trichome density may explain why O₃ sensitivity varies among plant species. However, the formation of glandular trichomes and their chemical composition can be significantly influenced by environmental factors such as humidity and water availability, implying the protective mechanism by glandular trichomes is a highly adaptive trait (Prozherina *et al.* 2003; Lihavainen *et al.* 2017).

In this thesis, I also investigated the O₃ depletion capacity of *P. vulgaris* under dark and light conditions. In fact, stomatal O₃ uptake rate by leaves exposed to 600 nmol mol⁻¹ O₃ under illumination was significantly higher than that in darkness, indicating that stomatal conductance plays a crucial role in regulating stomatal O₃ uptake rate (Fig. 3 in **Paper II**). In addition, stomatal conductance was often modified by pre-exposure to lower O₃ concentrations because the pre-exposure induced partial stomatal closure. This can be significant in field conditions, for example, pre-exposure of plants to O₃ in the morning can enhance stomatal closure and thus, reduce O₃ uptake rate during the rest of the day when ambient O₃ concentrations are higher (Nolle *et al.* 2002; Ribas and Peñuelas 2004; Xu *et al.* 2008).

6.2. Impact of elevated O₃ on foliage photosynthetic characteristics

O₃-induced reduction in net assimilation rate in exposed leaves is often associated with a decline in stomatal conductance and a reduced Rubisco activity (Fiscus *et al.* 2005). *Phaseolus vulgaris* leaves in darkness had a lower stomatal conductance and this resulted in lower stomatal O₃ uptake upon O₃ fumigation. In turn, this was associated with a minor degree of foliage visible injury and a moderate reduction in photosynthetic characteristics (Fig. 2 and 3 in **Paper II**), confirming the key role of stomatal conductance in controlling leaf damage under O₃ stress. Despite *P. vulgaris* leaves pre-exposed to the lower concentration of 200 nmol mol⁻¹ O₃ for 30

min under illumination followed by exposure to 600 nmol mol⁻¹ O₃ for additional 30 min had a lower stomatal conductance, the total O₃ uptake through stomata, and the degree of ultimate leaf damage were similar to leaves exposed to only 600 nmol mol⁻¹ for 30 min under illumination (Fig. 3 in **Paper II**). This non-significant difference suggested that the cumulative stress resulting from exposures to both 200 and 600 nmol mol⁻¹ was almost equivalent to the stress resulting from 600 nmol mol⁻¹ treatment alone, further underscoring that O₃ impacts foliage photosynthetic characteristics in a dose-dependent manner. Weak correlations between stomatal O₃ uptake rate and reductions in net assimilation, stomatal conductance and F_v/F_m were found across species (**Paper I**), suggesting that plant response to O₃ is a complex process which involving several biological levels.

6.3. Emission of VOCs upon acute O₃ and MeJA treatments in *P. vulgaris* and *C. sativus*

Abiotic stresses including temperature, mechanical damage and O₃ exposure typically induce the release of plant stress volatiles such as methanol, LOX products and MeSA (Heiden *et al.* 1999; Beauchamp *et al.* 2005; Copolovici and Niinemets 2010; Loreto and Schnitzler 2010; Niinemets 2010a; Peñuelas and Staudt 2010; Brilli *et al.* 2011; Copolovici *et al.* 2012, 2014; Portillo-Estrada *et al.* 2015; Pazouki *et al.* 2016). O₃ exposure resulted in multiphasic methanol emissions and monophasic LOX and MeSA emissions from *P. vulgaris* leaves during and after O₃ exposure, consistent with the past observations in *N. tabacum* (Beauchamp *et al.* 2005). However, higher methanol emissions were induced immediately after *P. vulgaris* leaves were treated with 200 nmolmol⁻¹ and 600 nmol mol⁻¹ O₃ in our study (Fig. 4 in **Paper II**), while in *N. tabacum*, methanol emissions were observed at 1-2 hours after 500 nmol mol⁻¹ O₃ fumigation in the study of Beauchamp *et al.* (2005), suggesting that *N. tabacum* is more tolerant to O₃ than *P. vulgaris*.

The release of methanol and LOX volatiles upon O₃ exposure was found in all cases (Fig. 4 in **Paper II**). Methanol release, which is highly dependent on stomatal conductance due to high methanol water solubility, results from actication of pectin methylesterases in cell walls and concomitant demethylation of cell wall pectins under O₃ fumigation (Niinemets and Reichstein 2003; Beauchamp *et al.* 2005; Harley *et al.* 2007; Hüve *et al.*

2007; Pelloux *et al.* 2007). In addition, constitutive pectin methylesterase activity and *de novo* expression of these enzymes also contribute to the total methanol emission during and after O₃ treatments (Pelloux *et al.* 2007).

O₃ generates reactive oxygen species (ROS) and leads to oxidative stress in leaves, directly triggering emissions of LOX products (Beauchamp *et al.* 2005). In this study, both methanol and LOX product emissions strongly scaled with O₃ exposure concentration, demonstrating strong stress dose vs. emission responses. However, no MeSA emission was detected from the leaves pre-exposed to 200 nmol mol⁻¹ O₃ prior to the exposure to 600 nmol mol⁻¹ O₃ in *P. vulgaris*, suggested that O₃-induced priming could likely inhibit MeSA biosynthesis via the inhibition of both *de novo* synthesis and release from a glycosidically bonded salicylate pool (Tikunov *et al.* 2010; Mhlango *et al.* 2017).

The release of plant stress volatiles such as methanol, LOX products, GGDP pathway volatiles and benzenoids is also strongly enhanced by a variety of biotic stresses including herbivore attack and pathogen invasion (Kessler and Baldwin 2001; Baldwin *et al.* 2006; Dicke *et al.* 2009; Kappers *et al.* 2010; Niinemets 2010a; Niinemets *et al.* 2013; Copolovici *et al.* 2014). In this study, different concentrations of exogenous MeJA were used to simulate the impact of biotic stresses on elicitation of plant stress volatiles. Both methanol and LOX emissions were observed immediately after *C. sativus* leaves were treated with exogenous MeJA and the induced emission bursts resembled those observed in response to wounding due to herbivore feeding (Brilli *et al.* 2011; Portillo-Estrada *et al.* 2015). Differently from O₃ treatments, LOX products showed a biphasic emission responses and methanol showed a monophasic emission response throughout the recovery. In addition, monoterpenes (limonene and linalool) and sesquiterpenes (β -farnesene, α -cedrene, and β -caryophyllene) were also released from treated leaves, and both mono- and sesquiterpene emissions showed a monophasic emission pattern. However, emissions of these volatiles were not detected immediately after leaf treatment with MeJA, indicating that terpene biosynthesis was likely regulated by gene expression level controls through recovery (Pazouki *et al.* 2016). The second burst of LOX compounds occurred simultaneously with terpenoid emissions (Fig. 2 in **Paper III**). This might indicate the onset of jasmonate-dependent gene expression (Bell and Mullet 1991; Wasternack and Parthier 2007). Furthermore, both the maximum emission rates and total amount of emissions were positively correlated with MeJA concentrations indicating

a dose-dependent response to simulated biotic stress.

6.4. Time- and dose-dependent modifications of stress volatiles emitted upon acute O₃ treatments in *P. vulgaris* leaves

We demonstrated that temporal shapes of O₃-induced volatile emissions of methanol, LOX products and MeSA from *P. vulgaris* were characterized by an initial exponential or sigmoidal rise to a maximum level, followed by a decline until they reached the pre-stress level. The first methanol emission burst reached to a maximum level faster (Fig. 7d in **Paper II**), and both the rate of increase and decrease of the first methanol emission burst were much higher in leaves exposed to 600 nmol mol⁻¹ under illumination than in leaves treated with 200 + 600 nmol mol⁻¹ O₃ under illumination, and with 600 nmol mol⁻¹ O₃ in darkness (Fig. 8a and b in **Paper II**) suggesting that methanol can be induced faster under higher dose of O₃ fumigation. However, factors triggering the second methanol peak during post O₃ exposure have not been explained in previous studies. In this study, the second methanol emission peak showed the highest emission rate, and a greater total emissions and longer time duration than the first burst. The rise of second methanol emission burst occurred faster and declined slower in leaves exposed to O₃ in darkness (Fig. 8a and b in **Paper II**) than that emitted by leaves under illumination, suggesting that the biochemical processes such as activation of demethylation of pectins and related gene expressions were likely linked to O₃ exposure conditions and stomatal O₃ uptake.

The fast emission bursts of LOX products in leaves exposed to 600 nmol mol⁻¹ under illumination (Fig. 7b in **Paper II**) indicated that there was a faster production of ROS upon 600 nmol mol⁻¹ exposure under illumination than that in leaves treated with 200 + 600 nmol mol⁻¹ O₃ under illumination, and 600 nmol mol⁻¹ O₃ in darkness. However, it is not clear why LOX emissions raised and decreased faster in leaves exposed to O₃ in darkness than in other treatments. In our study, MeSA release was observed only from leaves exposed to high O₃ concentrations of 600 nmol mol⁻¹ under illumination and in darkness, and it showed no correlation with total stomatal O₃ uptake. Overall, the relationship between O₃ dose vs stress volatile emission responses suggested that emission kinetics of stress volatiles in response to O₃ treatments are more complicated than generally thought and include both immediate stress response and

longer-term gene expression level responses.

6.5. Time- and dose-dependent modifications of stress volatiles emitted upon MeJA treatments in *C. sativus* leaves

Exogenous MeJA application led to a biphasic emission pattern of LOX products, whereas the second emission peak was much larger than the first peak. The emission bursts of monoterpenes (Fig. 2C in **Paper III**), sesquiterpenes and the second LOX volatile emission burst (Fig. 2B in **Paper III**) were started and reached to the maximum level much later, in 16–25 h after MeJA treatments. Such a long-term elicitation reflects a *de novo* emission response, likely regulated by jasmonate-dependent gene- and/or enzyme-level controls (Arimura *et al.* 2000; Martin *et al.* 2003; Byun-McKay *et al.* 2006; Tamogami *et al.* 2008). However, we cannot rule out that the substrate level controls were simultaneously operative with gene- and enzyme-level regulations.

In this study, we quantitatively characterized the rise and decay kinetics of volatile release from *C. sativus* leaves upon MeJA treatment. In some cases, the increase and decrease rates did not follow similar correlations with MeJA treatment concentrations. For example, both the rate of increase and the decrease of LOX compounds and terpenoids were strongly enhanced by increasing MeJA concentrations, but they decreased with the severity of MeJA treatments ranging between 0.2–5 mM. Particularly, the rate of rise and decline of methanol was weakly affected by MeJA concentrations >5 mM. This evidence emphasizes the highly dynamic nature of the MeJA dose dependency of volatile emissions during the recovery phase. Indeed, the quantitative relationships between MeJA dose and timing and magnitude of early and late emission responses are obviously more complex and probably reflect a systemic response. Although exogenous MeJA application is not sufficient to fully mimic the natural herbivory responses, the induced blend of volatiles such as LOX compounds dose play crucial roles in attraction of enemies of herbivores and in priming of neighboring plants similarly to genuine herbivore feeding responses (Dicke *et al.* 1999; Kappers *et al.* 2010). In agreement with these past observations, this study indicates that foliage emission responses upon MeJA treatments resemble biotic stress responses (Zhao and Chye 1999; Heijari *et al.* 2008; Tamogami *et al.* 2008; Kegge *et al.* 2013).

Taken together, our data suggest that strong quantitative relationships among stress dose vs. timing, magnitude and kinetics of emissions are determined by the type and length of stress applications, and the plant species used.

CONCLUSIONS

This thesis provides conclusive insight into the impact of the type and density of leaf trichomes on the severity of oxidative stress caused by O_3 across a wide range of plant species, and the dose- and time-dependent modifications in foliage photosynthetic characteristics and stress volatiles emitted upon acute O_3 and exogenous MeJA applications in *P. vulgaris* and *C. sativus*. Based on the results of this thesis, it can be concluded that:

Exposure of leaves to high concentration of O_3 leads to severe visible leaf injuries and remarkable reductions in leaf physiological characteristics including net assimilation rate, stomatal conductance to water vapor and the maximum dark-adapted photosystem II (PSII) quantum yield estimated by chlorophyll fluorescence (F_v/F_m). However, the degree of reductions in leaf physiological characteristics was significantly determined by O_3 dose, stomatal O_3 uptake and exposure conditions.

Both non-glandular and glandular trichomes were present on the leaf surfaces of the 24 species studied, but there was no relationship observed between the density of non-glandular trichomes and the percentage of non-stomatal O_3 deposition. However, the glandular trichome density was strongly correlated with the percentage of non-stomatal O_3 deposition. The O_3 dose threshold triggering acute physiological responses increased with increasing glandular trichome density. In addition, changes in leaf damage and LOX product emissions caused by leaf O_3 uptake were strongly correlated with glandular trichome density, demonstrating that species with low glandular trichome density were more sensitive to O_3 stress than the species with high glandular trichome density.

Emission bursts of methanol, LOX volatiles and methyl salicylate (MeSA) were observed during and after the exposure of *P. vulgaris* leaves to O_3 , but enhanced MeSA emission was not detected in any of the leaves pre-exposed to lower O_3 concentrations. Emission of all elicited volatiles exhibited a sigmoidal rise to a peak and then, they achieved pre-stress levels. The emission of methanol and LOX products was dose-dependent, but MeSA emission was not strictly dose-dependent. Overall, the emission responses after all stress treatments were broadly similar and has a clear long-lasting component observed through the recovery.

Changes in stomatal conductance to water vapour is an important factor in regulating O_3 entry into leaves and thus, it determines the necrotic damage in plants due to acute O_3 treatments. The quantity of methanol and LOX products released into the atmosphere demonstrated that stomatal closure in darkness and pre-exposure to low O_3 protects leaves against the damage caused by higher acute O_3 treatments.

MeJA treatment resulted in a burst of methanol, LOX products, and monoterpene and sesquiterpene emissions and these volatile emissions were linked to stress severity in a dose dependent manner. In addition, the strong relationships among stress dose, and the kinetics and magnitude of volatile emission were found in leaves treated with both acute O_3 and MeJA, emphasizing the importance of stress severity in determining the downstream biological impacts.

REFERENCES

- Adams RP (2001) Identification of essential oil components by gas chromatography/quadrupole mass spectroscopy. Allured Publishing, Carol Stream, IL
- Ainsworth EA (2017) Understanding and improving global crop response to ozone pollution. *Plant J* 90: 886-897
- Ainsworth EA, Yendrek CR, Sitch S, Collins WJ, Emberson LD (2012) The effects of tropospheric ozone on net primary productivity and implications for climate change. *Ann Rev Plant Biol* 63: 637-661
- Amme S, Rutten T, Melzer M, Sonsmann G, Vissers JPC, Schlesier B, Mock HP (2005) A proteome approach defines protective functions of tobacco leaf trichomes. *Proteomics* 5: 2508-2518
- Arimura GI, Ozawa R, Shimoda T, Nishioka T, Boland W, Takabayashi J (2000) Herbivory-induced volatiles elicit defence genes in lima bean leaves. *Nature* 406: 512-515
- Ascensão L, Pais MS (1998) The leaf capitate trichomes of *Leonotis leonurus*: histochemistry, ultrastructure and secretion. *Ann Bot* 81: 263-271
- Avnery S, Mauzerall DL, Liu J, Horowitz LW (2011a) Global crop yield reductions due to surface ozone exposure. 1. Year 2000 crop production losses and economic damage. *Atmos Environ* 45: 2284-2296
- Avnery S, Mauzerall DL, Liu J, Horowitz LW (2011b) Global crop yield reductions due to surface ozone exposure. 2. Year 2030 potential crop production losses and economic damage under two scenarios of O₃ pollution. *Atmos Environ* 45: 2297-2309
- Baldwin IT, Halitschke R, Paschold A, von Dahl CC, Preston CA (2006) Volatile signaling in plant-plant interactions: “Talking Trees” in the genomics era. *Science* 311: 812-815
- Baldwin IT, Zhang Z-P, Diab N, Ohnmeiss TE, McCloud ES, Lynds GY, Schmelz EA (1997) Quantification, correlations and manipulations of wound-induced changes in jasmonic acid and nicotine in *Nicotiana sylvestris*. *Planta* 201: 397-404
- Baran P, Özdemir C, Aktas K (2010) Structural investigation of the glandular trichomes of *Salvia argentea*. *Biologia* 65: 33-38
- Beauchamp J, Wisthaler A, Hansel A, Kleist E, Miebach M, Niinemets Ü, Schurr U, Wildt J (2005) Ozone induced emissions of biogenic VOC from tobacco: relationships between ozone uptake and emission of LOX products. *Plant Cell Environ* 28 (10): 1334-1343

- Bell E, Mullet JE (1991) Lipoxygenase gene expression is modulated in plants by water deficit, wounding, and methyl jasmonate. *Mol Gen Genet* 230: 456–62
- Benjamin MT, Winer AM (1998) Estimating the ozone-forming potential of urban trees and shrubs. *Atmos Environ* 32: 53–68
- Betzberger AM, Yendrek CR, Sun J, Leisner CP, Nelson RL, Ort DR, Ainsworth EA (2012) Ozone exposure response for U.S. soybean cultivars: linear reductions in photosynthetic potential, biomass, and yield. *Plant Physiol* 160: 1827–1839
- Brilli F, Ruuskanen TM, Schnitzhofer R, Müller M, Breitenlechner M, Bittner V, Wohlfahrt G, Loreto F, Hansel A. (2011) Detection of plant volatiles after leaf wounding and darkening by Proton Transfer Reaction “Time-of-Flight” Mass Spectrometry (PTR-TOF). *PLoS One* 6 (5): e20419
- Byun-McKay A, Godard KA, Toudefallah M, Martin DM, Alfaro R, King J, Bohlmann J, Plant AL (2006) Wound-induced terpene synthase gene expression in Sitka spruce that exhibit resistance or susceptibility to attack by the white pine weevil. *Plant Physiol* 140: 1009–1021
- Calatayud A, Iglesias D, Talon M, Barreno E (2003) Effects of 2 months ozone exposure in spinach leaves on photosynthesis, antioxidant systems and lipid peroxidation. *Plant Physiol Bioch* 41: 839–845
- Calfapietra C, Fares A, Manes F, Morani A, Sgrigna G, Loreto F (2013) Role of biogenic volatile organic compounds (BVOC) emitted by urban trees on ozone concentration in cities: a review. *Environ Pollut* 183: 71–80
- Carlton AG, Wiedinmyer C, Kroll JH (2009) A review of secondary organic aerosol (SOA) formation from isoprene. *Atmos Chem Phys* 9: 4987–5005
- Carter WPL (1994) Development of ozone reactivity scales for volatile organic compounds. *J Air Waste Man Ass* 44: 881–899
- Cheong JJ, Choi YD (2003) Methyl jasmonate as a vital substance in plants. *Trends Genet* 19: 409–413
- Claeys M, Graham B, Bas G, Wang W, Vermeylen R, Pashynska V, Cafmeyer J, Guyon P, Andreae MO, Artaxo P, Maenhaut W (2004) Formation of secondary organic aerosols through photooxidation of isoprene. *Science* 303: 1173–1176

- Conrath U, Beckers GJM, Flors V, García-Agustín P, Jakab G, Mauch F, Newman M-A, Pieterse CMJ, Poinssot B, Pozo MJ, Pugin A, Schaffrath U, Ton J, Wendehenne D, Zimmerli L, Mauch-Mani B (2006) Priming: getting ready for battle. *Mol. Plant-Microbe Interact* 19: 1062–71
- Coplovici L, Kännaste A, Niinemets Ü (2009) Gas chromatography-mass spectrometry method for determination of monoterpene and sesquiterpene emissions from stressed plants. *Stud Univ Babeş-Bol* 54 (4): 329–339
- Coplovici L, Kännaste A, Pazouki L, Niinemets Ü (2012) Emissions of green leaf volatiles and terpenoids from *Solanum lycopersicum* are quantitatively related to the severity of cold and heat shock treatments. *J Plant Physiol* 169: 664–672
- Coplovici L, Kännaste A, Remmel T, Niinemets Ü (2014) Volatile organic compound emissions from *Alnus glutinosa* under interacting drought and herbivory stresses. *Environ Exp Bot* 100: 55–63
- Coplovici L, Niinemets Ü (2010) Flooding induced emissions of volatile signalling compounds in three tree species with differing water-logging tolerance. *Plant Cell Environ* 33 (9): 1582–1594
- Corsi G, Bottega S (1999) Glandular hairs of *Salvia officinalis*: new data on morphology, localization and histochemistry in relation to function. *Ann Bot* 84: 657–664
- Dicke M, Gols R, Ludeking D, Posthumus MA (1999) Jasmonic acid and herbivory differentially induce carnivore-attracting plant volatiles in lima bean plants. *J Chem Ecol* 25: 1907–1922
- Dicke M, van Loon JJA, Soler R (2009) Chemical complexity of volatiles from plants induced by multiple attack. *Nat Chem Biol* 5: 317–324
- Dudareva N, Negre F, Nagegowda DA, Orlova I (2006) Plant volatiles: recent advances and future perspectives. *CRC Crit Rev Plant Sci* 25 (5): 417–440
- Ehleringer J (1981) Leaf absorptances of Mohave and Sonoran desert plants. *Oecologia* 49: 366–370
- Emberson LD, Püker P, Ashmore MR, Mills G, Jackson LS, Agrawal M, Atikuzzaman MD, Cinderby S, Engardt M, Jamir C, Kobayashi K, Oanh NTK, Quadir QF, Wahid A (2009) A comparison of North American and Asian exposure-response data for ozone effects on crop yields. *Atmos Environ* 43: 1945–1953
- Fahn A (2000) Structure and function of secretory cells. In: Hallahan DL and Gray JC (eds) *Plant Trichomes*, Academic Press: New York, NY, USA, pp 37

- Fares S, Barta C, Brilli F, Centritto M, Ederli L, Ferranti F, Pasqualini S, Reale L, Tricoli D, Loreto F (2006) Impact of high ozone on isoprene emission, photosynthesis and histology of developing *Populus alba* leaves directly or indirectly exposed to the pollutant. *Physiol Plant* 128: 456-465
- Fares S, Goldstein AH, Loreto F (2010a) Determinants of ozone fluxes and metrics for ozone risk assessment in plants. *J Exp Bot* 61: 629-633
- Fares S, Loreto F, Kleist E, Wildt J (2008) Stomatal uptake and stomatal deposition of ozone in isoprene and monoterpene emitting plants. *Plant Biol* 10: 44-54
- Fares S, Matteucci G, Scarascia Mugnozza G, Morani A, Calfapietra C, Salvatori E, Fusaro L, Manes F, Loreto F (2013a) Testing of models of stomatal ozone fluxes with field measurements in a mixed Mediterranean forest. *Atmos Environ* 67: 242-251
- Fares S, McKay M, Holzinger R, Goldstein AH (2010b) Ozone fluxes in a *Pinus ponderosa* ecosystem are dominated by non-stomatal processes: evidence from long-term continuous measurements. *Agric For Meteorol* 150: 420-431
- Fares S, Park J-H, Ormeno E, Gentner DR, McKay M, Loreto F, Karlik J, Goldstein AH (2010c) Ozone uptake by citrus trees exposed to a range of ozone concentrations. *Atmos Environ* 44: 3404-3412
- Fares S, Savi F, Muller J, Matteucci G, Paoletti E (2014) Simultaneous measurements of above and below canopy ozone fluxes help partitioning ozone deposition between its various sinks in a Mediterranean Oak Forest. *Agric For Meteorol* 198-199: 181-191
- Fares S, Vargas R, Detto M, Goldstein AH, Karlik J, Paoletti E, Vitale M (2013b) Tropospheric ozone reduces carbon assimilation in trees: estimates from analysis of continuous flux measurements. *Global Change Biol* 19: 2427-2443
- Farmer EE, Ryan CA (1990) Interplant communication: airborne methyl jasmonate induces synthesis of proteinase inhibitors in plant leaves. *Proc Nat Acad Sci USA* 87: 7713-7716
- Fehsenfeld F, Calvert J, Fall R, Goldan P, Guenther AB, Hewitt CN, Lamb B, Liu S, Trainer M, Westberg H, Zimmerman P (1992) Emissions of volatile organic compounds from vegetation and the implications for atmospheric chemistry, *Global Biogeochem Cycles* 6: 389-430
- Fiscus EL, Brooker FL, Burkey KO (2005) Crop responses to ozone: uptake, models of action, carbon assimilation and partitioning. *Plant Cell Environ* 28: 997-1011

- Flowers MD, Fiscus EL, Burkey KO, Booker FL, Dubois J-JB (2007) Photosynthesis, chlorophyll fluorescence, and yield of snap bean (*Phaseolus vulgaris* L.) genotypes differing in sensitivity to ozone. *Environ Exp Bot* 61: 190–198
- Fowler D, Amann M, Anderson R, Ashmore M, Cox P, Depledge M, Derwent D, Grennfelt P, Hewitt N, Hov O, Jenkin M, Kelly F, Liss PS, Pilling M, Pyle J, Slingo J, Steffenson D. (2008) *Ground-Level Ozone in the 21st Century: Future Trends, Impacts and Policy Implications*. The Royal Society, London, UK
- Franzaring J, Dueck TA, Tonneijck AEG (1999) Can plant traits be used to explain differences in ozone sensitivity between native European species? In: Fuhrer J, Achermann B (eds) *Critical levels for ozone-level II*, Swiss Agency for the Environment, Forests and Landscape, Bern, Switzerland, pp 271–274.
- Fuentes JD, Wang D (1999) On the seasonality of isoprene emissions from a mixed temperate forest. *Ecol Appl* 9: 1118–1131
- Gang DR, Wang J, Dudareva N, Nam KH, Simon JE, Lewinsohn E, Pichersky E (2001) An investigation of the storage and biosynthesis of phenylpropenes in sweet basil. *Plant Physiol* 125: 539–555
- Glas JJ, Schimmel BC, Alba JM, Escobar-Bravo R, Schuurink RC, Kant MR (2012) Plant glandular trichomes as targets for breeding or engineering of resistance to herbivores. *Int J Mol Sci* 13: 17077–17103
- Graus M, Müller M, Hansel A. (2010) High resolution PTR-TOF: quantification and formula confirmation of VOC in real time. *J Am Soc Mass Spectrom* 21: 1037–1044
- Guenther A, Geron C, Pierce T, Lamb B, Harley P, Fall R (2000) Natural emissions of non-methane volatile organic compounds, carbon monoxide, and oxides of nitrogen from North America. *Atmos Environ* 34: 2205–2230
- Guenther A, Hewitt CN, Erickson D, Fall R, Geron C, Graedel T, Harley P, Klinger L, Lerdau M, McKay WA, Pierce T, Scholes B, Steinbrecher R, Tallamraju R, Taylor J, Zimmerman P, (1995) A global model of natural volatile organic compound emissions. *J Geophys Res- Atmos* 100: 8873–8892
- Guenther AB, Zimmerman PR, Harley PC, Monson RK, Fall R (1993) Isoprene and monoterpene emission rate variability: model evaluations and sensitivity analyses. *J Geophys Res* 98 (D7): 12609–12617
- Guidi L, Degl’Innocenti E, Martinelli F, Piras M. (2009) Ozone effects on carbon metabolism in sensitive and insensitive *Phaseolus* cultivars. *Environ Exp Bot* 66, 117–125.

- Harley P, Greenberg J, Niinemets Ü, Guenther A (2007) Environmental controls over methanol emission from leaves. *Biogeosciences* 4: 1083–1099
- Hayes F, Jones MLM, Mills G, Ashmore M (2007) Meta-analysis of the relative sensitivity of semi-natural vegetation species to ozone. *Environ Pollu* 146: 754–762
- Heiden AC, Hoffmann T, Kahl J, Kley D, Klockow D, Langebartels C, Mehlhorn H, Jr Sandermann H, Schraudner M, Schuh G, Wildt J (1999) Emission of volatile organic compounds from ozone-exposed plants. *Ecol Appl* 9 (4): 1160–1167
- Heijari J, Nerg AM, Kainulainen P, Vuorinen M, Holopainen JK (2008) Long-term effects of exogenous methyl jasmonate application on Scots pine (*Pinus sylvestris*) needle chemical defence and diprionid sawfly performance. *Entomol Exp Appl* 128: 162–171
- Heil M, Kost C (2006) Priming of indirect defences. *Ecol Lett* 9: 813–817
- Heil M, Ton J (2008) Long-distance signalling in plant defence. *Trends Plant Sci* 13: 264–272
- Hüve K, Christ MM, Kleist E, Uerlings R, Niinemets Ü, Walter A, Wildt J (2007) Simultaneous growth and emission measurements demonstrate an interactive control of methanol release by leaf expansion and stomata. *J Exp Bot* 58: 1783–1793
- IPCC (2013) Summary for Policymakers. In: *Climate Change 2013: The Physical Science Basis. Contribution of Working Group I to the Fifth Assessment Report of the Intergovernmental Panel on Climate Change*. Cambridge University Press, Cambridge, United Kingdom and New York, NY, USA
- Ivanov AV, Trakhtenberg S, Bertram AK, Gershenson YM, Molina MJ (2007) OH, HO₂, and ozone gaseous diffusion coefficients. *J Phys Chem A* 111:1632–1637
- Jiang Y, Ye J, Li S, Niinemets Ü (2016) Regulation of floral terpenoid emission and biosynthesis in sweet basil (*Ocimum basilicum*). *J Plant Growth Regul* 35: 921–935
- Jordan A, Haidacher S, Hanel G, Hartungen E, Märk L, Seehauser H, Schotchkowsky R, Sulzer P, Märk TD (2009) A high resolution and high sensitivity proton-transfer-reaction time-of-flight mass spectrometer (PTR-TOF-MS). *Int J Mass Spectrom* 286: 122–128
- Jud W, Fischer L, Canaval E, Wohlfahrt G, Tissier A, Hansel A (2016) Plant surface reactions: an opportunistic ozone defense mechanism impacting atmospheric chemistry. *Atmos Chem Phys* 16: 277–292

- Kangasjärvi J, Talvinen J, Utriainen M, Karjalainen R (1994) Plant defence systems induced by ozone. *Plant Cell Environ* 17: 783–794
- Kännaste A, Copolovici L, Niinemets Ü (2014) Gas chromatography mass-spectrometry method for determination of biogenic volatile organic compounds emitted by plants. In: Rodríguez-Concepción M (ed) *Plant isoprenoids: methods and protocols*, vol 1153. *Methods in molecular biology*. Humana Press, New York, pp 161–169. Doi: 10.1007/978-1-4939-0606-2_11
- Kappers IF, Verstappen FW, Luckerhoff LL, Bouwmeester HJ, Dicke M (2010) Genetic variation in jasmonic acid- and spider mite-induced plant volatile emission of cucumber accessions and attraction of the predator *Phytoseiulus persimilis*. *J Chem Ecol* 36: 500–512
- Kegge W, Weldegergis BT, Soler R, Vergeer-Van Eijk M, Dicke M, Voesenek LA, Pierik R (2013) Canopy light cues affect emission of constitutive and methyl jasmonate-induced volatile organic compounds in *Arabidopsis thaliana*. *New Phytol* 200:861–874
- Kessler A, Baldwin IT (2001) Defensive function of herbivore-induced plant volatile emissions in nature. *Science* 291:2141–44
- Ko KN, Lee KW, Lee SE, Kim ES (2007) Development and ultrastructure of glandular trichomes in *pelargonium x fragrans* ‘mabel grey’ (geraniaceae). *J Plant Biol* 50: 362–368
- Kollist T, Moldau H, Rasulov B, Oja V, Rämme H, Hüve K, Jaspers P, Kangasjärvi J, Kollist H (2007) A novel device detects a rapid ozone-induced transient stomatal closure in intact *Arabidopsis* and its absence in *abi2* mutant. *Physiol Plant* 129: 796–803
- Laisk A, Kull O, Moldau H (1989) Ozone concentration in leaf intercellular air spaces is close to zero. *Plant Physiol* 90: 1163–1167
- Li P, Calatayud V, Gao F, Uddling J, Feng Z (2016) Differences in ozone sensitivity among woody species are related to leaf morphology and antioxidant levels. *Tree Physiol* 36: 1105–1116
- Lihavainen J, Ahonen V, Keski-Saari S, Söber A, Oksanen E, Keinänen M (2017) Low vapor pressure deficit reduces glandular trichome density and modifies the chemical composition of cuticular waxes in silver birch leaves. *Tree Physiol* 37: 1166–1181
- Long SP, Naidu SL (2002) Effect of oxidants at the biochemical, cell and physiological levels, with particular reference to ozone. In: Bell JNB, Treshow M (eds) *Air Pollution and Plant Life*, John Wiley & Sons, Ltd., West Sussex, pp 69–88

- Loreto F, Fares S (2007) Is ozone flux inside leaves only a damage indicator? Clues from volatile isoprenoid studies. *Plant Physiol* 143: 1096-1100
- Loreto F, Mannoizzi M, Maris C, Nascetti P, Ferranti F, Pasqualini S (2001) Ozone quenching properties of isoprene and its antioxidant role in leaves. *Plant Physiol* 126:993-1000
- Loreto F, Pinelli P, Manes F, Kollist H (2004) Impact of ozone on monoterpene emissions and evidence for an isoprene-like antioxidant actions of monoterpenes emitted by *Quercus ilex* leaves. *Tree Physiol* 24: 361-367
- Loreto F, Schnitzler JP (2010) Abiotic stresses and induced BVOCs. *Trends in Plant Sci* 15: 154-166
- Loreto F, Velikova V (2001) Isoprene produced by leaves protects the photosynthetic apparatus against ozone damage, quenches ozone products, and reduces lipid peroxidation of cellular membranes. *Plant Physiol* 127: 1781-1787
- Maffei ME (2010) Sites of synthesis, biochemistry and functional role of plant volatiles. *S Afr J Bot* 76: 612–631
- Martin DM, Gershenzon J, Bohlmann J (2003) Induction of volatile terpene biosynthesis and diurnal emission by methyl jasmonate in foliage of Norway spruce. *Plant Physiol* 132: 1586–1599
- Mathur J, Chua N-H (2000) Microtubules stabilization leads to growth reorientation in *Arabidopsis* trichomes. *Plant Cell* 12: 465-477
- McGrath JM, Betzelberger AM, Wang SW, Shook E, Zhu XG, Long SP, Ainsworth EA (2015) An analysis of ozone damage to historical maize and soybean yields in the United States. *Proc Natl Acad Sci USA* 112: 14390-14395
- Mhlongo MI, Tugizimana F, Piater LA, Steenkamp PA, Madala NE, Dubery IA (2017) Untargeted metabolomics analysis reveals dynamic changes in azelaic acid- and salicylic acid derivatives in LPS-treated *Nicotiana tabacum* cells. *Biochem Biophys Res Commun* 482: 1497-1503
- Moldau H, Bichele I (2002) Plasmalemma protection by the apoplast as assessed from above-zero ozone concentrations in leaf intercellular air spaces. *Planta* 214: 484-487
- Monks PS, Archibald AT, Colette A, Cooper O, Coyle M, Derwent R, Fowler D, Granier C, Law KS, Mills GE, Stevenson DS, Tarasova O, Thouret V, von Schneidemesser E, Sommariva R, Wild O, Williams ML (2015) Tropospheric ozone and its precursors from the urban to the global scale from air quality to short-lived climate forcer. *Atmos Chem Phys* 15: 8889–8973

- Mur LAJ, Laarhoven LJJ, Harren FJM, Hall MA, Smith AR (2008) Nitric oxide interacts with salicylate to regulate biphasic ethylene production during the hypersensitive response. *Plant Physiol* 148: 1537-1546
- Niinemets Ü (2010a) Mild versus severe stress and BVOCs: thresholds, priming and consequences. *Trends in Plant Sci* 15: 145-153
- Niinemets Ü (2010b) Responses of forest trees to single and multiple environmental stresses from seedlings to mature plants: past stress history, stress interactions, tolerance and acclimation. *For Ecol Manag* 260 (10): 1623–1639
- Niinemets Ü, Kännaste A, Copolovici L (2013) Quantitative patterns between plant volatile emissions induced by biotic stresses and the degree of damage. *Front Plant Sci* 4: 262
- Niinemets Ü, Kuhn U, Harley PC, Staudt M, Arneth A, Cescatti A, Ciccioli P, Copolovici L, Geron C, Guenther A, Kesselmeier J, Lerdau MT, Monson RK, Peñuelas J (2011) Estimations of isoprenoids emission capacity from enclosure studies: measurements, data processing, quantity and standardized measurement protocols. *Biogeosciences* 8: 2209-2246
- Niinemets Ü, Loreto F, Reichstein M (2004) Physiological and physico-chemical controls on foliar volatile organic compound emissions. *Trends Plant Sci* 9: 180–186.
- Niinemets Ü, Reichstein M (2003) Controls on the emission of plant volatiles through stomata: sensitivity or insensitivity of the emission rates to stomatal closure explained. *J Geophys Res* 108: 4208 DOI: 10.1029/2002JD002620
- Nolle M, Ellul R, Heinrich G, Güsten H (2002) A long-term study of background ozone concentrations in the central Mediterranean-diurnal and seasonal variations on the island of Gozo. *Atmos Environ* 36: 1391–1402
- Pasqualini S, Piccioni c, Reale L, Ederli L, Della TG, Ferranti F (2003) Ozone-induced cell death in tobacco cultivar Bel W3 plant. The role of programmed cell death in lesion formation. *Plant Physiol* 133: 1122-1134
- Pazouki L, Kanagendran A, Li S, Kännaste A, Memari HR, Bichele R, Niinemets Ü (2016) Mono- and sesquiterpene release from tomato (*Solanum lycopersicum*) leaves upon mild and severe heat stress and through recovery: from gene expression to emission response. *Environ Exp Bot* 132: 1-15
- Pelloux J, Rustérucci C, Mellerowicz EJ (2007) New insights into pectin methylesterase structure and function. *Trends Plant Sci* 12: 267–277

- Peñuelas J, Staudt M (2010) BVOCs and global change. *Trends Plant Sci* 15: 133-144
- Portillo-Estrada M, Kazantsev T, Talts E, Tosens T, Niinemets Ü (2015) Emission timetable and quantitative patterns of wound-induced volatiles across different leaf damage treatments in aspen (*Populus tremula*). *J Chem Ecol* 41(12): 1105-1117
- Prozherina N, Freiwald V, Rousi M, Oksanen E (2003) Interactive effect of springtime frost and elevated ozone on early growth, foliar injuries and leaf structures of birch (*Betula pendula*). *New Phytol* 159: 623-636
- Rao MV, Davis KR (2001) The physiology of ozone-induced cell death. *Planta* 213: 682-690
- Ribas À, Peñuelas J (2004) Temporal patterns of surface ozone levels in different habitats of the North Western Mediterranean basin. *Atmos Environ* 38: 985-992
- Rodriguez-Saona C, Crafts-Brandner SJ, Paré PW, Henneberry TJ (2001) Exogenous methyl jasmonate induces volatile emissions in cotton plants. *J Chem Ecol* 27: 679-695
- Sallaud C, Giacalone C, Töpfer R, Goepfert S, Bakaher N, Rösti S, Tissier A (2012) Characterization of two genes for the biosynthesis of the labdane diterpene Z-abienol in tobacco (*Nicotiana tabacum*) glandular trichomes. *Plant J* 72: 1-17
- Semiz G, Blande JD, Heijari J, Isik K, Niinemets Ü, Holopainen JK (2012) Manipulation of BVOC emissions with methyl jasmonate and carra-geenan in the evergreen conifer *Pinus sylvestris* and evergreen broadleaf *Quercus ilex*. *Plant Biol* 14: 57-65
- Sharkey TD, Chen X, Yeh S (2001) Isoprene increases thermotolerance of fosmidomycin-fed leaves. *Plant Physiol* 125: 2001-2006
- Sharkey TD, Singaas EL (1995) Why plants emit isoprene. *Nature* 374: 769
- Sharkey TD, Wiberley AE, Donohue AR, (2008) Isoprene emission from plants: why and how. *Ann Bot* 101: 5-18
- Sun J, Ariya PA (2006) Atmospheric organic and bio-aerosols as cloud condensation nuclei (CCN): a review. *Atmos Environ* 40: 795-820
- Tamogami S, Rakwal R, Agrawal GK (2008) Interplant communication: airborne methyl jasmonate is essentially converted into JA and JA-Ile activating jasmonate signaling pathway and VOCs emission. *Biochem Biophys Res Commun* 376:723-727

- Tikunov YM, de Vos RCH, González Paramás AM, Hall RD, Bovy AG (2010) A role for differential glycoconjugation in the emission of phenylpropanoid volatiles from tomato fruit discovered using a metabolic data fusion approach. *Plant Physiol* 152: 55-70
- Tissier A (2012) Glandular trichomes: What comes after expressed sequence tags? *Plant J* 70: 51–68
- Toome M, Randjārv P, Copolovici L, Niinemets Ü, Heinsoo K, Luik A, Noe SM (2010) Leaf rust induced volatile organic compounds signalling in willow during the infection. *Planta* 232: 235-243
- Turner GW, Gershenzon J, Croteau RB (2000) Distribution of peltate glandular trichomes on developing leaves of peppermint. *Plant Physiol* 124: 655–663
- Vahisalu T, Kollist H, Wang Y-F, Nishimura N, Chan W-Y, Valerio G, Lamminmäki A, Brosché M, Moldau H, Desikan R, Schroeder JI, Kangasjärvi J (2008) SLAC1 is required for plant guard cell S-type anion channel function in stomatal signalling. *Nature* 452: 487-491
- Vahisalu T, Puzõrjova I, Brosché M, Valk E, Lepiku M, Moldau H, Pechter P, Wang Y-S, Lindgren O, Salojärvi J, Loog M, Kangasjärvi J, Kollist H (2010) Ozone-triggered rapid stomatal response involves the production of reactive oxygen species, and is controlled by SLAC1 and OST1. *Plant J* 62: 442–453
- VanReken TM, Ng NL, Flagan RC, Seinfeld JH (2005) Cloud condensation nucleus activation properties of biogenic secondary organic aerosol. *J Geophys Res* 110: D07206
- Vickers CE, Possell M, Cojocariu CI, Velikova VB, Laothawornkitkul J, Ryan A, Mullineaux PM, Hewitt CN (2009) Isoprene synthesis protects transgenic tobacco plants from oxidative stress. *Plant Cell Environ* 32: 520-531
- Vingarzan R (2004) A review of surface ozone background levels and trend. *Atmos Environ* 38: 3431-3442
- von Caemmerer S, Farquhar GD (1981) Some relationships between the biochemistry of photosynthesis and the gas exchange of leaves. *Planta* 153: 376–387
- Wagner GJ, Wang E, Shepherd RW (2004) New approaches for studying and exploiting an old protuberance, the plant trichome. *Ann Bot* 93: 3–11
- Wasternack C, Parthier B (2007) Jasmonate-signalled plant gene expression. *Trends Plant Sci* 2: 302–307

- Werker E (2000) Trichome diversity and development. *Adv Bot Res* 31: 1–35
- Wi SJ, Ji NR, Park KY (2012) Synergistic biosynthesis of biphasic ethylene and reactive oxygen species in response to hemibiotrophic *Phytophthora parasitica* in tobacco plants. *Plant Physiol* 159: 251–265
- Wieser G, Hecke K, Tausz M, Matyssek R (2013) Foliage type specific susceptibility to ozone in *Picea abies*, *Pinus cembra* and *Larix decidua* at treeline: a synthesis. *Environ Exp Bot* 90: 4–11
- Wilkinson S, Mills G, Illidge R, Davies WJ (2012) How is ozone pollution reducing our food supply? *J Exp Bot* 63: 527–536
- Wittig VE, Ainsworth EA, Naidu AL, Karnosky DF, Long SP (2009) Quantifying the impact of current and future tropospheric ozone on the tree biomass, growth, physiology and biochemistry: a quantitative meta-analysis. *Global Change Biol* 15: 396–424
- Wohlgemuth H, Mittelstrass S, Kschieschan S, Bender J, Weigel HJ, Overmyer K, Kangasjarvi J, Sandermann H, Langebartels C (2002) Activation of an oxidative burst is a general feature of sensitive plants exposed to the air pollutant ozone. *Plant Cell Environ* 25: 717–726
- Xu X, Lin W, Wang T, Yan P, Tang J, Meng Z, Wang Y (2008) Long-term trend of surface ozone at a regional background station in eastern China 1991–2006: enhanced variability. *Atmos Chem Phys* 8: 2595–2607.
- Zhao KJ, Chye ML (1999) Methyl jasmonate induces expression of a novel *Brassica juncea* chitinase with two chitin-binding domains. *Plant Mol Biol* 40: 1009–1018

SUMMARY IN ESTONIAN

TAIMELEHTEDE LENDUVÜHENDITE EMISSIONI INDUKTSIOON OSOONI JA METÜÜL JASMONAADI MÕJUL

Taimed biosünteesivad mitmesuguseid lenduvaid orgaanilisi ühendeid (BVOCs) nagu näiteks isoprenoidid, lipoksügenaasirajaproduktid (LOX-d) ehk rohulõhnakomponendid, küllastunud aldehüüdid, bensenoidid, ning erinevad süsivesinikud. Kõikidel eelpool nimetatud BVOC-del on oluline roll biosfääri ning atmosfääri vahelistes suhetes. Biogeensed lenduvühendid kaitsevad taime abiootilise stressi eest, milleks võib olla üleliigne valgus, temperatuur ja oksüdatiivne stress. Lisaks meelitavad biogeensed lenduvühendid tolmeldajaid ning pakuvad kaitset patogeenide ja kahjurputukate rünnaku eest. Mainimata ei saa jätta ka biogeensete lenduvühendite rolli taimede kasvus ja arengus ning taimede omavahelistes suhetes. Kõik taimed ei emiteeri lenduvühendeid pidevalt, kuid nii abiootilised või biootilised stressitekitajad võivad põhjustada pideva lenduvühendite emissiooni kõikidel taimedel. Üldiselt on abiootiliste stressitekitajate mõju taimede lenduvühenditele laialdaselt uuritud. Kuid oksüdatiivse stressori nagu näiteks osooni (O_3) ja eksogeennse stressori nagu metüül jasmonaadi (MeJA) üldine mõju lehepinnalt või mesofüllist emiteeruvatele ühenditele, või O_3 -i ja MeJA-i dooside mõju lenduvühendite kineetikale, on palju vähem uuritud.

Kõrge O_3 -i kontsentratsioon mõjutab taimede kasvu ja arengut ning seetõttu kannatab ka saagikus. Keemiliselt on O_3 tugev polaarne oksüdeerija, mis siseneb taimelehte peamiselt õhulõhede kaudu. Seetõttu mõjutab taime õhulõhede juhtivus O_3 -stressi kulgemist taimerakkudes oluliselt, sest stressi ulatus taimes ei sõltu O_3 -i kontsentratsioonist väljapool taimelehte. Vähenenud õhulõhede juhtivus takistab süsihappegaasi (CO_2) sisenemist taimelehte, mis omakorda vähendab fotosünteesi kiirust. Lisaks eelpool kirjeldatule võivad taime lehepinnal asetleidvad O_3 -ga seotud reaktsioonid alandada taimelehtedesse sisenevat O_3 -i kogust. Näiteks vääristubaka (*Nicotiana tabacum*) näärmekarvad sisaldavad poollenduvaid orgaanilisi ühendeid, mis reageerivad O_3 -ga. Selle tagajärjel siseneb taimelehte vähem O_3 -i. Taimelehes reageerib O_3 koheselt rakumembraanidega ning käivitab reaktiivsete hapnikuühendite (ROS-de) vabanemise, mis muudavad rakukomponentide funktsioneerimist ning lõpuks kahjustavad rakke või hävitavad need.

Erinevalt abiootilisest stressist kutsuvad ka biootilise stressi tekitajad, nagu näiteks kahjurputukate või patogeenide rünnak, esile lenduvühendite emissiooni taime vegetatiivsetest osadest. Peale taime mehaanilist vigastamist või kahjurite poolt tekitatud kahjustusi, on leitud mõnede taimede emissioonidest jasmoonhapet (JA) ja selle metüülestrit, MeJA. Stressis taimelt lendunud MeJA on kui signaal stressist puutumata naabertaimedele, sest ta aktiveerib viimastes kaitsevõime. Seetõttu töödeldakse taimi MeJA-ga ka välispidisel, et vallandada biootilisest stressist tulenevaid ja JA-st sõltuvaid kaitsereaktsioone.

Töö eesmärk:

Doktoritöö üldine eesmärk oli uurida O_3 -i ja MeJA-i mõju erinevate taimeliikidele, et saada ülevaade lenduvühendite varieeruvusest sõltuvalt mesofüllist ja lehepinnal asetsevatest näärmekarvadest ja mehaanilistest kattekarvadest.

Doktoritöö eesmärgid väljatoodult:

1. Uurida, kuidas mõjutab O_3 ja MeJA erinevate taimede fotosünteesi ja lenduvate ühendite emissioone (**I-III**)
2. Hinnata, kas lehe kattekarvad ja näärmekarvad kaitsevad taime O_3 -i eest (**I**).
3. Testida hüpoteesi, et madal õhulõhede juhtivus, mis tekib taime hoidmisel pimedas ja taime eeltöötlemisel madala O_3 -i kontsentratsiooniga, kaitseb hariliku aedoa (*Phaseolus vulgaris*) lehti kõrge O_3 -i kontsentratsiooni poolt tekitatavate kahjude eest (**II**).
4. Hinnata, kuidas erinevad O_3 -i ja MeJA-i kogused mõjutavad taimede lenduvühendite emissioone ning milliseks kujuneb lenduvühendite emissioon kohe peale stressi rakendamist ja hiljem stressist taastumise ajal (**I, III**).

Põhilised tulemused:

Akuutne O_3 põhjustas tõsiseid ja nähtavaid kahjustusi taimelehtedel ning vähendas märkimisväärselt lehe füsioloogilist aktiivsust sealhulgas fotosünteesi kiirust, õhulõhede juhtivust ja fotosüsteem II tootlikkust (F_v/F_m), kuid kõigi fotosünteesinäitajate muutuste ulatus sõltus O_3 -i kontsentratsioonist ja selle rakendamise tingimustest (**I, II**).

Kõigil 24 uuritud taimeliigil esinesid nii näärmekarvad kui ka mehaanilised kattekarvad. Uuringust selgus, et erinevalt mehaaniliste kattekarvade tiheduset sõltus lehepinna kaudu sisenenud O_3 -i hulk näärmekarvade tihedusest. O_3 -doosidest tingitud akuutse füsioloogilise reaktsiooni ulatus oli seda suurem, mida suurem oli näärmekarvade tihedus taimelehel. Lisaks oli O_3 -st tekkinud lehepinna kahjustuste ulatus seotud LOX-de emissiooniga, mis näitab seda, et madalama näärmekarvade tihedusega taimeliigid olid O_3 -stressile vastuvõtlikumad kui tihedamate näärmekarvade taimeliigid (**I**).

O_3 -ga töötlemise ajal ning peale O_3 -i kasutamist emiteeris harilik aeduba *P.vulgaris* metanooli, LOX-e ja MeJA-i. Juhul kui enne kõrge O_3 -i kontsentratsiooni kasutamist oli taimelehte hoitud madala O_3 -i kontsentratsiooniga keskkonnas, MeJA-i emissioon ei suurenenud (**II**). Teatud ajahetkel saavutas kõigi eelpool nimetatud lenduvühendite emissioon maksimumi ja seejärel langes stressieelsele tasemele. Erinevalt MeJA-st sõltus metanooli ja LOX-de emissioon O_3 -i doosist. Üldiselt põhjustas O_3 talle omase lenduvühendite emissiooni, lisaks olid emissioonid pikaajalised (**I**, **II**).

See, kuivõrd ulatuslik on taimelehe kärbumine peale taime fumigeerimist O_3 -ga, sõltub õhulõhede juhtivusest taime osoneerimise ajal. Hariliku aedoa poolt emiteeritud metanooli ja LOX-de tase viitab sellele, et pimeduse ja madala O_3 -i kontsentratsiooniga eeltöötlemise poolt tingitud õhulõhede sulgumine kaitseb taime hilisemate O_3 -i kahjustuste eest, mida tekitab O_3 -i kõrge kontsentratsioon (**II**).

Taime töötlemine MeJA-ga põhjustas metanooli, LOX-de ning mono- ja seskviterpeenide emissiooni. Kõigi eelpool nimetatud volatiilide emissioonide tase sõltus MeJA-i doosist. Lenduvühendite emissiooni tase ja emissiooni kineetika oli seotud nii O_3 -i kui ka MeJA-i doosiga (**I**, **III**).

ACKNOWLEDGEMENTS

First, I am most grateful to my supervisor Prof. Dr. Ülo Niinemets for giving me the opportunity to study in his lab, with unforgettable experiences in Estonia. Thanks for his insightful guidance, valuable discussions and for his enthusiasm and friendship. This work would never have been happened without his full support and intellectual input.

I am particularly grateful to Dr. Peter C. Harley for his valuable advice and discussions, excellent cooperation, and for his encouragement, kindness and friendship. Thanks for his guidance and helps in instrument operations, planning and executing experiments, and writing scientific papers.

I am thankful to my collaborators who listed as co-authors of my publications for their support and friendly advice, particularly to Dr. Yifan Jiang and Arooran Kanagendran for their friendly cooperation and help throughout my PhD study.

I would like to thank Prof. Ülo Niinemets, Arooran Kanagendran and Dr. Astrid Kännaste for their suggestions and comments during the English language editing process of the thesis. I thank to Dr. Astrid Kännaste and Kaia Kask for their translation and editing of the summary of my dissertation. I would thank Prof. Francesco Loreto and Dr. Federico Brilli for reviewing my thesis.

I would also like to thank Tiia Kurvits, Evi Vaino, Eda Tursk, Lilian Ariva-Türmaa and Veronika Sulg for their academic and administrative support during my study years

I sincerely thank to all the staff members in the Department of Plant Physiology, and also to all my friends and colleagues that I could not mention their names here.

Finally, I would like to wholeheartedly thank my family for their continuous and invaluable love, understanding and support throughout this whole process.

This study was funded by grants from the European Research Council (advanced grant 322603, SIP-VOL+), the European Commission

through the European Regional Fund (Centers of Excellence ENVIRON and EcolChange) and the Estonian Ministry of Science and Education (institutional grant IUT8-3). This study was also supported by Internationalisation Programme DoRa and DoRa Plus. Programmes DoRa and DoRa Plus are carried out by Archimedes Foundation.

ORIGINAL PUBLICATIONS

Li, S., Tosens, T., Harley, P.C., Jiang, Y., Kanagendran, A.,
Grosberg, M., Jaamets, K., Niinemets, Ü. (2018)
Glandular trichomes as a barrier against atmospheric oxidative stress:
relationships with ozone uptake, leaf damage and emission of LOX
products across a diverse set of species.
Plant Cell & Environment, in press.

Glandular trichomes as a barrier against atmospheric oxidative stress: relationships with ozone uptake, leaf damage and emission of LOX products across a diverse set of species

Shuai Li¹, Tiina Tosens¹, Peter C. Harley¹, Yifan Jiang¹, Arooran Kanagendran¹, Mirjam Grosberg¹, Kristen Jaamets¹ & Ülo Niinemets^{1,2}

¹ Institute of Agricultural and Environmental Sciences, Estonian University of Life Sciences, Kreutzwaldi 1, 51014 Tartu, Estonia

² Estonian Academy of Sciences, Kohtu 6, 10130 Tallinn, Estonia

Author for correspondence: Ülo Niinemets, Tel: +372 53457189, Email: ylo.niinemets@emu.ee

Running title: Glandular trichomes promote ozone resistance

This article has been accepted for publication and undergone full peer review but has not been through the copyediting, typesetting, pagination and proofreading process which may lead to differences between this version and the Version of Record. Please cite this article as doi: 10.1111/pce.13128

This article is protected by copyright. All rights reserved.

SUMMARY STATEMENT

Glandular and non-glandular trichomes are widely distributed on leaf surfaces, but the role of different trichome types and trichome density in protection from atmospheric oxidative stress is poorly understood. This study analyzed ozone stress resistance of photosynthesis and induction of stress volatiles in 24 species with widely varying trichome characteristics and taxonomy, and demonstrated that the presence of glandular trichomes strongly reduced stomatal ozone uptake and ozone-dependent damage. This highlights a key role of glandular trichomes in maintenance and physiological homeostasis under atmospheric oxidative stress.

ABSTRACT

There is a spectacular variability in trichome types and densities and trichome metabolites across species, but the functional implications of this variability in protection from atmospheric oxidative stresses remain poorly understood. The aim of the present study was to evaluate the possible protective role of glandular and non-glandular trichomes against ozone stress. We investigated the interspecific variation in types and density of trichomes and how these traits were associated with elevated impacts on visible leaf damage, net assimilation rate, stomatal conductance, chlorophyll fluorescence and emissions of lipoxygenase (LOX) pathway products in 24 species with widely varying trichome characteristics and taxonomy. Both peltate and capitate glandular trichomes played a critical role in reducing leaf ozone uptake, but no impact of non-glandular trichomes was observed. Across species, the visible ozone damage varied 10.1-fold, reduction in net assimilation 3.3-fold and release of LOX compounds 14.4-fold, and species with lower glandular trichome density were more sensitive to ozone stress and more vulnerable to ozone damage compared to species with high glandular trichome density. These results demonstrate that leaf surface glandular trichomes constitute a major factor in reducing ozone toxicity and function as a chemical barrier which neutralizes the ozone before it enters the leaf.

Key words: glandular trichomes, leaf damage, LOX products, ozone stress, ozone uptake, photosynthesis, PTR-TOF-MS

INTRODUCTION

Average global ozone (O₃) concentration has approximately doubled during the 20th century and is expected to increase further (Vingarzan, 2004; Fowler *et al.*, 2008; Logan *et al.*, 2012; Hartmann *et al.*, 2013; Oltmans *et al.*, 2013). Currently, the ambient O₃ concentration in the northern hemisphere is around 20-45 nmol mol⁻¹ and it occasionally reaches 120 nmol mol⁻¹ or more (Fowler *et al.*, 2008; Lai *et al.*, 2012; Yuan *et al.*, 2015; Gao *et al.*, 2016). Numerous studies have revealed that elevated O₃ negatively impacts plant growth and development and decreases forest productivity and crop yields as well as plant biodiversity (Ainsworth *et al.*, 2012; Leisner & Ainsworth, 2012; Wilkinson *et al.*, 2012; Fares *et al.*, 2013). It is well-established that some plant species are more tolerant to elevated O₃ concentrations than others, but the complexity of underlying mechanisms that lead to enhanced O₃ tolerance is not fully understood (Flowers *et al.*, 2007; Ainsworth *et al.*, 2012; Li *et al.*, 2016; Ainsworth, 2017; Feng *et al.*, 2017).

Plant response to O₃ is a complex process involving several biological levels from molecular to organ and whole plant responses. O₃ enters plants mainly through the stomata, and once inside the leaf, it reacts with organic molecules in the apoplast leading to direct formation of reactive oxygen species (ROS) as well as induction of endogenous formation of ROS that can collectively lead to the onset of cell damage and programmed cell death when the O₃ concentration exceeds critical levels (Wohlgenuth *et al.*, 2002; Pasqualini *et al.*, 2003; Beauchamp *et al.*, 2005; Fiscus *et al.*, 2005; Cho *et al.*, 2011; Ainsworth, 2017; Li *et al.*, 2017; Kanagendran *et al.*, 2017). Generally, progressive and irreversible reductions in photosynthetic activity occur upon acute O₃ exposure, and direct injury to leaf cells in O₃-exposed leaves is also associated with the release of ubiquitous stress-induced

volatiles such as volatile products of lipoxygenase (LOX) reactions comprising of various C6 aldehydes and alcohols (Heiden *et al.*, 1999; Beauchamp *et al.*, 2005; Loreto & Schnitzler, 2010; Li *et al.*, 2017). Reductions in the quantum yield of primary photochemistry in the dark-adapted state and emissions of LOX and other volatile organic compounds (VOC) are widely used characteristics to assess plant response to O₃ stress (Nussbaum *et al.*, 2001; Beauchamp *et al.*, 2005; Bussotti *et al.*, 2011; Chutteang *et al.*, 2016; Li *et al.*, 2017).

O₃ sensitivity varies across species and depends on several species-specific biochemical, physiological and morphological traits (Li *et al.*, 2016). Regarding the physiological and biochemical traits, differences in O₃ sensitivity have been related to inherent differences in stomatal conductance and to the leaf antioxidant capacity (Brosché *et al.*, 2010; Fares *et al.*, 2013). Very few studies have been conducted to understand to which extent morphological traits such as trichome morphology and density or differences in exposed mesophyll cell surface or other structural traits such as leaf mass per unit area, leaf nitrogen content and life form may affect interspecific variation in O₃ sensitivity when exposed to acute rather than chronic low to moderate level O₃ (Franzaring *et al.*, 1999; Prozherina *et al.*, 2003; Hayes *et al.*, 2007; Li *et al.*, 2016).

The leaf surface is covered by glandular and/or non-glandular trichomes in many species. Non-glandular trichomes, which are not able to produce or secrete phytochemicals, serve to increase herbivore resistance by interfering mechanically with herbivore movement and/or feeding (Eisner *et al.*, 1998; Corsi & Bottega, 1999; Kennedy, 2003). In addition, by increasing surface reflectance they contribute to reduced solar radiation interception and thus, to enhanced resistance to low water availabilities and photoinhibition stress (Ehleringer, 1981, 1982; Cescatti & Niinemets, 2004; Hallik *et al.*, 2017). However, due to increasing surface area, non-glandular trichomes could potentially participate in chemical reactions on leaf surface as well, e.g. in O₃ adsorption, but little is known of relationships between non-glandular trichome density and species O₃ resistance. However, given that non-glandular trichomes are covered by a wax layer that consists of saturated hydrocarbons that have low reactivity with O₃ (Corsi & Bottega, 1999), it might also be that the effect of non-glandular trichomes in leaf O₃ resistance is minor despite greater surface area.

Glandular trichomes, which store and secrete various secondary metabolites such as flavonoids, monoterpenes or sesquiterpene lactones, are widely distributed on leaf surfaces and may contribute significantly to defense against diverse biotic and environmental challenges (Ehleringer *et al.*, 1976; Huci *et al.*, 1982; Rieseberg *et al.*, 1987; Wagner, 1991; Fahn & Shimony, 1996; Kostina *et al.*, 2001; Heinrich *et al.*, 2002; Amme *et al.*, 2005; Paoletti *et al.*, 2007; Peiffer *et al.*, 2009; Agati *et al.*, 2012; Jud *et al.*, 2016; Lihavainen *et al.*, 2017; Thitz *et al.*, 2017). Two major types of glandular trichomes, peltate and capitate, have been discerned. There are various types of capitate trichomes varying in stalk and head size, and although the basic morphology of peltate trichomes varies less, there is still a significant variation in the shapes and sizes of peltate trichomes as well (Ascensão *et al.*, 1995; Ascensão & Pais, 1998; Baran *et al.*, 2010; Glas *et al.*, 2012). Capitate trichomes are specialized to produce and store a large amount of diterpenes and a wide array of non-volatile or poorly volatile compounds such as defensive proteins, acylated sugars and esters that are directly exuded onto trichome surface (Sallaud *et al.*, 2012; Jud *et al.*, 2016). Their primary function is thought to repel pests. Peltate glandular trichomes, on the other hand, mostly produce and store biogenic volatile or semi-volatile organic compounds related to plant abiotic or biotic stress induced responses (Corsi & Bottega, 1999; Gang *et al.*, 2001; Wagner *et al.*, 2004). Recently, Jud *et al.* (2016) showed that semi-volatile organic compounds such as various diterpenoids exuded by the glandular trichomes of *Nicotiana tabacum* act as an efficient chemical protection shield against stomatal O₃ uptake by reacting with and thereby depleting O₃ at the leaf surface. However, the shape and size of glandular trichomes as well as the metabolites stored vary greatly across plant species, and the generality of this finding is currently unclear. Although several studies have demonstrated the important protective role of trichomes in O₃ stress resistance in a given species (Huci *et al.*, 1982; Prozherina *et al.*, 2003; Paoletti *et al.*, 2007; Riikonen *et al.*, 2010), their potential role in O₃ resistance across different plant species, in particular under acute exposure, has not been investigated to date.

Considering leaf surface reactions, it is important to distinguish between O₃ exposure, O₃ uptake by leaf and uptake through the stomata to accurately characterize the thresholds for acute responses. However, this is not fully possible until we discern the extent of O₃ neutralization at the leaf surface

(Jud *et al.*, 2016) and determine the extent to which leaf internal O₃ concentrations can build up (Moldau & Bichele, 2002; Niinemets *et al.*, 2014). To fill the gap in understanding the role of trichomes in defense against O₃ stress, we examined interspecific variation in O₃ sensitivity in 24 species with varying densities of non-glandular and glandular trichomes on the leaf surface. The main hypotheses tested were (1) leaves with a high density of glandular trichomes have higher rates of non-stomatal O₃ uptake, resulting in greater O₃ resistance as evidenced by less negative effects on their physiology at the given O₃ exposure concentration; (2) non-glandular trichomes have no significant protective role under O₃ exposure; (3) peltate glandular trichomes have a major impact on non-stomatal O₃ uptake. We demonstrate a broad relationship between O₃ resistance and glandular trichome density across a highly diverse set of species, suggesting that glandular trichomes do serve as an important antioxidative barrier. To our knowledge, this is the first study to provide information on how non-glandular and glandular trichomes can contribute to plant ability to cope with increased O₃ levels and maintain physiological homeostasis under atmospheric oxidative stress.

MATERIALS AND METHODS

Plant materials and growth conditions

Twenty three herbaceous species, selected for their wide range of trichome characteristics (trichome density, glandular vs. non-glandular, capitate vs. peltate) were chosen for this study (*Anchusa officinalis* L., *Arctium tomentosum* Mill, *Carduus crispus* L., *Cucumis sativus* L. cv. Libelle F1, *Cucurbita pepo* L., *Erigeron acer* L., *Erigeron canadensis* L., *Erodium cicutarium* L., *Geranium palustre* L., *Geranium pratense* L., *Geranium robertianum* L., *Lavandula angustifolia* Mill, *Mentha × piperita* L., *Nicotiana tabacum* L. cv. W38, *Ocimum basilicum* L., *Phaseolus vulgaris* L. cv. Saxa, *Rosmarinus officinalis* L., *Salvia officinalis* L., *Silene latifolia* Poir, *Solanum lycopersicum* L. cv. Pontica, *Tussilago farfara* L., *Urtica dioica* L. and *Verbascum thapsus* L.). In addition, although woody species generally exhibit greater tolerance to O₃ than herbaceous species, we chose a single woody species, *Betula pendula* Roth, was included. Plants of *C. sativus*, *N. tabacum*, *O. basilicum*, *P. vulgaris*, *S. lycopersicum* and *V. thapsus* were grown from seed (seed sources: *C. sativus*: Seston

Seemned OÜ, Estonia; *N. tabacum*: gift of I. Bichele, University of Tartu; *O. basilicum* and *S. lycopersicum*: SC Agrosel SRL, Romania; *P. vulgaris*: Dalema UAB, Vilnius, Lithuania; the seed of *V. thapsus* were collected in the field in Tartu, Estonia). After germination, seedlings were replanted in 2 L plastic pots containing a commercial potting mix (Kekkilä Group, Vantaa, Finland) and maintained in a plant room with light intensity at plant level of 400 $\mu\text{mol m}^{-2} \text{s}^{-1}$ (HPI-T Plus 400 W metal halide lamps, Philips) during 12 h photoperiod. The day/night temperatures were maintained at 24/20 °C and daytime humidity at 60%. Seedlings of *B. pendula*, and plants of *G. palustre*, *G. pratense* and *U. dioica* were collected from the campus of the Estonian University of Life Sciences (EULS), Tartu, Estonia (58°23' N, 27°05' E, elevation 40 m), the plants of *E. acer*, *E. canadensis*, *E. cicutarium* and *S. latifolia* from Ihaste, Tartu (58°21' N, 26°46' E, elevation 41 m), and plants of *G. robertianum* from Pühajärve, Estonia (58°03' N, 26°28' E, elevation 131 m). The plants were replanted in 2 L plastic pots containing the same potting mix, and maintained on the roof of the plant biology lab building at the campus of EULS and were exposed to full sunlight under ambient conditions. All plants were fertilized once in two weeks with Biolan NPK (N of 100 mg L⁻¹, P of 30 mg L⁻¹, and K of 200 mg L⁻¹) complex fertilizer with microelements (Biolan Oy, Kekkilä Group, Vantaa, Finland) and they were watered every day to maintain optimal growth conditions.

In the case of *N. tabacum* and *V. thapsus* that had leafed petioles making it difficult to achieve a good seal upon enclosure of the leaf to the gas-exchange chamber, we removed the part of the lamina attached to the base of the leaf, while avoiding cutting through first- and second-order veins. In order to minimize the influence of leaf damage on volatile organic compound (VOC) emissions, at least two days were allowed for recovery before conducting measurements. According to previous measurements, the effect of lamina wounding is short-living with the bulk of the stress volatiles released within first 5-10 min after wounding (Portillo-Estrada *et al.*, 2015). We also did not observed any subsequent induction of stress volatiles and volatile isoprenoids after wounding, and leaf photosynthesis measurements with clip-on type gas-exchange system (Walz GFS-3000, Walz GmbH, Effeltrich, Germany) demonstrated that the wounding also did not alter foliage photosynthesis rate and stomatal conductance at 48 h since wounding stress (data not shown).

The leaves of *A. officinalis*, *A. tomentosum*, *C. crispus*, and *T. farfara* were collected from the campus of the EULS and leaves of *C. pepo*, *L. angustifolia*, *M. × piperita*, *R. officinalis* and *S. officinalis* were collected from the gardens of Tartu city. All plants sampled had developed in open areas exposed to full sunlight. Early in the morning, high light exposed terminal shoots with multiple leaves were excised with a sharp razor blade under water and immediately transported to the laboratory. Once in the laboratory, the cut ends of the shoots were recut under water and a representative leaf was selected for measurements. All measurements were conducted with fully-expanded non-senescent leaves.

Gas-exchange system for photosynthesis, stomatal conductance, volatile organic compound and ozone concentration measurements

We used a custom-built gas-exchange system with a temperature-controlled 1.2 L glass chamber described in detail by Copolovici & Niinemets (2010) to fumigate leaves with O₃ and to measure leaf gas exchange characteristics (net photosynthesis and stomatal conductance) and VOC. The ambient air was drawn from outside, passed through a 10 L buffer volume, purified by an O₃ trap and a charcoal filter, humidified by a custom-made humidifier to standard air humidity of 60% and then passed at a flow rate of 1.6 L min⁻¹ to the glass chamber. The air entering or leaving the chamber was analyzed alternately, with an electronic valve switching between incoming (reference) and outgoing (measurement) air streams. To mix the chamber air and to minimize leaf boundary layer resistance, a fan was mounted inside the chamber. The leaf temperature was maintained at 25 °C, ambient CO₂ concentration at 400 μmol mol⁻¹ and light intensity at the leaf surface was 1000 μmol m⁻² s⁻¹ during the experiment.

An infra-red dual-channel gas analyzer (CIRAS II, PP-Systems, Amesbury, MA, USA) operated in absolute mode was used to measure CO₂ and H₂O concentrations, a proton transfer reaction-time of flight-mass spectrometer (PTR-TOF-MS, Ionicon Analytik GmbH, Innsbruck, Austria) to determine VOC concentration and a UV-photometric O₃ sensor (Model 49i, Thermo Scientific, Massachusetts, USA) to measure O₃ concentrations. All instruments were operated continuously and CO₂ and H₂O

concentrations and all PTR-TOF-MS signals were recorded every 10 s and the range of O₃ concentrations was recorded for every 15 min interval. Reference measurements (incoming air) were conducted every 10-15 min.

Ozone fumigation treatments

Ozone exposure treatments were carried out using O₃ concentrations that constituted a moderately severe stress leading to visible leaf damage but not resulting in leaf death during more than 20 hours following the experimental treatment. After the leaves were enclosed in the chamber, continuous measurements of photosynthetic characteristics and trace gas exchange were begun immediately. O₃ fumigation was started after stabilization of net photosynthesis and VOC emissions, typically 20-30 min after leaf enclosure. O₃ was generated in a quartz glass reaction chamber (Stable Ozone Generator, Ultra-Violet Products Ltd, Cambridge, UK) under UV light ($\lambda=185$ nm) and monitored by a UV-photometric O₃ sensor (Model 49i, Thermo Scientific, Massachusetts, USA). The O₃ enriched air from the reaction chamber was mixed with the air stream entering the leaf chamber. The leaf was fumigated with a step-wise increase in O₃ concentration as follows: 100 ± 5 nmol mol⁻¹ of O₃ for 30 min, followed by 200 ± 10 nmol mol⁻¹ for 30 min, and so on progressively, increasing O₃ concentration by 100 nmol mol⁻¹ in half-hour steps until the final maximum O₃ concentration that lead to a sharp decrease in net assimilation rate and stomatal conductance was reached. This final O₃ concentration varied by plant species. Due to logistic difficulties, PTR-TOF-MS measurements could be carried out in six species with different glandular trichome density (*C. sativus*, *N. tabacum*, *O. basilicum*, *P. vulgaris*, *S. lycopersicum* and *V. thapsus*). In order to further investigate the effect of O₃ concentration rather than O₃ uptake on volatile LOX product emissions, we applied the same O₃ stress with a step-wise increase from 100 to 500 nmol mol⁻¹ for these six species. In all cases, the duration of exposures at each O₃ concentration was 30 min and the stability of O₃ concentration within the leaf chamber was \pm 5-10% of the target. The gas-exchange characteristics and trace gas-exchange were also continuously monitored for 21 h after each of the treatments. The treated leaves were then harvested and their area (*S*) and the quantitative degree of damage visible as necrotic or chlorotic lesions were estimated using ImageJ software (National Institutes of Health, Bethesda, MD, USA).

Operation of the PTR-TOF-MS and online monitoring of the kinetics of volatile release

The main advantages of PTR-TOF-MS are simultaneous detection of all masses rather than predetermined masses, and higher sensitivity, higher mass resolution as well as improved accuracy over the traditional quadrupole PTR (PTR-QMS); this allows quantification of a larger number of organic compounds at trace levels in real time (Jordan *et al.*, 2009; Graus *et al.*, 2010). The PTR-TOF-MS was operated according to the method described in detail in Graus *et al.* (2010), Brilli *et al.* (2011) and Portillo-Estrada *et al.* (2015). The drift tube voltage was kept at 600 V at 2.3 mbar drift pressure and 60°C temperature, corresponding to an $E/N \approx 130$ Td in H_3O^+ reagent ion mode. The PTR-TOF-MS system was calibrated with a calibration standard mixture containing key volatiles from different compound families (Ionimed Analytic GmbH, Austria). The data acquisition software TofDaq (Tofwerk AG, Switzerland) was used to acquire the raw data and the data were further post-processed by PTR-MS Viewer software (PTR-MS Viewer v3.1, Tofwerk AG, Switzerland) (Jordan *et al.*, 2009; Portillo-Estrada *et al.*, 2015; Li *et al.*, 2017).

The total amount of lipoxygenase pathway products (LOX products) emission presented in this study is the sum of the dominant compounds with mass signals m/z 81.070 [hexenal (fragment)], m/z 83.085 [hexenol + hexenal (fragments)], m/z 85.101 [hexanol (fragment)], m/z 99.080 [(Z)-3-hexenal + (E)-3-hexenal (main)], m/z 101.096 [(Z)-3-hexenol + (E)-3 hexenol + (E)-2-hexenol + hexenal (main)] (Brilli *et al.*, 2011; Portillo-Estrada *et al.*, 2015; Li *et al.*, 2017).

Chlorophyll fluorescence measurements

To visualize the distribution of photosynthetic electron transport activity of leaves before and after the O_3 treatment, a portable Imaging-PAM chlorophyll fluorometer with ImagingWin software (Imaging-MIN/B, Heinz Walz GmbH, Effeltrich, Germany) was used. The Mini version of the Imaging-PAM M-series has a measurement window area of 24×32 mm and uses a CCD camera (640×480 pixel) for fluorescence imaging and 12 high-power LED lamps to provide actinic light and high-intensity light flashes. After the leaf was fixed in the leaf holder of the Imaging PAM, and dark-adapted for 30 min at 25°C, the minimum fluorescence yield (F_0) was measured, the maximum dark-adapted fluorescence

yield (F_m) was then determined by illuminating the leaves with a 500 ms pulse of saturating irradiance of 2700 $\mu\text{mol quanta m}^{-2} \text{s}^{-1}$. The spatially-averaged maximum dark-adapted quantum yield of PSII, F_v/F_m was calculated as $(F_m - F_0)/F_m$.

Scanning electron microscopy and analyses of density and morphology trichomes

To quantify the trichome characteristics, a Zeiss EVO LS15 Environmental Scanning Electron Microscope (ESEM, Carl Zeiss AG, Jena, Germany) was used. A fresh leaf adjacent to the leaf used for O_3 fumigation was mounted on brass stubs. The samples were viewed and images taken with the ESEM at an acceleration voltage of 15 kV under the low vacuum mode. Images acquired from ESEM were analyzed with the ImageJ software. Trichome density was estimated from the middle zones of both leaf surfaces (adaxial and abaxial) avoiding major veins. Three to ten areas of view were selected for measurements, and all trichomes were counted within 1 mm^2 areas. The type of glandular trichomes - peltate or capitate - was identified from ESEM images as suggested by Ascensão *et al.* (1995), Ascensão & Pais (1998), Ko *et al.* (2007) and Baran *et al.* (2010), and averages were calculated for all fields of view for the given leaf on both upper and lower surface.

Empty chamber corrections

The background volatile samples were measured from the empty chamber before the plant measurements to correct for possible emission of volatiles adsorbed previously on gas-exchange system components. Although such corrections were minor ($\leq 1\%$), they were included in the calculations for consistency (Niinemets *et al.*, 2011). O_3 destruction due to surface reactions (“uptake”) by the empty chamber ($C_{\text{O}_3}^{\text{chamber}}$, nmol mol^{-1}) was measured before the plant measurements and calculated as:

$$C_{\text{O}_3}^{\text{chamber}} = C'_{\text{in}} - C'_{\text{out}} \quad \text{Eqn 1}$$

where C'_{in} is the O_3 concentration at the chamber inlet and C'_{out} that at the chamber outlet. The values obtained were subsequently used to correct all measurements of leaf O_3 uptake. Overall, this correction was minor, less than 5% of total O_3 uptake when leaves were enclosed in the chamber.

Calculations of photosynthesis, stomatal conductance, trace gas emission rates and ozone uptake

Net assimilation rate (A_n) and stomatal conductance (g_s) per leaf area were calculated according to von Caemmerer & Farquhar (1981).

Volatile emissions rates (ϕ_x , nmol m⁻² s⁻¹) were calculated as

$$\phi_x = \frac{F}{S} [C_o(X) - C_i(X) - C_c(X)] \quad \text{Eqn 2}$$

where F is the flow rate through the chamber (1.19×10^{-3} mol s⁻¹), and S is the leaf area enclosed in the chamber (m²), $C_o(X)$ is the concentration (nmol mol⁻¹) of the target VOC (compound X) measured at the chamber outlet and $C_i(X)$ of that measured at the chamber inlet, $C_c(X)$ is the correction to account for the possible release of the given compound released from the gas-exchange system components (Beauchamp *et al.*, 2005; Li *et al.*, 2017).

The total amount of target VOC emitted over a certain time (Φ_x) (nmol m⁻²) was integrated as:

$$\Phi_x = \sum_{t_{PS}}^{t_{PE}} \Delta t \phi_x \quad \text{Eqn 3}$$

where t_{PS} and t_{PE} are the start and end times of the target VOC emission release, Δt is the measurement time interval (10 s), and ϕ_x is the emission rate of the target VOC measured over this time interval (Beauchamp *et al.*, 2005; Li *et al.*, 2017). The total emission values correspond to the whole experiment, from elicitation to 21 h since the end of the experiment.

The rate of O₃ uptake by the leaf (ϕ_{LO_3} , nmol m⁻² s⁻¹) was calculated as:

$$\phi_{LO_3} = \frac{F}{S} (C_{in} - C_{out} - C_{O_3}^{chamber}) \quad \text{Eqn 4}$$

where C_{in} and C_{out} are the O₃ concentrations in the air entering and exiting the leaf chamber (nmol mol⁻¹). We calculated C_{in} and C_{out} as the average value over the given time interval due to the fluctuations of O₃ concentration produced by the ozone generator and manual adjustment of C_{in} to account for changes in O₃ uptake during the exposure.

The rate of O₃ uptake by stomata (ϕ_{GO_3} , nmol m⁻² s⁻¹) was determined by:

$$\phi_{\text{GO}_3} = (C_{\text{out}} - C_{\text{O}_3}^i) \frac{g_s}{2.03} \quad \text{Eqn 5}$$

where $C_{\text{O}_3}^i$ is intercellular O₃ concentration (nmol mol⁻¹), and 2.03 is the ratio of water vapor to O₃ diffusivities (Li *et al.*, 2017). Given that $C_{\text{O}_3}^i$ is typically small compared with C_{out} , and it cannot be estimated from these measurements, it was assumed to be zero (Laisk *et al.*, 1989; but see Moldau & Bichele, 2002). To be consistent with the C_{out} calculations, stomatal conductance (g_s) was also determined as the average value over the same time interval.

The total amount of leaf and stomatal O₃ uptake (Φ_Y , where Y stands either for leaf, LO₃, or for stomatal, GO₃, O₃ uptake) over the given exposure period (O₃ dose) was integrated as:

$$\Phi_Y = \sum_{t_s}^{t_E} \Delta t \phi_Y \quad \text{Eqn 6}$$

where t_s and t_E are the start and end times of O₃ exposure, Δt is the time interval of the O₃ exposure, and ϕ_Y is either the mean rate of ϕ_{LO_3} or the mean rate of ϕ_{GO_3} measured during this time interval (Beauchamp *et al.*, 2005). Ultimately, the total amount of non-stomatal O₃ uptake (Φ_{NGO_3}), i.e. presumably O₃ uptake by the leaf surface was determined by:

$$\Phi_{\text{NGO}_3} = \Phi_{\text{LO}_3} - \Phi_{\text{GO}_3} \quad \text{Eqn 7}$$

where Φ_{LO_3} is the total measured amount of O₃ uptake by the whole leaf and Φ_{GO_3} is the calculated O₃ uptake through the stomata. We note that chemical quenching of O₃ in chamber air by volatiles in the leaf chamber or by volatiles on the leaf surface is also possible and is incorporated in the value of Φ_{NGO_3} .

Quantitative characterization of the protective role of glandular trichomes against O₃ stress

To further characterize the functional role of glandular trichomes in ameliorating changes in leaf physiological characteristics and LOX product emission under O₃ stress, the plant response per unit O₃ taken up by the leaf (γ , O₃ uptake weighted response) was calculated as:

$$\gamma_{Z/\Phi_Y} = Z / \Phi_Y$$

Eqn 8

where Z represents the percentage decrease of A_n , g_s and F_v/F_m or the total amount or maximum rate of LOX products emitted over a certain time (Eqn 3). Analogously, the plant response per unit O_3 taken up by stomata was also calculated for each of these traits.

Data analysis

All O_3 fumigation treatments were conducted in three to five replications ($n=3-5$) with different plants in each species. Linear- and non-linear regressions were used to analyze the effects of O_3 on foliage traits and relationships between leaf trichome density and physiological traits. All relationships were considered significant at $P < 0.05$.

RESULTS

Trichome morphology, distribution and density

Non-glandular and glandular trichomes were both present on the leaf surfaces of the 24 studied species (Fig. 1). The density of non-glandular trichomes varied 250-fold across species (Table 1). Two types of glandular trichomes (peltate and capitate) were identified (Fig. 1). Capitate glandular trichomes were present in all species, but peltate glandular trichomes were found only in 12 species belonging to the family Lamiaceae (*L. angustifolia*, *M. × piperita*, *O. basilicum*, *R. officinalis* and *S. officinalis*) and Geraniaceae (*E. cicutarium*, *G. pratense* and *G. robertianum*) and in *B. pendula*, *E. canadensis*, *S. latifolia* and *U. dioica* (Table 1). The density of capitate glandular trichomes varied from 1 mm⁻² in *C. pepo* to 90 mm⁻² in *R. officinalis*, and peltate glandular trichome density varied from 5.9 mm⁻² in *G. robertianum* to 60 mm⁻² in *R. officinalis* (Table 1). No significant correlation between glandular and non-glandular trichome density was found in the species with only capitate trichomes and with both capitate and peltate glandular trichomes (Fig. S1).

Kinetics of O₃ uptake flux and stomatal conductance with rising O₃ concentration

During stepwise increases in O₃ in all species, stomatal conductance (g_s) declined with increasing O₃ exposure (filled symbols, Fig. 2a for representative responses in *P. vulgaris*, *N. tabacum* and *S. lycopersicum*). Relative to the values prior to low-level O₃ fumigation (100 nmol mol⁻¹), stomatal conductance (g_s) decreased by 27% in *P. vulgaris*, 66% in *N. tabacum* and 55% in *S. lycopersicum* in response to higher-level O₃ exposure treatment (400-700 nmol mol⁻¹). Despite of sharp decreases in g_s , O₃ uptake by the leaf (ϕ_{LO_3}) increased in all three species (Fig. 2a) although the continuing decrease in g_s at high O₃ concentration eventually caused O₃ uptake to level off and then decline in *N. tabacum* and *S. lycopersicum*. In *P. vulgaris*, the percentage of non-stomatal O₃ uptake increased with rising O₃ concentration (Fig. 2b). The changes in total O₃ uptake and stomatal conductance (g_s) during O₃ fumigation in *N. tabacum* and *S. lycopersicum* were generally similar to *P. vulgaris* up to O₃ concentration of 400 nmol mol⁻¹. However, when O₃ concentration was raised to 600 or 700 nmol mol⁻¹ O₃ uptake by the leaf (ϕ_{LO_3}) and stomata (ϕ_{GO_3}) started to decrease because of the lower stomatal conductance (Fig. 2). The percentage of non-stomatal O₃ uptake (i.e., O₃ removal at the leaf surface) in leaves of *N. tabacum* and *S. lycopersicum* declined somewhat over the course of the experiment as O₃ concentrations increased (Fig. 2b). These responses were analogous in other species studied (data not shown).

The relationships between non-stomatal O₃ uptake and trichome types and density

There was no correlation between non-glandular trichome density and the percentage of non-stomatal O₃ uptake (Fig. 3a), and we also found no correlation between the size (length and width) of non-glandular trichomes with the amount of non-stomatal O₃ uptake (data not shown). In contrast, the glandular trichome density was strongly correlated with the percentage of non-stomatal O₃ uptake ($P < 0.0001$; Fig. 3b). The correlations were even stronger when species with capitate glandular trichomes only and species with both peltate and capitate type glandular trichomes were examined separately although the latter group had overall greater non-stomatal O₃ uptake (Fig. 3c).

The glandular trichome density showed highly significant correlations with the threshold of total leaf O₃ uptake that induced a sharp decrease in net assimilation rate and stomatal conductance ($P < 0.0001$; Fig. 4a,c), but it was not correlated with the threshold of total stomatal O₃ uptake (Fig. 4b,d).

In the case of induction of volatile LOX product emissions, glandular trichome density showed a non-significant correlation ($P = 0.09$) with the threshold of total leaf O₃ uptake for all species pooled (Fig. 4e), but a significant correlation ($P < 0.01$) in the case of species with only capitate glandular trichomes (inset in Fig. 4e), and no significant correlation with the threshold of total stomatal O₃ uptake (Fig. 4f). However, a significant negative relationship ($P < 0.0001$) between the total amount of volatile LOX pathway products released and glandular trichome density was observed (Fig. 5).

Changes in physiological characteristics and LOX product emissions in response to O₃ exposure in relation to glandular trichome density

Both net assimilation rate (A_n) and stomatal conductance (g_s) were significantly decreased after O₃ exposure compared to the rates prior to O₃ fumigation. O₃-induced relative reductions in A_n and g_s were strongly determined by glandular trichome density ($P < 0.05$; Fig. 6a,b). Visible leaf injury was also less in species with greater glandular trichome density at the same amount of leaf O₃ uptake ($P < 0.05$; Fig. 6c). There was overall reduction of F_v/F_m per ppb O₃ taken up by the leaf (O₃ uptake weighted F_v/F_m , Eq. 8), but the correlation with glandular trichome density was not significant (Fig. 6d). Additionally, no significant correlations were observed between glandular trichome density and relative reduction in stomatal uptake weighted A_n , g_s , F_v/F_m and visible leaf injury (Fig. S2a-d). However, glandular trichome density was negatively correlated with O₃ uptake weighted total LOX product emission and maximum LOX product emission rate, regardless of whether the calculations were based on O₃ taken up by the entire leaf ($P < 0.05$; Fig. 6e,f) or by stomata ($P=0.05$ and $P=0.06$, Fig. S2e,f), and the data were best fitted by nonlinear regressions (Fig. 6e,f and Fig. S2e,f). Across all treatments, visible leaf damage assessed at the end of the O₃ exposure was a good indicator of reductions in foliage physiological characteristics and elicitation of LOX volatiles, except for reductions in stomatal conductance (Fig. 7).

Correlations among O₃ uptake and leaf damage and with emissions of LOX products

To estimate O₃ damage across different species, we compared the correlations of modification in leaf physiological traits and leaf damage with O₃ uptake by the whole leaf (Φ_{LO_3}), stomatal O₃ uptake (Φ_{GO_3}) and non-stomatal O₃ uptake (Φ_{NGO_3}). Φ_{LO_3} was not correlated with the percentage of decrease in A_n , g_s and F_v/F_m , but a significant positive correlation ($P < 0.0005$) with the percentage of visibly damaged leaf area was observed (Fig. S3a-d). Furthermore, Φ_{LO_3} was also positively correlated with the total LOX product emission and maximum LOX product emission rate ($P < 0.05$; Fig. S3e,f). Apart from the protective role of glandular trichomes against O₃ stress, the O₃ dose ultimately entering into the leaf is crucial in understanding the magnitude of reductions in photosynthesis, appearance of visible lesions, and emission of LOX products. Φ_{GO_3} was strongly correlated with the amount of visible leaf damage ($P < 0.05$; Fig. 8c), but there was no correlation between Φ_{GO_3} and the percent decrease in A_n , g_s or F_v/F_m (Fig. 8a,b,d). Furthermore, a positive non-linear relationship was found between Φ_{GO_3} and both the total LOX product emission and maximum LOX product emission rate across the species ($P < 0.05$; Fig. 8e,f).

Φ_{NGO_3} was not correlated with the percentage decrease in A_n , g_s and F_v/F_m , and total amount of visible leaf damage and LOX product emissions (Fig. S4). Finally, the percentage of non-stomatal O₃ uptake showed highly significant correlation with the percentage decrease in F_v/F_m ($P < 0.005$) but it was correlated with the percentage decrease in A_n and g_s , amount of visible leaf damage and LOX product emissions (Fig. S5).

DISCUSSION

Variation in trichome types and density across species

Non-glandular and glandular trichomes were found on the surfaces of all studied leaves. Specifically, two types of glandular trichomes on the surface were identified: peltate and capitate (Fig. 1). All species had capitate trichomes whereas peltate trichomes were observed only on the surface of 12 species. This agrees with previous observations by Glas *et al.* (2012), demonstrating more frequent

occurrence of capitate glandular trichomes. According to past reports available for some of the species studied here, peltate and capitate trichome densities vary between 1-140 mm² (Wilkens *et al.*, 1996; Ranger & Hower, 2001; Valkama *et al.*, 2004; Kapoor *et al.*, 2007; Lihavainen *et al.*, 2017; Thitz *et al.*, 2017). Correspondingly, the species studied here fell in the same range.

As outlined in the introduction, glandular and non-glandular trichomes play different roles in plant defense. Non-glandular trichomes are linked to mechanical defense against biotic and environmental stressors, while glandular trichomes produce metabolites for the alleviation of those stressors (Levin, 1973; Lihavainen *et al.*, 2017). Glandular and non-glandular trichome density was not correlated suggesting that various selection pressures have occurred independently.

Glandular trichomes affect stomatal O₃ uptake and increase the threshold of acute O₃ responses

Stomata exert a strong control over leaf interior O₃ concentrations and thus, play a major role in protecting leaves from O₃ stress (Beauchamp *et al.*, 2005; Li *et al.*, 2017). Likewise, in this study, the step-wise increases in O₃ concentration induced simultaneous stomatal closure (Fig. 2). In addition, data on non-stomatal O₃ uptake (Φ_{NGO_3}) during the exposure revealed that O₃ was significantly destroyed by leaf surface reactions. Factors that reduce O₃ concentrations at leaf surface will reduce O₃ entry into the leaf interior through the stomata and lower the effective O₃ dose received by the plant. In our study, capitate and peltate glandular trichomes were both related to Φ_{NGO_3} (Fig 3), whereas peltate glandular trichomes were more strongly related to reduced stomatal O₃ uptake than capitate glandular trichomes, but surprisingly, non-glandular trichomes did not affect at all leaf O₃ uptake.

Across species, a wide variety of metabolites are stored and exuded by glandular trichomes at the leaf surface (Rieseberg *et al.*, 1987; Wagner, 1991; Fahn & Shimony, 1996; Heinrich *et al.*, 2002; Amme *et al.*, 2005; Peiffer *et al.*, 2009; Agati *et al.*, 2012; Jud *et al.*, 2016; Lihavainen *et al.*, 2017). It has been suggested that unsaturated semi-volatile compounds destroy O₃ before it enters the leaf (Jud *et al.*, 2016). Furthermore, high glandular trichome density is often associated with the presence of high concentrations of more volatile terpenoids, but also other non-volatile defense compounds such

as acylated sugars and proteins (Gang *et al.*, 2001; Amme *et al.*, 2005). As different types of trichomes may have vastly different composition of secreted compounds (e.g. Fahn & Shimony, 1996; Heinrich *et al.*, 2002; Amme *et al.*, 2005; Kant *et al.*, 2009; Jud *et al.*, 2016), such differences among capitate and peltate glandular trichomes might reflect differences in the chemical reactivity with O₃ of main chemical constituents synthesized in different trichomes. Peltate glandular trichomes are a major site of semi-volatile compound production and contain a much larger oil sac into which these compounds are secreted (e.g. Fahn, 1979; Gang *et al.*, 2001; Amme *et al.*, 2005). Nevertheless, tobacco lacks peltate trichomes, but in this species, the degree of non-stomatal O₃ uptake also correlates strongly with the density of capitate trichomes and their exudates, indicating that capitate trichomes also contribute strongly to surface reactions with O₃ (Jud *et al.*, 2016). In fact, Jud *et al.* (2016) suggested that diterpenes exuded from tobacco trichomes were responsible for O₃ quenching.

Non-glandular trichomes can form a dense indumentum on leaf surface that serve as a mechanical barrier against herbivores and pathogens (Eisner *et al.*, 1998; Corsi & Bottega, 1999; Kennedy, 2003), but their role in antioxidative responses is less clear. Several species in our study had a massive amount of non-glandular trichomes (Table 1), but we found no correlation between the density of non-glandular trichomes with the amount of non-stomatal O₃ uptake in the present study (Fig. 3a). This likely reflects the circumstance that non-glandular trichomes possess no secretory structures and are covered by a wax layer that consists of long-chained saturated oxygenated and non-oxygenated hydrocarbons (Corsi & Bottega, 1999) that have very low reactivity with O₃.

O₃ dose ultimately entering the plant interior is known to determine the amount of visible leaf damage, but in the case of mild O₃ uptake not exceeding a certain O₃ threshold, neither damage to the leaf biochemical apparatus nor induction of VOC emission have been observed (Nussbaum *et al.*, 2001; Beauchamp *et al.*, 2005; Velikova *et al.*, 2005; Niinemets, 2010). In our study, we found a stronger relationship between glandular trichome density and the threshold for acute responses caused by O₃ taken up by leaf than with that taken up through stomata (Fig. 4), indicating that trichome density promotes O₃ tolerance of plants. However, once O₃ enters the leaf, all species had similar threshold values regardless of trichome density. Moreover, the total emission of volatile LOX

products was related to glandular trichome density under the same stepwise increase of O₃ concentration and duration of fumigation (Fig. 5). By combining the correlations between glandular trichome density and non-stomatal O₃ uptake, we have further demonstrated that glandular trichomes directly reduce O₃ concentration at the leaf surface and thus indirectly reduce stomatal O₃ uptake. While previously this has been shown for tobacco (Jud *et al.*, 2016), our results extend this observation to a highly diverse set of plants with a large variability in trichome types, densities and likely also with exudates with highly diverse chemical nature. These results further confirm the previous suggestions that the plants' acute responses are determined directly by O₃ dose taken up by stomata (Φ_{GO_3}) (Beauchamp *et al.*, 2005; Jud *et al.*, 2016; Li *et al.*, 2017), but also emphasize that these responses are importantly modified by glandular trichome density.

Effects of elevated O₃ concentration on foliage photosynthetic characteristic and LOX product emission

Effects of elevated O₃ concentration on plant growth, development, biodiversity, forest productivity and crop yields have been studied extensively in the last 30 years (Feng & Kobayashi, 2009; Ainsworth *et al.*, 2012; Leisner & Ainsworth, 2012; Wilkinson *et al.*, 2012; Fares *et al.*, 2013; Ainsworth, 2017). The stepwise increase in O₃ concentrations in this study caused reductions in net assimilation rates (A_n), stomatal conductance (g_s) and F_v/F_m and induced formation and emission of LOX products, in agreement with previous reports for single species exposed to a given O₃ concentration (Beauchamp *et al.*, 2005; Chutteang *et al.*, 2016; Li *et al.*, 2017). We observed that there was a stronger relationship between the density of glandular trichomes and the absolute response per unit of O₃ taken up by the whole leaf (i.e., through both surface reactions and via the stomata) than per unit of O₃ taken up through the stomata (Fig. 6, S2), suggesting that trichomes provide protection against O₃ damage on leaf surface. Furthermore, the evidence that visible leaf damage across species correlates more strongly with stomatal O₃ uptake than with whole leaf O₃ uptake (Fig. 8, S3) suggests that plant injuries are more strongly linked to the uptake of O₃ through stomatal pores. These relationships clearly show that glandular trichomes directly reduce stomatal O₃ uptake by depleting O₃ at the leaf surface and thus indirectly alleviate O₃ damage.

Given that glandular trichomes play multiple role in defence, the questions is whether the protection provided by glandular trichomes is directly driven by selection for greater oxidative stress resistance or whether it is primarily coincidental and reflects adaptation to other abiotic and biotic stresses. While the selection for atmospheric pollutant resistance was likely of minor significance in the past, human-driven pollution clearly increases the significance of selection for traits protecting against pollution and thus, the variation in glandular trichome density can importantly alter the fitness of given species in multispecies stands where different species exhibit differences in glandular trichome density. The fact that trichome number is not fixed at the time of leaf emergence and that trichome distribution changes with leaf position also implies that protection by glandular trichomes is a highly adaptive trait (Maffei *et al.*, 1989; Prozhertina *et al.*, 2003; Deschamps *et al.*, 2006; Jud *et al.*, 2016). Thus, the severity of abiotic and biotic stresses during leaf development can importantly alter leaf vulnerability to stress such as O₃ during their lifetime (Jud *et al.*, 2016), and further studies should examine whether long-term increases in atmospheric O₃ concentration alter trichome density and the capacity for protection against atmospheric oxidants.

Although different species exhibited different O₃ tolerance, O₃-induced leaf damage occurred in all species (Fig. 7). The reductions in A_n and F_v/F_m and the induction of LOX product emissions were associated with O₃-induced leaf damage across different species (Fig. 7). Such interspecific relationships have not been well studied, but finding uniform correlations across species suggests that the damage, once induced, alters foliage physiological characteristics similarly in all species. In previous studies, quantitative within-species relationships among LOX product emission and the severity of abiotic (Copolovici *et al.*, 2012; Copolovici & Niinemets, 2016; Li *et al.*, 2017) and biotic stresses (Niinemets *et al.*, 2013) have been observed. The interspecific correlations with the degree of damage observed in our study provide also encouraging evidence that not only modifications in foliage photosynthetic characteristics, but also LOX product emissions can provide a quantitative measure to estimate the deleterious effects of O₃ across species.

CONCLUSIONS

Our study provides conclusive evidence that glandular trichomes play a protective role against O₃ stress, and that this protection is associated with the type and density of glandular trichomes across a highly diverse set of species. A stepwise increase in O₃ concentration during fumigation led to severe visible leaf injury, and reductions in maximum quantum yield of PSII, leaf net assimilation rate and stomatal conductance, and increase in emissions of volatile products of lipoxygenase (LOX) pathway. We demonstrated that the presence of both peltate and capitate glandular trichomes are strongly related to reduced stomatal O₃ uptake. Because glandular trichomes reduce O₃ concentrations surrounding the open stomata on leaf surface, the O₃ dose threshold triggering acute responses increased with increasing glandular trichome density. In addition, absolute differences in leaf damage and LOX product emissions caused by leaf O₃ uptake were strongly linked to glandular trichome density. In summary, our study demonstrates that species with low glandular trichome density were more sensitive to O₃ stress compared to species with high trichome density, suggesting that leaf trichominess might importantly drive species dispersal in polluted environments. Further work is needed to gaining an insight into the distribution of species with different level of glandular trichome density in different communities and to understanding how various types of glandular trichomes containing different organic compounds affect plant O₃ resistance.

ACKNOWLEDGMENTS

We thank Märt Rahi for the help with SEM analyses. This work was supported by grants from the European Research Council (advanced grant 322603, SIP-VOL+), the European Regional Development Fund (Centre of Excellence EcolChange), and the Estonian Ministry of Science and Education (institutional grant IUT-8-3) and personal investigator grant PUT 1473. This manuscript greatly benefited from the comments of two anonymous reviewers and the Handling Editor, Lisa Ainsworth.

CONFLICT OF INTEREST

The authors declare that they have no conflicts of interest.

REFERENCES

- Agati G., Azzarello E., Pollastri S. & Tattini M. (2012) Flavonoids as antioxidants in plants: location and functional significance. *Plant Science* **196**, 67-76.
- Ainsworth E.A. (2017) Understanding and improving global crop response to ozone pollution. *The Plant Journal* **90**, 886–897.
- Ainsworth E.A., Yendrek C.R., Stich S., Collins W.J. & Emberson L.D. (2012) The effects of tropospheric ozone on net primary productivity and implications for climate change. *Annual Review of Plant Biology* **63**, 637-661.
- Amme S., Rutten T., Melzer M., Sonnsmann G., Vissers J.P.C., Schlesier B. & Mock H.-P. (2005) A proteome approach defines protective functions of tobacco leaf trichomes. *Proteomics* **5**, 2508–2518.
- Ascensão L., Marques N. & Pais M.S. (1995) Glandular trichomes on vegetative and reproductive organs of *Leonotis leonurus* (Lamiaceae). *Annals of Botany* **75**, 619-626.
- Ascensão L. & Pais M.S. (1998) The leaf capitate trichomes of *Leonotis leonurus*: histochemistry, ultrastructure and secretion. *Annals of Botany* **81**, 263-271.
- Baran P., Özdemir C. & Aktaş K. (2010) Structural investigation of the glandular trichomes of *Salvia argentea*. *Biologia* **65**, 33-38.
- Beauchamp J., Wisthaler A., Hansel A., Kleist E., Miebach M., Niinemets Ü., ..., Wildt J. (2005) Ozone induced emissions of biogenic VOC from tobacco: relationships between ozone uptake and emission of LOX products. *Plant, Cell and Environment* **28**, 1334-1343.

- Brilli F., Ruuskanen T.M., Schnitzhofer R., Müller M., Breitenlechner M., Bittner V., ..., Hansel A. (2011) Detection of plant volatiles after leaf wounding and darkening by Proton Transfer Reaction “Time-of-Flight” Mass Spectrometry (PTR-TOF). *PLoS One* **6**, e20419.
- Brosché M., Merilo E., Mayer F., Pechter P., Puzđrjova I., Brader G., Kangasjärvi J., Kollist H. (2010) Natural variation in ozone sensitivity among *Arabidopsis thaliana* accessions and its relation to stomatal conductance. *Plant, Cell and Environment* **33**, 914-925.
- Bussotti F., Desotgiu R., Cascio C., Pollastrini M., Gravano E., Gerosa G., ..., Strasser R.J. (2011) Ozone stress in woody plants assessed with chlorophyll a fluorescence. A critical reassessment of exiting data. *Environmental and Experimental Botany* **73**, 19-30.
- Cescatti A. & Niinemets Ü. (2004) Sunlight capture. Leaf to landscape. In *Photosynthetic adaptation. Chloroplast to landscape* (eds W.K. Smith, T.C. Vogelmann & C. Chritchley), pp. 42-85. Springer Verlag, Berlin, Germany.
- Cho K., Tiwari S., Agrawal S.B., Torres N.L., Agrawal M., Sarkar A., ..., Rakwal R. (2011) Tropospheric ozone and plants: absorption, responses, and consequence. *Reviews of Environmental Contamination and Toxicology* **212**, 61-111.
- Chutteang C., Booker F.L., Na-Ngern P., Burton A., Aoki M. & Burkey K.O. (2016) Biochemical and physiological processes associated with the differential ozone response in ozone-tolerant and sensitive soybean genotypes. *Plant Biology* **18**, 28-36.
- Copolovici L., Kännaste A., Pazouki L. & Niinemets Ü. (2012) Emissions of green leaf volatiles and terpenoids from *Solanum lycopersicum* are quantitatively related to the severity of cold and heat shock treatments. *Journal of Plant Physiology* **169**, 664-672.
- Copolovici L. & Niinemets Ü. (2010) Flooding induced emissions of volatile signaling compounds in three tree species with differing waterlogging tolerance. *Plant, Cell and Environment* **33**, 1582-1594.

- Copolovici L. & Niinemets Ü. (2016) Environmental impacts on plant volatile emission. In *Deciphering chemical language of plant communication* (eds J. Blande & R. Glinwood), pp. 35-59. Springer International Publishing, Berlin, Germany.
- Corsi G. & Bottega S. (1999) Glandular hairs of *Salvia officinalis*: new data on morphology, localization and histochemistry in relation to function. *Annals of Botany* **84**, 657-664.
- Deschamps C., Gang D., Dudareva N. & Simon J.E. (2006) Developmental regulation of phenylpropanoid biosynthesis in leaves and glandular trichomes of basil (*Ocimum basilicum* L.). *International Journal of Plant Sciences* **167**, 447-454.
- Ehleringer J. (1981) Leaf absorptances of Mohave and Sonoran desert plants. *Oecologia* **49**, 366-370.
- Ehleringer J. (1982) The influence of water stress and temperature on leaf pubescence development in *Encelia farinosa*. *American Journal of Botany* **69**, 670-675.
- Ehleringer J., Björkman O. & Mooney H.A. (1976) Leaf pubescence: effects on absorptance and photosynthesis in a desert shrub. *Science* **192**, 376-377.
- Eisner T., Eisner M. & Hoebeke E.R. (1998) When defense backfires: detrimental effect of a plant's protective trichomes on an insect beneficial to the plant. *Proceedings of the National Academy of Sciences of the United States of America* **95**, 4410-4414.
- Fahn A. (1979) *Secretory Tissues in Plants*. Academic Press, London, UK.
- Fahn A. & Shimony C. (1996) Glandular trichomes of *Fagonia* L. (Zygophyllaceae) species: structure, development and secreted materials. *Annals of Botany* **77**, 25-34.
- Fares A., Vargas R., Detto M., Goldstein A.H., Karlik J., Paoletti E. & Vitale M. (2013) Tropospheric ozone reduces carbon assimilation in trees: estimates from analysis of continuous flux measurements. *Global Change Biology* **19**, 2427-2443.
- Feng Z. & Kobayashi K. (2009) Assessing the impacts of current and future concentrations of surface ozone on crop yield with meta-analysis. *Atmospheric Environment* **43**, 1510-1519.

- Feng Z., B ker P., Pleijel H., Emberson L., Karlsson P.E., & Uddling J. (2017) A unifying explanation for variation in ozone sensitivity among woody plants. *Global Change Biology* DOI:10.1111/gcb.13824.
- Fiscus E.L., Booker F.L. & Burkey K.O. (2005) Crop responses to ozone: uptake, models of action, carbon assimilation and partitioning. *Plant, Cell and Environment* **28**, 997-1011.
- Flowers M.D., Fiscus E.L., Burkey K.O., Booker F.L. & Dubois J.-J.B. (2007) Photosynthesis, chlorophyll fluorescence, and yield of snap bean (*Phaseolus vulgaris* L.) genotypes differing in sensitivity to ozone. *Environmental and Experimental Botany* **61**, 190–198.
- Fowler D., Amann M., Anderson R., Ashmore M., Cox P., Depledge M., ..., Stevenson D. (2008) *Ground-level ozone in the 21st century: future trends, impacts and policy implications*. The Royal Society, London, UK.
- Franzaring J., Dueck T.A. & Tonneijck A.E.G. (1999) Can plant traits be used to explain differences in ozone sensitivity between native European species? In *Critical levels for ozone-level II* (eds J. Fuhrer & B. Achermann), pp. 271–274. Swiss Agency for the Environment, Forests and Landscape, Bern, Switzerland.
- Gang D.R., Wang J., Dudareva N., Nam K.H., Simon J.E., Lewinsohn E. & Pichersky E. (2001) An investigation of the storage and biosynthesis of phenylpropenes in sweet basil. *Plant Physiology* **125**, 539–555.
- Gao J., Zhu B., Xiao H., Kang H., Hou X. & Shao P. (2016) A case study of surface ozone source apportionment during a high concentration episode, under frequent shifting wind conditions over the Yangtze River Delta, China. *Science of the Total Environment* **544**, 853-863.
- Glas J.J., Schimmel B.C.J., Alba J.M., Escobar-Bravo R., Schuurink R.C. & Kant M.R. (2012) Plant glandular trichomes as targets for breeding or engineering of resistance to herbivores. *International Journal of Molecular Sciences* **13**, 17077-17103.

- Graus M., Müller M. & Hansel A. (2010) High resolution PTR-TOF: quantification and formula confirmation of VOC in real time. *Journal of the American Society for Mass Spectrometry* **21**, 1037-1044.
- Hallik L., Kazantsev T., Kuusk A., Galmés J., Tomás M. & Niinemets Ü. (2017) Generality of relationships between leaf pigment contents and spectral vegetation indices in Mallorca (Spain). *Regional Environmental Change* **17**, 2097-2109.
- Hartmann D.L., Klein Tank A.M.G., Rusticucci M., Alexander L.V., Brönnimann S., Charabi Y.A.R., ..., Zhai P. (2013) Observations: Atmosphere and Surface. In *Climate Change 2013: The Physical Science Basis. Contribution of Working Group I to the Fifth Assessment Report of the Intergovernmental Panel on Climate Change* (eds T.F. Stocker, D. Qin, G.-K. Plattner, M. Tignor, S.K. Allen, J. Boschung, ..., P.M. Midgley). Cambridge University Press, Cambridge, United Kingdom and New York, NY, USA.
- Hayes F., Jones M.L.M., Mills G. & Ashmore M. (2007) Meta-analysis of the relative sensitivity of semi-natural vegetation species to ozone. *Environmental Pollution* **146**, 754-762.
- Heiden A.C., Hoffmann T., Kahl J., Kley D., Klockow D., Langebartels C., ..., Wildt J. (1999) Emission of volatile organic compounds from ozone-exposed plants. *Ecological Applications* **9**, 1160-1167.
- Heinrich G., Pfeifhofer H.W., Stabentheiner E. & Sawidis T. (2002) Glandular hairs of *Sigesbeckia jorullensis* Kunth (Asteraceae): morphology, histochemistry and composition of essential oil. *Annals of Botany* **89**, 459-469.
- Huci P., Beversdorf W.D. & McKersie B.D. (1982) Relationship of leaf parameters with genetic ozone insensitivity in selected *Phaseolus vulgaris* cultivars. *Canadian Journal of Botany* **60**, 2187-2191.

- Jordan A., Haidacher S., Hanel G., Hartungen E., Märk L., Seehauser H., ..., Märk T.D. (2009) A high resolution and high sensitivity proton-transfer-reaction time-of-flight mass spectrometer (PTR-TOF-MS). *International Journal of Mass Spectrometry* **286**, 122-128.
- Jud W., Fischer L., Canaval E., Wohlfahrt G., Tissier A. & Hansel A. (2016) Plant surface reactions: an opportunistic ozone defence mechanism impacting atmospheric chemistry. *Atmospheric Chemistry and Physics* **16**, 277-292.
- Kanagendran A., Pazouki L., Li S., Liu B., Kännaste A., Niinemets Ü. (2017) Stress volatile emissions upon acute ozone exposure scale with foliage surface ozone uptake in ozone-resistant *Nicotiana tabacum* 'Wisconsin'. *Journal of Experimental Botany* DOI:10.1093/jxb/erx431.
- Kant M.R., Bleeker P.M., Van Wijk M., Schuurink R.C. & Haring M.A. (2009) Plant volatiles in defence. In *Advances in botanical research (volume 51. plant Innate Immunity)* (eds L.C. Van Loon), pp. 613–666. Academic press, VT, USA.
- Kapoor R., Chaudhary V. & Bhatnagar A.K. (2007) Effects of arbuscular mycorrhiza and phosphorus application on artemisinin concentration in *Artemisia annua* L. *Mycorrhiza* **17**, 581-587.
- Kennedy G.G. (2003) Tomato, pests, parasitoids, and predators: tritrophic interactions involving the genus *Lycopersicon*. *Annual Review of Entomology* **48**, 51–72.
- Ko K.N., Lee K.W., Lee S.E. & Kim E.S. (2007) Development and ultrastructure of glandular trichomes in *pelargonium x fragrans* 'mabel grey' (geraniaceae). *Journal of Plant Biology* **50**, 362-368.
- Kostina E., Wulff A. & Julkunen-Tiitto R. (2001) Growth, structure, stomatal responses and secondary metabolites of birch seedlings (*Betula pendula*) under elevated UV-B radiation in the field. *Trees* **15**, 483-491.
- Lai T.-L., Talbot R. & Mao H. (2012) An investigating of two highest ozone episodes during the last decade in New England. *Atmosphere* **3**, 59-86.

- Laisk A., Kull O. & Moldau H. (1989) Ozone concentration in leaf intercellular air spaces is close to zero. *Plant Physiology* **90**, 1163–1167.
- Leisner C.P. & Ainsworth E.A. (2012) Quantifying the effects of ozone on plant reproductive growth and development. *Global Change Biology* **18**, 606-616.
- Levin D.A. (1973) The role of trichomes in plant defense. *Quarterly Review of Biology* **48**, 3–15.
- Li P., Calatayud V., Gao F., Uddling J. & Feng Z. (2016) Differences in ozone sensitivity among woody species are related to leaf morphology and antioxidant levels. *Tree Physiology* **36**, 1105-1116.
- Li S., Harley P.C. & Niinemets Ü. (2017) Ozone-induced foliar damage and release of stress volatiles is highly dependent on stomatal openness and priming by low-level ozone exposure in *Phaseolus vulgaris*. *Plant, Cell and Environment* **40**, 1984-2003.
- Lihavainen J., Ahonen V., Keski-Saari S., Söber A., Oksanen E. & Keinänen M. (2017) Low vapor pressure deficit reduces glandular trichomes density and modifies the chemical composition of cuticular waxes in silver birch leaves. *Tree Physiology* **37**, 1166-1181.
- Logan J.A., Staehelin J., Megretskaia I.A., Cammas J.-P., Thouret V., Claude H., ..., Derwent R. (2012) Changes in ozone over Europe: analysis of ozone measurements from sondes, regular aircraft (MOZAIC) and alpine surface sites. *Journal of Geophysical Research* **117**, D09301.
- Loreto F. & Schnitzler J.-P. (2010) Abiotic stresses and induced BVOCs. *Trends in Plant Science* **15**, 154-166.
- Maffei M., Chialva F. & Sacco T. (1989) Glandular trichomes and essential oil in developing peppermint leaves. *New Phytologist* **111**, 707-716.
- Moldau H. & Bichele I. (2002) Plasmalemma protection by the apoplast as assessed from above-zero ozone concentrations in leaf intercellular air spaces. *Planta* **214**, 484-487.
- Niinemets Ü. (2010) Mild versus severe stress and BVOCs: thresholds, priming and consequences. *Trends in Plant Science* **15**, 145-153.

- Niinemets Ü., Fares S., Harley P. & Jardine K.J. (2014) Bidirectional exchange of biogenic volatiles with vegetation: emission sources, reactions, breakdown and deposition. *Plant, Cell and Environment* **37**, 1790-1809.
- Niinemets Ü., Kännaste A. & Copolovici L. (2013) Quantitative patterns between plant volatile emissions induced by biotic stresses and the degree of damage. *Frontiers in Plant Science* **4**, 262.
- Niinemets Ü., Kuhn U., Harley P.C., Staudt M., Arneth A., Cescatti A., ..., Peñuelas J. (2011) Estimations of isoprenoid emission capacity from enclosure studies: measurements, data processing, quality and standardized measurement protocols. *Biogeosciences* **8**, 2209-2246.
- Nussbaum S., Geissmann M., Eggenberg P., Strasser R.J. & Fuhrer J. (2001) Ozone sensitivity in herbaceous species as assessed by direct and modulated chlorophyll fluorescence techniques. *Journal of Plant Physiology* **158**, 757-766.
- Oltmans S.J., Lefohn A.S., Shadwick D., Harris J.M., Scheel H.E., Galbally I., ..., Kawasaki T. (2013) Recent tropospheric ozone changes- a pattern dominated by slow or no growth. *Atmospheric Environment* **67**, 331-351.
- Paoletti E., Seufert G., Della Rocca G. & Thomsen H. (2007) Photosynthetic responses to elevated CO₂ and O₃ in *Quercus ilex* leaves at a natural CO₂ spring. *Environmental Pollution* **147**, 516-524.
- Pasqualini S., Piccioni C., Reale L., Ederli L., Della Torre G. & Ferranti F. (2003) Ozone-induced cell death in tobacco cultivar Bel W3 plant. The role of programmed cell death in lesion formation. *Plant Physiology* **133**, 1122-1134.
- Peiffer M., Tooker J.F., Luthe D.S. & Felton G.W. (2009) Plants on early alert: glandular trichomes as sensors for insect herbivores. *New Phytologist* **184**, 644-656.
- Portillo-Estrada M., Kazantsev T., Talts E., Tosens T. & Niinemets Ü. (2015) Emission timetable and quantitative patterns of wound-induced volatiles across different leaf damage treatments in aspen (*Populus tremula*). *Journal of Chemical Ecology* **41**, 1105-1117.

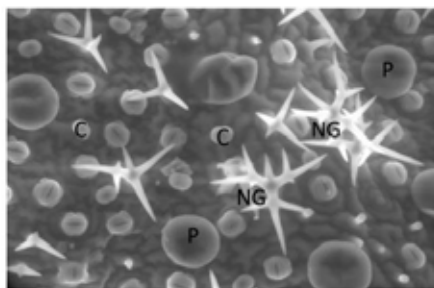
- Prozherina N., Freiwald V., Rousi M. & Oksanen E. (2003) Interactive effect of springtime frost and elevated ozone on early growth, foliar injuries and leaf structure of birch (*Betula pendula*). *New Phytologist* **159**, 623-636.
- Ranger C.M. & Hower A.A. (2001) Glandular morphology from a perennial alfalfa clone resistant to the potato leafhopper. *Crop Science* **41**, 1427-1434.
- Rieseberg L.H., Soltis D.E. & Arnold D. (1987) Variation and localization of flavonoid aglycones in *Helianthus annuus* (Compositae). *American Journal of Botany* **74**, 224-233.
- Riikonen J., Percy K.E., Kivimäenpää M., Kubiske M.E., Nelson N.D., Vapaavuori E. & Karnosky D.F. (2010) Leaf size and surface characteristics of *Betula papyrifera* exposed to elevated CO₂ and O₃. *Environmental Pollution* **158**, 1029-1035.
- Sallaud C., Giacalone C., Töpfer R., Goepfert S., Bakaher N., Rösti S. & Tissier A. (2012) Characterization of two genes for the biosynthesis of the labdane diterpene Z-abienol in tobacco (*Nicotiana tabacum*) glandular trichomes. *Plant Journal* **72**, 1-17.
- Thitz P., Possen B.J.H.M., Oksanen E., Mehtätalo L., Virjamo V. & Vapaavuori E. (2017) Production of glandular trichomes responds to water stress and temperature in silver birch (*Betula pendula*) leaves. *Canadian Journal of Forest Research* **47**, 1075-1081.
- Valkama E., Salminen J.-P., Koricheva J. & Pihlaja K. (2004) Changes in leaf trichomes and epicuticular flavonoids during leaf development in three birch taxa. *Annals of Botany* **94**, 233-242.
- Velikova V., Tsonev T., Pinelli P., Alessio G.A. & Loreto F. (2005) Localized ozone fumigation system for studying ozone effects on photosynthesis, respiration, electron transport rate and isoprene emission in field-grown Mediterranean oak species. *Tree Physiology* **25**, 1523-1532.
- Vingarzan R. (2004) A review of surface ozone background levels and trends. *Atmospheric Environment* **38**, 3431-3442.

- von Caemmerer S. & Farquhar G.D. (1981) Some relationships between the biochemistry of photosynthesis and the gas exchange of leaves. *Planta* **153**, 376-387.
- Wagner G.J. (1991) Secreting glandular trichomes: more than just hairs. *Plant Physiology* **96**, 675-679.
- Wagner G.J., Wang E. & Shepherd R.W. (2004) New approaches for studying and exploiting an old protuberance, the plant trichomes. *Annals of Botany* **93**, 3-11.
- Wohlgemuth H., Mittelstrass K., Kschieschan S., Bender J., Weigel H.-J., Overmyer K., ..., Langebartels C. (2002) Activation of an oxidative burst is a general feature of sensitive plants exposed to the air pollutant ozone. *Plant, Cell and Environment* **25**, 717-726.
- Wilkens R.T., Shea G.O., Halbreich S. & Stamp N.E. (1996) Resource availability and the trichome defenses of tomato plants. *Oecologia* **106**, 181-191.
- Wilkinson S., Mills G., Illidge R. & Davies W.J. (2012) How is ozone pollution reducing our food supply? *Journal of Experimental Botany* **63**, 527-536.
- Yuan X., Calatayud V., Jiang L., Manning W.J., Hayes F., Tian Y. & Feng Z. (2015) Assessing the effects of ambient ozone in China on snap bean genotypes by using ethylenediurea (EDU). *Environmental Pollution* **205**, 199-208.

Table 1 Mean \pm SE densities (number mm⁻²) of non-glandular (NGT), peltate (PGT) and capitate (CGT) glandular trichomes in the 24 plant species investigated.

Species	Family	NGT (number mm ⁻²)	CGT (number mm ⁻²)	PGT (number mm ⁻²)
<i>Anchusa officinalis</i>	Boraginaceae	6.8 \pm 0.9	12.9 \pm 3.5	
<i>Arctium tomentosum</i>	Asteraceae	30.1 \pm 1.1	60.7 \pm 1.3	
<i>Betula pendula</i>	Betulaceae	20.1 \pm 1.3	10.02 \pm 0.41	60.2 \pm 1.5
<i>Carduus crispus</i>	Asteraceae	30.1 \pm 1.1	14.0 \pm 1.2	
<i>Cucumis sativus</i>	Cucurbitaceae	15.036 \pm 0.021	28.1 \pm 0.8	
<i>Cucurbita pepo</i>	Cucurbitaceae	50.1 \pm 2.0	1.0274 \pm 0.0011	
<i>Erigeron acer</i>	Asteraceae	26.4 \pm 3.2	9.32 \pm 0.09	
<i>Erigeron canadensis</i>	Asteraceae	15.2 \pm 2.3	19 \pm 5	7.8 \pm 2.2
<i>Erodium cicutarium</i>	Geraniaceae	9.3 \pm 1.3	20.9 \pm 2.0	6.3 \pm 2.4
<i>Geranium palustre</i>	Geraniaceae	17 \pm 10	33 \pm 16	
<i>Geranium pratense</i>	Geraniaceae	20 \pm 7	58 \pm 10	6.35 \pm 0.35
<i>Geranium robertianum</i>	Geraniaceae	8.13 \pm 0.20	15.6 \pm 1.7	5.9 \pm 2.1
<i>Lavandula angustifolia</i>	Lamiaceae	65.3 \pm 1.5	65.2 \pm 1.4	30.0 \pm 1.2
<i>Mentha \times piperita</i>	Lamiaceae	21.0 \pm 1.3	37.1 \pm 1.1	50.2 \pm 1.7
<i>Nicotiana tabacum</i>	Solanaceae	5.172 \pm 0.011	70.2 \pm 1.2	
<i>Ocimum basilicum</i>	Lamiaceae	1.034 \pm 0.011	1.215 \pm 0.021	9.13 \pm 0.05
<i>Phaseolus vulgaris</i>	Fabaceae	2.041 \pm 0.007	10.132 \pm 0.012	
<i>Rosmarinus officinalis</i>	Lamiaceae	250.3 \pm 2.2	90.4 \pm 2.7	60.3 \pm 2.0
<i>Salvia officinalis</i>	Lamiaceae	70.2 \pm 1.2	10.114 \pm 0.012	45.2 \pm 1.1
<i>Silene latifolia</i>	Caryophyllaceae	15.1 \pm 3.3	7.9 \pm 1.1	8.3 \pm 1.3
<i>Solanum lycopersicum</i>	Solanaceae	1.243 \pm 0.021	9.035 \pm 0.022	
<i>Tussilago farfara</i>	Asteraceae	3.053 \pm 0.011	37.3 \pm 0.9	
<i>Urtica dioica</i>	Urticaceae	93 \pm 40	5.7 \pm 2.0	29 \pm 12
<i>Verbascum thapsus</i>	Scrophulariaceae	10.217 \pm 0.042	47.03 \pm 0.07	

(a) *Lavandula angustifolia*, abaxial surface



(b) *Cucumis sativus*, abaxial surface

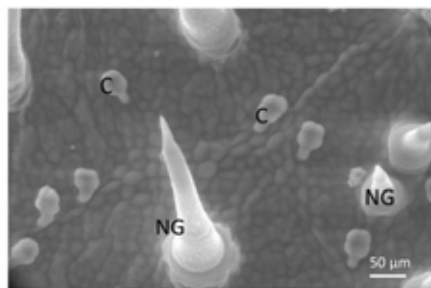


Fig. 1 Environmental scanning electron microscope (ESEM) micrographs of (a) non-glandular (NG) and peltate (P) and capitate (C) glandular trichomes on the lower surface of *Lavandula angustifolia* and (b) lower surface of *Cucumis sativus* containing non-glandular (NG) and glandular capitate trichomes (C). Scale bars on the bottom right.

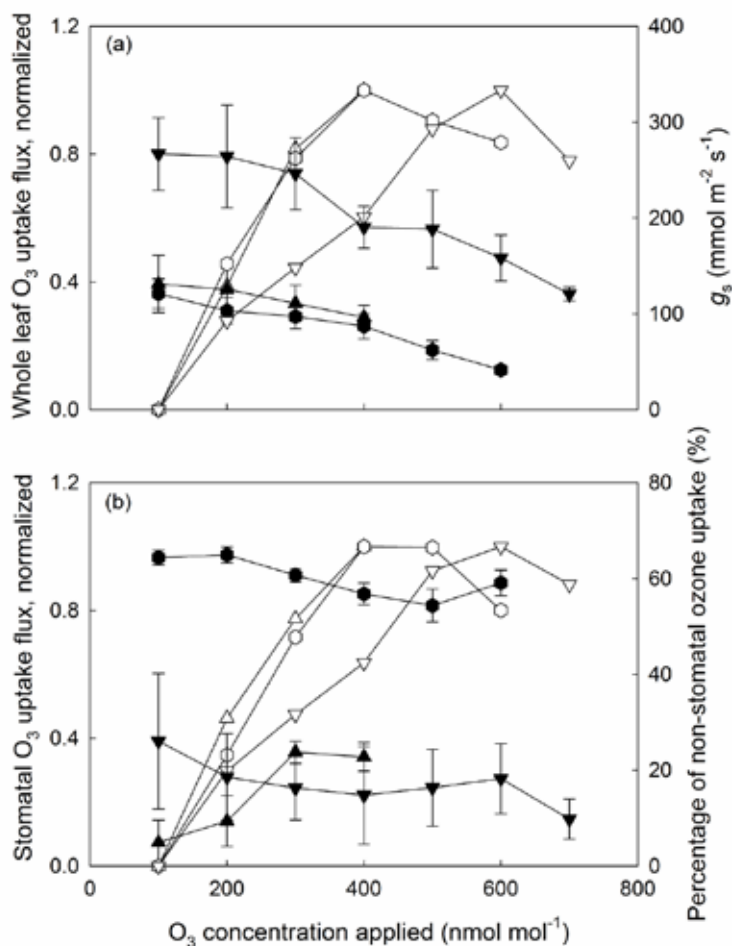


Fig. 2 Ozone uptake flux by the entire leaf (ϕ_{LO_3}) (a) and via the stomata (ϕ_{GO_3}) (b) normalized to the uptake fluxes at applied O_3 concentration of $100\ nmol\ mol^{-1}$, stomatal conductance (g_s ; a) and percentage of O_3 uptake by leaf surface (%; b) in relation to applied O_3 concentration in *P. vulgaris* (upward pointed triangles), *N. tabacum* (hexagons) and *S. lycopersicum* (downward pointed triangles). Open and filled symbols in (a) correspond to whole leaf normalized O_3 uptake flux (ϕ_{LO_3}) and stomatal conductance (g_s), and open and filled symbols in (b) to stomatal O_3 uptake flux (ϕ_{GO_3}) and percentage of O_3 uptake by leaf surface (%), respectively. Error bars indicate \pm SE.

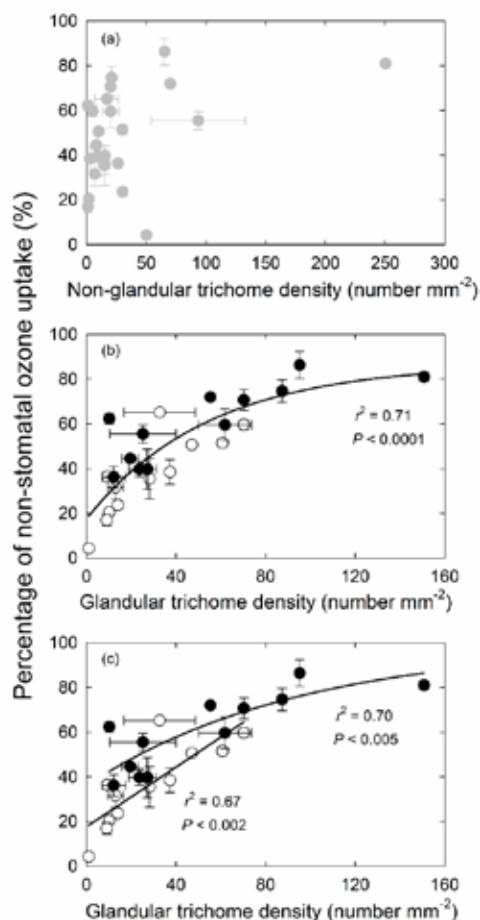


Fig. 3 Relationships between the percentage of non-stomatal ozone uptake and non-glandular trichome density (a), between the percentage of non-stomatal ozone uptake and glandular trichome density (b), and percentage of non-stomatal ozone uptake and glandular trichome density in species with capitate or both capitate and peltate trichomes (c). In (b) and (c), open symbols represent species with only capitate glandular trichomes and filled symbols species with both capitate and peltate glandular trichomes. The data in (b) were fitted by a non-linear regression ($y=17.5+69.3(1-0.982^x)$) and in (c) by a linear regression, $y=0.667x+17.7$, for species with capitate glandular trichomes and by a non-linear regression, $y=35.9+63.4(1-0.989^x)$, for species with capitate and peltate glandular trichomes.

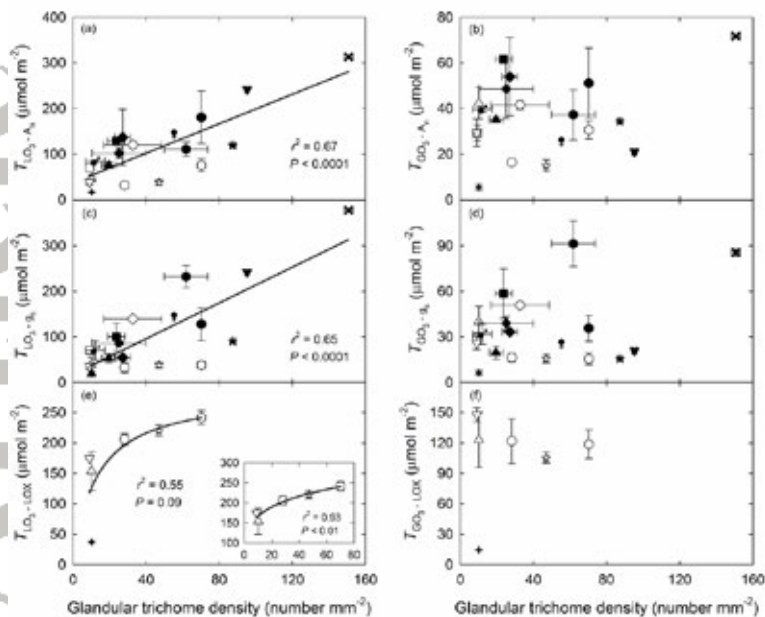


Fig. 4 Correlations of average glandular trichome density with average physiological thresholds of O_3 uptake by leaf (a, c, e) and stomata (b, d, f). The O_3 uptake thresholds were defined as uptake values inducing a significant decrease of net assimilation rate ($T_{LO_3-A_n}$ for leaf, and $T_{GO_3-A_n}$ for stomatal uptake) and stomatal conductance ($T_{LO_3-g_s}$, and $T_{GO_3-g_s}$), and emissions of volatile products of the lipoxygenase pathway (LOX products, also called green leaf volatiles) (T_{LO_3-LOX} and T_{GO_3-LOX}). In (e), the inset does not include *O. basilicum* that had both capitate and peltate glandular trichomes. The data were fitted by linear or non-linear regressions ($y=37.6+1.62x$ for (a); $y=17.9+1.96x$ for (c), $y=22.5x/(1+0.0788x)$ for (e, main panel) and $y=108.1x^{0.188}$ for (e, inset)). *B. pendula* (filled circles, ●), *C. sativus* (open circles, ○), *E. acer* (open squares, □), *E. canadensis* (filled squares, ■), *E. cicutarium* (filled diamonds, ◆), *G. palustre* (open diamonds, ◇), *G. pratense* (filled hexagons, ●), *G. robertianum* (filled upward pointing triangles, ▲), *L. angustifolia* (filled downward pointing triangles, ▼), *M. × piperita* (filled stars, ★), *N. tabacum* (open hexagons, ⬡), *O. basilicum* (filled plus symbols, +), *P. vulgaris* (open upward pointing triangles, △), *R. officinalis* (filled crosses, ✕), *S. officinalis* (filled Venus symbols, ♀), *S. latifolia* (filled Mars symbols, ♂), *S. lycopersicum* (open downward

pointing triangles, ∇), *U. dioica* (filled Christian crosses, \oplus), *V. thapsus* (open stars, \star). In all cases, open symbols represent species with only capitate glandular trichomes and filled symbols species with both capitate and peltate glandular trichomes. Error bars indicate \pm SE.

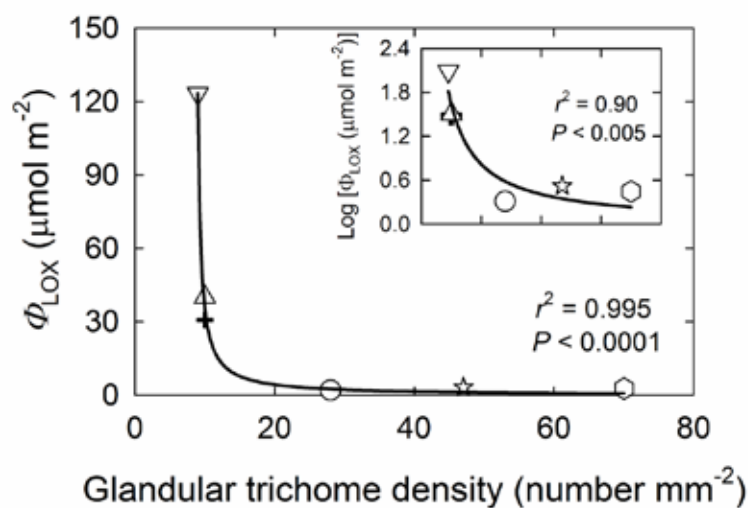


Fig. 5 Total LOX product emissions (Φ_{LOX}) over 21 hours following O_3 exposure in relation to glandular trichome density for six species with different density of glandular trichomes. The y axis is Log_{10} -transformed in the inset. In all cases, O_3 concentration was increased in a stepwise fashion in 30 minute intervals, 100 nmol mol⁻¹ increments, from 100 to 500 nmol mol⁻¹. The data were fitted by a non-linear regression ($y = -5.79 / (1 - 0.116x)$) for the main panel, and $y = 16.8 \cdot 10^6 / (1 + 10.3 \cdot 10^5 x)$ for the inset). Symbols are as defined in Fig. 4.

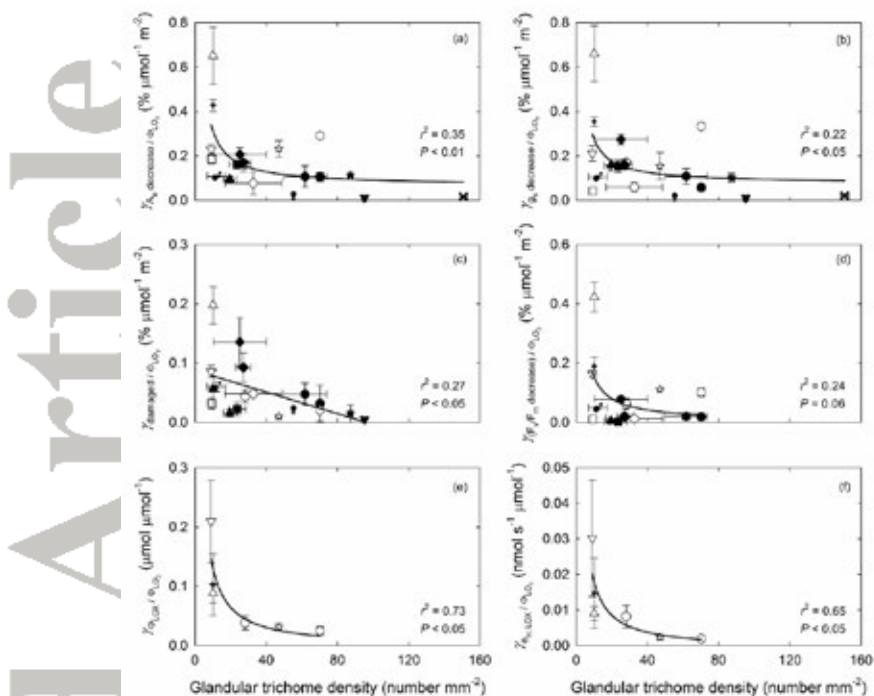


Fig. 6 (a) The percentage decrease in net assimilation rate ($\gamma_{A_n \text{ decreased}} / \phi_{LO_3}$), (b) the percentage decrease in stomatal conductance ($\gamma_{g \text{ decreased}} / \phi_{LO_3}$), (c) the percentage of leaf area visibly damaged ($\gamma_{\text{damaged}} / \phi_{LO_3}$), (d) the percentage decrease in the dark-adapted maximum quantum efficiency of PSII (F_v/F_m) ($\gamma_{(F_v/F_m \text{ decreased})} / \phi_{LO_3}$), (e) the induction of total amount of LOX product emission ($\gamma_{\phi_{LOX}} / \phi_{LO_3}$) and (f) the maximum rate of induced LOX product emission ($\gamma_{\phi_{M, LOX}} / \phi_{LO_3}$) per unit leaf O_3 uptake (Eq. 8) in relation to glandular trichome density. As in Fig. 5, the total LOX product emission is the sum of LOX products released since the induction until termination of the experiment at 21 h after the stop of O_3 exposure. Leaf damage after O_3 fumigation was assessed as the presence of necrotic and/or chlorotic lesions on leaf surface. The data were fitted by linear or non-linear regressions ($y=0.0662+(2.49/x)$ for (a); $y=0.0755+(2.01/x)$ for (b); $y=0.0871-0.000912x$ for (c); $y=-0.00371+(1.50/x)$ for (d); $y=-0.00332+(1.35/x)$ for (e) and $y=-0.00112+(0.19/x)$ for (f)). Symbols as defined in Fig. 4. Error bars indicate \pm SE.

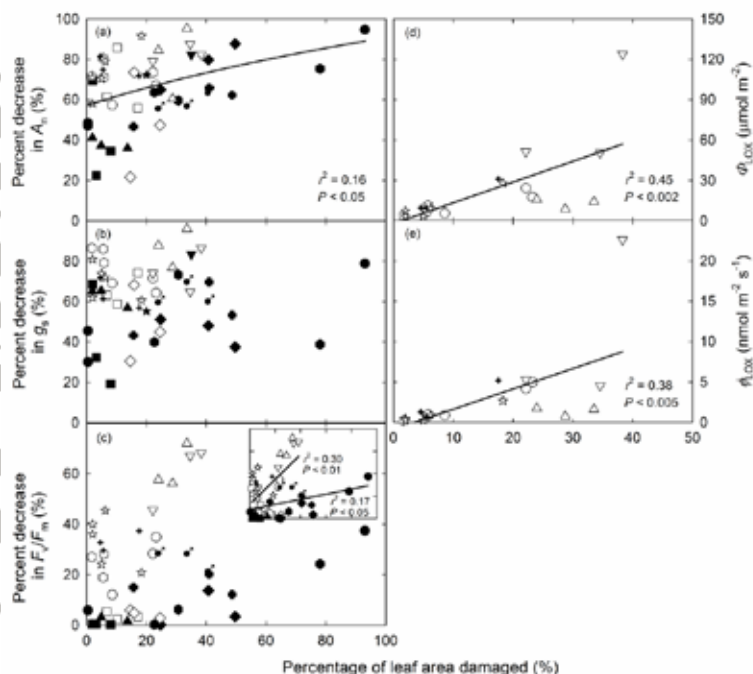


Fig. 7 Relative decreases in net assimilation rate (a) and stomatal conductance (b) and maximum dark-adapted quantum yield of PSII (F_v/F_m) (c), and total emission of LOX products (d) and maximum emission rate of LOX products (e) in O_3 -exposed leaves in relation to the percentage of leaf area visibly damaged. The data were fitted by linear or non-linear regressions ($y = -14.3 + 0.714(1 + 0.0188x)^{-0.366}$ for (a); $y = 1.54x - 1.99$ for (d) and $y = 0.252x - 0.899$ for (e)). The Data in the inset of (c) were fitted by linear regressions separately for species with only capitate trichomes ($y = 12.8 + 1.110x$, open symbols) and with both capitate and peltate glandular trichomes ($y = 8.09 + 0.227x$, filled symbols). Symbols as in Fig. 4.

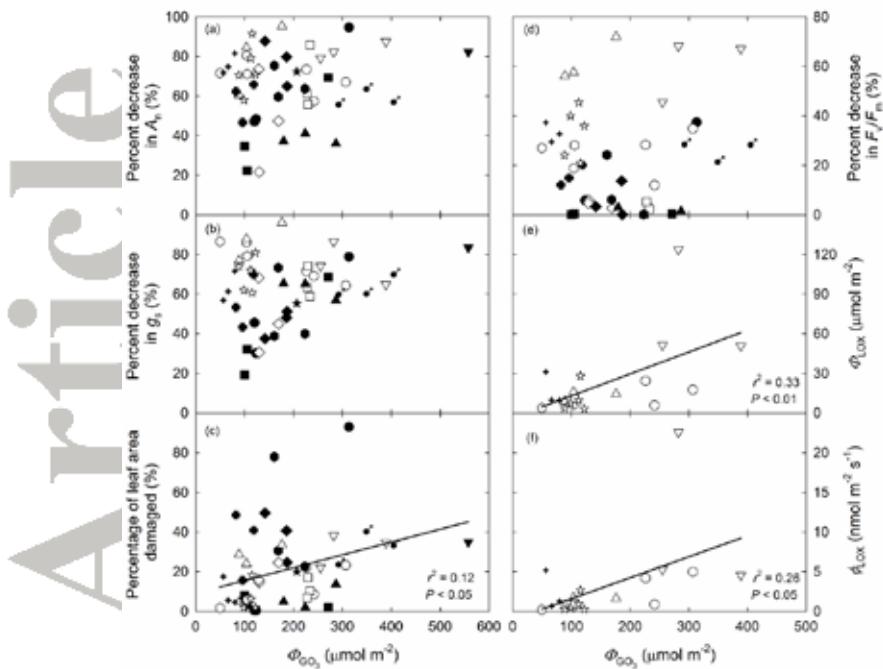


Fig. 8 The total amount of O_3 uptake by stomata (Φ_{GO_3}) in relation to the percentage decrease of net assimilation rate (a) and stomatal conductance (b), percentage leaf area visibly damaged (c) and percentage decrease of maximum dark-adapted chlorophyll fluorescence yield (F_v/F_m) (d), the total LOX product emission (e) and maximum emission rate of LOX products (f) from O_3 -exposed leaves. In (c), (e) and (f), the data were fitted by linear regressions ($y=9.03+0.0648x$; $y=0.166x-3.58$ and $y=0.0265x-1.06$). Symbols as in Fig. 4.

Li, S., Harley, P.C., Niinemets, Ü. (2017)
Ozone-induced foliar damage and release of stress volatiles is highly
dependent on stomatal openness and priming by low-level ozone
exposure in *Phaseolus vulgaris*.
Plant Cell & Environment 40, 1984-2003.

Original Article

Ozone-induced foliar damage and release of stress volatiles is highly dependent on stomatal openness and priming by low-level ozone exposure in *Phaseolus vulgaris*Shuai Li¹ , Peter C. Harley¹ & Ülo Niinemets^{1,2} ¹Institute of Agricultural and Environmental Sciences, Estonian University of Life Sciences, Kreutzwaldi 1, 51014 Tartu, Estonia and²Estonian Academy of Sciences, Kohtu 6, 10130 Tallinn, Estonia

ABSTRACT

Acute ozone exposure triggers major emissions of volatile organic compounds (VOCs), but quantitatively, it is unclear how different ozone doses alter the start and the total amount of these emissions, and the induction rate of different stress volatiles. It is also unclear whether priming (i.e. pre-exposure to lower O₃ concentrations) can modify the magnitude and kinetics of volatile emissions. We investigated photosynthetic characteristics and VOC emissions in *Phaseolus vulgaris* following acute ozone exposure (600 nmol mol⁻¹ for 30 min) under illumination and in darkness and after priming with 200 nmol mol⁻¹ O₃ for 30 min. Methanol and lipoxygenase (LOX) pathway product emissions were induced rapidly, followed by moderate emissions of methyl salicylate (MeSA). Stomatal conductance prior to acute exposure was lower in darkness and after low O₃ priming than in light and without priming. After low O₃ priming, no MeSA and lower LOX emissions were detected under acute exposure. Overall, maximum emission rates and the total amount of emitted LOX products and methanol were quantitatively correlated with total stomatal ozone uptake. These results indicate that different stress volatiles scale differently with ozone dose and highlight the key role of stomatal conductance in controlling ozone uptake, leaf injury and volatile release.

Key-words: LOX products; methanol; ozone stress; proton transfer reaction-time of flight-mass spectrometer (PTR-TOF-MS); stomatal conductance; volatile organic compounds (VOCs).

INTRODUCTION

Tropospheric ozone (O₃) is a major global air pollutant and an important greenhouse gas that seriously impacts human health and natural ecosystems worldwide from tropics to tundra (Fowler *et al.* 2008). Both plant growth and production as well as plant species biodiversity are significantly disturbed under elevated O₃ conditions, which portends a significant threat to

global food security (e.g. Schmidhuber & Tubiello 2007; Feng, Kobayashi, & Ainsworth 2008; Furlan *et al.* 2008; Wittig, Ainsworth, Naidu, Karnosky, & Long 2009; Ainsworth, Yendrek, Sitch, Collins, & Emberson 2012; Wilkinson, Mills, Illidge, & Davies 2012; Agathokleous, Saitanis, & Koike 2015; Cassimiro & Moraes 2016; Freire *et al.* 2017). It is estimated that the average current background concentration of O₃ in the northern hemisphere is around 20–50 nmol mol⁻¹ and O₃ concentrations are predicted to increase due to expected rise in O₃ precursor emissions in the future, implying even greater effects of tropospheric O₃ on global climate change and on atmospheric oxidative status by the end of this century (Vingarzan 2004; Fowler *et al.* 2008).

As a strong polar oxidant, O₃ enters plants mainly through the stomata. Thus, stomatal closure is a direct and highly effective way to limit O₃ damage, but it also limits CO₂ uptake, causing the reduction in net assimilation. Previous studies have observed that elevated O₃ concentrations induce both rapid stomatal closure (Kollist *et al.* 2007; Vahisalu *et al.* 2008; Vahisalu *et al.* 2010) and sluggish stomatal responses to changes in environmental conditions (Paoletti & Grulke 2010; Hoshika, Omasa, & Paoletti 2013), which may cause significant decline in photosynthesis and increase leaf water loss relative to net assimilation (leaf water use efficiency). Apart from stomata, semi-volatile and volatile organic compounds (VOCs) exuded by the glandular trichomes at leaf surface and volatiles emitted *de novo* from mesophyll cells constitute an efficient O₃ sink that can reduce O₃ concentrations on the leaf surface and in the gas-phase surrounding the leaf, thereby reducing O₃ entry through stomata (Loreto *et al.* 2001; Loreto, Pinelli, Manes, & Kollist 2004; Fares, Loreto, Kleist, & Wildt 2008; Fares, Goldstein, & Loreto 2010a; Fares, McKay, Holzinger, & Goldstein 2010b; Jud *et al.* 2016; Li *et al.* unpublished). Therefore, O₃-induced leaf damage may not be well correlated with the surrounding O₃ concentration but is related to the O₃ flux density into the plants through the stomata (Beauchamp *et al.* 2005; Loreto & Fares 2007; Fares *et al.* 2010a).

Once O₃ has entered the plant, it has to pass the cell wall aqueous phase where it can be partly quenched by water-soluble antioxidants such as ascorbate (e.g. Ranieri *et al.* 1999; Bichele *et al.* 2000). Once having passed the cell wall, O₃ can directly react with the plasmalemma lipids, resulting in direct damage, but it typically also elicits an endogenous

Correspondence to: Ü. Niinemets. E-mail: ylo.niinemets@emu.ee

generation of other reactive oxygen species (ROS), including hydrogen peroxide (H₂O₂), which collectively lead to a disruption and profound reprogramming of cellular metabolism, ultimately leading to major reduction of foliar photosynthetic activity, accelerated senescence and elicitation of programmed cell death (Long & Naidu 2002; Wohlgenuth *et al.* 2002; Calatayud, Iglesias, Talón, & Barreno 2003; Pasqualini *et al.* 2003; Beauchamp *et al.* 2005; Fiscus, Booker, & Burkey 2005). Foliage photosynthetic apparatus can be impaired by O₃ due to direct inactivation of ribulose-1,5-bisphosphate carboxylase/oxygenase (Rubisco) as well as reduction of expression of Rubisco synthase activity (Long & Naidu 2002; Calatayud *et al.* 2003; Fiscus *et al.* 2005). O₃ has also been shown to alter photosynthetic electron transport in some plants via reduction in efficiency of excitation energy capture by PSII (Fiscus *et al.* 2005; Flowers, Fiscus, Burkey, Booker, & Dubois 2007; Guidi, Degl'Innocenti, Martinelli, & Piras 2009). Visible symptoms of toxic O₃ exposure characteristically include chlorotic or necrotic lesions on the plant leaf surface, which can coalesce to form larger injured areas, ultimately resulting in whole leaf senescence and early abscission (Loreto *et al.* 2001; Long & Naidu 2002; Wohlgenuth *et al.* 2002; Pasqualini *et al.* 2003; Beauchamp *et al.* 2005; Vickers *et al.* 2009; Wilkinson *et al.* 2012). Although the basic principles of O₃ impacts on photosynthetic machinery have been uncovered, at quantitative level, O₃ dose versus plant response relationships are still poorly understood. In particular, in natural conditions, O₃ concentrations strongly fluctuate and studies have tried to use a certain threshold O₃ dose, for example AOT40, to characterize the impact of cumulative O₃ exposure on plant responses (e.g. Inclán, Ribas, Peñuelas, & Gimeno 1999; Bortier, Ceulemans, & De Temmerman 2000; Oksanen & Holopainen 2001). However, due to various O₃ quenching mechanisms operative across plant species, differences in stomatal reactions to fluctuating O₃ concentrations and differences in endogenous elicitation of ROS production, the plant dose responses can be very complex (Loreto & Fares 2007; Fares *et al.* 2010a). Furthermore, mild stress itself can elicit priming responses, enhancing or reducing the sensitivity to subsequent more severe stress episodes (Conrath *et al.* 2006; Heil & Kost 2006), but there is only limited body of information of possible modification of acute O₃ resistance by mild O₃ exposures.

In parallel with primary cellular damage due to O₃ reactions with plasmalemma unsaturated lipids, and/or secondary damage due to elicitation of endogenous ROS production by O₃, emissions of VOC such as methanol, lipoxygenase (LOX) pathway products (e.g. LOX products comprising various C6 aldehydes) and methyl salicylate (MeSA) are typically observed after O₃ fumigation (Heiden *et al.* 1999; Beauchamp *et al.* 2005). As discussed earlier, studies on volatile emissions have indicated that stomatal O₃ uptake is the primary driver for elicitation of volatile emissions (Beauchamp *et al.* 2005; Wieser, Hecke, Tausz, & Matyssek 2013; Jud *et al.* 2016). Detailed kinetic analysis of volatile emissions during fumigation and through recovery period allows for making inferences of engagement of different stress response pathways and evaluate the relationships between O₃ exposure dose and stress

response development and strength of plant response. In fact, because immediate photosynthetic responses during and after stress are primarily driven by modifications in stomatal conductance and the reductions due to direct damage occur later (Kollist *et al.* 2007; Vahisalu *et al.* 2008; Vahisalu *et al.* 2010), we argue that monitoring stress volatile fluxes through stress periods can be much more informative for gaining insight into the kinetics of stress development and propagation of lesions than monitoring changes in net assimilation rate (Beauchamp *et al.* 2005). However, volatile release during and after O₃ exposure is characterized by a complex kinetics with immediate emissions during or shortly after O₃ exposure followed by secondary emissions in hours after the stress event (Beauchamp *et al.* 2005). Due to the complex kinetics, quantitative relationships between different O₃ treatments and the timing and magnitude of induced volatile responses are still poorly understood. In particular, it is unclear whether the secondary emissions occurring during the recovery phase, often in many hours after the stress, are quantitatively linked to ozone dose. Especially limited is the information about secondary methanol emissions that might result both from the constitutive activity of cell wall pectin methylesterases, but also from *de novo* induction of stress-dependent pectin methylesterases (Pelloux, Rustérucchi, & Mellerowicz 2007).

In the present study, we used common bean (*Phaseolus vulgaris*) known for its sensitivity to O₃ (Wenzel & Mehlhorn 1995) to investigate the effects of acute O₃ exposure on net assimilation rate, stomatal conductance and biogenic VOC emissions combining high resolution measurements with a proton transfer reaction-time of flight-mass spectrometer (PTR-TOF-MS) and quantitative analysis of emission kinetics during exposure and through a 21 h recovery period (Table 1 and Fig. 1). Such long-term continuous VOC measurements after ozone exposure are rare in the literature, and to our knowledge, PTR-TOF-MS measurements have not been conducted during ozone exposure. The amount of O₃ uptake during acute O₃ exposure was altered by changing the light conditions and by pre-exposure to lower O₃ concentrations, that is using treatments known to lead to stomatal closure. We hypothesized that the lower rate of uptake of O₃ during acute exposure periods reduces O₃-induced damage and that this is associated with slower induction kinetics, with lower maximum rate of volatile emissions and lower total emissions. Because the leaves of *P. vulgaris* possess capitate glandular trichomes (Li *et al.* unpublished observations), which might contribute to total O₃ loss, total whole leaf O₃ absorption was separated among stomatal and non-stomatal components.

MATERIALS AND METHODS

Plant material and growth conditions

Phaseolus vulgaris L. cv. Saxa plants were grown from seed (seed source: DALEMA UAB, Vilnius, Lithuania). After germination, seedlings were replanted in 2 L plastic pots filled with commercial potting soil with NPK (N of 100 mg L⁻¹, P of 30 mg L⁻¹ and K of 200 mg L⁻¹) fertilizer (Biolan Oy, Kekkila Group, Vantaa, Finland). The plants were grown in a plant

Table 1. List of symbols used with definitions and units

Symbol	Definition	Units
ϕ_X	emission rates of given VOC	$\text{nmol m}^{-2} \text{s}^{-1}$
$\phi_{M1,X}$	maximum emission rate at the first emission peak	$\text{nmol m}^{-2} \text{s}^{-1}$
$\phi_{M2,X}$	maximum emission rate at the second emission peak	$\text{nmol m}^{-2} \text{s}^{-1}$
Φ_X	the total amount of given VOC emitted over a certain time	$\mu\text{mol m}^{-2}$
t_{P1S}	start of the first emission burst since the start of the O_3 exposure	h
t_{P1E}	end of the first emission burst since the start of the O_3 exposure	h
t_{P2S}	start of the second emission burst since the start of the O_3 exposure	h
t_{P2E}	end of the second emission burst since the start of the O_3 exposure	h
D_{P1}	duration of the first induced emission peak	h
D_{P2}	duration of the second induced emission peak	h
t_{E1}	time from the onset of O_3 exposure to the first emission elicitation	h
t_{E2}	time from the onset of O_3 exposure to the second emission elicitation	h
t_{M1}	time from elicitation to the first emission maximum	h
t_{M2}	time from elicitation to the second emission maximum	h
τ_{I1}	doubling-time for the increase of emissions during the first emission burst	h
τ_{D1}	half-time for the decrease of emissions during the second emission burst	h
τ_{I2}	doubling-time for the increase of emissions during the second emission burst	h
τ_{D2}	half-time for the decrease of emissions during the second emission burst	h
k_{I1}	rate constant for the initial increase of emissions during the first emission burst	h^{-1}
k_{D1}	rate constant for the decrease of emissions during the first emission burst	h^{-1}
k_{I2}	rate constant for the initial increase of emissions during the second emission burst	h^{-1}
k_{D2}	rate constant for the decrease of emissions during the second emission burst	h^{-1}
ϕ_{O_3}	the rate of ozone uptake by stomata	$\text{nmol m}^{-2} \text{s}^{-1}$
Φ_{O_3}	the total amount of ozone uptake by stomata	$\mu\text{mol m}^{-2}$
ϕ_{LO_3}	the rate of ozone uptake by whole leaf	$\text{nmol m}^{-2} \text{s}^{-1}$
Φ_{LO_3}	the total amount of ozone uptake by whole leaf	$\mu\text{mol m}^{-2}$

Fig. 1 demonstrates representative time courses of emissions and definition of symbols.

room with light intensity at plant level of $400 \mu\text{mol m}^{-2} \text{s}^{-1}$ (HPI-T Plus 400 W metal halide lamps, Philips) during a 12 h photoperiod. The day/night temperatures were maintained at 24/20 °C and daytime humidity at 60%. During growth, supply of nutrients and water was maintained at close to optimal levels.

The plants were grown under these conditions for 4 weeks before starting the experiments. In all experiments, we used similar-sized plants (average height of 30 cm) with similar number of leaves. All measurements were conducted with fully mature non-senescent trifoliate leaves.

Gas-exchange system for photosynthesis, stomatal conductance and volatile organic compound measurements and for ozone fumigation

A custom-built laboratory gas-exchange system described in detail by Copolovici & Niinemets (2010) was used to measure leaf gas exchange characteristics (photosynthetic rate and stomatal conductance) and VOC emissions and for O_3 fumigation. Briefly, ambient air was pumped from outside and passed through a 10 L buffer volume to minimize CO_2 fluctuations, purified by passing through a custom-made O_3 trap and charcoal filter and humidified to standard water vapour concentration. The conditioned air entered to a water-jacketed, temperature-controlled 1.2 L glass chamber. Chamber flow rate was fixed at 1.6 L min^{-1} , and a fan inside the chamber minimized leaf boundary layer resistance (Rasulov, Copolovici, Laisk, & Niinemets 2009), and thus, for

the first-order decay kinetics, the chamber response half-time was estimated to be 31 s (Niinemets 2012). The system had two identical gas lines, one passing to the leaf chamber (measurement) and the other passing through an equivalent flow resistance (reference). An electronic valve was used to switch between the air streams going to the gas analyser. In all measurements, leaf temperature was measured with thermocouple and maintained at 25 °C, ambient CO_2 concentration was $380\text{--}400 \mu\text{mol mol}^{-1}$ and light intensity at the leaf surface was set to $500 \mu\text{mol m}^{-2} \text{s}^{-1}$ when light was on.

O_3 was generated by an O_3 generator (Stable Ozone Generator, Ultra-Violet Products Ltd, Cambridge, UK) that has a quartz glass reaction chamber illuminated with UV light ($\lambda = 185 \text{ nm}$) for O_3 production. Ambient air was passed through the reaction chamber, and the air enriched with O_3 was mixed with the air stream entering the leaf chamber. The O_3 flux into the chamber was controlled by a custom-made flow restrictor. As the O_3 concentration in the chamber also depends on plant uptake that can vary through the experiment, the O_3 -enriched air flow was adjusted during the treatment to compensate for changes in O_3 uptake such that the stability of O_3 concentration achieved was $\pm 5\text{--}10\%$ of the target concentration.

An infra-red gas analyser (CIRAS II, PP-Systems, Amesbury, MA, USA) operated in an absolute mode was used to measure CO_2 and H_2O concentrations. A PTR-TOF-MS (Ionicon Analytik GmbH, Innsbruck, Austria) was employed to determine volatile concentrations, and a chemiluminescence O_3 sensor (Model 49i, Thermo Scientific, Massachusetts, USA)

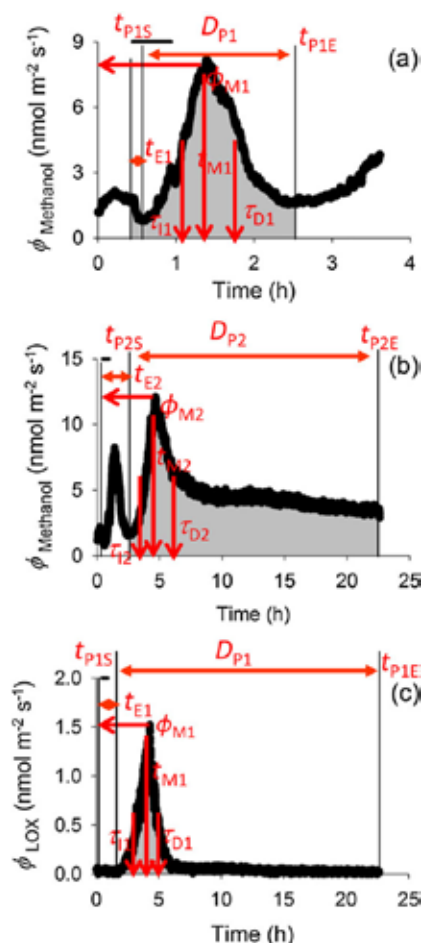


Figure 1. A typical time course of biogenic volatile organic compound (VOC) emissions from ozone-exposed *Phaseolus vulgaris* leaves, and definition of key quantitative emission characteristics: (a) first emission burst of methanol, (b) second emission burst of methanol and (c) emission burst of LOX pathway volatile products (mainly various C6 aldehydes and alcohols). The emission pattern of methyl salicylate (MeSA) resembles LOX emissions in (c). In all cases, t_{E1} and t_{E2} are the times from the onset of O₃ exposure to the elicitation of the first and (if present) the second burst of the given VOC species, respectively. ϕ_{M1} and ϕ_{M2} correspond to the emission maxima for the two bursts and t_{M1} and t_{M2} denote the corresponding times from the start of the elicitation to reaching the maxima. t_I and t_D indicate the initial doubling and decay times for the bursts. Integrated emissions for different emission bursts correspond to the shaded area for the duration of induced-emission bursts, D_P , that is from the start of the given VOC emission elicitation (t_{PS}) until the end of the given compound emission release (t_{PE} ; Eqn 3). As the experiment continued for 21 h after the O₃ exposure, methanol emissions might not have always reached the initial level (b), and thus, D_P and integrated emissions are somewhat underestimated in these cases. The vertical bars indicate periods for exposure to 600 nmol mol⁻¹ O₃.

was used to measure O₃ concentrations. All instruments were interchangeably connected to the chamber inlets and outlets (Copolovici & Niinemets 2010) and operated continuously. Average CO₂ and H₂O concentrations and all PTR-TOF-MS signals were recorded every 10 s, and the range and average O₃ concentrations were recorded for every 15 min period. Reference measurements (ingoing air) were conducted frequently, typically every 10–15 min.

O₃ fumigation treatments

Three different experimental treatments with individual leaves were carried out by using O₃ concentrations that constituted a moderately severe stress and led to visible leaf damage. In contrast to some other studies (e.g. Beauchamp *et al.* 2005), these exposures did not result in leaf death, at least during 24 h following the experimental treatment.

After leaf enclosure, continuous measurements of photosynthetic characteristics and trace gas exchange were begun immediately. When photosynthesis and VOC emission rates had stabilized, typically 20–30 min after leaf enclosure, O₃ fumigation was started. In Treatment 1, the illuminated leaf was fumigated with 600 ± 33 nmol mol⁻¹ O₃ for 30 min. In Treatment 2, the leaf acclimated to chamber light conditions was darkened by turning off the light and covering the chamber with an aluminium foil. Following stomatal closure (after 20–30 min in darkness), the leaf was exposed to 600 ± 30 nmol mol⁻¹ O₃ for 30 min in darkness. After the O₃ exposure, the light was turned on again. Finally, in Treatment 3, the illuminated leaf was exposed first to 200 ± 11 nmol mol⁻¹ O₃ for 30 min, after which the O₃ concentration was raised to 600 ± 32 nmol mol⁻¹ for an additional 30 min. After each of the three treatments, foliage gas-exchange characteristics and trace gas-exchange were continuously monitored for 21 h under illumination as detailed in the succeeding texts. The treated leaves were then removed from the chamber and their area, and the quantitative degree of damage was estimated by using an image analysis software (Image J, National Institutes of Health, Bethesda, MD, USA). For each treatment, we chose three mature and healthy plant individuals with the same age and same number of leaves and selected from each plant individual a representative fully mature same-aged and similar-sized leaf for the measurements.

Operation of PTR-TOF-MS and stress volatile estimation

PTR-TOF-MS allows for real-time monitoring of key plant stress-elicited volatiles, and its main advantages over the traditional quadrupole PTR (PTR-QMS) are higher mass resolution and a simultaneous rather than sequential detection of all VOC masses (Jordan *et al.* 2009; Graus, Müller, & Hansel 2010). Operation of the PTR-TOF-MS followed the method described in detail in Graus *et al.* (2010), Brilli *et al.* (2011) and Portillo-Estrada, Kazantsev, Talts, Tosens, & Niinemets (2015). In short, the conditions for PTR-TOF-MS operation were 60 °C drift tube temperature, 600 V drift voltage and

2.3 mbar drift pressure, corresponding to an $E/N \approx 130$ Td in H_3O^+ reagent ion mode. PTR-TOF-MS was calibrated with a commercial volatile standard containing representatives of key plant volatiles (Ionimed GmbH, Innsbruck, Austria) in the beginning and at the end of the experiment, and no changes in sensitivity were observed between these calibration events. In addition, measurements with pure standards, simultaneously with PTR-TOF-MS and GC-MS were further used to check for stability of the compound concentration in the commercial standard and obtain calibration factors for individual volatiles missing in the calibration mixture. The raw data were acquired by the TofDaq software (Tofwerk AG, Switzerland) and post-processed by PTR-MS Viewer software (PTR-MS Viewer v3.1, Tofwerk AG, Switzerland) (Jordan *et al.* 2009; Portillo-Estrada, Kazantsev, & Niinemets 2017).

Methanol and methyl salicylate (MeSA) were detected as the protonated parent ions at m/z of 33.034 and 153.088, respectively (Brilli *et al.* 2011; Tasin, Cappellin, & Biasoli 2012; Maja *et al.* 2014; Brilli *et al.* 2016; Giacomuzzi *et al.* 2016; Portillo-Estrada *et al.* 2017; Yener *et al.* 2016; Portillo-Estrada *et al.* 2017). To identify the signals of volatile products of the LOX pathway in the blend of parent and fragment masses detected by PTR-TOF-MS, pure chemicals (Sigma-Aldrich, St. Louis, MO, USA) were individually analysed and mass signals consistent with previous studies were found (e.g. Brilli *et al.* 2011; Portillo-Estrada *et al.* 2017). The total LOX product emission presented in this study is the sum of the dominant compounds with m/z of 81.070, 83.085, 85.101, 99.080, 101.096 and 143.107, representing 2-hexenal and 3-hexenal ($C_6H_{10}O$) H^+ , 3-hexenol ($C_6H_{12}O$) H^+ , 1-hexanol ($C_6H_{14}O$) H^+ , 3-hexenol ($C_6H_{12}O$) H^+ and hexenyl acetate ($C_8H_{14}O_2$) H^+ , respectively (Beauchamp *et al.* 2005; Giacomuzzi *et al.* 2016; Portillo-Estrada *et al.* 2017; Portillo-Estrada *et al.* 2017). The identity of O_3 -induced LOX compounds and MeSA from *P. vulgaris* leaves was also confirmed in pilot experiments by separate GC-MS analyses carried out according to the protocol of Copolovici, Kännaste, Pazouki, & Niinemets (2012) and Kännaste, Copolovici, & Niinemets (2014). We estimated that for MeSA and LOX volatiles, the detection limit with our setup was better than $0.05 \text{ nmol m}^{-2} \text{ s}^{-1}$ and for methanol better than $0.2 \text{ nmol m}^{-2} \text{ s}^{-1}$. Given that the key volatiles elicited upon ozone exposure are relatively non-reactive with ozone (Arnell & Niinemets 2010; Holopainen, Nerg, & Blande 2013 for the reaction rate constants for ozone), and that the emissions were elicited mostly after the ozone exposure (Fig. 1), we did not consider possible volatile losses during ozone exposure.

Chlorophyll fluorescence measurements

Photosystem II (PS II) activity was assessed for each individual leaf before and after the O_3 treatment with a portable Imaging PAM chlorophyll fluorimeter and ImagingWin software (IMAG-MIN/B, Heinz Walz GmbH, Effeltrich, Germany). The MINI version of the Imaging PAM M-series has a measurement window area of $24 \times 32 \text{ mm}$. A CCD camera (640×480 pixels) serves for fluorescence imaging and 12 high-power LED lamps provide actinic light and high-intensity

light flashes. After the leaf was fixed in the leaf holder of the Imaging PAM and dark adapted for 30 min, the minimum (F_o) fluorescence yield was measured. The leaf was further illuminated with a 500 ms pulse of saturating irradiance ($2700 \mu\text{mol quanta m}^{-2} \text{ s}^{-1}$) to measure the maximum (F_m) dark-adapted fluorescence yield. The spatial-average maximum dark-adapted quantum yield of PSII, F_v/F_m was calculated as $(F_m - F_o)/F_m$.

Empty chamber corrections

Before inserting the leaves in the gas-exchange chamber, the background VOC emission rates from the empty chamber were measured to correct for possible release of volatiles adsorbed previously on the gas-exchange system components. In general, such corrections were minor (1%) but are included in the calculations for consistency (Niinemets *et al.* 2011). In addition, O_3 destruction due to surface reactions ('uptake') by an empty chamber ($C_{O_3}^{\text{chamber}}$, nmol mol^{-1}) was measured before inserting the leaves in the chamber and calculated as:

$$C_{O_3}^{\text{chamber}} = C'_{\text{in}} - C'_{\text{out}} \quad (1)$$

where C'_{in} is the O_3 concentration at the chamber inlet (either 200 or 600 nmol mol^{-1}) and C'_{out} that at the chamber outlet. The obtained values were subsequently used to correct all measurements of leaf O_3 uptake. Overall, this correction was small, less than 5% of total O_3 uptake when leaves were enclosed in the chamber.

Calculations of photosynthetic characteristics, trace gas emission rates and O_3 uptake

The net assimilation rate (A) and stomatal conductance for water vapour (g_s) were calculated per unit enclosed leaf area according to the equations of von Caemmerer & Farquhar (1981). We estimated that with our measurement system, the accuracy was better than $0.3 \mu\text{mol m}^{-2} \text{ s}^{-1}$ for net assimilation rate and better than $0.15 \text{ mmol m}^{-2} \text{ s}^{-1}$ for the transpiration rate.

Volatile emissions rates (ϕ_X , $\text{nmol m}^{-2} \text{ s}^{-1}$) were calculated as

$$\phi_X = [C_o(X) - C_i(X) - C_c(X)] \frac{F}{S} \quad (2)$$

where $C_o(X)$ is the concentration (nmol mol^{-1}) of the target VOC (compound X) measured at the chamber outlet and $C_i(X)$ that measured at the chamber inlet, $C_c(X)$ is the correction to account for possible release of the given compound from system components as explained earlier (generally negligible in the current study), F is the molar flow rate through the chamber ($1.19 \times 10^{-3} \text{ mol s}^{-1}$) and S is the leaf area enclosed in the chamber (m^2) (Beauchamp *et al.* 2005).

The temporal pattern of VOC emissions showed an exponential increase shortly after initiation of O_3 exposure, followed by a non-linear decay after the emission had reached a maximum value. Various aspects of the kinetics of the rise and decay of VOC emission rates were analysed, and the key quantitative emission characteristics were estimated by using

first-order exponential rise and decay models for different parts of the time kinetics of emissions (Table 1 for acronyms and definitions of all quantitative characteristics). The exponentially increasing part of the response was quantitatively analysed according to

$$\phi(t) = \phi(t_{PS})e^{k_1(t)} \quad (3)$$

where $\phi(t)$ is the emission rate at time t and $\phi(t_{PS})$ is the VOC emission rate measured at the start of the emission burst following the start of O₃ exposure. The parameter k_1 is the rate constant for the initial increase of VOC emission rate, and the corresponding doubling-time (τ_1) for the emission burst is calculated as $\ln(2)/k_1$.

The decreasing part of the emission burst was analysed quantitatively by

$$\phi(t) = \phi_M e^{-k_D t}, \quad (4)$$

where ϕ_M is the maximum VOC emission rate. Analogously, the parameter k_D is the rate constant for the decrease of VOC emission rate, and the corresponding half-time (τ_D) for the emission burst is calculated as $\ln(2)/k_D$. Figure 1 shows a typical example of VOC emission release patterns of this experiment, as well as the definition of key quantitative emission characteristics used earlier. When a second emission burst was present, decay and rise characteristics for this second rise of emissions were also calculated (Fig. 1 and Table 1).

The total amount of given VOC emitted over a certain time (Φ_X) (nmol m⁻²) was calculated as

$$\Phi_X = \sum_{t_{PS}}^{t_{PE}} \Delta t \phi_X \quad (5)$$

where t_{PS} and t_{PE} are the start and end times of the release of given VOC species, respectively, Δt is the measurement time interval (10 s) and ϕ_X is the emission rate of the given compound measured over this time interval (Beauchamp *et al.* 2005). The total emission values presented here correspond to 21 h after starting of elicitation of given compound (D_p) (Table 1 and Fig. 1).

The rate of O₃ uptake by whole leaf (ϕ_{LO_3} , nmol m⁻² s⁻¹) was calculated as

$$\phi_{LO_3} = (C_{in} - C_{out} - C_{O_3}^{chamber}) \frac{F}{S} \quad (6)$$

where C_{in} and C_{out} are the O₃ concentrations of the air entering and exiting the leaf chamber (nmol mol⁻¹) and $C_{O_3}^{chamber}$ is the amount of O₃ removed by the empty chamber (nmol mol⁻¹). In this study we calculated C_{in} and C_{out} as the average values over a certain time due to the fluctuations of concentration produced by O₃ generator and manual adjustment of C_{in} to account for changes in O₃ uptake during the exposure.

The rate of O₃ uptake by stomata (ϕ_{O_3} , nmol m⁻² s⁻¹) was determined by

$$\phi_{O_3} = (C_{out} - C_{O_3}^i) \frac{g_s}{2.03} \quad (7)$$

where C_{out} is the O₃ concentrations of the air exiting the leaf chamber (nmol mol⁻¹) and $C_{O_3}^i$ is intercellular O₃

concentration (nmol mol⁻¹), and 2.03 is the ratio of water vapour to O₃ diffusivities. This estimate was derived from O₃ diffusion coefficient in air of 1.267×10^{-5} m² s⁻¹ at 22.84 °C (Ivanov, Trakhtenberg, Bertram, Gershenzon, & Molina 2007) and water vapour diffusion coefficient in air of 2.569×10^{-5} m² s⁻¹ at the same temperature calculated according to Chapman and Enskog (Niinemets & Reichstein 2003a). Analysis of possible temperature effects on the collision integral for both water vapour and O₃ (Tucker & Nelken 1982) suggested that temperature effects on this ratio were minor (the ratio differed less than 0.1% for 25 °C used for leaf measurements and 22.84 °C used to estimate O₃ diffusivity).

Although it has for long been considered that the internal O₃ concentration is close to zero because of its high reactivity once taken up (Laisk, Kull, & Moldau 1989), Moldau & Bichele (2002) showed that very high ambient concentrations of O₃ led to low, but not zero, internal O₃ concentrations ($C_{O_3}^i$), biasing O₃-uptake flux calculations up to 5%. Because the internal O₃ concentration was unknown, this correction was not considered in our study. Given that an average value had to be used for C_{out} , the corresponding average value of stomatal conductance (g_s) was used in these calculations. The rate of non-stomatal O₃ uptake was calculated as the difference between total (Eqn 6) and stomatal uptake rates (Eqn 7).

The total amount of O₃ uptake (Φ_Y) over the given exposure period (O₃ dose) was calculated as:

$$\Phi_Y = \sum_t \Delta t \phi_Y \quad (8)$$

where t is the time after starting O₃ exposure, Δt is the time interval duration of the O₃ exposure (30 min) and ϕ_Y is the mean rate of O₃ uptake by the whole leaf through stomata measured during this time interval (Beauchamp *et al.* 2005). Total and non-stomatal O₃ uptakes were calculated analogously.

Statistical analyses

All treatments were conducted in three replications with different plants. The statistical significance of the effects of O₃ exposure treatment were tested with one-way ANOVA followed by Tukey's post hoc test using SPSS 16.0 (SPSS, Chicago, Illinois, USA). In addition, linear and non-linear regressions were fitted to the data based on the shape of the response. All statistical tests were considered significant at $P < 0.05$.

RESULTS

Leaf damage, ozone uptake, chlorophyll fluorescence and photosynthesis

Although necrotic spots on leaves were visible in all treatments after O₃ exposure, the area of necrotic lesions in Treatment 2 (exposure to 600 nmol mol⁻¹ O₃ in the darkness) was much less than in Treatments 1 (exposure to 600 nmol mol⁻¹ O₃ in the light) and 3 (exposure first to 200 nmol mol⁻¹ and then to 600 nmol mol⁻¹ O₃ in the light; Fig. 2a,b). Photosynthetic rates (A) and the maximum quantum efficiency of PSII (F_v/F_m) obtained from chlorophyll fluorescence measurements were

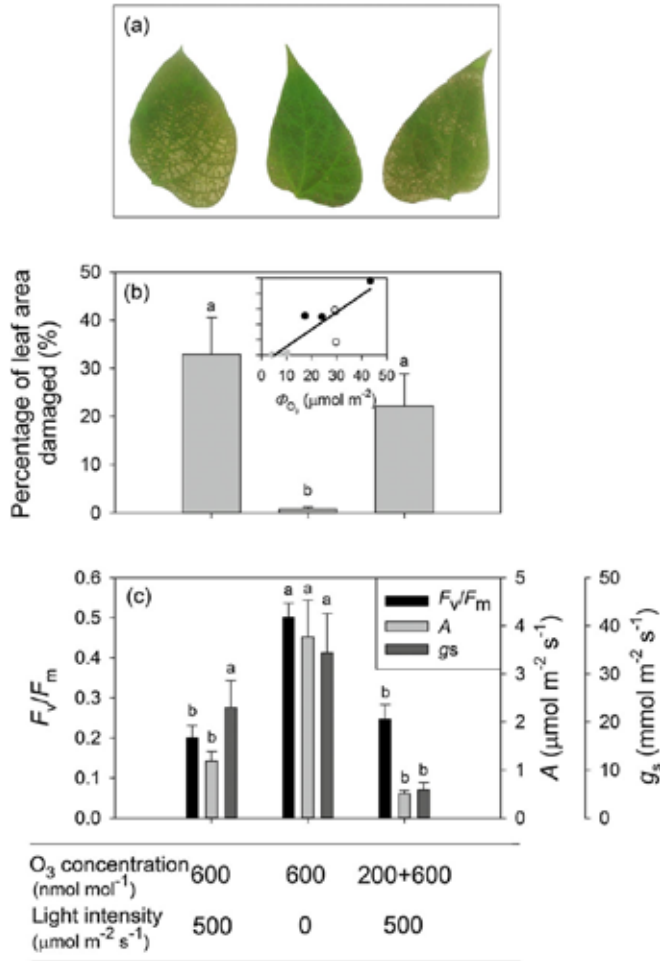


Figure 2. Illustration of visible leaf injury in representative O_3 -fumigated leaves (a), percentage of leaf area damaged (b) and physiological data collected from *P. vulgaris* leaves before O_3 fumigation and 21 h after O_3 fumigation (c). The relationship between the percentage of leaf area damaged and total amount of O_3 uptake (Φ_{O_3}) in (b) were fitted by a linear regression ($y = 1.12x - 5.69$; $r^2 = 0.74$, $P < 0.005$). The error bars denote \pm standard error (SE). The means were compared by ANOVA and the means separated by Tukey's tests. Significant differences ($P < 0.05$) between means are indicated by different letters.

significantly reduced in *P. vulgaris* leaves after O_3 exposure in both Treatments 1 and 3 compared with Treatment 2 (Fig. 2c). However, there was no statistical difference in average stomatal conductance (g_s) after treatment between Treatments 1 and 2 (Fig. 2c; $P > 0.10$). Relative to the values prior to O_3 fumigation, F_v/F_m decreased on average (\pm SE) by $74 \pm 3.9\%$ in Treatment 1, $31 \pm 6.6\%$ in Treatment 2 and $67 \pm 4.8\%$ in Treatments 3. The declines were also observed in photosynthetic rate (A) under O_3 exposure in all treatments, $87 \pm 3.6\%$ for Treatment 1, $59 \pm 8.3\%$ for Treatment 2 and $93 \pm 1.7\%$ for Treatment 3.

Correlations between O_3 uptake and stomatal conductance

A strong linear relationship was found between O_3 uptake flux and stomatal conductance when leaves were fumigated under a constant O_3 concentration of $600 \text{ nmol mol}^{-1}$ ($P < 0.0001$; circles in Fig. 3a). Although the range of stomatal conductance for fumigations with $200 \text{ nmol mol}^{-1}$ O_3 was small (triangles, Fig. 3a), the rate of O_3 uptake at a given conductance of about $110 \text{ mmol m}^{-2} s^{-1}$ was approximately 30% of that obtained at $600 \text{ nmol mol}^{-1}$ O_3 ; that is, the difference in uptake between

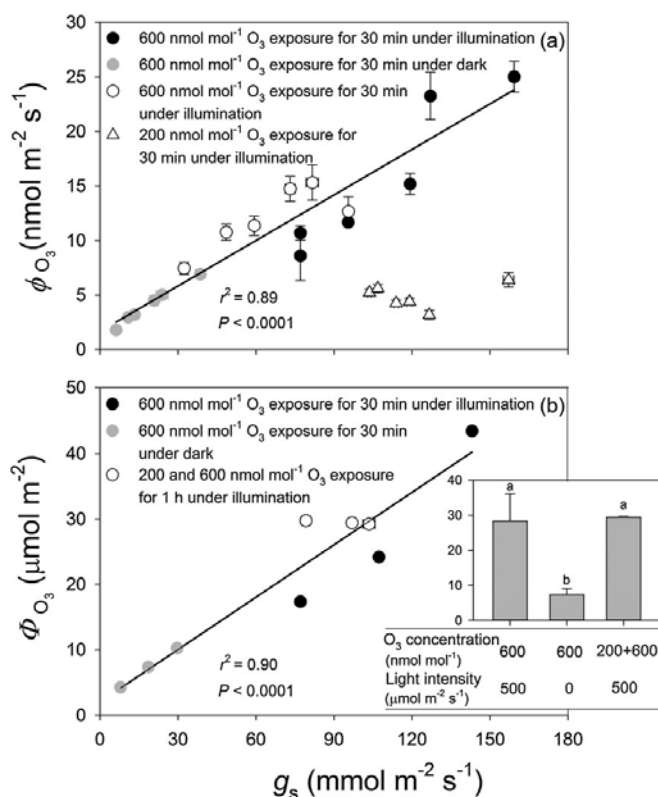


Figure 3. Stomatal conductance (g_s) in relation to O₃ uptake rate per leaf area (ϕ_{O_3}) (a) and total amount of O₃ uptake (Φ_{O_3}) over the given exposure period (b and inset) in O₃-exposed leaves of *P. vulgaris*. The black circles correspond to illuminated leaves fumigated with 600 ± 33 nmol mol⁻¹ of O₃ for 30 min. The grey circles correspond to leaves exposed to 600 ± 30 nmol mol⁻¹ of O₃ for 30 min in darkness. The white triangles and circles correspond to the same treatment, for illuminated leaves exposed first to 200 ± 11 nmol mol⁻¹ of O₃ for 30 min (white triangles) and then to 600 ± 32 nmol mol⁻¹ of O₃ for an additional 30 min (white circles). Data for 600 nmol mol⁻¹ O₃ fumigation for 30 min were fitted by linear regressions (for (a): $y = 0.139x + 1.67$; $r^2 = 0.89$, $P < 0.0001$; for (b): $y = 0.267x + 2.07$; $r^2 = 0.90$, $P < 0.0001$). Error bars indicate \pm SE.

these treatments scaled was strongly driven by the ambient O₃ concentration. In addition, the total rate of O₃ uptake (non-stomatal + stomatal) (ϕ_{LO_3}) was similarly correlated with stomatal uptake (data not show), which indicates that the O₃ uptake rate was highly dependent on the O₃ concentration during fumigation (Table 2).

The amount of O₃ taken up by leaves in the three treatments shown in Fig. 3b reflects differences in stomatal conductance over the course of the O₃ fumigation period. Thus, total O₃ uptake in Treatment 1, in which fumigation took place under illuminated conditions, was substantially greater than the uptake in Treatment 2, in which fumigation occurred in darkness and stomatal conductance was substantially less ($84.7 \pm 3.1\%$ less) than in Treatment 1. Although the leaves in Treatment 3 were exposed to 200 nmol mol⁻¹ O₃ for 30 min prior to further 30 min exposure to 600 nmol mol⁻¹, the total amount of O₃ taken up was not statistically different from that taken up by the leaves in Treatment 1 because of

more rapid stomatal closure during 600 nmol mol⁻¹ fumigation (Table 2). In addition, a strong non-linear relationship ($P < 0.0001$) was found between the total amount of O₃ taken up (Φ_{O_3}) and the percentage of leaf area damaged (Fig. 2b). More than half of total O₃ uptake (ϕ_{LO_3}) was due to leaf surface deposition, and there were no significant differences in the percentage of non-stomatal O₃ uptake among the treatments (Table 2).

Time courses of gas-exchange during and after O₃ exposure

Both photosynthetic rate (A) and stomatal conductance (g_s) rapidly decreased in all *Phaseolus vulgaris* leaves after O₃ exposure, and representative kinetics in each of the three Treatments used to estimate the key kinetic characteristics (Fig. 1, Table 1) are analysed in the following (Fig. 4). For the

Table 2. Average \pm SE O_3 uptake by the entire leaf (Φ_{LO_3} , $\mu\text{mol m}^{-2}$) and via the stomata (Φ_{O_3} , $\mu\text{mol m}^{-2}$) and percentage of non-stomatal O_3 uptake (%) from leaves of *Phaseolus vulgaris* in response to different O_3 treatments under illumination and in darkness

O_3 uptake	O_3 concentration (nmol mol^{-1})		
	600	600	200 + 600
	Light intensity ($\mu\text{mol m}^{-2} \text{s}^{-1}$)		
	500	0	500
O_3 uptake by the entire leaf (Φ_{LO_3} , $\mu\text{mol m}^{-2}$)	66.2 \pm 9.6 a ^a	24.3 \pm 4.9 b	64.9 \pm 5.7 a
O_3 uptake via the stomata (Φ_{O_3} , $\mu\text{mol m}^{-2}$)	28.3 \pm 7.8 a	7.3 \pm 1.7 b	29.5 \pm 0.15 a
Percent of non-stomatal O_3 uptake (%)	58.4 \pm 6.5 a	70.3 \pm 1.4 a	53.9 \pm 4.0 a

The O_3 treatment 200 + 600 nmol mol^{-1} denotes a 30 min pre-exposure to 200 nmol mol^{-1} O_3 (priming) followed by a further 30 min exposure to 600 nmol mol^{-1} O_3 .

^aDifferent letters indicate statistical significance at $P < 0.05$.

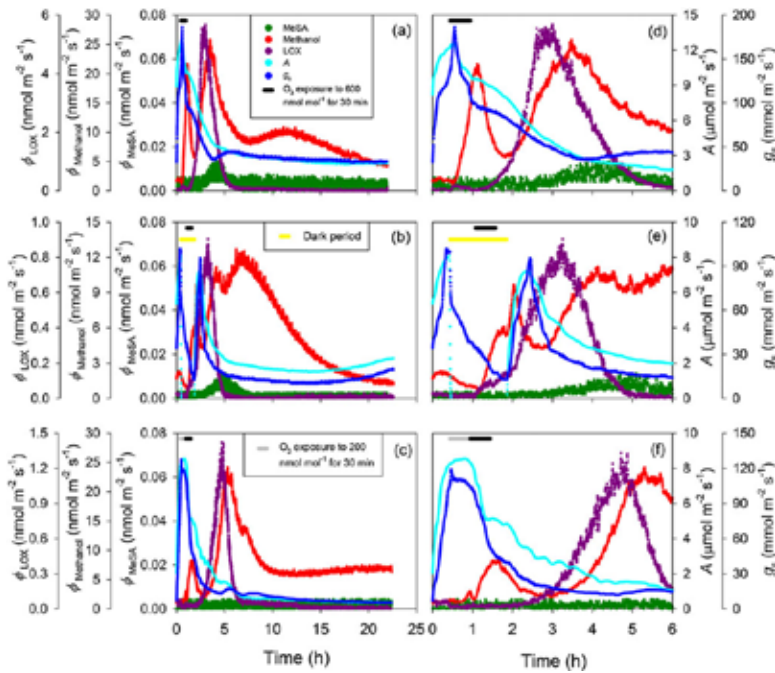


Figure 4. Representative time courses of photosynthetic rates, stomatal conductance and induced volatile emissions in O_3 -exposed *P. vulgaris* leaves for three different treatments. In the first treatment (a and d), the leaf was exposed to 600 nmol mol^{-1} O_3 under continuous illumination for 30 min, in the second treatment (b and e), the leaf was exposed to 600 nmol mol^{-1} O_3 in darkness for 30 min, and in the third treatment (c and f), the leaf was exposed to 200 nmol mol^{-1} O_3 for 30 min and to 600 nmol mol^{-1} O_3 for 30 min under continuous illumination. In (a)–(c), the whole measurement period including the period for leaf adaptation within the leaf chamber prior to fumigation, fumigation period and recovery period after fumigation until 21 h is shown. In (d)–(f), the same data are zoomed out for the period from the onset of measurement until 6 h. In all cases, the black bars on the top left indicate the period of 600 nmol mol^{-1} O_3 fumigation, the grey bar denotes the period of 200 nmol mol^{-1} O_3 fumigation and the yellow bar denotes the leaf darkening period. LOX stands for volatile products of the lipoxygenase pathway and MeSA for methyl salicylate.

representative leaf in Treatment 1, the photosynthetic rate (A) was approximately $9.6 \pm 1.3 \mu\text{mol m}^{-2} \text{s}^{-1}$ prior to O_3 fumigation, but began to decline shortly after the start of fumigation, declining by $\sim 20\%$ over the 30 min fumigation period

(Fig. 4a,d). Following fumigation, photosynthetic rate continued to decline almost linearly for approximately 3 h, reaching a value of $5.2 \pm 0.2 \mu\text{mol m}^{-2} \text{s}^{-1}$. Photosynthetic rate continued to decline slowly before levelling off at $\sim 1.4 \mu\text{mol m}^{-2} \text{s}^{-1}$

after about 12 h. Stomatal conductance (g_s) evinced a sudden transient increase at the beginning of O₃ fumigation and then declined in parallel with photosynthetic rate (A) for the first 3 h following fumigation (Fig. 4a,d). Stomatal conductance then recovered slightly and remained stable for the remaining 18 h of the experiment at a value approximately 30% of the pre-fumigation value.

For the representative leaf in Treatment 2 (Fig. 4b,e), the pre-fumigation rate of photosynthesis in the light was $7.97 \pm 0.08 \mu\text{mol m}^{-2} \text{s}^{-1}$. When the leaf was darkened, including the 30 min O₃ fumigation period, A became negative, and g_s declined by about 86% from its previous value in the light. During the first 30 min after the light was turned back on, both the photosynthetic rate (A) and stomatal conductance recovered rapidly, returning to nearly the same levels as before darkening, but both then declined sharply over the next 60 min to only ~50% of their initial values. Both A and g_s then continued to decline slowly over the next 11 h, and then both started to recover at about 12 h after the fumigation. Although the photosynthetic rate in Treatment 2 declined significantly from pre-fumigation values, A was less affected than in Treatment 1, never falling below about 30% of the pre-fumigation value.

In Treatment 3, neither photosynthetic rate (A) nor stomatal conductance (g_s) was affected by the 30-min exposure to 200 nmol mol⁻¹ O₃, but when O₃ concentration was raised to 600 nmol mol⁻¹ for 30 min, changes in photosynthetic characteristics were similar to those in the Treatment 1 (Fig. 4c,f). Both A and g_s fell by 41% during the 600 nmol mol⁻¹ fumigation period, then continued to decline more slowly over the following 4 h before levelling off at low values about 11 h after stopping the fumigation (Fig. 4c,f). Although g_s exhibited two slight transient periods of recovery, between ~4–6 h and 7–9 h (Fig. 4c), g_s was more strongly affected by O₃ fumigation in Treatment 3 than in either Treatments 1 or 2. The effects of fumigation on A were very similar in Treatments 1 and 3, and more severe than in Treatment 2. In addition, during the 21 h following the end of O₃ exposure, a significant recovery of photosynthetic rate (A) and stomatal conductance (g_s) was observed only in the Treatment 2 (Fig. 4b).

Time courses of emissions of methanol, LOX products and MeSA

Prior to ozone exposure, methanol emission rates did not differ significantly among plants used in different treatments ($1.77 \pm 0.158 \text{ nmol m}^{-2} \text{s}^{-1}$, $1.76 \pm 0.368 \text{ nmol m}^{-2} \text{s}^{-1}$ and $1.66 \pm 0.247 \text{ nmol m}^{-2} \text{s}^{-1}$ for Treatments 1, 2 and 3, respectively), and the emissions of volatile LOX products and MeSA were not detectable. During and following the exposure to O₃, characteristic emissions bursts of methanol, LOX volatiles and MeSA were observed (Fig. 4 for the temporal patterns emissions for representative leaves in each of the three treatments). All elicited VOC emissions exhibited a sigmoidal rise to a peak value and then decayed to near pre-fumigation values (Fig. 4), and the emissions of these key volatile classes followed the same general pattern in all leaves, but there were specific compound and treatment differences as discussed in the following.

Methanol emissions exhibited a bi-phasic or tri-phasic response pattern. A few minutes after the onset of fumigation with high O₃ of 600 nmol mol⁻¹, methanol emissions began to rise, peaking shortly after the fumigation ended and then declined rapidly (methanol burst 1; Fig. 4). A second, much larger burst of methanol emissions was observed in all experiments beginning 1–2 h after the end of the fumigation and peaking several hours later (methanol burst 2; Fig. 4). In most cases, a third rise of methanol emission was also observed (Fig. 4a,b).

For the first methanol emission burst, in Treatments 1 and 3 where O₃ fumigation was carried out in the light (Fig. 4a,c,d,f), methanol emissions increased within 10 min since the start of the fumigation and began to fall rapidly within 10 min after cessation of the fumigation. In Treatment 2 where O₃ fumigation occurred in darkness (Fig. 4b,e), the elicitation response was similar, but in contrast to illuminated leaves, when the fumigation period ended, methanol emissions remained constant in the dark for an additional 15 min. When the leaf was then illuminated, a second short burst of methanol emissions was observed, perhaps associated with rapid stomatal opening (Fig. 4e). In Treatment 3 where the leaves were exposed first to a lower O₃ dose of 200 nmol mol⁻¹, the induction of methanol emissions was very slight (Fig. 4f). When the exposure concentration was raised to 600 nmol mol⁻¹, methanol emissions increased rapidly, exhibiting dynamics similar to Treatment 1.

The second burst of methanol emission was similar in all treatments (Fig. 4a,b,c). However, in Treatment 1, a broad, but a smaller late rise of methanol emission occurred at about 12 h since the start of fumigation, while in Treatment 2, this tertiary rise occurred earlier, at ca. 6 h and partly run into the second emission burst (Fig. 4b). In Treatment 3, this tertiary peak was almost absent, and overall, the long-term methanol emissions decreased earlier than in the two other treatments (Fig. 4c,f).

No enhancement of LOX product emissions was observed during and immediately after O₃ exposure, but in all cases, exposure to O₃ resulted in a single large burst of LOX product emissions beginning 1–2 h after the exposure, and peaking just before the second methanol emission burst. A burst of MeSA emissions was observed in all leaves of Treatments 1 and 2 (Fig. 4a,b,d,e), but not in any of the leaves in Treatment 3 (Fig. 4c,f). The onset, duration and magnitude of LOX product and MeSA emissions varied with treatment as discussed in the succeeding texts.

Maximum and total integrated O₃-elicited volatile emissions

Despite qualitatively similar emission dynamics discussed earlier, quantitatively, the size of the VOC emission bursts and the total amount of methanol and LOX products emitted over the 21 h recovery period following O₃ exposure differed between the three treatments. The maximum emission rates observed during the initial burst of methanol (burst 1) were significantly greater in Treatment 1 than in either Treatments 2 or 3, which did not differ significantly from each other (Fig. 5a). In addition, a strong non-linear relationship

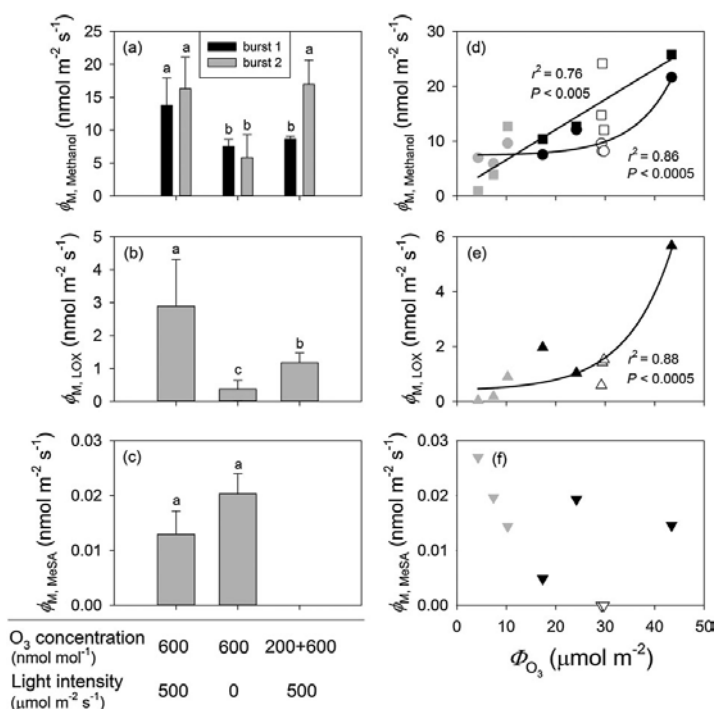


Figure 5. Maximum emission rates of methanol (a), LOX products (b) and MeSA (c) and corresponding correlations with the total amount of O₃ uptake (Φ_{O_3}) (d–f) in O₃-exposed *P. vulgaris* leaves. The MeSA emission burst was absent in Treatment 3 in (c). In all cases, the black symbols denote data from the illuminated leaves fumigated with 600 ± 33 nmol mol⁻¹ O₃ for 30 min (Treatment 1), the grey symbols correspond to leaves exposed to 600 ± 30 nmol mol⁻¹ O₃ for 30 min in darkness (Treatment 2), and the white symbols denote the illuminated leaves first exposed to 200 ± 11 nmol mol⁻¹ O₃ for 30 min and then to 600 ± 32 nmol mol⁻¹ for additional 30 min (Treatment 3). In (d), the data for the first methanol emission burst (circles) were fitted by an exponential regression ($y = 0.0569 \cdot 1.14^x + 7.40$; $r^2 = 0.86$, $P < 0.0005$) and the data for the second methanol emission burst (squares) were fitted by a linear regression ($y = 0.55x + 1.10$; $r^2 = 0.76$, $P < 0.005$). In (e), the data were fitted by an exponential regression ($y = 0.0453 \cdot 1.11^x + 0.389$; $r^2 = 0.88$, $P < 0.0005$). The error bars indicate \pm SE. Statistical data analysis as in Fig. 2.

($P < 0.0005$) was found between the total amount of O₃ taken up (Φ_{O_3}) and the maximum emission rate of the first methanol burst (Fig. 5d). In contrast, the maximum methanol emission rates observed during the second burst were significantly higher in both Treatments 1 and 3 than in Treatment 2, and the correlation between total amount of O₃ taken up (Φ_{O_3}) and the maximum emission rate of the second methanol emission burst was linear ($P < 0.005$; Fig. 5d).

The maximum emission rate of LOX products was greater in Treatment 1 than in either Treatment 2 or 3 (Fig. 5b), and it was strongly correlated with the total amount of O₃ taken up (Φ_{O_3}) ($P < 0.0005$; Fig. 5e). No significant differences in maximum emission rates of MeSA between Treatments 1 and 2 leaves were found, while MeSA emission was undetectable in Treatment 3 (Fig. 5c), and the maximum MeSA emission rate was not correlated with the O₃ dose (Fig. 5f).

Overall, the amount of methanol released during the second bursts (after the initial methanol burst; Fig. 4a,b,c) was much greater, 10-fold to 25-fold greater, than the amount of

methanol released during the first burst, reflecting the circumstance that the second burst of methanol emission persisted for over 5 h (Fig. 6a). Differently from the maximum methanol emission rate during burst 1 (Fig. 5a), no significant difference was observed in the total amount of methanol released during burst 1 between Treatments 1 and 3 (Fig. 6a). Leaves in both these treatments, however, released significantly more methanol during the first burst than those in Treatment 2 (Fig. 6a). Consistent with observed differences in maximum peak height (Fig. 4a,b,c), the total amount of methanol emissions during methanol burst 2 was significantly lower in Treatment 2 than in either Treatments 1 or 3, which did not differ significantly from each other (Fig. 6a). The total emission of methanol during O₃ exposure and through the recovery phase in Treatments 1 and 3 exceeded more than twice that in Treatment 2, because the emissions during the secondary bursts dominated the total emissions (Fig. 6b).

Total LOX emissions were vastly different among treatments and the treatments ranked according to total emission

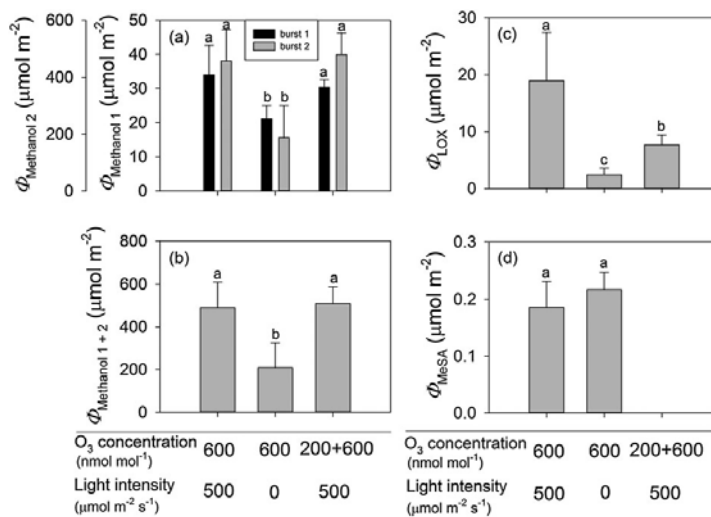


Figure 6. Total amount of emitted methanol for the first and for the second methanol emission burst (a), the sum two methanol emission bursts (b), total LOX product emission (c) and total MeSA emission (d) for three O₃ treatments in *P. vulgaris* leaves. The error bars stand for \pm SE. Treatments as in Fig. 5 and statistics as in Fig. 2.

of LOX products as Treatment 1 > Treatment 3 > Treatment 2 (Fig. 6c). Consistent with the data on maximum emission rates of MeSA (Fig. 5c), total amount of MeSA released did not differ significantly between Treatments 1 and 2 (Fig. 6d).

Start and rate of elicitation and decay of volatile emissions

The delay between the onset of O₃ exposure and the initiation of the first methanol burst (t_{E1} ; Fig. 1 for definitions) was about 10 min, and it did not differ significantly between the treatments (Fig. 7a). The time from the onset of elicitation to the maximum of the first methanol burst (t_{M1}) was significantly lower in Treatment 1 than in Treatments 2 and 3 (Fig. 7d), and this was also similar for the duration of the emission burst lasting on average (\pm SE) 1.28 ± 0.145 h, 1.87 ± 0.196 h and 1.76 ± 0.375 h for Treatments 1, 2 and 3, respectively (the mean for the Treatment 1 is significantly different from the two other treatments at $P < 0.05$). However, the time until the second burst was initiated (t_{E2}) was significantly less in Treatments 1 and 2 than in Treatment 3 (Fig. 7a). There was no significant difference in the time from the onset of elicitation to the second methanol peak in all cases (Fig. 7d), but the duration of the second methanol emission burst (Fig. 4) was longer in Treatments 1 (19.5 ± 0.164 h) and 3 (19.0 ± 0.125 h) than in Treatment 2 (14.8 ± 2.23 h, means are significantly different at $P < 0.02$). The burst of LOX products after the onset of O₃ fumigation occurred earlier in Treatment 1 than in Treatment 2 and 3 (Fig. 7b), and the time from the onset of elicitation to the peak in emissions of LOX products was significantly greater in Treatments 1 and 3 than in Treatment 2 (Fig. 7c). In contrast,

the duration of the LOX burst (Fig. 4) was the greatest in Treatment 3 (9.10 ± 1.77 h), followed by Treatment 1 (5.53 ± 0.206 h) and Treatment 2 (3.36 ± 0.058 h; the means are statistically significant at $P < 0.01$). The MeSA emission burst occurred earlier in Treatment 2 than in Treatment 1 (Fig. 7c), but the time from the onset of elicitation to the peak of MeSA emission did not differ among Treatments 1 and 2 (Fig. 7f).

To further characterize O₃ effects on the emission kinetics, the rate constants for induction (k_1 , Eqn 4) and decay (k_D , Eqn 5) were determined. For the first burst of methanol emission, both the initial increase and decrease of emissions were faster in Treatment 1 than in either Treatments 2 or 3 (Fig. 8a,b). For the second burst of methanol release, the initial increase of emissions was faster and decrease was slower in Treatment 2 than in either Treatments 1 or 3 (Fig. 8a,b). Both the rise and decline kinetics were much faster for the LOX product emission burst in Treatment 2 than in either Treatments 1 or 3 (Fig. 8c). However, for MeSA emission, there were no significant differences in k_1 and k_D among Treatments 1 and 2 (Fig. 8d).

The total emissions of the first and second methanol emission bursts and LOX products were strongly correlated with total amount of O₃ taken up (Φ_{O_3}) (Fig. 9a,b). The time from the onset of elicitation to the peak in emissions of the first methanol burst and LOX emission burst were nonlinearly correlated with total amount of O₃ taken up (Φ_{O_3}) (Fig. 9c,d). The correlations between total amount of O₃ taken up (Φ_{O_3}) and k_1 and k_D broadly reflected differences among the treatments with k_{12} for methanol (Fig. 9e), k_1 (Fig. 9f) and k_D (Fig. 9h) for LOX products decreasing and k_D values for both the first and

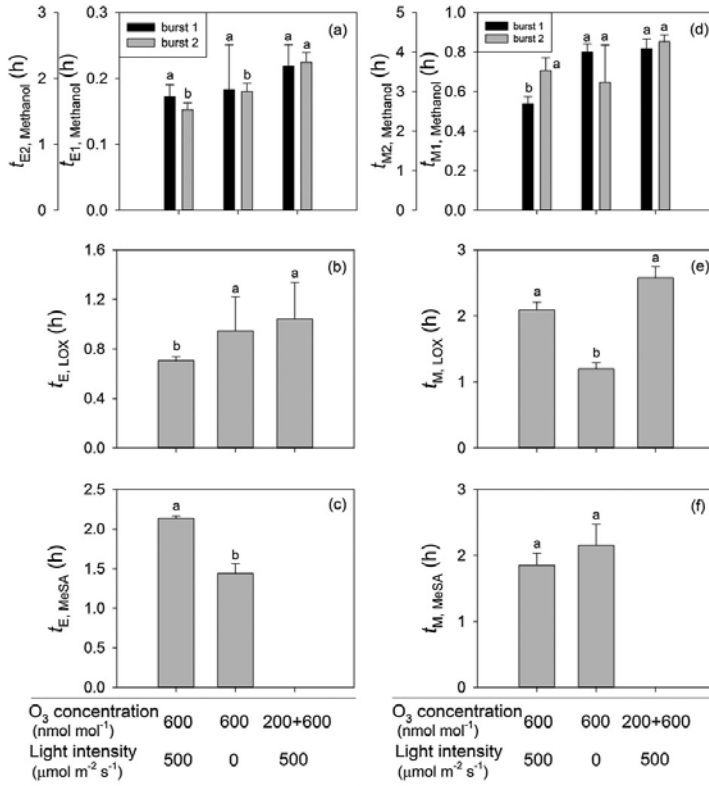


Figure 7. The lag time from the onset of O₃ exposure to the elicitation (a–c), and from elicitation to the maximum emission (d–f) for the first and second burst of methanol (a, d), LOX products (b, e) and MeSA (c, f) for three O₃ treatments in *P. vulgaris* leaves. The error bars indicate \pm SE. Treatments as in Fig. 5 and statistical analysis as in Fig. 2.

subsequent methanol emission burst (Fig. 9g) increasing with increasing the amount of O₃ taken up.

DISCUSSION

O₃ exposure and uptake via stomata

Ambient ozone concentrations significantly vary over the land surface, and large-scale predictions of O₃ effects on plant growth, production and biodiversity are commonly based on this variation in surrounding air O₃ concentrations (e.g. Feng *et al.* 2008; Wittig *et al.* 2009; Ainsworth *et al.* 2012). However, O₃ sensitivity varies among plant species (Flowers *et al.* 2007; Brauer *et al.* 2016; Li, Calatayud, Gao, Uddling, & Feng 2016; Osborne *et al.* 2016), and plant responses to chronic low to moderate level O₃ exposure can quantitatively and qualitatively differ from the responses to acute O₃ exposure (Beauchamp *et al.* 2005; Calfapietra, Pallozzi, Lusini, & Velikova 2013; Heiden *et al.* 1999). Furthermore, the overall physiological effects can be importantly driven by O₃ uptake

via stomata (Beauchamp *et al.* 2005; Jud *et al.* 2016). Given that stomatal conductance is affected by light level, modifications in light availability as occurring commonly during the day and among the days can importantly alter plant responses to O₃. Furthermore, stomatal effects can also be altered by pre-exposure to lower O₃ concentrations, for example exposure to the morning low O₃ concentrations can force stomatal closure, thereby reducing O₃ uptake during the rest of the day when ambient concentrations are higher (Nolle, Ellul, Heinrich, & Güsten 2002; Ribas & Peñuelas 2004; Xu *et al.* 2008). Thus, quantitative characterization of initial responses of plants to elevated O₃ under different light levels and pre-exposure to lower-level O₃ can provide important insight into factors affecting plant responses to acute O₃ stress.

Stomatal uptake at the given ambient O₃ concentration can be significantly affected by surface reactions due to high-reactivity volatile and non-volatile compounds stored in the trichomes on leaf surface or released from the leaf interior. Previously, Jud *et al.* (2016) found that the glandular trichomes of *Nicotiana tabacum* are an efficient chemical barrier against

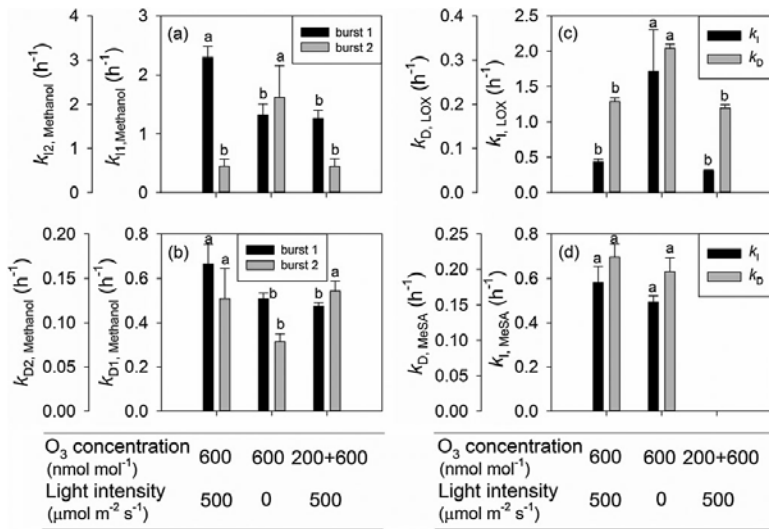


Figure 8. The rate constant for the initial increase for the first and the second emission burst of methanol (a), LOX products (c) and MeSA (d) and the rate constant for decrease for the first and the second emission burst of methanol (b), LOX products (c) and MeSA (d) for three treatments in O₃-exposed *P. vulgaris* leaves. The error bars indicate \pm SE. Treatments as in Fig. 5 and statistical analysis as in Fig. 2.

stomatal O₃ uptake due to amplification of surface reactions that deplete O₃ at the leaf surface. Indeed, peltate glandular trichomes have been found to produce and store biogenic VOCs and alter plant abiotic or biotic stress induced responses (Corsi & Bottega 1999; Gang *et al.* 2001; Wagner, Wang, & Shepherd 2004). However, *Phaseolus vulgaris* has capitate glandular trichomes (Bahafid *et al.* 2017; Li *et al.* unpublished observations), the role of which as the storage of biogenic volatiles is less clear (Levin 1973; Corsi & Bottega 1999), but which nevertheless might contribute to depleting O₃ at the leaf surface. In this study, we investigated the O₃ depletion by *Phaseolus vulgaris* under dark and light conditions and found that the percentage of non-stomatal O₃ uptake in all three treatments was actually higher than the stomatal uptake (Table 2). This is a direct indication for the high O₃ depletion capacity of the surface, and indeed such a strong surface deposition capacity can directly reduce stomatal O₃ uptake. In our study, the variation in total O₃ uptake among treatments was mainly driven by variation in stomatal O₃ uptake (Table 2) with Treatment 2, 600 nmol mol⁻¹ O₃ exposure in darkness exhibiting the lowest O₃ uptake due to stomatal closure in the darkness (Table 2). While the total O₃ uptakes did not differ among O₃ exposure treatments in the light, exposure to the lower O₃ concentration of 200 nmol mol⁻¹ in Treatment 3 reduced stomatal conductance such that during the subsequent exposure to the higher O₃ concentration of 600 nmol mol⁻¹, O₃ uptake was less than in Treatment 1 where the leaves were immediately exposed to the high O₃ concentration (Table 2). This could allow plants to respond faster to oxidative stress caused by O₃, preventing O₃ entry and minimizing potential damage and preventing the over-accumulation ROS. These data collectively indicate

that both the modification of light level and initial exposure to lower O₃ concentration significantly reduced the O₃ uptake due to acute exposure.

Impact of elevated O₃ on photosynthetic characteristics

Generally, O₃ exposure results in decreased net photosynthetic carbon assimilation (*A*), stomatal conductance (*g_s*) and the maximum quantum efficiency of PSII (*F_v/F_m*) (Long & Naidu 2002; Calatayud *et al.* 2003; Fiscus *et al.* 2005; Flowers *et al.* 2007; Kollist *et al.* 2007; Vahisalu *et al.* 2008; Guidi *et al.* 2009; Vahisalu *et al.* 2010). A reduction of *A* in O₃ exposed leaves typically results from decreases in *g_s* and losses in Rubisco activity (Fiscus *et al.* 2005). In our study, the reductions in photosynthetic characteristics and total O₃ uptake through stomata (Φ_{O_3}) were strongly related (Fig. 2), consistent with past observations (e.g. Calatayud *et al.* 2003). In fact, leaves in Treatment 2 showed a minor degree of foliage visible injury and a moderate reduction in photosynthetic characteristics with some changes in only *A* and *g_s* (Fig. 2). Because the pre-exposure to the lower concentration of 200 nmol mol⁻¹ led to a significant decline in *g_s*, and thus, O₃ uptake during the subsequent exposure to the higher concentration of 600 nmol mol⁻¹ was less in Treatment 3 than in Treatment 1. However, the total O₃ uptake through stomata (Φ_{O_3}) was similar in Treatments 1 and 3, and the degree of final leaf damage and reduction in *F_v/F_m* and *A* were statistically not different among these treatments (Fig. 2), suggesting that the cumulative stress resulting from exposures to both 200 and 600 nmol mol⁻¹ in Treatment

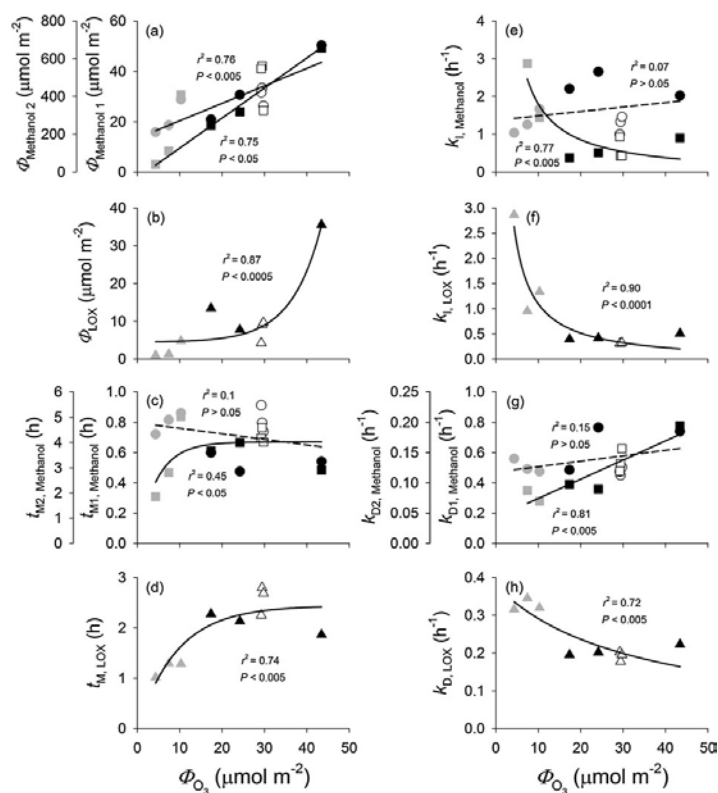


Figure 9. Correlation of total emissions (a and b), the lag time from elicitation to the maximum emission (c and d), the rate constant for the initial increase (e and f) and decrease (g and h) for the two methanol bursts (a, c, e, g) and LOX products (b, d, f, h) with the total amount of O_3 taken up (Φ_{O_3}) in O_3 -exposed leaves of *P. vulgaris*. In all cases, the black symbols denote illuminated leaves fumigated with $600 \pm 33 \text{ nmol mol}^{-1} O_3$ for 30 min (Treatment 1), the grey symbols denote the leaves exposed to $600 \pm 30 \text{ nmol mol}^{-1} O_3$ for 30 min in darkness (Treatment 2), and the white symbols denote the illuminated leaves exposed first to $200 \pm 11 \text{ nmol mol}^{-1} O_3$ for 30 min and then to $600 \pm 32 \text{ nmol mol}^{-1} O_3$ for additional 30 min (Treatment 3). In (a), (c), (e) and (g), the circles correspond to the first and squares to the second methanol emission burst. In (a), the data for both the first (circles; $y = 0.695x + 13.4$; $r^2 = 0.76$, $P < 0.005$) and second (squares; $y = 13.9x + 72.2$; $r^2 = 0.75$, $P < 0.005$) methanol emission burst were fitted by linear regressions. In (b), the data for LOX products were fitted by a non-linear regression ($y = 0.0607 \cdot 1.15^x + 4.46$; $r^2 = 0.87$, $P < 0.0005$). In (c), the data for the first methanol emission burst were fitted by a linear (circles; $y = -0.00370x + 0.798$; $r^2 = 0.1$, $P > 0.05$) and the data for the second burst by a non-linear regression (squares; $y = 4.02(1 - \exp(-0.215x))$; $r^2 = 0.45$, $P < 0.05$). In (d), the LOX product data were fitted by an exponential regression ($y = 2.44 \cdot (1 - 0.898^x)$; $r^2 = 0.74$, $P < 0.005$). In (e), the data for the first methanol emission burst were fitted by a linear (circles; $y = 0.0117x + 1.37$; $r^2 = 0.07$, $P > 0.05$) and the data for the second burst by a non-linear regression (squares; $y = 18.9/x - 0.0904$; $r^2 = 0.77$, $P < 0.005$). In (f), the data for LOX products were fitted by a non-linear regression ($y = 11.6/x - 0.0612$; $r^2 = 0.90$, $P < 0.0001$). In (g), the data for both the first (circles; $y = 0.471 + 0.00360x$; $r^2 = 0.15$, $P > 0.05$) and second (squares; $y = 0.00320x + 0.0426$; $r^2 = 0.81$, $P < 0.005$) methanol emission burst were fitted by linear regressions. In (h), the data for LOX product were fitted by a non-linear regression ($y = 12.6/(33.1 + x)$; $r^2 = 0.72$, $P < 0.005$).

3 was equivalent to the stress resulting from $600 \text{ nmol mol}^{-1}$ only in Treatment 1, and further underscoring that O_3 effect on foliage photosynthetic characteristics is dose-dependent.

Different application of O_3 has varying effects on VOC emissions

The release of plant stress volatiles such as methanol, LOX products and MeSA is highly enhanced by a variety of abiotic stresses including temperature, mechanical damage and O_3

exposure (Beauchamp *et al.* 2005; Loreto & Schnitzler 2010; Niinemets 2010; Brilli *et al.* 2011; Copolovici, Kännaste, Pazouki, & Niinemets 2012; Portillo-Estrada *et al.* 2015; Pazouki *et al.* 2016). As the emissions of stress volatiles are often quantitatively related to the severity of stress (Beauchamp *et al.* 2005; Copolovici *et al.* 2012; Portillo-Estrada *et al.* 2015; Pazouki *et al.* 2016), they can serve as an important tool to monitor development of stress response and recovery and gain insight into overall stress severity under given environmental conditions.

Ozone-induced multiphasic methanol emissions that were quantitatively related to ozone dose constitute one of the most conspicuous findings of this study. In particular, a major rapid burst of methanol was induced in all treatments, followed by a subsequent longer-term burst or multiple overlapping bursts (Fig. 4) consistent with past observations in *Nicotiana tabacum* (Beauchamp *et al.* 2005). However, in our study with *P. vulgaris*, large methanol emissions were induced almost immediately upon fumigation with 600 nmol mol⁻¹ O₃, and methanol emissions were also increased during fumigation with the lower O₃ concentration of 200 nmol mol⁻¹ (Fig. 4). In contrast, in *N. tabacum* in the study of Beauchamp *et al.* (2005), there was a certain delay in the rise of methanol emissions after fumigation, and methanol emissions were elicited upon exposure to O₃ concentrations larger than 500 nmol mol⁻¹. These results show that *P. vulgaris* is more vulnerable to O₃ than *N. tabacum*.

Although the maximum emission rate of the first methanol peak correlated with total O₃ uptake through stomata (Φ_{O_3}) (Fig. 5d), the leaves in Treatments 2 and 3 exhibited a much lower maximum emission rate than the leaves in Treatment 1 (Fig. 5a), suggesting that the magnitude of the first methanol emission peak was driven by the initial O₃ uptake that was greater in Treatment 1 than in the two other treatments. Interestingly, we observed that the maximum methanol emission rate was greater for the second than for the first methanol emission burst in Treatment 3, and this second emission peak in this treatment was similar to that in Treatment 1 (Fig. 5a). Furthermore, the total integrated emissions during the second peak were also much greater (Fig. 6a) due to longer duration (Fig. 7d), and scaled with total O₃ uptake through the exposure (Fig. 9a). The question of what triggers the second methanol peak during post-O₃-exposure has not been explained in previous studies, but O₃-driven methanol release likely results from the activation of pectin methylesterases in cell walls and concomitant demethylation of the cell wall pectins (Pelloux *et al.* 2007; Beauchamp *et al.* 2005). There is a certain constitutive pectin methylesterase activity that is likely responsible for the initial methanol release, but plants have multiple pectin methylesterases (Pelloux *et al.* 2007) and the subsequent methanol release might be partly associated with *de novo* expression of these enzymes. While the first methanol emission burst likely reflects the response to the immediate damage, accumulation of lesions post-O₃-exposure and/or elicitation of repair processes or hypersensitive programmed cell death like processes might explain why the post-exposure second methanol peak emission was strongly correlated with the total amount of O₃ uptake (Φ_{O_3}).

Notably, the pronounced decline in both stomatal conductance and methanol emissions observed when the leaves were darkened (Fig. 4e) indicates that stomata can exert short-term control over methanol release as previously reported (Nemecek-Marshall, MacDonald, Franzen, Wojciechowski, & Fall 1995; Niinemets & Reichstein 2003a, 2003b; Niinemets, Loreto, & Reichstein 2004; Hüve *et al.* 2007; Harley, Greenberg, Niinemets, & Guenther 2007). Stomatal control on methanol emissions is due to high methanol water solubility such that the rise of intercellular gas-phase methanol concentrations upon stomatal closure cannot keep up with stomatal

movements (Niinemets & Reichstein 2003a, 2003b; Niinemets *et al.* 2004; Hüve *et al.* 2007; Harley *et al.* 2007). However, when stomata open, methanol stored in the leaf liquid phase is rapidly released, resulting in a burst of methanol emission as was observed upon switching on the light in our study (Fig. 4e). Clearly, stomatal responses can interfere with the kinetics of methanol synthesis in cell walls and might explain the multiphasic nature of methanol emission during the recovery phase (Fig. 4). Further studies are needed to gain an insight into the physiological and gene expression controls on methanol emissions after O₃ exposure.

Large O₃-induced post-exposure bursts of LOX product emissions were found in this study (Fig. 4), and both maximum LOX emission rate (Fig. 5e) and total emissions (Fig. 9b) depended on total O₃ uptake (Φ_{O_3}) as has been observed in *N. tabacum*, albeit at higher O₃ exposures (Beauchamp *et al.* 2005). Lower emissions of LOX products in Treatment 2 imply that stomatal closure under darkness limited both O₃ uptake and acute responses. Despite the similar O₃ uptake in both Treatments 1 and 3, Treatment 3 displayed lower values of maximum emission rate and total emissions of LOX products than expected based on total O₃ uptake, suggesting that formation of ROS was less in this treatment. In our study, the initial methanol and LOX product emissions behaved similarly across the treatments (Fig. 4), suggesting that it is the initial level of ROS formation that is responsible for the magnitude of these emissions.

MeSA is a volatile plant stress hormone, release of which has been observed in several cases upon severe O₃ exposure (Heiden *et al.* 1999; Vuorinen, Nerg, & Holopainen 2004; Beauchamp *et al.* 2005). In *P. vulgaris* in our study, MeSA release was observed following exposures to high O₃ concentrations of 600 nmol mol⁻¹ in Treatments 1 and 2. However, no MeSA emission was detected in Treatment 3, where the leaves were first exposed to the lower-level O₃ of 200 nmol mol⁻¹ prior to the exposure to high concentration of O₃ of 600 nmol mol⁻¹. Apparently, prior low-level O₃ exposure can inhibit MeSA formation both due to *de novo* synthesis as well as release from glycosidically bonded form during subsequent high-level O₃ fumigation. In Treatments 1 and 2, MeSA maximum emission rate and total emissions were not correlated with total O₃ uptake (Φ_{O_3}). In light of the dose response of LOX products and methanol, the non-dose response for MeSA is puzzling, but it could be indicative of the circumstance that elicitation of MeSA emissions is associated with exceeding a certain threshold for damage rather than with damage per se. This non-dose response resembles effects of herbivory stress where across diverse volatiles elicited, some are strongly correlated with the severity of damage, while the others are not and seem to serve as infochemicals of the presence of stress (Copolovici, Kännaste, Rimmel, Vislap, & Niinemets 2011).

Kinetics of O₃-elicited volatile release upon different O₃ stresses

On the basis of experiments in *N. tabacum*, it has been suggested that the temporal shapes of O₃-induced volatile

emissions for different compounds are similar and characterized by an initial exponential or sigmoidal increase to a maximum level, followed by a decrease until the baseline emissions have been reached (Beauchamp *et al.* 2005). We have studied the kinetics of O₃-elicited volatile release in *P. vulgaris* by fitting the temporal shapes of increase and decrease by first-order exponential relationships. We observed that both the rate of increase and decrease of methanol and LOX products were strongly enhanced by O₃ exposure (Fig. 8). Albeit the emission kinetics was similar for MeSA (Fig. 4), timing of its release was not dependent on the O₃ dose, again suggesting that once a certain threshold O₃ concentration was reached, the emission was initiated and the subsequent fading of these emissions were unrelated to accumulated O₃ dose.

In the present study, a similar induction time for the initiation of the methanol burst among the three treatments (Fig. 7a) might indicate that activation of demethylation of pectins is primarily driven by the presence of stress elicitor. However, the faster increase of the first burst of methanol emission in Treatment 1 (Fig. 8) indicates that the degree of activation is much greater upon higher initial O₃ uptake. However, it is less clear why the rate of decrease of emissions was greater in the Treatments 1 and 3 than in Treatment 2 (Fig. 8b). It might indicate a faster quenching of the initial rise of ROS, but further studies are needed to gain an insight into the downregulation of methanol emissions during the initial impact response. In the case of the secondary methanol emission bursts, the onset of these emissions was similar, but the rise occurred faster and decline more slowly in Treatment 2 (Fig. 8a,b) than in the two other treatments. As discussed earlier, activation of this late-induced response was likely linked to the plant-internal long-term processes, indicating activation of a gene expression response, and it is plausible that pre-exposure to lower O₃ concentration of 200 nmol mol⁻¹ already primed the leaf for these later-occurring responses.

The faster emission burst of LOX products in Treatment 1 than in the other treatments (Fig. 7b), indicates that in this treatment the processes downstream of the activation of pectin methylsterases were induced earlier, again suggesting that this was the most severe treatment. Provided that LOX emissions are typically associated with an oxidative burst (e.g. Beauchamp *et al.* 2005), this evidence might indicate that ROS were triggered more quickly in Treatment 1 than in Treatments 2 and 3. However, once induced, LOX emissions raised and decreased faster in Treatment 2 than in the two other treatments (Fig. 8c). This faster increase and decrease kinetics of LOX products in this treatment is unclear. However, several LOX compounds have low volatility (e.g. Henry's law constant for 2-hexenol of 0.90 Pa m³ mol⁻¹ at 25 °C (Vempati 2014) is only moderately greater than that for methanol of 0.46 Pa m³ mol⁻¹ (Niinemets & Reichstein 2003a) and it is also relatively low, 5.1 Pa m³ mol⁻¹ for 2-hexenal according to webbook: nist.gov/chemistry/), and thus, such response might indicate an interference of low stomatal conductance with LOX release similarly to methanol (Niinemets & Reichstein 2003a for detailed analyses of stomatal controls on emissions of compounds with different values of Henry's law constant). When light was switched on, LOX products synthesized in

darkness and temporarily stored in leaf liquid phase might have contributed to the total emission flux, resulting in a larger emission flux than the rate of LOX product synthesis. However, previous studies have also suggested that darkness itself can induce a temporary burst of LOX products which could be triggered by changes of foliar pH due to transitions from light to dark conditions (Hauser, Eichelmann, Oja, Heber, & Laisk 1995; Graus *et al.* 2004; Brilli *et al.* 2011). However, in our study, such a LOX burst upon switch-off the light was only observed in one leaf from Treatment 2 (data not shown). On the other hand, switching on light can also contribute to modified leaf redox status and thereby alter leaf ROS concentrations in Treatment 2.

Despite similar total amount of O₃ uptake in Treatments 1 and 3, leaves in Treatment 3 had significantly lower total emission and maximum emission rate of LOX products and needed a longer time to reach the maximum value (Figs. 4, 5b and 6c), suggesting that priming by low-level O₃ played an important role in coping with higher-level O₃.

Taken together, analyses of the volatile elicitation kinetics are partly consistent with the hypothesis that more severe O₃ stress resulted in earlier and faster induction of stress volatiles. However, there were several surprising differences among the treatments which might be partly related to stomatal effects on water-soluble volatile emission, but might also be associated with modified timing of ROS burst. Further studies should examine O₃-driven volatile emissions in relation to the kinetics of ROS development.

CONCLUSIONS

Our results demonstrated that short-term (30 min) exposure to relatively high O₃ concentrations (~600 nmol mol⁻¹) can lead to severe visible leaf injury and reductions in leaf physiological activity in *Phaseolus vulgaris*. These changes are accompanied by a characteristic release of stress volatiles methanol, LOX products and MeSA during the exposure and through recovery in dose-dependent manner for methanol and LOX products and non-dose-dependent manner for MeSA. Overall, the emission responses after stress impact were long-lasting, and emission bursts were observed many hours after the stress impact, especially for methanol, indicating a major elicitation of the stress response pathways. Photosynthetic data and emissions of LOX products and methanol during the early emission burst suggested that stomatal closure due to darkness and pre-exposure to low-level O₃ protect leaves against high-level O₃-induced injury in *Phaseolus vulgaris*. Reduced stomatal conductance is an important factor preventing O₃ entry into plant leaves, thus reducing plant damage and the amount of methanol and LOX products released into the atmosphere. These observations have important implications for understanding plant responses to O₃ in natural environments where both light and O₃ concentrations strongly vary during the day and among the days, and could drive ecological success of species with different sensitivity to O₃ and stomatal responses to environmental changes. Surprisingly, MeSA emission was inhibited by pre-exposure of leaves to lower O₃ concentration of 200 nmol mol⁻¹, but longer-term methanol emissions, albeit

being multiphasic, scaled with total O₃ uptake. This suggests that different pathways are differently regulated during exposure and through recovery, resulting in different dose responses. Further work is needed to gain insight into the kinetics and dose responses of stress volatile release as determined by plant-internal processes and application of O₃. Our study also demonstrates that there is evidence of both quantitative dose-dependent relationships between O₃ dose and the kinetics and magnitude of elicitation of volatiles, but also provide evidence of non-dose emission responses, especially during the recovery phase. These non-dose responses suggest that O₃ responses are more complicated than generally thought.

ACKNOWLEDGMENTS

This work was supported by grants from the European Research Council (advanced grant 322603, SIP-VOL+), and the European Regional Development Fund (Centre of Excellence EcolChange) and the Estonian Ministry of Science and Education (institutional grant IUT-8-3). We thank two anonymous referees for their helpful comments.

CONFLICT OF INTEREST

The authors declare that they have no conflicts of interest.

REFERENCES

- Agathokleous E., Saitanis C.J. & Koike T. (2015) Tropospheric O₃, the nightmare of wild plants: a review study. *Journal of Agricultural Meteorology* **71**, 142–152.
- Ainsworth E.A., Yendrek C.R., Stith S., Collins W.J. & Emberson L.D. (2012) The effects of tropospheric ozone on net primary productivity and implications for climate change. *Annual Review of Plant Biology* **63**, 637–661.
- Arnth J. & Niinemets Ü. (2010) Induced BVOCs: how to bug our models? *Trends in Plant Science* **15**, 118–125.
- Bahafid W., Joutey N.T., Sayel H., Asri M., Laachari F. & Ghachtouli N.E.L. (2017) Soil bioaugmentation with *Cyberlindnera fabianii* diminish phytotoxic effects of chromium (VI) on *Phaseolus vulgaris* L. *Journal of Materials and Environmental Sciences* **8**, 438–443.
- Beauchamp J., Wisthaler A., Hansel A., Kleist E., Miebach M., Niinemets Ü., ... Wildt J. (2005) Ozone induced emissions of biogenic VOC from tobacco: relationships between ozone uptake and emission of LOX products. *Plant, Cell and Environment* **28**, 1334–1343.
- Bichele I., Moldau H. & Padu E. (2000) Estimation of plasmalemma conductivity to ascorbic acid in intact leaves exposed to ozone. *Physiologia Plantarum* **108**, 405–412.
- Bortier K., Ceulemans R. & De Temmerman L. (2000) Effects of ozone exposure on growth and photosynthesis of beech seedlings (*Fagus sylvatica*). *New Phytologist* **146**, 271–280.
- Brauer M., Freedman G., Frostad J., van Donkelaar A., Martin R.V., Dentener F., ... Cohen A. (2016) Ambient air pollution exposure estimation for the global burden of disease 2013. *Environmental Science & Technology* **50**, 79–88.
- Brilli F., Gioli B., Fares S., Terenzio Z., Zona D., Gielen B., ... Ceulemans R. (2016) Rapid leaf development drives the seasonal pattern of volatile organic compound (VOC) fluxes in a 'coppiced' bioenergy poplar plantation. *Plant, Cell and Environment* **39**, 539–555.
- Brilli F., Ruuskanen T.M., Schnitzhofer R., Müller M., Breitenlechner M., Bittner V., ... Hansel A. (2011) Detection of plant volatiles after leaf wounding and darkening by Proton Transfer Reaction 'Time-of-Flight' Mass Spectrometry (PTR-TOF). *PLoS One* **6**, e20419.
- Calatayud A., Iglesias D.J., Talón M. & Barreno E. (2003) Effects of 2-month ozone exposure in spinach leaves on photosynthesis, antioxidant system and lipid peroxidation. *Plant Physiology and Biochemistry* **41**, 839–845.
- Calfapietra C., Pallozzi E., Lusini I. & Velikova V. (2013) Modification of BVOC emissions by changes in atmospheric [CO₂] and air pollution. In *Biology, controls and models of tree volatile organic compound emissions* (eds Niinemets Ü. & Monson R.K.), pp. 253–284. Springer, Berlin.
- Cassimiro J.C. & Moraes R.M. (2016) Response of a tropical tress species to ozone: visible leaf injury, growth, and lipid peroxidation. *Environmental Science and Pollution Research* **23**, 8085–8090.
- Conrath U., Beckers G.J.M., Flors V., García-Agustín P., Jakab G., Mauch F., ... Mauch-Mani B. (2006) Priming: getting ready for battle. *Molecular Plant-Microbe Interactions* **19**, 1062–1071.
- Copolovici L., Kännaste A., Pazouki L. & Niinemets Ü. (2012) Emissions of green leaf volatiles and terpenoids from *Solanum lycopersicum* are quantitatively related to the severity of cold and heat shock treatments. *Journal of Plant Physiology* **169**, 664–672.
- Copolovici L., Kännaste A., Remmel T., Vislap V. & Niinemets Ü. (2011) Volatile emissions from *Alnus glutinosa* induced by herbivory are quantitatively related to the extent of damage. *Journal of Chemical Ecology* **37**, 18–28.
- Copolovici L. & Niinemets Ü. (2010) Flooding induced emissions of volatile signaling compounds in three tree species with differing waterlogging tolerance. *Plant, Cell and Environment* **33**, 1582–1594.
- Corsi G. & Bottega S. (1999) Glandular hairs of *Salvia officinalis*: new data on morphology, localization and histochemistry in relation to function. *Annals of Botany* **84**, 657–664.
- Fares S., Goldstein A.H. & Loreto F. (2010a) Determinants of ozone fluxes and metrics for ozone risk assessment in plants. *Journal of Experimental Botany* **61**, 629–633.
- Fares S., Loreto F., Kleist E. & Wildt J. (2008) Stomatal uptake and stomatal deposition of ozone in isoprene and monoterpene emitting plants. *Plant Biology* **10**, 44–54.
- Fares S., McKay M., Holzinger R. & Goldstein A.H. (2010b) Ozone fluxes in a *Pinus ponderosa* ecosystem are dominated by non-stomatal processes: evidence from long-term continuous measurements. *Agricultural and Forest Meteorology* **150**, 420–431.
- Feng Z., Kobayashi K. & Ainsworth E.A. (2008) Impact of elevated ozone concentration on growth, physiology, and yield of wheat (*Triticum aestivum* L.): a meta-analysis. *Global Change Biology* **14**, 2696–2708.
- Fiscus E.L., Booker F.L. & Burkey K.O. (2005) Crop responses to ozone: uptake, models of action, carbon assimilation and partitioning. *Plant, Cell and Environment* **28**, 997–1011.
- Flowers M.D., Fiscus E.L., Burkey K.O., Booker F.L. & Dubois J.-J.B. (2007) Photosynthesis, chlorophyll fluorescence, and yield of snap bean (*Phaseolus vulgaris* L.) genotypes differing in sensitivity to ozone. *Environmental and Experimental Botany* **61**, 190–198.
- Fowler D., Amann M., Anderson R., Ashmore M., Cox P., Depledge M., ... Stefenson D. (2008) *Ground-Level Ozone in the 21st Century: Future Trends, Impacts and Policy Implications*. The Royal Society, London, UK.
- Freire L.S., Gerken T., Ruiz-Plancarte J., Wei D., Fuentes J.D., Katul G.G., ... Chamercki M. (2017) Turbulent mixing and removal of ozone within an Amazon rainforest canopy. *Journal of Geophysical Research – Atmospheres* **122**, 2791–2811.
- Furlan C.M., Moraes R.M., Bulbovas P., Sanz M.J., Domingos M. & Satatino A. (2008) *Tibouchina pulchra* (Cham.) Cogn., a native Atlantic Forest species, as a bio-indicator of ozone: visible injury. *Environmental Pollution* **152**, 361–365.
- Gang D.R., Wang J., Dudareva N., Nam K.H., Simon J.E., Lewinsohn E. & Pichersky E. (2001) An investigation of the storage and biosynthesis of phenylpropanes in sweet basil. *Plant Physiology* **125**, 539–555.
- Giacomuzzi V., Cappellin L., Khomenko I., Biasioli F., Schütz S., Tasin M., ... Angeli S. (2016) Emission of volatile compounds from apple plants infested with *Pandemis heparana* larvae, antennal response of conspecific adults, and preliminary field trial. *Journal of Chemical Ecology* **42**, 1265–1280.
- Graus M., Müller M. & Hansel A. (2010) High resolution PTR-TOF: quantification and formula confirmation of VOC in real time. *Journal of the American Society for Mass Spectrometry* **21**, 1037–1044.
- Graus M., Schnitzler J.-P., Hansel A., Cojocariu C., Rennenberg H., Wisthaler A. & Kreuzwieser L. (2004) Transient release of oxygenated volatile organic compounds during light-dark transitions in grey poplar leaves. *Plant Physiology* **135**, 1967–1975.
- Guidi L., Degl'Innocenti E., Martinelli F. & Piras M. (2009) Ozone effects on carbon metabolism in sensitive and insensitive *Phaseolus* cultivars. *Environmental and Experimental Botany* **66**, 117–125.
- Harley P., Greenberg J., Niinemets Ü. & Guenther A. (2007) Environmental controls over methanol emission from leaves. *Biogeosciences* **4**, 1083–1099.
- Hauser M., Eichelmann H., Oja V., Heber U. & Laik A. (1995) Stimulation by light of rapid pH regulation in the chloroplast stroma in vivo as indicated by CO₂ solubilization in leaves. *Plant Physiology* **108**, 1059–1066.

- Heiden A.C., Hoffmann T., Kahl J., Kley D., Klockow D., Langebarts C., ... Wildt J. (1999) Emission of volatile organic compounds from ozone-exposed plants. *Ecological Applications* **9**, 1160–1167.
- Heil M. & Kost C. (2006) Priming of indirect defences. *Ecology Letters* **9**, 813–817.
- Holopainen J.K., Nerg A.-M. & Blande J.D. (2013) Multitrophic signalling in polluted atmospheres. In *Biology, controls and models of stress volatile organic compound emissions* (eds Niinemets Ü. & Monson R.K.), pp. 285–314. Springer, Berlin.
- Hoshika Y., Omasa K. & Paoletti E. (2013) Both ozone exposure and soil water stress are able to induce stomatal sluggishness. *Environmental and Experimental Botany* **88**, 19–23.
- Hüve K., Christ M.M., Kleist E., Uerlings R., Niinemets Ü., Walter A. & Wildt J. (2007) Simultaneous growth and emission measurements demonstrate an interactive control of methanol release by leaf expansion and stomata. *Journal of Experimental Botany* **58**, 1783–1793.
- Inclán R., Ribas A., Peñuelas J. & Gimeno B.S. (1999) The relative sensitivity of different Mediterranean plant species to ozone exposure. *Water, Air, and Soil Pollution* **116**, 273–277.
- Ivanov A.V., Trakhtenberg S., Bertram A.K., Gershenzon Y.M. & Molina M.J. (2007) OH, HO₂, and ozone gaseous diffusion coefficients. *Journal of Physical Chemistry A* **111**, 1632–1637.
- Jordan A., Haidacher S., Hanel G., Hartungen E., Märk L., Seehauser H., ... Märk T.D. (2009) A high resolution and high sensitivity proton-transfer-reaction time-of-flight mass spectrometer (PTR-TOF-MS). *International Journal of Mass Spectrometry* **286**, 122–128.
- Jud W., Fischer L., Canaval E., Wohlfahrt G., Tissier A. & Hansel A. (2016) Plant surface reactions: an ozone defence mechanism impacting atmospheric chemistry. *Atmospheric Chemistry and Physics* **16**, 277–292.
- Kännaste A., Copolovici L. & Niinemets Ü. (2014) Gas chromatography mass-spectrometry method for determination of biogenic volatile organic compounds emitted by plants. In *Plant Isoprenoids: Methods and Protocols* (ed Rodríguez-Concepción M.), pp. 161–169. Humana Press, New York.
- Kollist T., Moldau H., Rasulov B., Oja V., Rämha H., Hüve K., ... Kollist H. (2007) A novel device detects a rapid ozone-induced transient stomatal closure in intact Arabidopsis and its absence in abi2 mutant. *Physiologia Plantarum* **129**, 796–803.
- Laisk A., Kull O. & Moldau H. (1989) Ozone concentration in leaf intercellular air spaces is close to zero. *Plant Physiology* **90**, 1163–1167.
- Levin D.A. (1973) The role of trichomes in plant defence. *QUARTERLY REVIEW OF BIOLOGY* **48**, 3–15.
- Li P., Calatayud V., Gao F., Uddling J. & Feng Z. (2016) Differences in ozone sensitivity among woody species are related to leaf morphology and antioxidant levels. *Tree Physiology* **36**, 1105–1116.
- Long S.P. & Naidu S.L. (2002) Effect of oxidants at the biochemical, cell and physiological levels, with particular reference to ozone. In *Air Pollution and Plant Life* (eds Bell J.N.B. & Treshow M.), pp. 69–88. John Wiley & Sons, Ltd., West Sussex.
- Loreto F. & Fares S. (2007) Is ozone flux inside leaves only a damage indicator? Clues from volatile isoprenoid studies. *Plant Physiology* **143**, 1096–1100.
- Loreto F., Mannozi M., Maris C., Nascetti P., Ferranti F. & Pasqualini S. (2001) Ozone quenching properties of isoprene and its antioxidant role in leaves. *Plant Physiology* **126**, 993–1000.
- Loreto F., Pinelli P., Manes F. & Kollist H. (2004) Impact of ozone on monoterpene emissions and evidence for an isoprene-like antioxidant action of monoterpenes emitted by *Quercus ilex* leaves. *Tree Physiology* **24**, 361–367.
- Loreto F. & Schnitzler J.P. (2010) Abiotic stress and induced BVOCs. *Trends in Plant Science* **15**, 154–166.
- Maja M.M., Kasurinen A., Yli-Pirilä P., Joutsensaari J., Klemola T., Holopainen T. & Holopainen J. (2014) Contrasting responses of silver birch VOC emissions to short- and long-term herbivory. *Tree Physiology* **34**, 241–252.
- Moldau H. & Bichele I. (2002) Plasmalemma protection by the apoplast as assessed from above-zero ozone concentrations in leaf intercellular air spaces. *Planta* **214**, 484–487.
- Nemecek-Marshall M., MacDonald R.C., Franzen J.F., Wojciechowski C.L. & Fall R. (1995) Methanol emission from leaves: enzymatic detection of gas-phase methanol and relation of methanol fluxes to stomatal conductance and leaf development. *Plant Physiology* **108**, 1359–1368.
- Niinemets Ü. (2010) Mild versus severe stress and BVOCs: thresholds, priming and consequences. *Trends in Plant Science* **15**, 145–153.
- Niinemets Ü. (2012) Whole plant photosynthesis. In *Terrestrial Photosynthesis in a Changing Environment. A Molecular, Physiological and Ecological Approach* (eds Flexas J., Loreto F. & Medrano H.), pp. 399–423. Cambridge University Press, Cambridge.
- Niinemets Ü., Kuhn U., Harley P.C., Staudt M., Arneth A., Cescatti A., ... Peñuelas J. (2011) Estimations of isoprenoid emission capacity from enclosure studies: measurements, data processing, quality and standardized measurement protocols. *Biogeosciences* **8**, 2209–2246.
- Niinemets Ü., Loreto F. & Reichstein M. (2004) Physiological and physicochemical controls on foliar volatile organic compound emissions. *Trends in Plant Science* **9**, 180–186.
- Niinemets Ü. & Reichstein M. (2003a) Controls on the emission of plant volatiles through stomata: differential sensitivity of the emission rates to stomatal closure explained. *Journal of Geophysical Research - Atmospheres* **108**, 4208 <https://doi.org/10.1029/2002JD002620>.
- Niinemets Ü. & Reichstein M. (2003b) Controls on the emission of plant volatiles through stomata: a sensitivity analysis. *Journal of Geophysical Research - Atmospheres* **108**, 4211 <https://doi.org/10.1029/2002JD002626>.
- Nolle M., Ellul R., Heinrich G. & Gisten H. (2002) A long-term study of background ozone concentrations in the central Mediterranean-diurnal and seasonal variations on the island of Gozo. *Atmospheric Environment* **36**, 1391–1402.
- Oksanen E. & Holopainen T. (2001) Responses of two birch (*Betula pendula* Roth) clones to different ozone profiles with similar AOT40 exposure. *Atmospheric Environment* **35**, 5245–5254.
- Osborne S.A., Mills G., Hayes F., Ainsworth E.A., Büker P. & Emberson L. (2016) Has the sensitivity of soybean cultivars to ozone pollution increased with time? An analysis of published dose-response data. *Global Change Biology* **22**, 3097–3111.
- Paoletti E. & Grulke N.E. (2010) Ozone exposure and stomatal sluggishness in different plant physiognomic classes. *Environmental Pollution* **158**, 2664–2671.
- Pasqualini S., Piccioni C., Reale L., Ederli L., Della T.G. & Ferranti F. (2003) Ozone-induced cell death in tobacco cultivar Bel W3 plant. The role of programmed cell death in lesion formation. *Plant Physiology* **133**, 1122–1134.
- Pazouki L., Kanagendran A., Li S., Kännaste A., Memari H.R., Bichele R. & Niinemets Ü. (2016) Mono- and sesquiterpene release from tomato (*Solanum lycopersicum*) leaves upon mild and severe heat stress and through recovery: from gene expression to emission responses. *Environmental and Experimental Botany* **132**, 1–15.
- Pelloux J., Rustérucci C. & Mellerowicz E.J. (2007) New insights into pectin methyltransferase structure and function. *Trends in Plant Science* **12**, 267–277.
- Portillo-Estrada M., Kazantsev T. & Niinemets Ü. (2017) Fading of wound-induced volatile release during *Populus tremula* leaf expansion. *Journal of Plant Research* **130**, 157–165.
- Portillo-Estrada M., Kazantsev T., Talts E., Tosens T. & Niinemets Ü. (2015) Emission timetable and quantitative patterns of wound-induced volatiles across different leaf damage treatments in aspen (*Populus tremula*). *Journal of Chemical Ecology* **41**, 1105–1117.
- Ranieri A., Castagna A., Padu E., Moldau H., Rahi M. & Soldatini G.F. (1999) The decay of O₃ through direct reaction with cell wall ascorbate is not sufficient to explain the different degrees of O₃-sensitivity in two poplar clones. *Journal of Plant Physiology* **154**, 250–255.
- Rasulov B., Copolovici L., Laisk A. & Niinemets Ü. (2009) Postillumination isoprene emission: in vivo measurements of dimethylallyldiphosphate pool size and isoprene synthesis kinetics in aspen leaves. *Plant Physiology* **149**, 1609–1618.
- Ribas A. & Peñuelas J. (2004) Temporal patterns of surface ozone levels in different habitats of the North Western Mediterranean basin. *Atmospheric Environment* **38**, 985–992.
- Tasin M., Cappellin L. & Biasioli F. (2012) Fast direct injection mass-spectrometric characterization of stimuli for insect electrophysiology by proton transfer reaction-time of flight mass-spectrometry (PTR-ToF-MS). *Sensors* **12**, 4091–4104.
- Tucker W.A. & Nelken L.H. (1982) Diffusion coefficients in air and water. In *Handbook of Chemical Property Estimation Methods: Environmental Behavior of Organic Compounds* (eds Lyman W.J., Reehl W.F. & Rosenblatt D.H.), pp. 17/11–17/25. McGraw-Hill, New York.
- Vahisalu T., Kollist H., Wang Y.-F., Nishimura N., Chan W.-Y., Valerio G., ... Kangasjärvi J. (2008) SLAC1 is required for plant guard cell S-type anion channel function in stomatal signalling. *Nature* **452**, 487–491.
- Vahisalu T., Puzõrjova I., Brosché M., Valk E., Lepiku M., Moldau H., ... Kollist H. (2010) Ozone-triggered rapid stomatal response involves the production of reactive oxygen species, and is controlled by SLAC1 and OST1. *The Plant Journal* **62**, 442–453.
- Vempati H.S. (2014) Physico-chemical properties of green leaf volatiles. MSc. Thesis, pp. 20–24. Graduate Faculty of the Louisiana State University and Agriculture and Mechanical College.

- Vickers C.E., Possell M., Cojocariu C.I., Velikova V.B., Laothawornkitkul J., Ryan A., Mullineaux P.M. & Hewitt C.N. (2009) Isoprene synthesis protects transgenic tobacco plants from oxidative stress. *Plant, Cell and Environment* **32**, 520–531.
- Vingarzan R. (2004) A review of surface ozone background levels and trends. *Atmospheric Environment* **38**, 3431–3442.
- von Caemmerer S. & Farquhar G.D. (1981) Some relationships between the biochemistry of photosynthesis and the gas exchange of leaves. *Planta* **153**, 376–387.
- Vuorinen T., Nerg A.-M. & Holopainen J.K. (2004) Ozone exposure triggers the emission of herbivore-induced plant volatiles, but does not disturb tritrophic signalling. *Environmental Pollution* **131**, 305–311.
- Wagner G.J., Wang E. & Shepherd R.W. (2004) New approaches for studying and exploiting an old protuberance, the plant trichomes. *Annals of Botany* **93**, 3–11.
- Wenzel A.A. & Mehlhorn H. (1995) Zinc deficiency enhances ozone toxicity in bush beans (*Phaseolus vulgaris* L. cv. Saxa). *Journal of Experimental Botany* **46**, 867–872.
- Wieser G., Hecke K., Tausz M. & Matyssek R. (2013) Foliage type specific susceptibility to ozone in *Picea abies*, *Pinus cembra* and *Larix decidua* at treeline: a synthesis. *Environmental and Experimental Botany* **90**, 4–11.
- Wilkinson S., Mills G., Illidge R. & Davies W.J. (2012) How is ozone pollution reducing our food supply? *Journal of Experimental Botany* **63**, 527–536.
- Wittig V.E., Ainsworth E.A., Naidu A.L., Karnosky D.F. & Long S.P. (2009) Quantifying the impact of current and future tropospheric ozone on the tree biomass, growth, physiology and biochemistry: a quantitative meta-analysis. *Global Change Biology* **15**, 396–424.
- Wohlgemuth H., Mittelstrass K., Kschieschan S., Bender J., Weigel H.J., Overmyer K., ... Langebartels C. (2002) Activation of an oxidative burst is a general feature of sensitive plants exposed to the air pollutant ozone. *Plant, Cell and Environment* **25**, 717–726.
- Xu X., Lin W., Wang T., Yan P., Tang J., Meng Z. & Wang Y. (2008) Long-term trend of surface ozone at a regional background station in eastern China 1991–2006: enhanced variability. *Atmospheric Chemistry and Physics* **8**, 2595–2607.
- Yener S., Sánchez-López J.A., Granitto P.M., Cappellin L., Märk T.D., Zimmermann R., ... Biasioli F. (2016) Rapid and direct volatile compound profiling of black and green teas (*Camellia sinensis*) from different countries with PTR-ToF-MS. *Talanta* **152**, 45–53.

Received 19 April 2017; received in revised form 7 June 2017; accepted for publication 8 June 2017

Jiang, Y., Ye, J., **Li, S.**, Niinemets, Ü. (2017)
Methyl jasmonate-induced emission of biogenic volatiles is biphasic
in cucumber: a high-resolution analysis of dose dependence.
Journal of Experimental Botany 68 (16), 4679-4694.



RESEARCH PAPER

Methyl jasmonate-induced emission of biogenic volatiles is biphasic in cucumber: a high-resolution analysis of dose dependence

Yifan Jiang^{1,2}, Jiayan Ye¹, Shuai Li¹ and Ülo Niinemets^{1,3,*}

¹ Institute of Agricultural and Environmental Sciences, Estonian University of Life Sciences, Kreutzwaldi 1, Tartu 51014, Estonia

² College of Art, Changzhou University, Gehu 1, Changzhou 213164, Jiangsu, China

³ Estonian Academy of Sciences, Kohtu 6, 10130 Tallinn, Estonia

* Correspondence: ylo.niinemets@emu.ee

Received 4 January 2017; Editorial decision 24 June 2017; Accepted 25 June 2017

Editor: Peter Bozhkov, Swedish University of Agricultural Sciences

Abstract

Methyl jasmonate (MeJA) is a key airborne elicitor activating jasmonate-dependent signaling pathways, including induction of stress-related volatile emissions, but how the magnitude and timing of these emissions scale with MeJA dose is not known. Treatments with exogenous MeJA concentrations ranging from mild (0.2 mM) to lethal (50 mM) were used to investigate quantitative relationships among MeJA dose and the kinetics and magnitude of volatile release in *Cucumis sativus* by combining high-resolution measurements with a proton-transfer reaction time-of-flight mass spectrometer (PTR-TOF-MS) and GC-MS. The results highlighted biphasic kinetics of elicitation of volatiles. The early phase, peaking in 0.1–1 h after the MeJA treatment, was characterized by emissions of lipoxygenase (LOX) pathway volatiles and methanol. In the subsequent phase, starting in 6–12 h and reaching a maximum in 15–25 h after the treatment, secondary emissions of LOX compounds as well as emissions of monoterpenes and sesquiterpenes were elicited. For both phases, the maximum emission rates and total integrated emissions increased with applied MeJA concentration. Furthermore, the rates of induction and decay, and the duration of emission bursts were positively, and the timing of emission maxima were negatively associated with MeJA dose for LOX compounds and terpenoids, except for the duration of the first LOX burst. These results demonstrate major effects of MeJA dose on the kinetics and magnitude of volatile response, underscoring the importance of biotic stress severity in deciphering the downstream events of biological impacts.

Key words: Biotic stress, cucumber, dose–response, LOX products, MeJA, proton-transfer reaction time-of-flight mass spectrometer (PTR-TOF-MS), terpenes.

Introduction

Endogenous levels of jasmonic acid (JA) and its methylated derivative methyl jasmonate (MeJA) are known to increase rapidly in response to herbivore attack or invasion by pathogens, subsequently activating downstream defense responses. Once released into the air, MeJA has been shown to act as

a long-distance airborne signal to trigger defense responses in non-impacted parts of the damaged plant or in neighboring plants (Heil and Ton, 2008; Tamogami *et al.*, 2008; Cheong and Choi, 2003). Thus, exogenous application of MeJA has often been used to simulate the impact of a biotic

© The Author 2017. Published by Oxford University Press on behalf of the Society for Experimental Biology.

This is an Open Access article distributed under the terms of the Creative Commons Attribution License (<http://creativecommons.org/licenses/by/4.0/>), which permits unrestricted reuse, distribution, and reproduction in any medium, provided the original work is properly cited.

stress on elicitation of jasmonate-dependent defenses (Zhao and Chye, 1999; Heijari *et al.*, 2008; Tamogami *et al.*, 2008; Suh *et al.*, 2013; Shi *et al.*, 2015; Jiang *et al.*, 2016a). Among these induced defenses, elicitation of the release of volatile emissions in MeJA-treated leaves is a characteristic MeJA response (Dicke *et al.*, 1999; Kappers *et al.*, 2010; Mäntylä *et al.*, 2014). The chemical classes of plant volatile blends induced by MeJA vary considerably in quantity, quality, and timing, with green leaf volatiles [lipoxygenase (LOX) compounds] and various terpene compounds (mainly monoterpenes and sesquiterpenes) being the typical elicited volatiles (Rodríguez-Saona *et al.*, 2001; Martin *et al.*, 2003; Semiz *et al.*, 2012; Kegeles *et al.*, 2013). These emissions occur as the result of both constitutive activity of key stress pathways (e.g. constitutive LOX activities leading to rapid emission of green leaf volatiles; Andreou and Feussner, 2009) and activation of expression of genes responsible for specialized volatile synthesis (e.g. elicitation of expression of terpene synthases leading to emissions of mono- and sesquiterpenes; Martin *et al.*, 2002, 2003; Byun-McKay *et al.*, 2006). Despite the diversity, these induced emissions resemble the emissions induced by herbivores or by physical wounding, and can serve as infochemicals in attracting herbivore enemies or in priming defenses in neighboring plants (Dicke *et al.*, 1999; Heil and Kost, 2006; Heil and Ton, 2008; Kappers *et al.*, 2010), thus underscoring the biological significance of MeJA as a model of chemical signaling.

So far, the majority of studies on the relationships of stress-driven volatile emissions and biotic stress, including herbivore infestation and exogenous MeJA application, have been non-quantitative and have not focused on understanding how much is emitted in response to a certain elicitor dose. The studies have rather mainly looked at the modifications in volatile profiles or at the ecological roles of the volatile induction, for example in plant indirect defenses. However, there is encouraging evidence that the stress-dependent elicitation of volatile emissions is linked to the severity of biotic impacts in a dose-dependent manner (Niinemets *et al.*, 2013). The severity of biotic stress has been modified by varying the degree of wounding (Mithöfer *et al.*, 2005; Portillo-Estrada *et al.*, 2015, 2017) or varying the number of feeding larvae (Copolovici *et al.*, 2011; Yli-Pirilä *et al.*, 2016; Copolovici *et al.*, 2017). However, the definition of the severity of biotic stress, the stress 'dose', is still difficult in biotic stress studies because of localized spread and complexity of timing of biotic impacts, especially for multiple biotic impacts occurring at somewhat different times, such as simultaneous herbivore feeding and spread of pathogen infections. Such complex impacts can lead to emission responses that are hard to decipher, complicating construction of mechanistic quantitative stress severity versus emission response models for prediction of signaling among neighboring plants and other organisms (Grote *et al.*, 2013). As exogenous MeJA can be applied in precisely defined doses, it can provide an invaluable model system to simulate dose dependencies of biotic impacts, and start resolving complex biological interactions, at least using volatile responses as a quantitative measure of biotic stress severity.

A dose dependence between the exogenous MeJA concentration and plant volatile response can be expected because treatments with a higher concentration probably result in a greater coverage of potential impact sites in cell wall and cellular membrane surfaces. Furthermore, MeJA exposure has also been related to the downstream components of signaling pathways in cell death regulation (Jonak *et al.*, 2002), and studies using higher concentrations of exogenous MeJA have reported hypersensitive responses including necrosis and/or activation of programmed cell death (PCD) (Popova *et al.*, 2003; Jung, 2004; Zhang and Xing, 2008; Repka *et al.*, 2013) that are expected to result in profound modifications in the total amount and profiles of volatile emission (Beauchamp *et al.*, 2005; Niinemets, 2010). Although the evidence suggests that MeJA activates defense pathways in a dose-dependent manner, to our knowledge, the way in which the MeJA dose alters the timing and magnitude of induced volatile responses has not been studied.

We used cucumber (*Cucumis sativus* L.), known to respond strongly to MeJA (Bouwmeester *et al.*, 1999; Kappers *et al.*, 2010), as the model to investigate the effect of different exogenous MeJA concentrations through early and late phases of MeJA response by combining high-resolution measurements with a proton-transfer reaction time-of-flight mass spectrometer (PTR-TOF-MS) and GC-MS measurements, and kinetic analyses (Table 1). We asked how MeJA dose alters the total amount of volatiles released, how it affects volatile composition, and how it modifies the kinetics of volatile release. We hypothesized that there are MeJA dose-dependent differences in the overall degree of elicitation and compositions of induced volatile emissions. The results of the current study highlight biphasic emission kinetics of volatile emission and strong quantitative relationships between MeJA concentration and the timing and magnitude of early and late emission responses.

Materials and methods

Plant growth conditions

Cucumber (*Cucumis sativus* cv. Libelle F1, Seston Seemned OÜ, Estonia) seeds were sown in 1 liter plastic pots filled with a mixture (1:1) of sand and commercial potting soil (Biolan Oy, Finland), and cultivated in an environment-controlled plant growth room (Copolovici *et al.*, 2012). In brief, light intensity of 300–400 $\mu\text{mol m}^{-2} \text{s}^{-1}$ at the level of plants was provided for 12 h by Philips HPI/T Plus 400 W metal halide lamps (Philips Eesti, Tallinn, Estonia). Air temperature was 24 °C during the day and 20 °C at night, and relative humidity was maintained at 60–70% through the day and night. Plants were watered daily to field capacity, and fertilized every 3 d with a commercial NPK fertilizer (N-P₂O₅-K₂O: 19-5-13). Approximately 3- to 4-week-old, 20–30 cm tall plants with four to five fully expanded leaves were used in the experiments.

Methyl jasmonate (MeJA) treatments

As studies have used widely different protocols for MeJA application (e.g. Thaler *et al.*, 2002; Loivamäki *et al.*, 2004; Heijari *et al.*, 2005; Liang *et al.*, 2006; Phillips *et al.*, 2007), we tested different methods in preliminary experiments. These tests included different solvents (water with 0.01% Triton X-100 versus 5% ethanol), mode of treatment (spraying versus brushing), treatment location (ventilated

Table 1. Definition of the traits characterizing the kinetics of volatile compounds released upon methyl jasmonate treatment (see Fig. 2 for representative emission kinetics)

Symbol (unit)	Definition
D_M (h)	Duration between the first and the second emission maxima
D_{P1} (h)	Duration of the first induced emission peak
D_{P2} (h)	Duration of the second induced emission peak
I_{T1} (nmol m ⁻²)	Integral of the first emission peak (Equation 1)
I_{T2} (nmol m ⁻²)	Integral of the second emission peak
I_{Tot} (nmol m ⁻²)	Integral of the total induced emissions, $I_{T1}+I_{T2}$
k_{I1} (h ⁻¹)	Rate constant for the initial increase of emissions during the first emission burst (Equation 2)
k_{D1} (h ⁻¹)	Rate constant for the decrease of emissions during the first emission burst (Equation 3)
k_{I2} (h ⁻¹)	Rate constant for the increase of emissions during the second emission burst
k_{D2} (h ⁻¹)	Rate constant for the decrease of emissions during the second emission burst
t_{M1} (h)	Time to the first emission maximum since the start of the treatment
t_{M2} (h)	Time to the second emission maximum since the start of the treatment
t_{P1S} (h)	Start of the first emission burst since the start of the treatment
t_{P1E} (h)	End of the first emission burst since the start of the treatment
t_{P2S} (h)	Start of the second emission burst since the start of the treatment
t_{P2E} (h)	End of the second emission burst since the start of the treatment
τ_{I1} (h)	Doubling time for the increase of emissions during the first emission burst
τ_{D1} (h)	Half-time for the decrease of emissions during the first emission burst
τ_{I2} (h)	Doubling time for the increase of emissions during the second emission burst
τ_{D2} (h)	Half-time for the decrease of emissions during the second emission burst
$\Phi(t)$ (nmol m ⁻² s ⁻¹)	Emission rate at time t
Φ_{M1} (nmol m ⁻² s ⁻¹)	Maximum emission rate at the first emission peak
Φ_{M2} (nmol m ⁻² s ⁻¹)	Maximum emission rate at the second emission peak

hood versus an experimental ventilated flow-through glass chamber; see the details in ‘Dynamic headspace collection of volatiles’). The key selection criteria for MeJA treatment were the repeatability of the treatment in terms of quantitative volatile response and minimization of non-specific effects as assessed by comparing the volatile emissions of non-treated plants and control plants treated with pure solvent identically to the MeJA treatment. Ultimately, application of MeJA (Sigma-Aldrich, St Louis, MO, USA) in 5% aqueous ethanol by spraying in the experimental glass chamber as in several previous studies (Martin *et al.*, 2003; Semiz *et al.*, 2012; Jiang *et al.*, 2016b) was selected as the most repeatable application procedure that was associated with minor non-specific effects in control treatments. In fact, volatile emissions in the control treatment (5% ethanol solution) did not significantly differ from non-treated plants.

To obtain the MeJA dose response, the following concentrations were used: 0 (control, 5% ethanol), 0.2, 2, 5, 10, 20, and 50 mM. The selected leaf with an area of ~40 cm² was sealed in the glass gas-exchange cuvette of one of the two gas-exchange systems described below, the baseline measurement of volatile emissions was taken, the cuvette was opened, and 10 ml of MeJA solution was sprayed over the entire leaf surface to obtain a complete and even coating. Immediately after the treatment, the treated leaf was sealed in the gas exchange cuvette again (within ~1 min) and, depending on the system used, volatiles were collected at intervals and analyzed offline by GC-MS or monitored continuously using an online PTR-TOF-MS. Three different plants were used for each MeJA concentration treatment.

Dynamic headspace collection of volatiles

Volatile collection for GC-MS analysis was carried out with a multichamber open gas-exchange system described in detail by Toome *et al.* (2010) and Copolovici *et al.* (2011) that was also used for MeJA treatments as described above. Each 3 liter glass chamber was operated individually using purified ambient air for the chamber inlet and maintaining an air flow rate of 1 l min⁻¹ through the chamber. Turbulent conditions inside the chambers were achieved by a fan

installed at the bottom of each individual chamber. The light regime during measurements followed growth light conditions, with light intensity of 200–400 μmol m⁻² s⁻¹ provided for 12 h per day with a Heliospectra LX60 plant growth LED lamp (Heliospectra AB, Sweden). The temperature inside the chambers was between 24 and 26 °C during the light period and 22 °C during the dark period, air humidity was ~60%, and CO₂ concentration was 380 μmol mol⁻¹.

Volatiles in the chamber air were collected onto multibed stainless steel cartridges (10.5 cm length, 4 mm inner diameter; Supelco, Bellefonte, PA, USA) using a constant flow air sample pump (210-1003MTX; SKC Inc., Houston, TX, USA) operated at a rate of 200 ml min⁻¹ for 20 min, resulting in quantitative adsorption of volatiles from 4 liters of air. The cartridges were filled with Carbotrap C 20/40 mesh (0.2 g), Carboxpack B 40/60 mesh (0.1 g), and Carbotrap X 20/40 (0.1 g) adsorbents (Supelco) for optimal adsorption of volatiles in the C5–C15 range (Kännaste *et al.*, 2014). Before the collection of volatiles, the traps were cleaned by passage of a stream of ultra pure helium at a flow rate of 200 ml min⁻¹ at 400 °C for 2 h using a SIM Clean-Cube cartridge thermo-conditioner (Scientific Instruments Manufacturer GmbH, Oberhausen, Germany). After each treatment, the chamber and tubing were flushed with a stream of ozone (~1000 ppm) to eliminate the volatiles adsorbed by the chamber and tubes that could contaminate the measurement system (mainly MeJA, and to a low degree stress-induced volatiles; Niinemets *et al.* 2011).

The volatile samples were collected before leaf treatment with MeJA and 20 min, 2, 10, and 24 h after treatment with MeJA. Blank empty chamber measurements were taken before and after the experiment. During and after the experiment, additional blank samples were taken from the adjacent empty chamber operated under identical conditions, and the baseline during the experiment was adjusted when needed using the blanks from the experimental chamber and empty chamber at the end of the experiment (the difference between the two blanks was small, indicating that the system memory effect was minor). After 36–48 h, the experiment was finished, and the treated leaf was removed, scanned, and its area was estimated with the UTHSCSA ImageTool 2.0 (Dental Diagnostic

Science, The University of Texas Health Science Center, San Antonio, TX, USA). These leaf images were further used to assess the quantitative degree of damage (Fig. 1A).

Gas-chromatographic analysis of volatiles

Adsorbent cartridges were analyzed according to the method of Kännaste et al. (2014) using a combined Shimadzu TD20 automated cartridge desorber and a Shimadzu 2010 Plus gas chromatograph with mass spectrometric detector (GC-MS; Shimadzu Corporation, Kyoto, Japan). A C8–C20 hydrocarbon standard (Sigma-Aldrich) was used to obtain the retention indices as in Pazouki et al. (2015) and in Jiang et al. (2016b) (Table 2). Compounds were identified using the NIST spectral library, the spectral and retention indices library of Adams (1995), and a custom-made library of retention times and mass spectra of commercially available mono- and sesquiterpene standards (GC purity, Sigma-Aldrich). The authentic standards were also used for GC-MS calibration as described in detail in Kännaste et al. (2014). The background (blank) concentrations of individual volatiles in the empty chamber were subtracted from the plant samples, and the emission rates were calculated according to the equations of Niinemets et al. (2011).

Online monitoring of the kinetics of volatile release

A high-resolution PTR-TOF-MS (TOF8000, Ionicon Analytik, Innsbruck, Austria) was used to track the volatile release in real time. The PTR-TOF-MS system was connected to a custom-designed two-channel gas-exchange system described in detail by Copolovici

and Niinemets (2010). The measurement cuvette (1.2 l) consisted of a stainless steel bottom and a double-walled glass upper part specially designed for volatile compound measurements. A thermostat was used to control the temperature of water circulating between the glass chamber walls, and the chamber air temperature was within ± 0.2 °C of the chamber wall temperature. Four wide-beam halogen lamps (Osram GmbH, Germany) were used for chamber illumination. Ambient air that was purified through the passage of a charcoal filter and an ozone trap, and humidified to the desired water vapor pressure was used (Copolovici and Niinemets, 2010). The flow rate through the system was 1.6 l min^{-1} , and the sample air was drawn into the PTR-TOF-MS drift tube at a flow rate of 100 ml min^{-1} . Background volatile concentrations in the ambient air pumped into the chamber were assessed in the reference mode, and volatile concentrations in the outgoing air stream were measured in the sample mode. In addition, measurements with the empty chamber were also conducted before and after plant measurements. In these experiments, chamber temperature was maintained at 25 °C, light intensity at the leaf surface at $500 \mu\text{mol m}^{-2} \text{ s}^{-1}$, chamber air humidity between 50% and 60% (vapor pressure deficit of 1.2–1.6 kPa), and CO_2 concentration between $370 \mu\text{mol mol}^{-1}$ and $400 \mu\text{mol mol}^{-1}$. After enclosure of the MeJA-treated leaf, all measurements were immediately started.

The operation of the PTR-TOF-MS, system calibration, and compound detection followed the protocol of Portillo-Estrada et al. (2015). In brief, the drift tube conditions were 2.3 mbar, 600 V, and 60 °C, the measurements were carried out continuously through the mass to charge ratio (m/z) range of 0–316, and data for 31 250 spectra s^{-1} were averaged. The raw PTR-TOF-MS data were post-processed with the PTR-MS Viewer 3.0.0.99 (Tofwerk AG, Switzerland), and relevant m/z peaks were integrated as explained in Portillo-Estrada et al. (2015). The time resolution used in this study is 10 s (the averaged data were recorded every 10 s). Methanol was detected as the protonated parent ion with an m/z of 33, while the total emission of volatiles produced within the octadecanoid pathway (LOX products) was taken as the sum of individual ion masses (m/z) of 57 [m_{57} , (*E*)-2-hexenal (frag)], 81 [m_{81} , (*Z*)-3-hexenal+(*E*)-3-hexenal (frag) after correction for the share of the fraction originating from monoterpenes; see below], 83 [m_{83} , hexenol+hexenal (frag)], 85 [m_{85} , hexanol (frag)], 103 [m_{103} , hexanol (main)], 99 [m_{99} , (*Z*)-3-hexenal+(*E*)-3-hexenal (main)], and 101 [m_{101} , (*Z*)-3-hexenol+(*E*)-3-hexenol+(*E*)-2-hexenol+hexenal (main)] (Copolovici and Niinemets, 2010; Portillo-Estrada et al., 2015). Total monoterpene emission was characterized by the parent ion with an m/z of 137 (m_{137}), and total sesquiterpene emission by the parent ion with m/z 205 (m_{205}). As even under the soft ionization conditions of the operation of PTR-TOF-MS used here, monoterpenes can partly fragment, with the fragment spectrum dominated by the mass fragments with m/z 67, 81, and 95 (Copolovici et al., 2005; Tani et al., 2003), use of parent ions somewhat underestimates the emissions of monoterpenes. Based on simultaneous GC-MS measurements, for total monoterpenes, we divided the concentration of the parent ion by m/z 137 by 0.46 to obtain total monoterpene emission. To consider the interference of the mass fragment with m/z 81 coming from monoterpene fragmentation with the detection of the LOX compound 3-hexenal, fragmentation of which also produces the identical mass fragment, we separately analyzed the PTR-TOF-MS fragmentation spectra of (*Z*)-3-hexenal and all emitted terpenoids, and developed appropriate equations to assess the share of m/z 81 from monoterpenes and 3-hexenal based on the concentration of corresponding parent ions.

The emission rates per unit leaf area were calculated according to Niinemets et al. (2011) considering both the incoming air measurements taken frequently during the experiments and empty chamber measurements before plant enclosure (typically only differing slightly from the incoming air concentrations). PTR-TOF-MS measurements were continued until the elicited emissions reached the background level, usually between 36 h and 48 h after the treatment (Fig. 2).

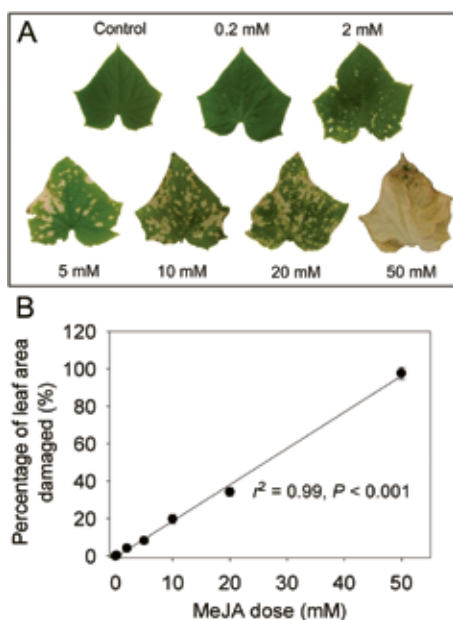


Fig. 1. Characteristic images of MeJA-treated cucumber (*Cucumis sativus*) leaves taken 36–48 h after treatment with MeJA concentrations of 0 (control), 0.2, 2, 5, 10, 20, and 50 mM (A), and corresponding relationship between the percentage of damage and applied MeJA concentration (B). The data in (B) were fitted by a linear regression ($y = 1.94x - 0.71$; $r^2 = 0.99$, $P < 0.001$).

Quantitative characterization of elicitation of volatile emissions by MeJA treatment

Time-courses of emissions induced by MeJA treatment were either biphasic with two maxima (LOX products; Fig. 2A, B) or monophasic (monoterpenes, sesquiterpenes, and methanol; Fig. 2C, D). The emission time-courses were used to derive the key quantitative emission characteristics (Fig. 2; Table 1), including the emission rates at the two emission maxima (Φ_{M1} and Φ_{M2}), the corresponding times for the emission maxima (t_{M1} and t_{M2}), the durations of the two emission peaks (D_{P1} and D_{P2}), the duration between the emission maxima (D_M), and the total volatile emissions corresponding to both emission bursts (I_{T1} and I_{T2}). For the first emission burst, the total integrated emission was calculated as:

$$I_{T1} = \int_{t_{P1S}}^{t_{P1E}} \Phi(t) dt, \quad (1)$$

where $\Phi(t)$ is the emission rate at time t , t_{P1S} is the start, and t_{P1E} is the end of the first induced emission release. In practice, numerical integration according to the trapezoidal rule was used and the infinitesimal time period dt was replaced by the measurement period Δt of 10 s. The integrated emission corresponding to the second emission burst was calculated analogously.

The emission kinetics of different volatiles followed a similar pattern characterized by an initial exponential increase, then by slowing down of the rate of increase until the emissions reached the maximum value, followed by a non-linear decay to the baseline emission (Fig. 2). We fitted the initial parts of the increase and decay of the emissions corresponding to the first and the second emission burst with simple first-order exponential models. For the first peak,

$$\Phi(t) = \Phi(t_{P1S})e^{k_{I1}t}, \quad (2)$$

for the increasing part, and

$$\Phi(t) = \Phi(t_{M1})e^{-k_{D1}t}, \quad (3)$$

for the decreasing part. Here, k_{I1} is the rate constant for the increase and k_{D1} is the rate constant for the decrease of emission of the given compound. If present, the rate constants for the increase and decrease for the second peak (k_{I2} and k_{D2}) were calculated analogously. From the rate constants, corresponding doubling times [e.g. for the first emission burst, $\tau_{I1} = \ln(2)/k_{I1}$] and decay half-times [$\tau_{D1} = \ln(2)/k_{D1}$] for both emissions bursts were also calculated.

Data analyses

All experiments were replicated three times with different plants, and all data shown are averages \pm SE. Effects of MeJA dose were studied by linear or non-linear regressions depending on the shape of the response. Emission rates of volatiles elicited by different MeJA concentrations at fixed time points estimated by GC-MS were compared by ANOVA followed by post-hoc Tukey's test. The analyses were conducted with SAS (Version 8.02; SAS Institute, Cary, NC, USA) and all statistical effects are considered significant at $P < 0.05$.

Results

Methyl jasmonate treatments in leaves of *Cucumis sativus*: general patterns and short- and long-term emission responses

Control plants were weak emitters of monoterpenes α -pinene, camphene, β -pinene, and Δ^3 -carene, several longer aliphatic

aldehydes C7–C10, some characteristic C6 lipoxygenase pathway volatiles (LOX), and benzaldehyde (Table 2). MeJA treatment resulted in rapid elevation of C6 and derivative LOX products, (Z)-3-hexen-1-ol, 3-hexenyl acetate, (Z)-3-hexen-1-ol, and *n*-hexanal, detectable with GC-MS already at 20 min after treatment. Moreover, 6-methyl-5-hepten-2-one and heptanal could also be induced significantly by higher concentrations of MeJA (10 mM and 20 mM). Emissions of C6-LOX compounds in the treated plants were strongly reduced at the second sampling event at 2 h, and the emissions increased again at 10 h, especially C6-LOX compounds and derivatives (Table 2). However, 3-hexenyl acetate was not detectable in any of the MeJA dose treatments after the initial elevation at 20 min. In 24 h after the treatment, (Z)-3-hexen-1-ol could not be identified in any of the MeJA dose treatments, and the emission rate of *n*-hexanal decreased dramatically compared with the emission rate at 10 h. However, nonanal and decanal emissions remained at a moderately high level throughout the treatments (Table 2).

In contrast to aliphatic aldehydes and LOX, no enhancement of monoterpene emissions and no sesquiterpene emissions in MeJA-treated leaves were observed at the first two measurement events (Table 2). However, monoterpene emissions, especially limonene and Δ^3 -carene emissions, were enhanced in MeJA-treated leaves at 10 h and, at this sampling event, emissions of the monoterpene linalool, and sesquiterpenes β -farnesene, α -cedrene, and β -caryophyllene were identified (Table 2). At 24 h after the treatment, terpenoid emissions had mostly reached the pre-treatment level (Table 2).

In 36–48 h after the exposure to MeJA, all treated leaves except those from the 0.2 mM treatment exhibited a certain degree of damage ranging from chlorotic spots in the 2 mM treatment to major chlorotic areas in 5–20 mM treatments, and at the lethal concentration of 50 mM, the damage was spread over the entire leaf area (Fig. 1A). The damaged leaf area was linearly correlated with the concentration of MeJA applied (Fig. 1B).

High time resolution measurements of kinetics of elicitation of volatile emissions in MeJA-treated leaves by PTR-TOF-MS broadly confirmed the timing of release of different compounds highlighted by GC-MS analyses (Fig. 2). PTR-TOF-MS measurements also confirmed the occurrence of two emission bursts for LOX, a fast burst elicited immediately after MeJA treatment and reaching a maximum in ~0.2–1 h, and a slower burst elicited in 6–10 h after MeJA treatment and reaching a maximum in ~16–20 h (Fig. 2A, B). In the case of mono- (*m/z* 137) and sesquiterpenes (*m/z* 205), only one slower burst was observed (Fig. 2C). This slower burst started in 2–6 h after MeJA treatment and reached a maximum in ~15–25 h (Fig. 2C). Apart from the compounds detected by GC-MS, PTR-TOF-MS measurements demonstrated a major burst of methanol emission (Fig. 2D). Methanol (*m/z* 33) emissions started almost immediately after MeJA treatment, and reached a maximum ~0.5–1.5 h after the treatment (Fig. 2D).

The MeJA threshold concentration for elicitation of both the rapid and the slow LOX emission bursts and the methanol

Table 2. Average (\pm SE) emission rates ($\text{pmol m}^{-2} \text{s}^{-1}$) of individual volatile compounds after treatment of MeJA with different doses over the time-course of 24 h identified by GC-MS

Volatile Compounds	Retention index	20 min					2 h				
		Control	2 mM	5 mM	10 mM	20 mM	Control	2 mM	5 mM	10 mM	20 mM
Lipoxygenase pathway products and saturated aldehydes											
(E)-3-Hexenal	802	120 ± 24a	167 ± 37a	608 ± 87ab	663 ± 87ab	860 ± 140b	80 ± 17	71 ± 11	110 ± 24	180 ± 24	130 ± 20
(Z)-3-Hexen-1-ol	863	ND ^a	ND	130 ± 17a	342 ± 68ab	1000 ± 140b	ND	ND	4.7 ± 1.9	5.7 ± 0.7	10.1 ± 2.4
Heptanal	899	ND	ND	101 ± 18	182 ± 39	152 ± 22	ND	ND	ND	115 ± 12	76 ± 17
Octanal	1074	105 ± 19	183 ± 32	110 ± 17	201 ± 30	161 ± 21	177 ± 24	223 ± 22	94 ± 22	219 ± 16	167 ± 24
(Z)-3-Hexen-1-yl acetate	1008	ND	ND	2160 ± 290	1930 ± 210	3270 ± 810	ND	ND	ND	ND	ND
2-Ethyl-1-hexanol	1046	130 ± 31	229 ± 63	137 ± 18	249 ± 37	201 ± 28	222 ± 27	278 ± 32	118 ± 22	273 ± 29	208 ± 27
Nonanal	1098	502 ± 74	868 ± 99	521 ± 99	950 ± 170	763 ± 124	843 ± 112	1050 ± 140	446 ± 81	1042 ± 81	790 ± 140
Decanal	1204	561 ± 99	977 ± 81	590 ± 120	1060 ± 150	857 ± 112	945 ± 87	1180 ± 170	505 ± 93	1166 ± 93	890 ± 120
Monoterpenes											
α-Pinene	932	76 ± 11	50 ± 11	81 ± 12	62.6 ± 9.9	86.2 ± 9.9	78 ± 11	57.0 ± 7.4	41.5 ± 9.3	58.9 ± 8.1	65.7 ± 8.7
Camphene	949	1.4 ± 0.4	1.4 ± 0.6	1.0 ± 0.4	2.0 ± 0.3	2.4 ± 0.6	1.9 ± 0.3	1.9 ± 0.5	1.4 ± 0.3	3.6 ± 0.6	2.9 ± 0.4
β-Pinene	980	3.3 ± 1.0	4.3 ± 1.2	3.6 ± 0.7	2.9 ± 0.6	3.3 ± 1.0	2.2 ± 0.6	3.5 ± 0.9	4.7 ± 1.1	6.4 ± 0.9	6.1 ± 0.9
Δ ³ -Carene	1011	36.6 ± 8.9	31.6 ± 8.7	55.8 ± 9.9	65.7 ± 8.7	71 ± 19	39.1 ± 5.6	64.5 ± 7.4	31.4 ± 5.6	26.0 ± 6.2	55.2 ± 6.8
Limonene	1029	ND	ND	ND	ND	ND	ND	ND	ND	ND	ND
Linalool	1098	ND	ND	ND	ND	ND	ND	ND	ND	ND	ND
Sesquiterpenes											
α-Cedrene	1409	ND	ND	ND	ND	ND	ND	ND	ND	ND	ND
β-Caryophyllene	1428	ND	ND	ND	ND	ND	ND	ND	ND	ND	ND
β-Farnesene	1455	ND	ND	ND	ND	ND	ND	ND	ND	ND	ND
Geranyl/geranyl diphosphate (GGDP) pathway derived volatiles ^b											
6-Methyl-5-hepten-2-one	985	158 ± 29a	366 ± 56ab	185.4 ± 29a	513 ± 58ab	1810 ± 320b	99 ± 17a	252 ± 32ab	231 ± 56ab	455 ± 56ab	1100 ± 170b
Geranylacetone	1453	34.2 ± 1.4	59 ± 13	36.0 ± 5.6	65 ± 11	52.1 ± 5.0	57.7 ± 6.2	73 ± 12	31.4 ± 9.3	71.3 ± 8.1	53.9 ± 8.7
Benzenoids											
Benzaldehyde	967	180 ± 37a	126 ± 19a	236 ± 62a	550 ± 87ab	890 ± 110b	148 ± 18	158 ± 22	167 ± 37	107.9 ± 7.4	137 ± 19

Three replicate treatments at each MeJA application concentration were carried out. Means among treatments and sampling times were compared by ANOVA followed by post-hoc Tukey's tests, and statistically significant differences are denoted by different lowercase letters. For compounds without labels, the emission rates did not differ significantly among treatments at different sampling events. The pathways leading to saturated aliphatic aldehydes are not yet fully resolved, although these emissions are also up-regulated upon abiotic and biotic stresses similarly to lipoxygenase volatiles (Wildt et al., 2003; Hu et al., 2009). The data of the 50 mM treatment are not shown in the table because this lethal dose caused a rapid necrosis in 1 h and no volatile emission was detected then from the leaves, implying the loss of the biological activity.

^a ND, below the detection limit of $\sim 0.1 \text{ pmol m}^{-2} \text{s}^{-1}$

^b Carotenoid breakdown products including geranyl acetone (Gao et al., 2008; Arimura et al., 2009; Kask et al., 2016).

emission burst was 2 mM, while for monoterpenes the threshold concentration was 0.2 mM and for sesquiterpenes 2 mM. The slower emission burst for LOX and the emission bursts for monoterpenes and sesquiterpenes were absent for leaves treated with the highest (lethal, Fig. 1A) MeJA concentration of 50 mM.

MeJA elicits volatile emissions in a dose-dependent manner

The maximum emission rate of MeJA-elicited emissions increased with increasing MeJA concentration for both the faster (Fig. 3A, B) and the slower (Fig. 3A, C, D) MeJA response. The dependencies of the maximum emission rates of volatiles on MeJA concentration were somewhat non-linear, implying that the increases of the maximum emission rates were greater at greater MeJA treatment

concentration, especially between the concentrations of 10 mM and 20 mM and 20 mM and 50 mM (Fig. 4). The emission maxima scaled positively with the degree or leaf damage (insets in Fig. 3). MeJA dose dependencies of emission rates of LOX in the early response phase and of LOX and mono- and sesquiterpenes in the late phase were also evident in GC-MS data. However, due to the lower time resolution, the variability in these responses was greater (Table 2).

The total integral emissions (Equation 1; Fig. 2 for definition) also scaled positively with the MeJA treatment concentration for both the faster (Fig. 4A, B) and the slower (Fig. 4A, C, D) emission responses. However, although the emission maxima at a given MeJA concentration were similar for the first and the second emission bursts of LOX compounds (Fig. 3A), the total LOX emission corresponding to the second emission burst was much larger than that for

10 h					24 h				
Control	2 mM	5 mM	10 mM	20 mM	Control	2 mM	5 mM	10 mM	20 mM
76 ± 20a	46.5 ± 6.8a	298 ± 62ab	820 ± 130b	720 ± 150b	63 ± 14	81 ± 12	123 ± 14	161 ± 22	169 ± 19
ND	18.9 ± 2.1a	64 ± 12ab	304 ± 43b	252 ± 23b	ND	ND	ND	ND	ND
ND	ND	102 ± 11	223 ± 37	233 ± 29	ND	ND	20.2 ± 3.3	27.9 ± 3.0	21.3 ± 1.9
101 ± 17	131 ± 18	167 ± 24	42.8 ± 9.9	98 ± 16	66 ± 14	137 ± 17	144 ± 15	109 ± 18	140 ± 19
ND	ND	ND	ND	ND	ND	ND	ND	ND	ND
127 ± 19	163 ± 23	208 ± 26	53.9 ± 9.3	122 ± 23	83 ± 16	172 ± 11	180 ± 17	136 ± 23	176 ± 24
484 ± 87	620 ± 110	794 ± 93	204 ± 29	465 ± 99	316 ± 63	650 ± 120	682 ± 99	515 ± 87	660 ± 120
542 ± 74	699 ± 81	888 ± 81	229 ± 31	523 ± 94	353 ± 62	731 ± 93	769 ± 87	580 ± 93	750 ± 81
64.5 ± 9.3	100 ± 11	99.2 ± 9.3	182 ± 38	246 ± 34	107 ± 14	52.7 ± 7.4	39.1 ± 4.3	36.0 ± 5.6	35.3 ± 4.3
2.2 ± 0.4	3.0 ± 0.3	5.1 ± 0.9	9.9 ± 2.1	15.5 ± 4.3	0.62 ± 0.09a	2.0 ± 0.4ab	3.41 ± 0.682b	6.51 ± 0.87bc	8.7 ± 1.1c
2.6 ± 0.4	2.9 ± 0.6	5.8 ± 1.1	5.8 ± 1.8	8.1 ± 1.6	0.66 ± 0.06	2.2 ± 0.4	1.8 ± 0.3	3.2 ± 0.6	2.9 ± 0.4
43.4 ± 5.0a	55.8 ± 8.7a	133 ± 19b	311 ± 50bc	477.4 ± 68c	53.3 ± 8.1	40.3 ± 6.2	29.1 ± 3.1	67.6 ± 8.1	57.0 ± 9.3
ND	ND	254 ± 37	428 ± 50	378 ± 50	ND	ND	42.0 ± 8.6	43.2 ± 8.4	99 ± 25
ND	ND	7.0 ± 1.0	22.2 ± 2.5	18.0 ± 3.7	ND	ND	ND	ND	ND
ND	ND	ND	18.3 ± 3.0	30.4 ± 4.3	ND	ND	ND	9.3 ± 3.1	ND
ND	ND	ND	4.6 ± 1.1	9.4 ± 2.2	ND	ND	ND	ND	ND
ND	7.1 ± 1.9	4.8 ± 0.7	8.7 ± 2.2	13.4 ± 3.0	ND	ND	ND	0.7 ± 0.3	ND
152 ± 19	179 ± 25	145 ± 19	199 ± 32	114 ± 12	15.2 ± 2.8	17.9 ± 2.8	214.5 ± 2.5	19.9 ± 2.2	70.1 ± 6.8
32.9 ± 7.4	42.2 ± 9.3	53.9 ± 7.4	14.0 ± 2.5	31.6 ± 5.0	21.5 ± 2.5	44.6 ± 8.7	46.5 ± 8.7	35.3 ± 3.1	45.9 ± 5.0
32.9 ± 7.4a	118 ± 12a	210 ± 25ab	515 ± 74ab	869 ± 99b	484 ± 87	205 ± 22	156 ± 19	113 ± 16	68.8 ± 4.3

the first emission burst (Fig. 4A), and thus the total release of LOX compounds during the whole experiment mainly scaled with the slower LOX response (Fig. 4A). Stronger elicitation of the slower emission response was particularly evident for lower concentrations of MeJA such that the ratio of the second ($I_{T,LOX2}$) to the first ($I_{T,LOX1}$) integrated emission scaled negatively with MeJA concentration (Fig. 5A).

For total integrated emission versus MeJA concentration relationships, the non-linearity was much less than for maximum emission versus MeJA relationships (cf. Figs 3 and 4). In fact, the total LOX emissions corresponding to both the first and the second emission bursts were best fitted by linear regressions (Fig. 4A). Analogously with the maximum emissions, total LOX emissions were strongly correlated with the degree of leaf damage through the MeJA treatments (insets in Fig. 4).

Timing and rate of elicitation of volatile emissions depend on MeJA concentration

MeJA concentration significantly affected the timing of volatile emission responses. The maxima for both the faster and the slower LOX emission bursts occurred earlier at higher MeJA concentration, whereas the change in the timing was greater for the faster LOX burst (Fig. 5B). In contrast, the maximum emission for the methanol burst occurred later at a greater MeJA concentration (Fig. 5C). Similarly to LOX, the maxima of monoterpene and sesquiterpene emissions also occurred earlier at higher MeJA concentrations, and this concentration response was stronger for monoterpenes (Fig. 5D).

To characterize further the MeJA effects on the emission kinetics, the induction (k_i , Equation 2) and decay (k_d , Equations 2 and 3) rate constants (see also Table 1) were determined. This analysis indicated that both the initial increase

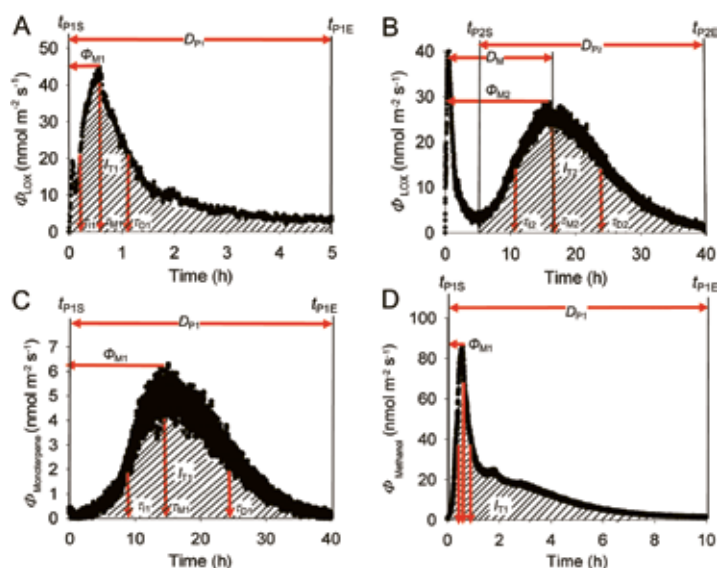


Fig. 2. Representative time-courses of methyl jasmonate (MeJA)-induced emissions from a *C. sativus* leaf, and definition of key variables characterizing the induction response (see Table 1 for further specifics). Volatile emissions were induced by application of 20 mM MeJA that elicited an early lipoxygenase pathway volatile (LOX) burst (A), and a second late LOX emission burst (B) with concomitant monoterpene emission burst (C) and an early slowly decaying methanol emission burst (D). Shaded areas in all panels indicate integrated emissions corresponding to individual emission bursts (I_{T1} for the first and I_{T2} for the second burst, Equation 1). Φ_{T1} and Φ_{T2} correspond to the emission maxima for the two bursts, and t_{M1} and t_{M2} denote the corresponding times from the start of the treatment. Different τ -s stand for the initial doubling and decay times for the two bursts (Table 1). In (D), the red vertical arrows show the positions of τ_{T1} , t_{M1} , and τ_{D1} as in the other panels. After the leaf treatment with MeJA, the release of emissions was continuously monitored with a proton-transfer reaction time-of-flight mass spectrometer (PTR-TOF-MS). The time kinetics of sesquiterpene emission is analogous to monoterpene emissions and is therefore not presented.

and decrease of emissions was faster at higher MeJA concentrations for LOX compounds (Fig. 6A, B) and terpenoids (Fig. 7A, B). However, for methanol, the rate constants k_1 and k_D initially decreased over the MeJA concentration range of 0.2–5 mM, and they were weakly affected by MeJA concentrations >5 mM (Fig. 6C). Both the rise and decline kinetics were much faster for the first than for the second LOX emission burst (Fig. 6A, B). In addition, MeJA concentration dependencies of k_1 and k_D were weaker for the second LOX emission burst, with a moderate change in the induction and decay rates over the MeJA concentration range of 5–20 mM (Fig. 6A, B). The induction and decay rates were similar for mono- and sesquiterpenes, except for the lowest MeJA treatment concentration of 0.2 mM that barely induced sesquiterpene release (Fig. 6C, D).

Despite a faster rate of decline at greater MeJA concentrations, induction to a higher maximum level at greater MeJA concentration (Fig. 3) implied that the total length of the emission burst increased with increasing MeJA concentration for all compound classes (Figs 6D, 7C), except for the first LOX burst (Fig. 6D). In the case of the early LOX release, the duration of the pulse length decreased between 2mM and 5 mM MeJA, and was thereafter invariable (Fig. 6D).

Discussion

Exposure to MeJA leads to rapid bursts of characteristic stress volatiles in *Cucumis sativus*

A variety of biotic stresses elicits emissions of volatile products of the lipoxygenase pathway (LOX compounds, also called green leaf volatiles) (Matsui *et al.*, 2012; Scala *et al.*, 2013). LOX compounds are synthesized by multiple lipoxygenases and fatty acid hydroperoxide lyases, several of which are constitutively active in leaves (Feussner and Wasternack, 2002), implying that as soon as the substrates, polyunsaturated fatty acids, are released from membranes, LOX products are rapidly emitted. Typically, the early LOX response occurs within 2–30 min after biotic stress treatment (Zhang and Xing, 2008; Bruinsma *et al.*, 2009; Brill *et al.*, 2011; War *et al.*, 2012; Portillo-Estrada *et al.*, 2015), and this rapid LOX burst has been shown to be involved in priming and triggering subsequent local and systemic stress responses (Farag and Paré, 2002; Mithöfer *et al.*, 2005; Niinemets *et al.*, 2013; Scala *et al.*, 2013).

In our study, LOX emissions were detected immediately after enclosure of treated leaves in the measurement system, and the emissions reached the first maximum in 0.1–1 h depending on MeJA concentration (Figs 2A, 5B). The increase was faster than the decrease (cf. Fig. 6A, B)

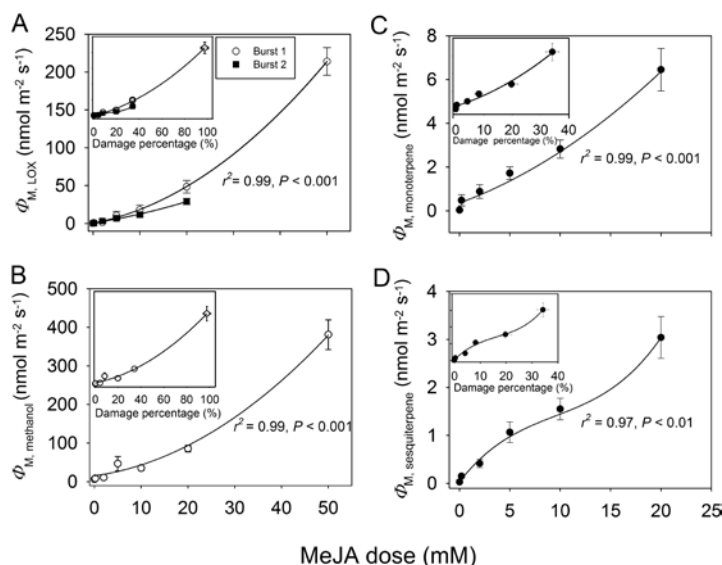


Fig. 3. Maximum emission rates of LOX ($\Phi_{M,LOX}$; A), methanol ($\Phi_{M,methanol}$; B), monoterpenes ($\Phi_{M,monoterpene}$; C), and sesquiterpenes ($\Phi_{M,sesquiterpene}$; D) as dependent on the applied MeJA dose and corresponding correlations with the degree of damage at the end of the experiment (insets) in leaves of *C. sativus* (see Fig. 2 for sample-induced emission kinetics). MeJA treatments as in Fig. 1. Treatment with 50 mM MeJA was lethal (Fig. 1) and, thus, the second LOX emission burst and monoterpene and sesquiterpene emission bursts were absent at this concentration. Data were fitted by second-order polynomial regressions, except that sigmoidal regressions were used for (D). For the first LOX burst in (A), $y = 0.062x^2 + 1.19x + 0.46$ (main panel) and $y = 0.013x^2 + 0.89x - 0.3$ (inset). For the second LOX burst in (A), $y = 0.0335x^2 + 0.94x + 0.46$ (main panel) and $y = 0.013x^2 + 0.37x + 1.05$ (inset). For methanol in (B), $y = 0.11x^2 + 1.65x + 12.0$ (main) and $y = 0.026x^2 + 1.28x + 10.9$ (inset), for monoterpenes in (C), $y = 0.0037x^2 + 0.23x + 0.30$ (main) and $y = 0.0023x^2 + 0.098x + 0.36$ (inset), and for sesquiterpenes in (D), $y = 3.26/[1 + e^{(9.80 - x)/4.02}]$ (main) and $y = 3.72/[1 + e^{(21.5 - x)/8.72}]$ (inset). For the relationships in (A–C), $r^2 = 0.99$, $P < 0.001$, except for the second LOX burst versus damage percentage in (A) where $r^2 = 0.98$, $P < 0.01$. In (D), $r^2 = 0.97$, $P < 0.01$ for the main panel and $r^2 = 0.96$, $P < 0.01$ for the inset. Three replicate treatments at each MeJA application concentration were carried out.

such that the emissions corresponding to this initial burst were maintained at a moderately high level for several hours after the MeJA treatment (Fig. 2A). Thus, this early MeJA response clearly reflects activation of constitutive lipoxygenases (LOX), hydroperoxide lyase (HPL), allene oxide synthase (AOS), and alcohol dehydrogenase (ADH), resembling the rapid response to wounding herbivores (Brilli *et al.*, 2011; Portillo-Estrada *et al.*, 2015).

Concomitant with the start of LOX emissions, major methanol emissions were elicited (Fig. 2D). Release of methanol is a characteristic stress response that reflects activation of demethylation of cell wall pectins by constitutively expressed pectin methylsterases (Micheli, 2001; Pelloux *et al.*, 2007). Previous studies have demonstrated activation of methanol release upon leaf mechanical wounding (Brilli *et al.*, 2011; Portillo-Estrada *et al.*, 2015), insect feeding (Peñuelas *et al.*, 2005; von Dahl *et al.*, 2006), fungal infestation (Copolovici *et al.*, 2014b; Jiang *et al.*, 2016b), and ozone exposure (Beauchamp *et al.*, 2005). Such cell wall modifications can importantly enhance the penetration of downstream signaling compounds (Gális *et al.*, 2009), including MeJA diffusion. Furthermore, there is evidence that in addition to LOX volatiles, methanol is not only the by-product of stress-dependent

cell wall modifications, but also can serve as an important signal eliciting or modifying systemic stress responses (von Dahl *et al.*, 2006; Seco *et al.*, 2011; Hann *et al.*, 2014; Komarova *et al.*, 2014).

Biphasic MeJA elicitation of volatile emissions in *C. sativus*

The fast emission burst of LOX and methanol was followed by slower emission bursts of LOX (Fig. 2B), monoterpenes (Fig. 2C), and sesquiterpenes that reached a maximum in 16–25 h after MeJA treatment (Fig. 5B, C). Constitutive monoterpene emissions are very low in non-stressed cucumber (Table 2), and the emissions were not significantly elicited by MeJA over the short term, suggesting that the longer term elicitation of terpenoid emissions reflects a gene expression level response as has been observed in several studies looking at MeJA-dependent stress responses (Martin *et al.*, 2002, 2003; Byun-McKay *et al.*, 2006). Furthermore, the induced monoterpene blend significantly differed from the blend of constitutive emissions (Table 2), further supporting the argument that the induced monoterpene emissions reflected expression of

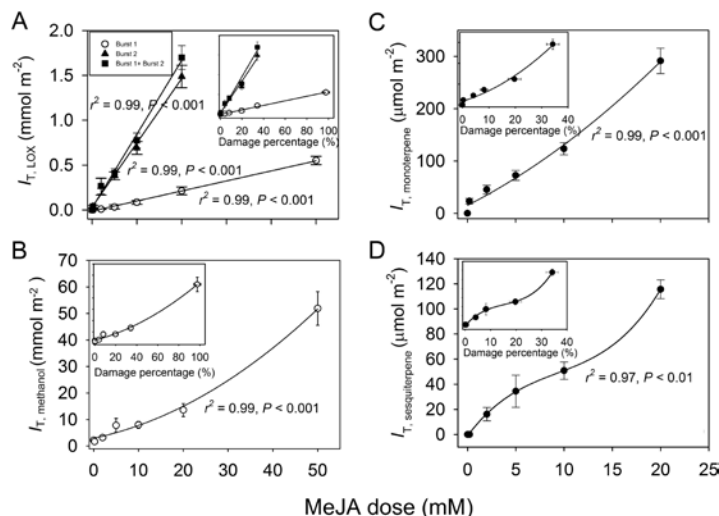


Fig. 4. Integrated emissions (I_T , Equation 1) of lipoxigenase pathway volatiles ($I_{T, LOX}$, A), methanol ($I_{T, methanol}$, B), monoterpenes ($I_{T, monoterpene}$, C), and sesquiterpenes ($I_{T, sesquiterpene}$, D) in relation to the applied MeJA concentration and corresponding relationships with the degree of damage (insets) in leaves of *C. sativus* (see Fig. 2 for the sample kinetics of the emissions). In (A), the data for the first and the second emission burst of LOX and the sum of the two are separately shown and fitted by linear regressions for the main panel, $y=0.0112x-0.0124$ for the first and $y=0.0716x+0.0322$ for the second LOX burst; for the inset, $y=0.00576x-0.0080$ for the first and $y=0.0409x+0.023$ for the second LOX burst. For $I_{T, methanol}$ in (B) and for $I_{T, monoterpene}$ in (C), the data were fitted by second-order polynomial regressions for the main panels, $y=0.0093x^2+0.99x+1.62$ for (B) and $y=0.22x^2+9.43x+15.2$ for (C); and for the insets, $y=0.0026x^2+0.25x+2.66$ for (B) and $y=0.12x^2+3.85x+17.8$ for (C). For $I_{T, sesquiterpene}$ in (D), the data were fitted by sigmoidal regressions [$y=127/[1+e^{(11.3-x)/4.20}]$ for the main panel and $y=161/[1+e^{(25.8-x)/9.19}]$ for the inset]. MeJA treatment is as in Fig. 1. For all relationships in (A) and (B) and for the main panel of (C), $r^2=0.99$, $P<0.001$. For the inset of (C), $r^2=0.98$, $P<0.01$ and for the main panel and the inset of (D), $r^2=0.96$, $P<0.01$. Three replicate treatments at each MeJA application concentration were carried out.

inducible terpenoid synthases not expressed under non-stressed conditions. The terpenoids elicited by MeJA in our study (Table 2), especially monoterpenes (limonene and linalool) and sesquiterpenes (β -farnesene, α -cedrene, and β -caryophyllene), are also induced in herbivore-infested cucumber (Bouwmeester et al., 1999; Kappers et al., 2010), and play key roles as airborne signals attracting herbivore enemies or in priming defenses in neighboring plants (Degenhardt and Lincoln, 2006; Brilli et al., 2009; Mäntylä et al., 2014).

As previous studies have demonstrated, biosynthesis of terpenes is delayed after the initiation of biotic stress (Arimura et al., 2008, 2009), reflecting the lags in signal transduction as well as the fact that the transcription and translation of terpene synthases are time-consuming. However, the existence of a second sustained burst of LOX compounds synchronously with the elicitation of induced terpene emissions after ~10 h is surprising. Because it occurred simultaneously with terpenoid emissions, this second burst of LOX compounds is unlikely to be the chemical elicitor inducing terpenoid release. In fact, there is evidence that the late MeJA response reflects the rise of endogenously synthesized jasmonate levels (Tamogami et al., 2008), and, thus, the second release of LOX might indicate the onset of jasmonate-dependent gene expression as reported in several previous studies for lipoxigenase

pathway genes (Bell and Mullet, 1991; Wasternack and Parthier, 2007).

From a biological perspective, LOX compounds are not only released upon immediate wounding in herbivore-damaged leaves, but also concomitantly with the synthesis of terpenoids elicited at the later stages of induction. Moreover, these LOX-containing compound blends play important roles in attraction of herbivore enemies and in priming of neighboring plants (Dicke et al., 1999; Bruinsma et al., 2007; Frost et al., 2008; Allmann and Baldwin, 2010; Copolovici et al., 2011, 2014a). Although the exposure to MeJA does not fully mimic the herbivory stress (Dicke et al., 1999; Degenhardt and Lincoln, 2006; Kappers et al., 2010), it still elicits a blend of volatiles that attracts enemies of herbivores similarly to genuine herbivore feeding (Dicke et al., 1999; Kappers et al., 2010). Thus, this second LOX burst concomitant with the induced terpenoid emissions might be part of the characteristic herbivory smell bouquet that is driving the plant–insect and plant–plant interactions.

Although longer term kinetic studies are rare, especially those considering the entire bouquet of volatiles, biphasic emission kinetics have been demonstrated in response to various stresses for several volatiles, including biphasic methanol emissions upon ozone stress (Beauchamp et al., 2005), biphasic ethylene emissions in response to treatments with the

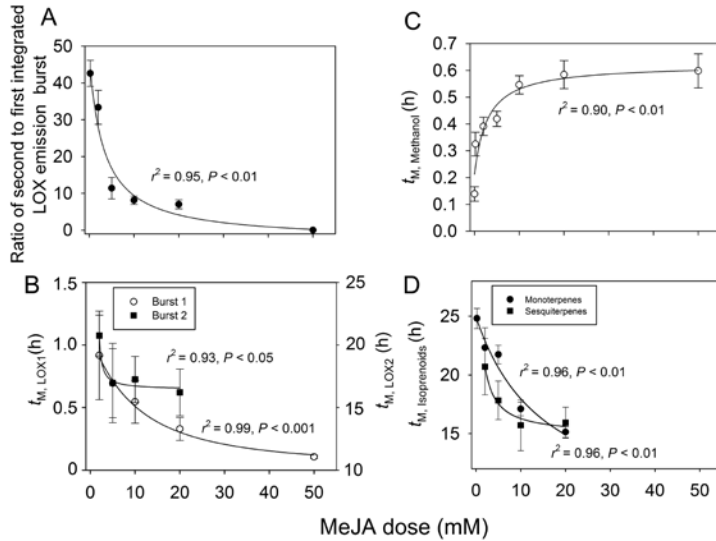


Fig. 5. The ratio of the second to the first integrated LOX emission burst (t_{LOX2}/t_{LOX1} , A), and the times to the maxima of the first ($t_{M,LOX1}$) and second ($t_{M,LOX2}$) LOX emission bursts (B), emission burst of methanol (C) and the times to the maxima of monoterpene ($t_{M,monoterpene}$) and sesquiterpene ($t_{M,sesquiterpene}$) emission bursts (D) in relation to MeJA dose in leaves of *C. sativus* (see Fig. 2 for the sample responses and definition of the characteristics). MeJA treatments are as in Fig. 1 and data coverage is as in Fig. 3. In all cases, the data were fitted by hyperbolic regressions. For t_{LOX2}/t_{LOX1} in (A), $y=162/(3.27+x)-2.83$, $r^2=0.95$, $P<0.01$; for $t_{M,LOX1}$ in (B), $y=14.1/(11.7+x)-0.12$, $r^2=0.99$, $P<0.001$; for $t_{M,LOX2}$ in (B), $y=9.69/(0.0027+x)+15.7$, $r^2=0.93$, $P<0.01$; for $t_{M,methanol}$ in (C), $y=0.41x/(2.90+x)+0.21$; for $t_{M,monoterpene}$ in (D), $y=281/(15.7+x)+7.03$, $r^2=0.96$, $P<0.01$; for $t_{M,sesquiterpene}$ in (D), $y=14.6/(0.50+x)+14.9$, $r^2=0.96$, $P<0.01$. Three replicate treatments at each MeJA application concentration were carried out.

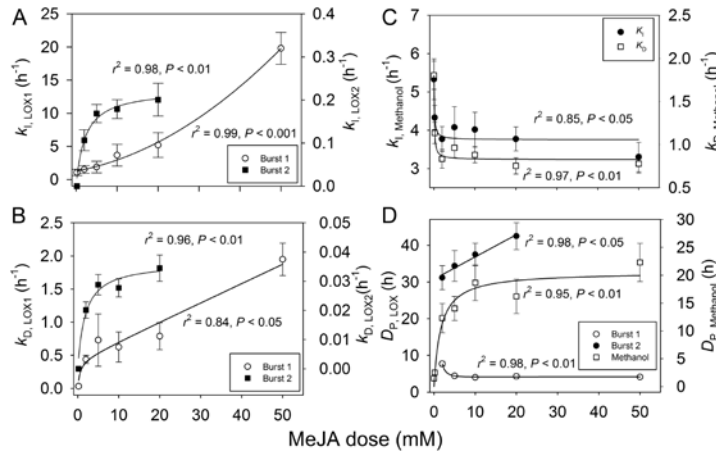


Fig. 6. First-order rate constants (k_0) for the initial increases (Equation 2, k_0 ; A, C) and decreases (Equation 3, k_0 ; B, C) of the MeJA-induced emissions for the first ($k_{I,LOX1}$ and $k_{D,LOX1}$) and the second ($k_{I,LOX2}$ and $k_{D,LOX2}$) emission burst (B) as dependent on the MeJA concentration in *C. sativus* leaves (see Fig. 2 for sample responses). Experimental treatments are as in Fig. 1 and data coverage is as in Fig. 3. The regressions describing the statistical effects of MeJA on the rate constants were the following: $y=0.0050x^2+0.12x+1.27$ for $k_{I,LOX1}$ and $y=0.214x/(1.87+x)$ for $k_{I,LOX2}$ in (A), $y=2.51(1-e^{-0.028x})$ for $k_{D,LOX1}$ and $y=0.0357x/(1.42+x)$ for $k_{D,LOX2}$ in (B), $y=3.75+0.194/(0.123+x)$ for $k_{I,methanol}$ and $y=0.826+0.0920/(0.094+x)$ for $k_{D,methanol}$ in (C), $y=4.24-3.11/x+20.1/x^2$ for $D_{P,LOX1}$, $y=30.8+0.604x$ for $D_{P,LOX2}$, and $y=20.6x/(1.65+x)$ for $D_{P,methanol}$ in (D). Three replicate treatments at each MeJA application concentration were carried out.

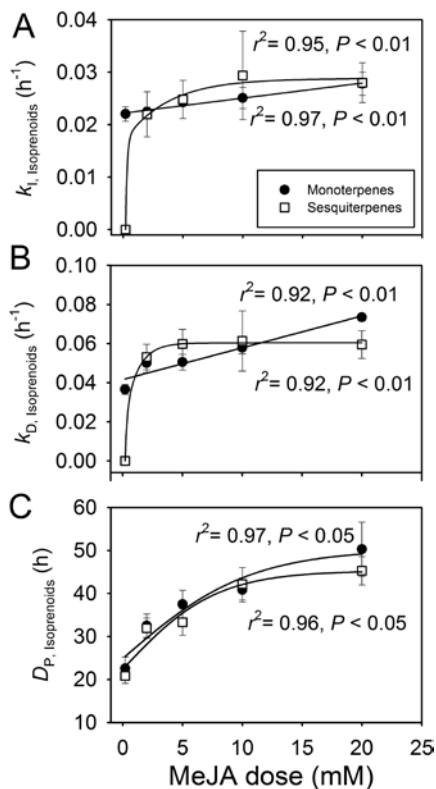


Fig. 7. First-order rate constants (k_i) for the initial increases (Equation 2, k_i ; A) and decreases (Equation 3, k_D ; B) of the MeJA-induced emissions for mono- ($k_{i,monoterpene}$ and $k_{D,monoterpene}$) and sesquiterpenes ($k_{i,sesquiterpene}$ and $k_{D,sesquiterpene}$) and the durations (C) of monoterpene ($D_{P,monoterpene}$) and sesquiterpene ($D_{P,sesquiterpene}$) emission bursts in relation to MeJA concentration in *C. sativus* leaves (see Fig. 2 for sample responses). Experimental treatments are as in Fig. 1 and data availability is as in Fig. 3. The regressions fitted to the data as: $y=0.0029x+0.22$ for $k_{i,monoterpene}$ and $y=0.297x/(0.736+x)$ for $k_{i,sesquiterpene}$ in (A), $y=0.0016x+0.041$ for $k_{D,monoterpene}$ and $y=0.061x/(0.295+x)$ for $k_{D,sesquiterpene}$ in (B), $y=50.3/[1+e^{(0.107-x)/5.26}]$ for $D_{P,monoterpene}$ and $y=45.3/[1+e^{(0.0784-x)/3.84}]$ for $D_{P,sesquiterpene}$ in (C). Altogether three replicate treatments at each MeJA application concentration were carried out.

fungal elicitor cryptogin and infections by *Phytophthora parasitica* (Wi et al., 2012) and *Pseudomonas syringae* (Mur et al., 2008), and biphasic LOX product and terpenoid emissions in response to infections by *Melampsora epitea* (Toome et al., 2010). However, with the exception of the ozone stress study of Beauchamp et al. (2005) that was carried out with a proton-transfer reaction quadrupole mass spectrometer (PTR-QMS), other kinetic studies had much lower time resolution than that (10 s) used in our study. While the elicitation of the volatile response to mechanical wounding and herbivory is characteristically very fast (Brilli et al., 2011; Copolovici et

al., 2011, 2014a; Portillo-Estrada et al., 2015), resembling the MeJA treatment response in our study, both the first and the second emission bursts in the pathogen-infected leaves (Mur et al., 2008; Toome et al., 2010; Wi et al., 2012) occurred later than in our study in MeJA-treated leaves (Fig. 2A, D). Clearly, different stresses can propagate differently, reflecting the diversity of biological characteristics of impacting organisms as well as differences in stress perception and signal transduction. Further research using high-resolution techniques as used here is needed to resolve the general and specific features of shorter and longer term elicitation responses induced by different stresses, including studies linking the emissions to pertinent gene expression patterns.

Emission rates and total emission of induced volatiles scale with MeJA dose

The level of biological stress varies greatly depending on the degree of infestation by herbivores and infection by pathogens (Niinemets et al., 2013), but biological stress severity versus stress response relationships have not been routinely studied. Here we observed that MeJA treatment concentration and the degree of leaf area damaged were quantitatively correlated (Fig. 1), in agreement with past observations indicating that exogenous application of MeJA can result in local phytotoxicity (Heijari et al., 2005). We also observed that both the total and maximum emissions of LOX compounds for both the early and the second emission burst (Figs 3A, 4A), for the early methanol emission burst (Figs 3B, 4B), and for the late monoterpene (Figs 3C, 4C) and sesquiterpene (Figs 3D, 4D) emission bursts were quantitatively associated with MeJA concentration and the proportion of leaf area damaged (damage severity). Thus, these results indicate that both the initial stress response due to activation of constitutive defenses and the later response due to activation of induced defenses are dose dependent.

MeJA that mainly enters through the stomata, and to a lower degree through the cuticle, is expected to become progressively diluted as it penetrates deeper into the leaf interior and dissolves in leaf water. Thus, the dose dependence of the early constitutive response as evident in the first LOX compound burst (Fig. 2A) and in the methanol burst (Fig. 2D) can result from quantitative scaling of the proportion of impacted cell wall and membrane sites with MeJA concentration. Such a positive scaling of early LOX and methanol emission responses with the degree of impact has been observed in wounding experiments (Brilli et al., 2011; Portillo-Estrada et al., 2015), and suggests that the control of the rapid elicitation response at the level of immediate impact is possible.

In the case of the late-induced response, the situation is less clear because in addition to MeJA *per se*, the primary MeJA-induced LOX volatile emissions can propagate the signal to cellular locations not necessarily directly impacted by MeJA (Cardoza et al., 2002; Engelberth et al., 2007; Kishimoto et al., 2008; Piesik et al., 2013; Castelyn et al., 2015).

The MeJA dose dependence of induced emissions resembles herbivory experiments where the rate of emissions of mono- and sesquiterpenes increases with the proportion of

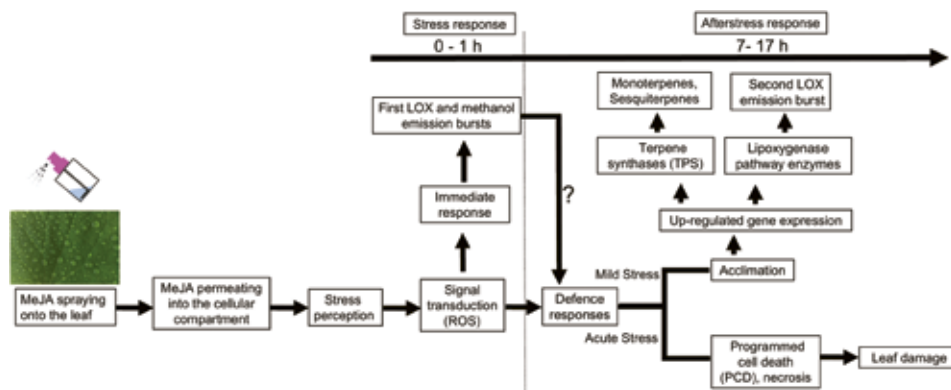


Fig. 8. A conceptual model of elicitation of short- and long-term volatile responses upon MeJA treatment of cucumber leaves. Gaseous MeJA is taken up into the leaf internal air space through stomata, permeates further through cell walls and plasmalemma, reaching ultimately the symplastic leaf compartments. This activates an oxidative burst due to rapid formation of reactive oxygen species (ROS; Garrido *et al.*, 2003; Zhang and Xing, 2008; Küpper *et al.*, 2009; Hazra *et al.*, 2017) and release of free polyunsaturated fatty acids from plant membranes (Dicke *et al.*, 1999; Feussner and Wasternack, 2002; Andreou and Feussner, 2009) in several minutes after the treatment at the immediate location of MeJA impact. Due to the constitutive activity of lipoxygenases, free fatty acids are rapidly converted to volatile lipoxygenase pathway products (LOX products; Feussner and Wasternack, 2002; Andreou and Feussner, 2009), resulting in the first burst of LOX emissions (Fig. 2A). Simultaneously with the release of free fatty acids or maybe even somewhat earlier, constitutive pectin methylsterases (Micheli, 2001; Pelloux *et al.*, 2007) are activated, resulting in major emissions of methanol (Fig. 2D). In a longer-term sequence of events probably involving endogenous jasmonate formation and interplay with jasmonate repressor proteins (JAZ) (Chini *et al.*, 2007; Wasternack and Song, 2017; Zhang *et al.*, 2017), plant defense responses depend on the initial stress severity. Mild and moderate stress caused by MeJA treatment (5, 10, and 20 mM) is expected to lead to elicitation of gene expression level defenses including enhanced expression of terpenoid synthase (TPS; Martin *et al.*, 2002, 2003; Byun-McKay *et al.*, 2006) and lipoxygenase pathway genes (Bell and Mullet, 1991; Wasternack and Parthier, 2007), resulting in volatile terpene and LOX emissions that are sustained for long time periods of ~20–30 h (Fig. 2B, C). In the case of moderate stress, propagation of necrotic lesions remains localized (Fig. 1A). In contrast, acute MeJA stress (50 mM) leads to enhanced progression of programmed cell death (PCD), and subsequent rapid propagation of necrosis over the entire leaf surface (Fig. 1A).

leaf area consumed (Copolovici *et al.*, 2011, 2014a), indicating that the rate of terpene synthesis becomes progressively greater in the remaining tissues. Analogously, in fungal-infected leaves, terpenoid emissions increase with increasing spread of the necrotic area (Jiang *et al.*, 2016b). We argue that the quantitative relationships between the dose of the model compound MeJA, severity of damage, and the volatile emission responses in cucumber have major biological consequences. Studies have demonstrated that different levels of induction of volatiles by MeJA treatment alter both plant attractiveness to herbivores (Heil, 2014) and the repellency to herbivores (Zas *et al.*, 2011). This suggests that the capacity to respond to a biotic stress in a dose-dependent manner as demonstrated here provides significant fitness advantages.

A conceptual model describing MeJA elicitation of defenses from stress response to acclimation

The induction of volatiles released upon MeJA treatment from cucumber leaves followed similar elicitation patterns for both the fast and slow phases, with an initial exponential or sigmoidal increase to a maximum level, followed by a decrease to the baseline emission (Fig. 2). We fitted the temporal shapes of the increase and decrease of volatiles by first-order exponential relationships to characterize the rise and decay kinetics (Equations 2 and 3) and further characterized

the timing of emission elicitation (Fig. 2; Table 1). Both the rate of increase and the decrease of LOX compounds and terpenoids were strongly enhanced by increasing MeJA concentrations (Figs 6A, B, 7A, B). Furthermore, both the first and the second LOX burst (Fig. 5B) and monoterpene and sesquiterpene emission bursts (Fig. 5D) occurred earlier, and were sustained for longer time periods (Figs 6D, 7C) at higher MeJA dose. This evidence emphasizes the highly dynamic nature of the MeJA concentration dependence of volatile emissions over both the short and long term.

For chronic biotic stresses such as herbivory infestation and pathogen attacks, quantitative relationships between the severity of biotic stress and release of induced volatiles have been suggested to result from the scaling of emissions with propagation of damage and the number of simultaneous stress impact sites (Niinemets *et al.*, 2013). As this study with MeJA elicitor demonstrates, the scaling relationships of volatile responses with MeJA dose, the ‘stress severity’, consist of both local and systemic responses. As for the local early response, it indeed can reflect scaling of emissions with the spread of the immediate stress impact sites (Fig. 8). However, the quantitative scaling of the subsequent slower gene-level responses with MeJA dose is obviously more complex and probably reflects a systemic response. The timing and magnitude of this systemic response is determined by the initial MeJA dose, but the way in which the early stress signal

determines the gene expression response is still unclear at a mechanistic level, and will require further studies looking at both the activation of expression of regulator and target genes. It is likely that the balance between the free transcription regulator MYC2 that activates downstream jasmonate transcriptional responses and jasmonate signaling repressor proteins (JAZ proteins) that negatively affect MYC2 levels (Gális *et al.*, 2009), together with the elicitation of endogenous jasmonate synthesis (Tamogami *et al.*, 2008), determines the onset of elicitation of gene expression and subsequent repression.

Furthermore, the set of events downstream of the initial MeJA impact consists of acclimation responses and localized acute necrotic or PCD-like responses with the share among them determined by the initial MeJA concentration (Figs 1, 8). Thus, with increasing MeJA concentration, a greater proportion of leaf area undergoes death, while the volatile emission capacity of the remaining cells is increasingly up-regulated. Stronger amplification of the emission capacity in those cells still alive resembles the emission response to herbivory where foliar terpenoid emissions in remaining leaf parts increase dependent on the proportion of leaf area consumed by herbivores (Copolovici *et al.*, 2011, 2014a, 2017).

What could be the biological significance of the dose dependence of the second elicited emission burst? Due to high reactivity in the ambient atmosphere, the volatile signal itself fades with the distance from the emission source (Holopainen and Blande, 2013; Holopainen *et al.*, 2013; Blande *et al.*, 2014). Thus, a stronger signal will reach more distant leaves, and also provides a farther reaching signal for other organisms such as herbivore predators. Furthermore, we suggest that the strength of the volatile signal might carry information about the severity of the biological impact and, as such, contribute to stronger priming responses in surrounding leaves of the same plant and neighboring plants. We argue that for quantitative prediction of biotic stress severity versus emission response relationships, further studies are needed to gain insight into the turnover of JAZ and MYC2 proteins and into the timing and magnitude of formation of endogenous jasmonate as driven by the severity of biotic stress impact.

Conclusions

High time resolution measurements conducted here have highlighted the biphasic kinetics of volatile emissions induced by MeJA treatment. Our study demonstrates rapid constitutive lipoxygenase pathway volatile (LOX) and methanol emissions and subsequent elicitation of terpenoid emission. Strong quantitative relationships between the timing and magnitude of early and late emissions and applied MeJA concentration collectively indicate high plant plastic capacity to respond to biotic stress, and emphasize the highly dynamic nature of the MeJA concentration dependence of volatile emissions over both the short and long term. Albeit that this study presented exciting evidence of quantitative scaling of local and systemic emission responses to MeJA treatment, we suggest that to gain insight into the mechanisms of regulation of the magnitude and kinetics of the downstream responses

and validate the differences in the sensitivity of gene expression in cucumber, further studies should look at expression of terpenoid synthase genes under treatments with different MeJA concentrations. In addition, higher resolution reactive oxygen species measurement techniques should be developed to obtain complementary information on leaf oxidative status through the emissions bursts recorded by PTR-TOF-MS.

Acknowledgements

We acknowledge the financial support from the European Commission through the European Research Council (advanced grant 322603, SIP-VOL+), the European Regional Development Fund (Centre of Excellence EcolChange), and the Estonian Ministry of Science and Education (institutional grant IUT-8-3).

References

- Adams RP. 1995. Identification of essential oil components by gas chromatography and mass spectrometry, 3rd edn. USA: Allured Publishing Corporation.
- Allmann S, Baldwin IT. 2010. Insects betray themselves in nature to predators by rapid isomerization of green leaf volatiles. *Science* **329**, 1075–1078.
- Andreou A, Feussner I. 2009. Lipoxygenases—structure and reaction mechanism. *Phytochemistry* **70**, 1504–1510.
- Arimura G, Matsui K, Takabayashi J. 2009. Chemical and molecular ecology of herbivore-induced plant volatiles: proximate factors and their ultimate functions. *Plant and Cell Physiology* **50**, 911–923.
- Arimura G, Garms S, Maffei M, Bossi S, Schulze B, Leitner M, Mithöfer A, Boland W. 2008. Herbivore-induced terpenoid emission in *Medicago truncatula*: concerted action of jasmonate, ethylene and calcium signaling. *Planta* **227**, 453–464.
- Beauchamp J, Wisthaler A, Hansel A, Kleist E, Miebach M, Niinemets U, Schurr U, Wildt J. 2005. Ozone induced emissions of biogenic VOC from tobacco: relations between ozone uptake and emission of LOX products. *Plant, Cell and Environment* **28**, 1334–1343.
- Bell E, Mullet JE. 1991. Lipoxygenase gene expression is modulated in plants by water deficit, wounding, and methyl jasmonate. *Molecular and General Genetics* **230**, 456–462.
- Blande JD, Holopainen JK, Niinemets Ü. 2014. Plant volatiles in polluted atmospheres: stress responses and signal degradation. *Plant, Cell and Environment* **37**, 1892–1904.
- Bouwmeester HJ, Verstappen FW, Posthumus MA, Dicke M. 1999. Spider mite-induced (3S)-(*E*)-nerolidol synthase activity in cucumber and lima bean. The first dedicated step in acyclic C11-homoterpene biosynthesis. *Plant Physiology* **121**, 173–180.
- Brilli F, Ciccioli P, Frattoni M, Prestinini M, Spanedda AF, Loreto F. 2009. Constitutive and herbivore-induced monoterpenes emitted by *Populus × euroamericana* leaves are key volatiles that orient *Chrysomela populi* beetles. *Plant, Cell and Environment* **32**, 542–552.
- Brilli F, Ruuskanen TM, Schnitzhofer R, Müller M, Breitenlechner M, Bittner V, Wohlfahrt G, Loreto F, Hansel A. 2011. Detection of plant volatiles after leaf wounding and darkening by proton transfer reaction 'time-of-flight' mass spectrometry (PTR-TOF). *PLoS One* **6**, e20419.
- Bruinsma M, Posthumus MA, Munn R, Mueller MJ, van Loon JJ, Dicke M. 2009. Jasmonic acid-induced volatiles of *Brassica oleracea* attract parasitoids: effects of time and dose, and comparison with induction by herbivores. *Journal of Experimental Botany* **60**, 2575–2587.
- Bruinsma M, Van Dam NM, Van Loon JJ, Dicke M. 2007. Jasmonic acid-induced changes in *Brassica oleracea* affect oviposition preference of two specialist herbivores. *Journal of Chemical Ecology* **33**, 655–668.
- Byun-McKay A, Godard KA, Toudefallah M, Martin DM, Alfaro R, King J, Bohlmann J, Plant AL. 2006. Wound-induced terpene synthase gene expression in Sitka spruce that exhibit resistance or susceptibility to attack by the white pine weevil. *Plant Physiology* **140**, 1009–1021.
- Cardoza YJ, Alborn HT, Tumlinson JH. 2002. In vivo volatile emissions from peanut plants induced by simultaneous fungal infection and insect damage. *Journal of Chemical Ecology* **28**, 161–174.

- Castelyn HD, Appelgryn JJ, Mafa MS, Pretorius ZA, Visser B. 2015. Volatiles emitted by leaf rust infected wheat induce a defence response in exposed uninfected wheat seedlings. *Australas Plant Pathology* **44**, 245–254.
- Cheong JJ, Choi YD. 2003. Methyl jasmonate as a vital substance in plants. *Trends in Genetics* **19**, 409–413.
- Chini A, Fonseca S, Fernández G, et al. 2007. The JAZ family of repressors is the missing link in jasmonate signalling. *Nature* **448**, 666–671.
- Copolovici LO, Filella I, Llusia J, Niinemets Ü, Peñuelas J. 2005. The capacity for thermal protection of photosynthetic electron transport varies for different monoterpenes in *Quercus ilex*. *Plant Physiology* **139**, 485–496.
- Copolovici L, Kännaste A, Pazouki L, Niinemets Ü. 2012. Emissions of green leaf volatiles and terpenoids from *Solanum lycopersicum* are quantitatively related to the severity of cold and heat shock treatments. *Journal of Plant Physiology* **169**, 664–672.
- Copolovici L, Kännaste A, Rimmel T, Niinemets Ü. 2014a. Volatile organic compound emissions from *Alnus glutinosa* under interacting drought and herbivory stresses. *Environmental and Experimental Botany* **100**, 55–63.
- Copolovici L, Kännaste A, Rimmel T, Vislap V, Niinemets Ü. 2011. Volatile emissions from *Alnus glutinosa* induced by herbivory are quantitatively related to the extent of damage. *Journal of Chemical Ecology* **37**, 18–28.
- Copolovici L, Niinemets Ü. 2010. Flooding induced emissions of volatile signalling compounds in three tree species with differing waterlogging tolerance. *Plant, Cell and Environment* **33**, 1582–1594.
- Copolovici L, Pag A, Kännaste A, Bodescu A, Tomescu D, Copolovici D, Soran ML, Niinemets Ü. 2017. Disproportionate photosynthetic decline and inverse relationship between constitutive and induced volatile emissions upon feeding of *Quercus robur* leaves by large larvae of gypsy moth (*Lymantria dispar*). *Environmental and Experimental Botany* **138**, 184–192.
- Copolovici L, Väärtnõu F, Portillo Estrada M, Niinemets Ü. 2014b. Oak powdery mildew (*Erysiphe alphitoides*)-induced volatile emissions scale with the degree of infection in *Quercus robur*. *Tree Physiology* **34**, 1399–1410.
- Degenhardt DC, Lincoln DE. 2006. Volatile emissions from an odorless plant in response to herbivory and methyl jasmonate exposure. *Journal of Chemical Ecology* **32**, 725–743.
- Dicke M, Gols R, Ludeking D, Posthumus MA. 1999. Jasmonic acid and herbivory differentially induce carnivore-attracting plant volatiles in lima bean plants. *Journal of Chemical Ecology* **25**, 1907–1922.
- Engelberth J, Seidl-Adams I, Schultz JC, Tumlinson JH. 2007. Insect elicitors and exposure to green leafy volatiles differentially upregulate major octadecanoids and transcripts of 12-oxo phytyldienoic acid reductases in *Zea mays*. *Molecular Plant-Microbe Interactions* **20**, 707–716.
- Farag MA, Paré PW. 2002. C6-Green leaf volatiles trigger local and systemic VOC emissions in tomato. *Phytochemistry* **61**, 545–554.
- Feussner I, Wasternack C. 2002. The lipoxygenase pathway. *Annual Review of Plant Biology* **53**, 275–297.
- Frost CJ, Mescher MC, Dervinis C, Davis JM, Carlson JE, De Moraes CM. 2008. Priming defense genes and metabolites in hybrid poplar by the green leaf volatile cis-3-hexenyl acetate. *New Phytologist* **180**, 722–734.
- Gális I, Gaquerel E, Pandey SP, Baldwin IT. 2009. Molecular mechanisms underlying plant memory in JA-mediated defence responses. *Plant, Cell and Environment* **32**, 617–627.
- Gao H, Zhu H, Shao Y, Chen A, Lu C, Zhu B, Luo Y. 2008. Lycopene accumulation affects the biosynthesis of some carotenoid-related volatiles independent of ethylene in tomato. *Journal of Integrative Plant Biology* **50**, 991–996.
- Garrido I, Espinosa F, Córdoba-Pedregosa MC, González-Reyes JA, Alvarez-Tinaut MC. 2003. Redox-related peroxidative responses evoked by methyl-jasmonate in axenically cultured aeroponic sunflower (*Helianthus annuus* L.) seedling roots. *Protoplasma* **221**, 79–91.
- Grote R, Monson RK, Niinemets Ü. 2013. Leaf-level models of constitutive and stress-driven volatile organic compound emissions. In: **Niinemets Ü, Monson RK**, eds. *Biology, controls and models of tree volatile organic compound emissions*. *Tree Physiology* 5. Berlin: Springer, 315–355.
- Hann CT, Bequette CJ, Dombrowski JE, Stratmann JW. 2014. Methanol and ethanol modulate responses to danger- and microbe-associated molecular patterns. *Frontiers in Plant Science* **5**, 550.
- Hazra S, Bhattacharyya D, Chattopadhyay S. 2017. Methyl jasmonate regulates podophyllotoxin accumulation in *Podophyllum hexandrum* by altering the ROS-responsive podophyllotoxin pathway gene expression additionally through the down regulation of few interfering miRNAs. *Frontiers in Plant Science* **8**, 164.
- Heijari J, Nerg AM, Kainulainen P, Viiri H, Vuorinen M, Holopainen JK. 2005. Application of methyl jasmonate reduces growth but increases chemical defence and resistance against *Hylobius abietis* in Scots pine seedlings. *Entomologia Experimentalis et Applicata* **115**, 117–124.
- Heijari J, Nerg AM, Kainulainen P, Vuorinen M, Holopainen JK. 2008. Long-term effects of exogenous methyl jasmonate application on Scots pine (*Pinus sylvestris*) needle chemical defence and diprionid sawfly performance. *Entomologia Experimentalis et Applicata* **128**, 162–171.
- Heil M. 2014. Herbivore-induced plant volatiles: targets, perception and unanswered questions. *New Phytologist* **204**, 297–306.
- Heil M, Kost C. 2006. Priming of indirect defences. *Ecology Letters* **9**, 813–817.
- Heil M, Ton J. 2008. Long-distance signalling in plant defence. *Trends in Plant Science* **13**, 264–272.
- Holopainen JK, Blande JD. 2013. Where do herbivore-induced plant volatiles go? *Frontiers in Plant Science* **4**, 185.
- Holopainen JK, Nerg AM, Blande JD. 2013. Multitrophic signalling in polluted atmospheres. In: **Niinemets Ü, Monson RK**, eds. *Biology, controls and models of tree volatile organic compound emissions*. *Tree Physiology* 5. Berlin: Springer, 285–314.
- Hu ZH, Shen YB, Su XH. 2009. Saturated aldehydes C₆–C₁₀ emitted from ashleaf maple (*Acer negundo* L.) leaves at different levels of light intensity, O₂, and CO₂. *Journal of Plant Biology* **52**, 289–298.
- Jiang Y, Ye J, Li S, Niinemets Ü. 2016a. Regulation of floral terpene emission and biosynthesis in sweet basil (*Ocimum basilicum*). *Journal of Plant Growth Regulation* **35**, 921–935.
- Jiang Y, Ye J, Veromann LL, Niinemets Ü. 2016b. Scaling of photosynthesis and constitutive and induced volatile emissions with severity of leaf infection by rust fungus (*Melampsora larici-populina*) in *Populus balsamifera* var. *suaveolens*. *Tree Physiology* **36**, 856–872.
- Jonak C, Okrész L, Bögre L, Hirt H. 2002. Complexity, cross talk and integration of plant MAP kinase signalling. *Current Opinion in Plant Biology* **5**, 415–424.
- Jung S. 2004. Effect of chlorophyll reduction in *Arabidopsis thaliana* by methyl jasmonate or niflurazon on antioxidant systems. *Plant Physiology and Biochemistry* **42**, 225–231.
- Kännaste A, Copolovici L, Niinemets Ü. 2014. Gas chromatography mass-spectrometry method for determination of biogenic volatile organic compounds emitted by plants. *Methods in Molecular Biology* **1153**, 161–169.
- Kappers IF, Verstappen FW, Luckerhoff LL, Bouwmeester HJ, Dicke M. 2010. Genetic variation in jasmonic acid- and spider mite-induced plant volatile emission of cucumber accessions and attraction of the predator *Phytoseiulus persimilis*. *Journal of Chemical Ecology* **36**, 500–512.
- Kask K, Kännaste A, Talts E, Copolovici L, Niinemets Ü. 2016. How specialized volatiles respond to chronic and short-term physiological and shock heat stress in *Brassica nigra*. *Plant, Cell and Environment* **39**, 2027–2042.
- Kegge W, Weldegergis BT, Soler R, Vergeer-Van Eijk M, Dicke M, Voosenek LA, Pierik R. 2013. Canopy light cues affect emission of constitutive and methyl jasmonate-induced volatile organic compounds in *Arabidopsis thaliana*. *New Phytologist* **200**, 861–874.
- Kishimoto K, Matsui K, Ozawa R, Takabayashi J. 2008. Direct fungicidal activities of C6-aldehydes are important constituents for defense responses in *Arabidopsis* against *Botrytis cinerea*. *Phytochemistry* **69**, 2127–2132.
- Komarova TV, Sheshukova EV, Dorokhov YL. 2014. Cell wall methanol as a signal in plant immunity. *Frontiers in Plant Science* **5**, 101.
- Küpper FC, Gaquerel E, Cosse A, Adas F, Peters AF, Müller DG, Kloareg B, Salaün JP, Potin P. 2009. Free fatty acids and methyl jasmonate trigger defense reactions in *Laminaria digitata*. *Plant and Cell Physiology* **50**, 789–800.
- Liang YS, Kim HK, Lefeber AW, Erkelens C, Choi YH, Verpoorte R. 2006. Identification of phenylpropanoids in methyl jasmonate treated *Brassica rapa* leaves using two-dimensional nuclear magnetic resonance spectroscopy. *Journal of Chromatography A* **1112**, 148–155.

- Loivamäki M, Holopainen JK, Nerg AM.** 2004. Chemical changes induced by methyl jasmonate in oilseed rape grown in the laboratory and in the field. *Journal of Agricultural and Food Chemistry* **52**, 7607–7613.
- Mäntylä E, Blande JD, Klemola T.** 2014. Does application of methyl jasmonate to birch mimic herbivory and attract insectivorous birds in nature? *Arthropod-Plant Interactions* **8**, 143–153.
- Martin DM, Gershenzon J, Bohlmann J.** 2003. Induction of volatile terpene biosynthesis and diurnal emission by methyl jasmonate in foliage of Norway spruce. *Plant Physiology* **132**, 1586–1599.
- Martin D, Tholl D, Gershenzon J, Bohlmann J.** 2002. Methyl jasmonate induces traumatic resin ducts, terpenoid resin biosynthesis, and terpenoid accumulation in developing xylem of Norway spruce stems. *Plant Physiology* **129**, 1003–1018.
- Matsui K, Sugimoto K, Mano J, Ozawa R, Takabayashi J.** 2012. Differential metabolisms of green leaf volatiles in injured and intact parts of a wounded leaf meet distinct ecophysiological requirements. *PLoS One* **7**, e36433.
- Micheli F.** 2001. Pectin methylesterases: cell wall enzymes with important roles in plant physiology. *Trends in Plant Science* **6**, 414–419.
- Mithöfer A, Wanner G, Boland W.** 2005. Effects of feeding *Spodoptera littoralis* on lima bean leaves. II. Continuous mechanical wounding resembling insect feeding is sufficient to elicit herbivory-related volatile emission. *Plant Physiology* **137**, 1160–1168.
- Mur LA, Laarhoven LJ, Harren FJ, Hall MA, Smith AR.** 2008. Nitric oxide interacts with salicylate to regulate biphasic ethylene production during the hypersensitive response. *Plant Physiology* **148**, 1537–1546.
- Niinemets Ü.** 2010. Mild versus severe stress and BVOCs: thresholds, priming and consequences. *Trends in Plant Science* **15**, 145–153.
- Niinemets Ü, Kännaste A, Copolovici L.** 2013. Quantitative patterns between plant volatile emissions induced by biotic stresses and the degree of damage. *Frontiers in Plant Science* **4**, 262.
- Niinemets Ü, Kuhn U, Harley PC, et al.** 2011. Estimations of isoprenoid emission capacity from enclosure studies: measurements, data processing, quality and standardized measurement protocols. *Bioessences* **8**, 2209–2246.
- Pazouki L, Memari HR, Kännaste A, Bichele R, Niinemets Ü.** 2015. Germacrene A synthase in yarrow (*Achillea millefolium*) is an enzyme with mixed substrate specificity: gene cloning, functional characterization and expression analysis. *Frontiers in Plant Science* **6**, 111.
- Pelloux J, Rustérucci C, Mellerowicz EJ.** 2007. New insights into pectin methylesterase structure and function. *Trends in Plant Science* **12**, 267–277.
- Peñuelas J, Filella I, Stefanescu C, Llusà J.** 2005. Caterpillars of *Euphydryas aurinia* (Lepidoptera: Nymphalidae) feeding on *Succisa pratensis* leaves induce large foliar emissions of methanol. *New Phytologist* **167**, 851–857.
- Phillips MA, Walter MH, Ralph SG, et al.** 2007. Functional identification and differential expression of 1-deoxy-D-xylulose 5-phosphate synthase in induced terpenoid resin formation of Norway spruce (*Picea abies*). *Plant Molecular Biology* **65**, 243–257.
- Piesik D, Panka D, Jeske M, Wenda-Piesik A, Delaney KJ, Weaver DK.** 2013. Volatile induction of infected and neighbouring uninfected plants potentially influence attraction/repellence of a cereal herbivore. *Journal of Applied Entomology* **137**, 296–309.
- Popova LP, Ananieva E, Hristova V, Christov K, Georgieva K, Alexieva V, Stoinova ZH.** 2003. Salicylic acid- and methyl jasmonate-induced protection on photosynthesis to parakeet oxidative stress. *Bulgarian Journal of Plant Physiology Special issue*, 133–152.
- Portillo-Estrada M, Kazantsev T, Niinemets Ü.** 2017. Fading of wound-induced volatile release during *Populus tremula* leaf expansion. *Journal of Plant Research* **130**, 157–165.
- Portillo-Estrada M, Kazantsev T, Taits E, Tosens T, Niinemets Ü.** 2015. Emission timetable and quantitative patterns of wound-induced volatiles across different leaf damage treatments in aspen (*Populus tremula*). *Journal of Chemical Ecology* **41**, 1105–1117.
- Repka V, Carna M, Pavlovkin J.** 2013. Methyl jasmonate-induced cell death in grapevine requires both lipoxygenase activity and functional octadecanoid biosynthetic pathway. *Biologia* **68**, 896–903.
- Rodríguez-Saona C, Crafts-Brandner SJ, Paré PW, Henneberry TJ.** 2001. Exogenous methyl jasmonate induces volatile emissions in cotton plants. *Journal of Chemical Ecology* **27**, 679–695.
- Scala A, Allmann S, Mirabella R, Haring MA, Schuurink RC.** 2013. Green leaf volatiles: a plant's multifunctional weapon against herbivores and pathogens. *International Journal of Molecular Sciences* **14**, 17781–17811.
- Seco R, Filella I, Llusà J, Peñuelas J.** 2011. Methanol as a signal triggering isoprenoid emissions and photosynthetic performance in *Quercus ilex*. *Acta Physiologiae Plantarum* **33**, 2413–2422.
- Semiz G, Blande JD, Heijari J, Işık K, Niinemets Ü, Holopainen JK.** 2012. Manipulation of VOC emissions with methyl jasmonate and carrageenan in the evergreen conifer *Pinus sylvestris* and evergreen broadleaf *Quercus ilex*. *Plant Biology* **14 Suppl 1**, 57–65.
- Shi J, Ma C, Qi D, Lv H, Yang T, Peng Q, Chen Z, Lin Z.** 2015. Transcriptional responses and flavor volatiles biosynthesis in methyl jasmonate-treated tea leaves. *BMC Plant Biology* **15**, 233.
- Suh HW, Hyun SH, Kim SH, Lee SY, Choi HK.** 2013. Metabolic profiling and enhanced production of phytochemicals by elicitation with methyl jasmonate and silver nitrate in whole plant cultures of *Lemma paucicostata*. *Process Biochemistry* **48**, 1581–1586.
- Tani A, Hayward S, Hewitt CN.** 2003. Measurement of monoterpenes and related compounds by proton transfer reaction-mass spectrometry (PTR-MS). *International Journal of Mass Spectrometry* **223–224**, 561–578.
- Tamogami S, Rakwal R, Agrawal GK.** 2008. Interplant communication: airborne methyl jasmonate is essentially converted into JA and JA-Ile activating jasmonate signaling pathway and VOCs emission. *Biochemical and Biophysical Research Communications* **376**, 723–727.
- Thaler JS, Fidantsef AL, Bostock RM.** 2002. Antagonism between jasmonate- and salicylate-mediated induced plant resistance: effects of concentration and timing of elicitation on defense-related proteins, herbivore, and pathogen performance in tomato. *Journal of Chemical Ecology* **28**, 1131–1159.
- Toome M, Randjäärv P, Copolovici L, Niinemets Ü, Heinsoo K, Luik A, Noe SM.** 2010. Leaf rust induced volatile organic compounds signalling in willow during the infection. *Planta* **232**, 235–243.
- von Dahl CC, Hävecker M, Schlögl R, Baldwin IT.** 2006. Caterpillar-elicited methanol emission: a new signal in plant–herbivore interactions? *The Plant Journal* **46**, 948–960.
- War AR, Paulraj MG, Ahmad T, Buhroo AA, Hussain B, Ignacimuthu S, Sharma HC.** 2012. Mechanisms of plant defense against insect herbivores. *Plant Signaling and Behavior* **7**, 1306–1320.
- Wasternack C, Parthier B.** 2007. Jasmonate-signalled plant gene expression. *Trends in Plant Science* **2**, 302–307.
- Wasternack C, Song S.** 2017. Jasmonates: biosynthesis, metabolism, and signaling by proteins activating and repressing transcription. *Journal of Experimental Botany* **68**, 1303–1321.
- Wi SJ, Ji NR, Park KY.** 2012. Synergistic biosynthesis of biphasic ethylene and reactive oxygen species in response to hemibiotrophic *Phytophthora parasitica* in tobacco plants. *Plant Physiology* **159**, 251–265.
- Wildt J, Kobel K, Schuh-Thomas G, Heiden AC.** 2003. Emissions of oxygenated volatile organic compounds from plants. Part II: Emissions of saturated aldehydes. *Journal of Atmospheric Chemistry* **45**, 173–196.
- Yli-Pirilä P, Copolovici L, Kännaste A, et al.** 2016. Herbivory by an outbreaking moth increases emissions of biogenic volatiles and leads to enhanced secondary organic aerosol formation capacity. *Environmental Science and Technology* **50**, 11501–11510.
- Zas R, Moreira X, Sampedro L.** 2011. Tolerance and induced resistance in a native and an exotic pine species: relevant traits for invasion ecology. *Journal of Ecology* **99**, 1316–1326.
- Zhang L, Xing D.** 2008. Methyl jasmonate induces production of reactive oxygen species and alterations in mitochondrial dynamics that precede photosynthetic dysfunction and subsequent cell death. *Plant and Cell Physiology* **49**, 1092–1111.
- Zhang L, Zhang F, Melotto M, Yao J, He SY.** 2017. Jasmonate signaling and manipulation by pathogens and insects. *Journal of Experimental Botany* **68**, 1371–1385.
- Zhao KJ, Chye ML.** 1999. Methyl jasmonate induces expression of a novel *Brassica juncea* chitinase with two chitin-binding domains. *Plant Molecular Biology* **40**, 1009–1018.

CURRICULUM VITAE

First name: Shuai
Surname: Li
Date of birth: 20.06.1985

Employment: Estonian University of Life Sciences, Institute of Agricultural and Environmental Sciences
Position: Junior researcher
email: shuai.li@emu.ee

Academic degree: Master's degree (MSc), 2013, (sup) K.-F. Cao, The Heterogeneity of Structure and Function in Giant Leaves: the Hydraulic and Thermal Limitations on Leaf Size.

Education:
2013.12-2018.1 PhD studies, Estonian University of Life Sciences, Institute of Agricultural and Environmental Sciences, Tartu-Estonia
2009.9-2013.7 MSc studies, University of Science and Technology of China, School of Life Sciences, Hefei-China
2005.9-2009.7 BSc studies, Dezhou University, Department of Biology, Dezhou-China

Professional employment:
2015.1- Estonian University of Life Sciences, Institute of Agricultural and Environmental Sciences, Junior Researcher
2014.1-2014.12 Estonian University of Life Sciences, Institute of Agricultural and Environmental Sciences, Specialist

Grants and projects: Centre of Excellence in Environmental Adaptation (F11100PKTF)
Stress-Induced Plant Volatiles in Biosphere-Atmosphere System (8-2/T13006PKTF)
Plant stress in changing climates: from stress responses to acclimation and adaptation (IUT8-3)
Ecology of Global Change: natural and managed ecosystems (8F160018PKTF)

CURRICULUM VITAE IN ESTONIAN

Nimi:	Shuai
Perekonnanimi:	Li
Sünniaeg:	20.06.1985
Töökoht:	Eesti Maaülikool, Põllumajandus- ja keskkonnainstituut
Ametikoht:	Nooremteadur
e-mail:	shuai.li@emu.ee
Teaduskraad:	Master's degree (MSc), 2013, (sup) K.-F. Cao, The Heterogeneity of Structure and Function in Giant Leaves: the Hydraulic and Thermal Limitations on Leaf Size.
Hariduskäik:	
2013.12-2018.1	PhD studies, Eesti Maaülikool, Põllumajandus- ja keskkonnainstituut, Tartu-Estonia
2009.9-2013.7	MSc studies, University of Science and Technology of China, School of Life Sciences, Hefei-China
2005.9-2009.7	BSc studies, Dezhou University, Department of Biology, Dezhou-China
Teenistuskäik:	
2015.1-	Eesti Maaülikool, Põllumajandus- ja keskkonnainstituut, Nooremteadur
2014.1-2014.12	Eesti Maaülikool, Põllumajandus- ja keskkonnainstituut, Specialist
Osalemine uuringisprojektides ja programmides:	Keskkonnamuutustele Kohanemise tippkeskus (F11100PKTF) Stressindutseeritud taimsed lenduvad ühendid biosfääri-atmosfääri süsteemis (8-2/t13006PKTF) Taimede stress muutuvast kliimas: stressivastustest kohanemiseni (IUT8-3) Globaalmuutuste ökoloogia looduslikes ja põllumajanduskooslustes (8F160018PKTF)

LIST OF PUBLICATIONS

Publications:

1. **Li S**, Tosens T, Harley PC, Jiang Y, Kanagendran A, Grosberg M, Jaamets K, Niinemets Ü (2018) Glandular trichomes as a barrier against atmospheric oxidative stress: relationships with ozone uptake, leaf damage and emission of volatiles across a diverse set of species. *Plant, Cell & Environment*, in press.
2. Kanagendran A, Pazouki L, **Li S**, Liu B, Kännaste A, Niinemets Ü (2017) Ozone-triggered surface uptake and stress volatile emissions in *Nicotiana tabacum* ‘Wisconsin’. *Journal of Experimental Botany*, doi:10.1093/jxb/erx431.
3. Jiang Y, Ye J, **Li S**, Niinemets Ü (2017) Methyl jasmonate-induced emission of biogenic volatiles is biphasic in cucumber: a high-resolution analysis of dose dependence. *Journal of Experimental Botany* **68**(16), 4679-4694.
4. **Li S**, Harley PC, Niinemets Ü (2017) Ozone-induced foliar damage and release of stress volatiles is highly dependent on stomatal openness and priming by low-level ozone exposure in *Phaseolus vulgaris*. *Plant, Cell & Environment* **40**, 1984-2003.
5. Pazouki L, Kanagendran A, **Li S**, Kännaste A, Rajabi Memari H, Bichele R, Niinemets Ü (2016) Mono- and sesquiterpene release from tomato (*Solanum lycopersicum*) leaves upon mild and severe heat stress and through recovery: from gene expression to emission responses. *Environmental and Experimental Botany* **132**, 1-15.
6. Jiang Y, Ye J, **Li S**, Niinemets Ü (2016) Regulation of floral terpenoids emission and biosynthesis in sweet basil (*Ocimum basilicum*). *Journal of Plant Growth Regulation* **35**(4), 921-935.
7. **Li S**, Cao K-F (2014) Heterogeneity of anatomical structure in giant leaves of *Musa balbisiana*. *Chinese Science Bulletin* **59**, 522-528 Chinese Version with English Abstract.

8. **Li S**, Zhang Y-J, Sack L, Scoffoni C, Ishida A, Chen Y-J, Cao K-F (2013) The heterogeneity and spatial patterning of structure and physiology across the leaf surface in giant leaves of *Alocasia macrorrhiza*. *PLoS ONE* **8(6)**, e66016.

Conference abstracts:

1. **Li S**, Harley P, Niinemets Ü (2017) Stomata closure and pre-exposure to low-level O₃ protect leaves against high-level O₃-induced damage in *Phaseolus vulgaris*. *3rd Global Summit on Plant Science*, Rome, Italy.
2. **Li S**, Tosens T, Harley PC, Jiang Y, Kanagendran A, Jaamets K, Niinemets Ü (2017) Glandular trichomes as a barrier against atmospheric oxidative stress. *3rd Global Summit on Plant Science*, Rome, Italy.
3. Kanagendran A, Pazouki L, **Li S**, Niinemets Ü (2017) Effects of acute ozone exposure on the release of stress volatiles, and the expression of a monoterpene synthase gene in *Nicotiana tabacum* leaves through recovery. *3rd Global Summit on Plant Science*, Rome, Italy.
4. Fernández-Marín B, Harley P, Kazantsev T, Kännaste A, **Li S**, Miguez F, Niinemets Ü, Portillo M, García-Plazaola JI (2014) Is β -Cyclocitral a Communication Molecule between Stressed Plants? *Plant Biology Europe FESPB/EPSO Congress*, Dublin, Ireland.

VIIS VIIMAST KAITSMIST

ANNE PÓDER

THE SOCIO-ECONOMIC DETERMINANTS OF ENTREPRENEURSHIP IN ESTONIAN
RURAL MUNICIPALITIES
ETTEVÕTLUST MÕJUTAVAD SOTSIAAL-MAJANDUSLIKUD TEGURID EESTI
VALDADES

Professor Rando Värnik

27. november 2017

ENE TOOMING

THE SUBLETHAL EFFECTS OF NEUROTOXIC INSECTICIDES ON THE BASIC
BEHAVIOURS OF AGRICULTURALLY IMPORTANT CARABID BEETLES
NEUROTOKSILISTE INSEKTITSIIDIDE SUBLETAALNE TOIME
PÕLLUMAJANDUSLIKULT OLULISTE JOOKSIKLASTE PÕHIKÄITUMISTELE

Vanemteadur Enno Merivee, teadur Anne Must

11. detsember 2017

KADI PALMIK

EFFECTS OF NATURAL AND ANTHROPOGENIC PRESSURES AND DISTURBANCES
ON THE MACROPHYTES OF LAKE PEIPSI
LOODUSLIKE JA INIMTEKKELISTE SURVETEGURITE MÕJU PEIPSI JÄRVE
SUURTAIMESTIKULE

Vanemteadur Helle Mäemets, PhD Külli Kangur

15. detsember 2017

AIMAR NAMM

EXPRESSION OF BMP AND PAX PROTEINS IN THE CENTRAL NERVOUS SYSTEM
OF HUMAN AND RAT EMBRYOS AT EARLY STAGES OF DEVELOPMENT
BMP JA PAX SIGNAALMOLEKULIDE AVALDUMINE INIMESE JA ROTI EMBRÜOTE
KESKNÄRVISÜSTEEMI VARAJASTEL ARENGUETAPPIDEL

Professor Marina Aunapuu, professor Andres Arend (Tartu Ülikool)

15. detsember 2017

LEA TUVIKENE

THE EFFECT OF NATURAL VARIABILITY ON THE ASSESSMENT OF ECOLOGICAL
STATUS OF SHALLOW LAKES
LOODUSLIKU MUUTLIKKUSE MÕJU MADALATE JÄRVEDE ÖKOSEISUNDI
HINDAMISELE

Juhtivteadur Peeter Nõges

16. veebruar 2018

ISSN 2382-7076

ISBN 978-9949-629-17-6 (trükis)

ISBN 978-9949-629-18-3 (pdf)



Trükitud taastoodetud paberile looduslike trükivärvidega © Ecoprint